Universida de Vigo

Escola Internacional de Doutoramento

TESE DE DOUTORAMENTO

Fuentes oceánicas y terrestres de precipitación en el Ártico: Nuevas metas y orientaciones desde una aproximación lagrangiana

Marta Vázquez Domínguez

2017

Universidade Vigo

Escola Internacional de Doutoramento

Marta Vázquez Domínguez

TESIS DOCTORAL

Fuentes oceánicas y terrestres de precipitación en el Ártico: Nuevas metas y orientaciones desde una aproximación Lagrangiana

Dirigida por los doctores Luis Gimeno Presa
y Raquel Olalla Nieto Muñiz

Año 2017

Universidade Vigo

Escola Internacional de Doutoramento

El Dr. Luis Gimeno Presa, Profesor Catedrático
y la Dra. Raquel-Olalla Nieto Muñiz, Profesora Titular
ambos pertenecientes al Departamento de Física Aplicada, dentro del área de Física de la Tierra, de la Universidad de Vigo

HACEN CONSTAR que el presente trabajo, titulado "***Fuentes oceánicas y terrestres de precipitación en el Ártico: Nuevas metas y orientaciones desde una aproximación Lagrangiana***", que presenta Marta Vázquez Domínguez para la obtención do título de **DOCTORA POR LA UNIVERSIDAD DE VIGO** bajo la modalidad de "Compendio de publicaciones", fue elaborado bajo su dirección en el programa de doctorado "**Ciencias Marinas, Tecnología y Gestión (DO*MAR)**".

Ourense, 28 de junio de 2017

Los Directores de la tesis doctoral

Dr. Luis Gimeno Presa Dra. Raquel Olalla Nieto Muñiz

A familia y amigos

On ne découvre pas de terre nouvelle sans consentir à perdre de vue, d'abord et longtemps, tout rivage

André Guide

Índice

Resumen

En este trabajo se ha realizado una caracterización del transporte de humedad en el Ártico a través de una perspectiva lagrangiana y se ha tratado de relacionar este transporte con el deshielo observado en la región. El estudio del transporte de humedad en el Ártico viene motivado por los recientes cambios observados en esta región, los cuales tienen una implicación importante en la rama atmosférica del ciclo hidrológico. Conocer su comportamiento climatológico constituye un primer paso en el estudio de estas implicaciones así como de las causas de los cambios observados.

El cuerpo de este trabajo consiste en un total de cinco artículos publicados en revistas especializadas. En ellos se analiza el transporte de humedad en dos sentidos: el transporte desde las principales fuentes de humedad hacia el Ártico, con el fin de estudiar su influencia sobre la región, y el transporte desde el propio Ártico, para analizar las posibles implicaciones de los cambios sufridos en él en las últimas cuatro décadas. Este análisis se ha realizado a través del modelo lagrangiano FLEXPART, mediante el cual se puede seguir la trayectoria de las partículas atmosféricas con el fin de localizar aquellas regiones donde toman o pierden humedad. Así, teniendo en cuenta el cambio en la humedad específica del total de las partículas, se pueden considerar como fuentes aquellas regiones donde la evaporación total excede a la precipitación y como sumideros a la situación contraria, cuando la precipitación excede a la evaporación.

Con este propósito, en primer lugar se han caracterizado las fuentes climatológicas de humedad para el sistema ártico. Para ello, usando FLEXPART, se han seguido las trayectorias de las partículas atmosféricas desde la región ártica hacia atrás en el tiempo y analizado el valor de la evaporación menos precipitación. A través de este análisis se puede concluir que existen cuatro fuentes de humedad principales para la región, dos fuentes oceánicas: Atlántico Norte y Pacífico Norte, y dos continentales: Norte América y Siberia. Las fuentes

oceánicas están presentes a lo largo de todo el año, si bien su importancia es mayor en la época invernal, mientras que las fuentes continentales solo aparecen en verano, cuando las oceánicas pierden importancia, convirtiéndose en las fuentes principales para este periodo.

Para comprobar la efectividad de las fuentes detectadas en el transporte de humedad que genera precipitación sobre el Ártico, se ha realizado un análisis de las trayectorias de las partículas desde las fuentes hacia adelante en el tiempo y se ha analizado la humedad perdida sobre la región ártica. Así se ha encontrado que, en general, el transporte desde las fuentes hasta la región es más efectivo en los meses de verano y menos en los meses de invierno, coincidiendo estos resultados con trabajos previos que usan otras metodologías.

Tanto la evaporación de las propias fuentes, como la circulación desde ellas hacia la región ártica pueden afectar al transporte de humedad. Con el fin de investigar esta relación, se ha estudiado la correlación entre la evaporación sobre las fuentes con la contribución de cada una de ellas sobre la región ártica, así como de la contribución de cada fuente con los principales índices de teleconexión. En general no se ha encontrado una relación significativa entre la evaporación y la contribución de humedad y solo cierta relación con algunos de los patrones de teleconexión; como el patrón del Pacífico/Norte América o el patrón del Pacífico Oeste con la contribución desde la fuente pacífica y el patrón de Atlántico Este con la contribución atlántica.

Además de la caracterización climatológica de las fuentes de humedad, puede resultar de interés estudiar el transporte de humedad asociado a situaciones concretas, como pueden ser los años de mínima extensión de hielo, con el fin de analizar su influencia. Por este motivo en este trabajo se han analizado las principales fuentes de humedad para el sistema en los años 2007 y 2012 (aquellos que muestran una menor extensión en las últimas décadas), encontrándose cierta variación en la posición, intensidad y contribución de las mismas con respecto a la situación climatológica.

La relación entre la disminución de hielo ártico y el transporte de humedad también se ha analizado en este trabajo basándose en un par de relevantes publicaciones previas, las cuales asocian el deshielo ártico con un proceso radiativo, referente a cambios en la nubosidad, y un proceso hidrológico, referente a la descarga de los ríos; ambos asociados con un mayor

transporte de humedad hacia la región ártica. En este trabajo hemos establecido una relación entre los cambios en la evaporación y el deshielo, que sugiere una intrincada cadena de eventos relacionados con un aumento en la evaporación sobre distintas fuentes, una intensificación en el transporte de humedad desde ellas y un incremento en la descarga de los ríos o la cobertura nubosa en la región ártica.

Además de analizar el transporte hacia la región ártica, en este trabajo también se ha analizado el Ártico como “fuente” de humedad, con el fin de poder analizar las implicaciones que los actuales cambios en esta región pueden tener en otras zonas del planeta. Para este fin se han localizado los principales sumideros de humedad para las masas de aire que surgen desde este océano. En general la mayor parte de la humedad ártica afecta al propio sistema, sin embargo también se puede observar cierta influencia sobre Eurasia y Norte América. Con respecto a la variación estacional, la máxima contribución de humedad se produce en verano y otoño coincidiendo con los valores mínimos en la extensión de hielo.

La influencia del transporte de humedad desde el Ártico se ilustra también con el análisis del papel que el deshielo tiene en la precipitación en forma de nieve en Eurasia. A través de las observaciones de cobertura de nieve en 820 estaciones distribuidas a lo largo de Rusia, usando FLEXPART y con la ayuda de diversos parámetros de diagnósticos dinámicos, se ha analizado la influencia del deshielo sobre los mares de Barents y Kara en la precipitación sobre Siberia en los meses de octubre y noviembre. Se ha encontrado una intensificación de estos mares como fuentes de humedad, habiendo también aumentado su contribución sobre la región suroeste de Siberia para los años de mínima extensión de hielo.

Agradecimientos

En primer lugar me gustaría mostrar mi agradecimiento a mis directores Luis y Raquel por la oportunidad que me brindaron. Porque me han guiado a lo largo de todo el camino, porque han confiado en mí desde el principio y han conseguido que yo confiara un poco más en mi misma.

Agradecer, sin duda, a mis compañeros de laboratorio; los que todavía están y los que han ido pasando a lo largo de estos cuatro años: Rogert, Milica, Danica, Lucía, Aleksandar, Iago, Moha, Zeinab, Marni, Isa, Luana, Luisa y Motjaba. Cada uno de ellos me ha aportado algo distinto, me han convertido en experta en relaciones internacionales y han hecho que este tiempo haya pasado volando. Agradecer también a Orlando, porque siempre ha estado disponible para ayudarme en cualquier cosa que he necesitado, y al grupo EPhysLab al completo por haberme acogido todos estos años.

Me gustaría mostrar especialmente mi agradecimiento a Anita, porque su ayuda ha ido siempre más allá de lo académico. Por resolverme cada duda cuando lo he necesitado, por darme los mejores consejos y por todas las conversaciones que hemos tenido, las cuales me han hecho mejor en muchos aspectos.

No podría dejar de dar las gracias a mis padres, a mi hermana y a Simón, porque desde el primer momento me ha apoyado y han recorrido conmigo todo este camino. Porque a veces no ha sido fácil tener que aguantarme pero siempre lo han hecho con la mejor sus sonrisas.

Por ultimo me gustaría dar las gracias a mis niñas y el resto de amigos que han estado ahí todo este tiempo, que me han escuchado siempre que lo he necesitado y que sin duda han contribuido a que haya llegado hasta aquí.

AGRADECIMIENTOS

Este trabajo ha sido financiado por la Xunta de Galicia a través del Plan galego de investigación, innovación e crecemento 2011–2015 (Plan I2C) en colaboración con el campus internacional do Mar (PRE/2012/431), por el programa europeo ERAnet.RUS a través del proyecto ACPCA y por el Ministerio de Economía y Competitividad a través del proyecto EVOCAR (CGL2015-65141-R) el cual es cofinanciado por el Fondo Europeo de desarrollo regional (FEDER)

Lista de Figuras

Lista de Tablas

Lista de Acrónimos

AO Oscilación Ártica

BKS mares de Barents y Kara

CFSR Climate Forecast System Reanalysis

COSMO Consortium for Small-scale Modeling

CPC Climate Prediction Center

EA Patrón del Atlántico Este

EATL/WRUS Patrón de Atlántico Este/Oeste de Rusia

ECMWF Centro Europeo de Predicción a Medio Plazo

EP-NP Patrón de Pacífico Este-Pacífico Norte

ERL revista Environmental Research Letters

ESD revista Earth System Dynamics

GFS Sistema de Predicción Global

GLEAM Global Land surface Evaporation: the Amsterdam Methodology

LISTA DE ACRÓNIMOS

HadISST1 Conjunto de datos de hielo marino y temperatura del mar en superficie (SST) del centro Hadley en su versión 1.

JCR Journal Citation Reports

JGR revista Journal of Geophysical Research.

MDPI Multidisciplinary Digital Publishing Institute.

MERRA Modern Era Retrospective-Analysis for Research and Applications

NAO Oscilación del Atlántico Norte

NCEP Centro Nacional de Predicción Medioambiental

NPO Oscilación del Pacífico Norte

NSIDC National Snow and Sea Ice Data Center

OAFlux Objectively analyzed air–sea fluxes

PNA Patrón del Pacífico/Norte América

PT Transición del Pacífico

SCAND Patrón Escandinavo

SST Temperatura del mar en superficie.

SW-Siberia suroeste de Siberia.

TNH Patrón Tropical/ Hemisferio Norte

UTC Tiempo Universal Coordinado

WP Patrón del Pacífico Oeste

WRF Weather Research and Forecasting

1

Introducción: El Ártico ante el cambio climático

Debido a la amenaza del cambio climático, conocer la intensidad del ciclo hidrológico y sus variaciones en el tiempo es uno de los principales retos de este siglo. Resulta especialmente importante conocer los procesos que gobiernan la evaporación [Yu and Weller, 2007], el transporte de humedad en la atmósfera [Trenberth et al., 2003], y los efectos de estos procesos en el ciclo hidrológico [Bales, 2003], todo esto en el contexto del actual paradigma del cambio climático global. Dentro de esta situación, la región ártica representa una de las regiones más vulnerables, siendo los cambios experimentados en ella especialmente drásticos. Uno de los cambios más relevantes es el aumento de la temperatura superficial, el cual es de más del doble de la media global (fenómeno conocido como Amplificación Ártica) [Winton et al. 2006, Screen and Simmonds, 2010; Tang et al., 2014; Cohen et al., 2014]. Además el sistema también está sufriendo un descenso más que significativo en la extensión de hielo y cobertura de nieve [Tang et al. 2014;

IPCC, 2013]. Entre los diferentes factores que pueden influenciar los cambios observados en la región del Ártico, el ciclo hidrológico resulta de especial interés. La intensificación del transporte de humedad desde latitudes medias [Lucarini and Ragone, 2011; Zhang et al., 2012] así como el incremento de la evaporación local [Bintanja and Selten, 2014] resultan especialmente relevantes en el desarrollo de los procesos radiativos en la región ártica, que desembocan tanto en el aumento de temperatura como en el descenso de la cobertura de hielo. Además el ciclo hidrológico no solo está involucrado en los cambios observados en la región, sino que estos cambios a su vez afectan al transporte de humedad, produciendo un efecto en el clima tanto a nivel local como a mayor escala. Por ejemplo, la reducción en la cobertura de hielo y nieve ha sido relacionado con la ocurrencia de eventos meteorológicos extremos en el Hemisferio Norte [Francis and Vavrus, 2012; Tang et al., 2014]. En general, la señal climática originada en la región ártica a través de la reducción en la extensión de hielo marino puede propagarse hasta latitudes más bajas a través de distintos procesos como cambios en la trayectoria de las tormentas, cambios en las características de los jet streams o cambios en la configuración de las ondas planetarias [Cohen et al., 2014].

Teniendo en cuenta todo esto, resulta evidente la importancia que el estudio de la región ártica, y en concreto de su ciclo hidrológico, supone en el análisis de los cambios e implicaciones del actual cambio climático. A pesar del creciente interés que la región ártica ha suscitado en los últimos años, el transporte de humedad en la región no ha sido extensamente analizado hasta el momento y a día de hoy todavía no se dispone de un entendimiento completo de su implicación en el clima actual y futuro. Por este motivo en este trabajo se trata de ofrecer una ayuda a través de la caracterización del transporte de humedad hacia y desde el Ártico.

Existen diversas formas de caracterizar la región ártica. En este trabajo se utiliza la definición realizada por Roberts et al. [2010] según la cual el sistema ártico está formado por "la biosfera y geosfera al norte de la isoterma boreal media decadal de 10ºC de la superficie oceánica, el contorno de 0ºC del aire superficial que encierra el Polo Norte, y el límite sur del terreno que drena en el Alto Ártico" (Figura 1.1). Según esta definición dentro de la región ártica se incluyen: el propio océano Ártico y una parte del Atlántico y Pacífico norte, Groenlandia, Islandia, la mayor parte de la Península Escandinava y la parte más septentrional de Norte América y Rusia. Teniendo en cuenta esta definición, el Ártico incluye cuencas de ríos, glaciares, regiones oceánicas y continentales con características muy diversas. Sin embargo la mayor parte de su extensión la constituyen zonas oceánicas cuya principal característica es la presencia de hielo marino durante gran parte del año.

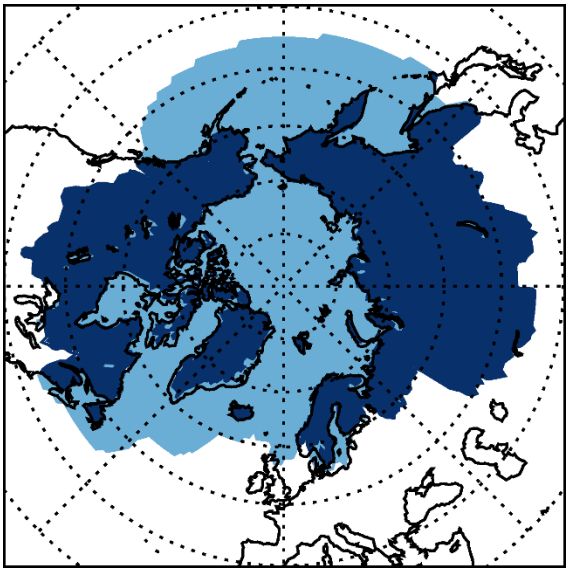

Figura 1.1. Extensión geográfica del sistema ártico como se ha empleado en este trabajo según la definición de Roberts et al. [2010]. En azul claro se representan las regiones oceánicas y en azul oscuro las regiones continentales que se incluyen en esta definición.

Como ya se ha mencionado, el sistema ártico representa una de las regiones más vulnerables al cambio climático, la cual ha sufrido cambios dramáticos en las últimas décadas [Comiso and Hall, 2014; Boisvert and Stroeve, 2015] y en la que se espera continúen durante los próximos años [Koenigk et al., 2013; Overland et al., 2014; Holland et al., 2006;

Smedsrud et al., 2008]. Uno de estos cambios es el fenómeno denominado Amplificación Ártica que consiste en un calentamiento más rápido de la región ártica con respecto al resto del hemisferio norte. Los factores por los que se ve afectado este fenómeno son diversos, encontrándose entre ellos el descenso del hielo marino [Screen and Simmonds, 2010], la cobertura nubosa y contenido de humedad [Graversen and Wang, 2009] o el transporte de calor hacia los polos [Yang et al., 2010], entre otros.

Con respecto al hielo marino en el Ártico, éste presenta un ciclo anual en su extensión muy claro, mostrando valores mínimos en el mes de septiembre y máximos en el mes de marzo. En los últimos años se han producido importantes descensos en su extensión, produciéndose mínimos históricos en ambas etapas del ciclo [Cavalieri and Parkinson, 2012; Polyakov et al., 2012]. Este descenso, que se ha visto acelerado en los últimos años [Comiso et al., 2008; Polyakov et al., 2012], es observable tanto a escala anual como estacional, siendo la tendencia más pronunciada en verano y otoño (cuando la extensión muestra su mínimo dentro del ciclo anual) [Cavalieri and Parkison, 2012]. Además esta disminución se ha producido en todas las regiones del océano Ártico, con la excepción del mar de Bering [Boisvert et al., 2015]. Pero no solo la extensión se ha visto reducida, también se ha producido un adelgazamiento de la capa de hielo [Lindsay and Zhang, 2005; Kwok and Rothrock, 2009], que a su vez produce un mayor derretimiento en verano [Lindsay et al., 2009] y afecta a la temporada de deshielo, que en los últimos años se ha estado alargando con una tendencia de cinco días por década aproximadamente [Stroeve et al., 2014].

Estos cambios observados en el hielo del Ártico tienen un efecto evidente en el albedo terrestre, disminuyéndolo de manera drástica y produciendo, a su vez, un aumento en la temperatura aún mayor del esperado. Todos los procesos descritos se encuentran mutuamente interrelacionados en un proceso de retroalimentación que favorece la aceleración del descenso de hielo, especialmente en septiembre. La figura 1.2 muestra de una manera esquemática cómo estos distintos factores se encuentran relacionados entre sí. Según este esquema y considerando las tendencias observadas, es esperable que la extensión de hielo siga disminuyendo a ritmo creciente en los próximos años, pudiendo llegar incluso a un escenario en el que el océano Ártico se encuentre libre de hielo en los meses estivales [Wang and Overland, 2009; Overland and Wang, 2013].

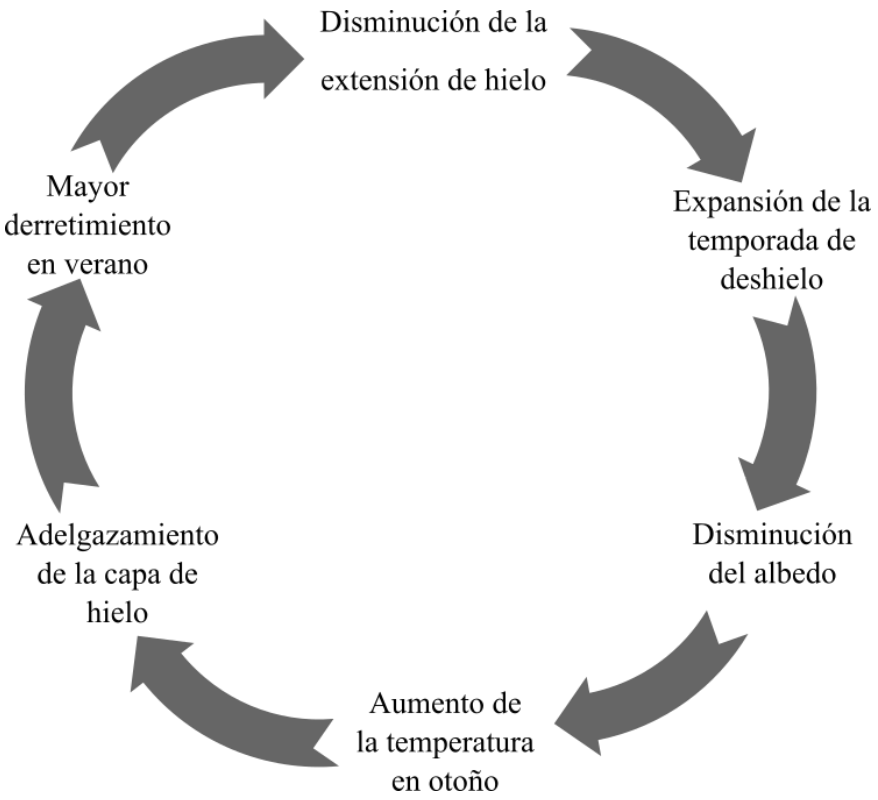

Figura 1.2. Relación y feedback entre los distintos cambios observados en el Ártico.

Teniendo en cuenta todos estos cambios observados sobre la región ártica y que sus diferentes subsistemas están interrelacionados entre sí, cabe esperar que éstos tengan un efecto más allá de lo local y que también afecten al clima global. Las consecuencias del deshielo ártico en el clima han sido ampliamente estudiadas en los últimos años [Overland and Wang, 2010; Honda et al., 2009; Singarayer et al., 2006, Strey et al., 2010], pudiéndose encontrar una revisión muy completa en el trabajo realizado por Vihma [2014]. Como ya se ha mencionado anteriormente, el descenso en la cobertura de hielo es una de las principales causas de la amplificación de las temperaturas observadas en el Ártico [Screen and Simmonds, 2010] pero también se ha observado un efecto del deshielo en la precipitación [Bintanja and Selten, 2014; Kopec et al., 2016], la cual se ve incrementada en la zonas árticas principalmente como consecuencia de la intensificación de la evaporación local.

Además de la evidente influencia del deshielo a nivel local, sus efectos también pueden ser observados a escala hemisférica. Así Overland and Wang [2010] han probado su influencia en los patrones de circulación atmosférica, encontrando una variación en la persistencia y variabilidad de la Oscilación Ártica y el dipolo ártico. Numerosos estudios también han

relacionado la disminución de hielo con fenómenos extremos en invierno [Cohen et al., 2014; Liu et al., 2012] o con el aumento en la precipitación en forma de nieve en Siberia [Liu et al., 2012; Park et al., 2013].

La humedad atmosférica presente en el Ártico tiene principalmente dos orígenes, la propia evaporación dentro del sistema y el transporte meridional desde latitudes más bajas, los cuales se han visto incrementados recientemente [Kapsch et al, 2013; Boisvert et al., 2015]. El aumento en el transporte de humedad ha sido tratado en diversos estudios recientes [eg. Kug et al., 2010; Kapsch et al., 2013] encontrándose dos posibles causas: un aumento en la evaporación en latitudes medias, un cambio en los patrones de circulación atmosférica, o una combinación de ambas [Gimeno et al., 2012; 2013]. Referente a los cambios en la circulación, numerosos trabajos señalan a un aumento en el número de ciclones que atraviesan la región ártica [Trigo, 2006; Sorteberg and Walsh, 2008; Sepp and Jaagus, 2011], produciendo un consecuente aumento en el transporte de humedad desde latitudes más bajas asociado a los mismos. Además las variaciones en el trasporte de humedad también se han relacionado con los principales patrones de teleconexión climática. Así, Jakobson and Vihma [2010] encontraron correlaciones positivas entre la Oscilación Ártica (AO) y el flujo meridional de humedad y el agua precipitable en primavera e invierno, mientras que Groves and Francis [2002] encontraron diferencias de hasta seis veces en el flujo de agua precipitable a través de la latitud 70ºN entre la fase positiva y negativa de AO en invierno, y de hasta dos veces en verano. Por otro lado Rogers et al. [2001] analizaron la relación entre la precipitación y la evaporación (P-E) con la Oscilación del Atlántico Norte (NAO), del Pacífico Norte (NPO) y de la AO encontrando correlaciones positivas con los tres patrones y siendo especialmente importante la influencia de NAO. Además de los patrones de teleconexión climática también se han encontrado influencias debidas a los jet streams [Kug et al., 2010], a los atmospheric rivers [Neff et al., 2014; Mundhenk et al., 2016; Gimeno et al., 2014] o las ondas planetarias [Liu and Barnes, 2015] en la disponibilidad de humedad en el Ártico.

Por otro la lado y referente a los cambios en la evaporación, Yu and Weller [2007] han observado un aumento en la evaporación oceánica en latitudes medias, siendo especialmente importante en los océanos Atlántico y Pacífico, existiendo por lo tanto una mayor disponibilidad de humedad para ser transportada por los mecanismos citados anteriormente. La evaporación local sobre la región ártica también ha sufrido cambios a causa del

deshielo. En el trabajo de Boisvert et al. [2015] se muestra cómo el flujo de humedad en el Ártico ha aumentado en la década 2003-2013, observándose una tendencia positiva sobre la mayor parte de la región oceánica a escala anual, con excepción del mar de Bering. Por otro lado Kopec et al. [2016] han encontrado un aumento en las fuentes locales en la precipitación sobre la región ártica.

La importancia de la cantidad de humedad presente en la atmósfera ártica radica en que ésta tiene una influencia directa en la transferencia radiativa, especialmente en la radiación de onda larga [Devasthale et al., 2011; Ohmura, 2001]. Además tiene un papel importante en los procesos de evaporación, formación nubosa y precipitación. Así los cambios en la humedad atmosférica en el Ártico afectarán a estos procesos, teniendo implicaciones en todo el sistema. En la figura 1.3 se muestra un esquema de las principales implicaciones de los cambios observados en la rama atmosférica del ciclo hidrológico.

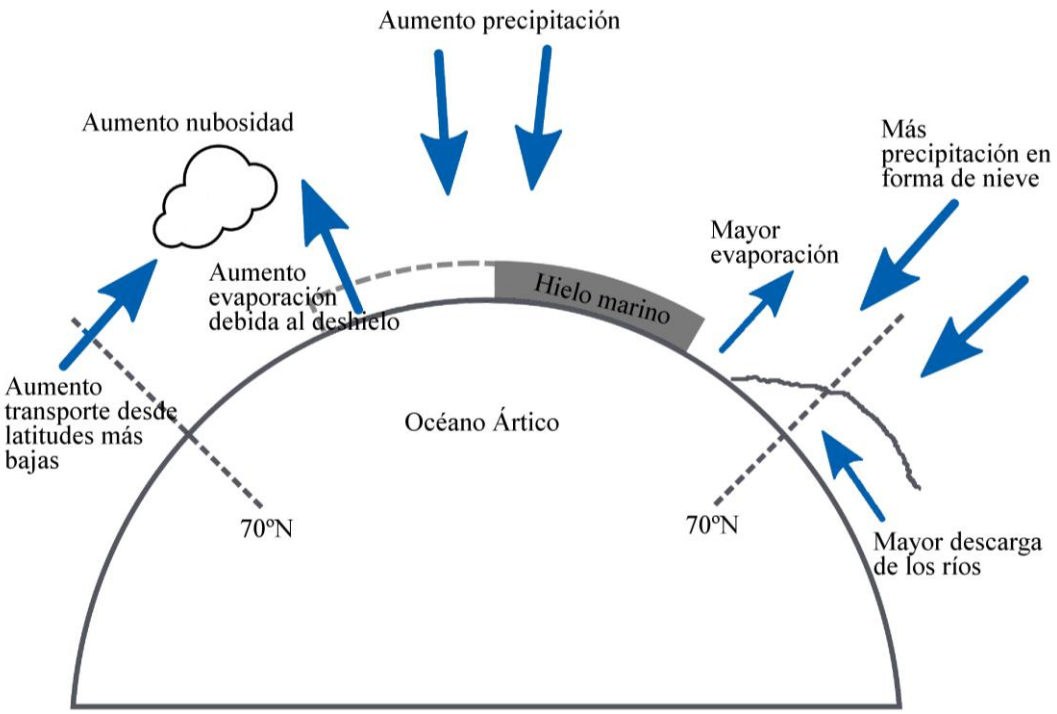

Figura 1.3. Esquema de los principales cambios referentes al ciclo hidrológico observados en el Ártico considerado como la región por encima de 70°N. Las flechas representan la dirección del flujo de humedad y la caja punteada en gris representa la disminución de hielo marino.

Los efectos de la nubosidad en la región ártica son diversos y varían según la época del año, la composición, fase o altura de la nube. La cobertura nubosa en el Ártico tiene un

ciclo anual muy marcado, siendo mayor en verano y otoño, y menor en invierno [Intrieri et al., 2002], pero con una presencia prácticamente constante a lo largo del año [Intrieri et al., 2002; Sedlar et al., 2011]. El papel más importante en el balance radiativo que ejerce la nubosidad en el Ártico es que retienen radiación de onda larga durante la mayor parte del año. Durante el invierno, la ausencia de radiación solar hace que las nubes creen un efecto invernadero al reflejar la radiación de onda larga saliente; efecto que se mantiene durante los meses estivales, a pesar de una presencia mayor de radiación solar (de onda corta), con la excepción del pleno verano, cuando la elevación del Sol es mayor y el hielo marino además se ha reducido [Shupe and Intrieri, 2004]. En los últimos años se ha observado también un aumento en la nubosidad en la región del Ártico, el cual se ha producido sobre todo en la cantidad de nubes bajas durante los meses de verano [Walsh et al., 2011]. Estos cambios en la cobertura nubosa se han asociado con los descensos en la extensión de hielo marino. Es el caso del trabajo de Kapsch et al. [2013] que han relacionado una mayor nubosidad en los meses de primavera con un descenso incrementado en la cobertura de hielo sobre el océano Ártico.

Otra de las variables que es fuente de cambios en el Ártico es la precipitación. La precipitación en esta región tiene su máximo entre los meses de julio y septiembre, y es mínima en primavera [Walsh et al., 1994]. Sus efectos son diversos y dependen de la su fase, tanto en forma de lluvia como de nieve, y de la región donde ésta se produzca. Sobre el océano Ártico, el efecto de la precipitación en forma de lluvia favorece la pérdida de hielo marino y disminuye el albedo [Screen and Simmonds, 2012; Parkinson and Comiso, 2013]. Sin embargo, en el caso de la precipitación en forma de nieve ésta aumenta el albedo, reduciendo el derretimiento en primavera y verano [Cheng et al., 2008] y favoreciendo el crecimiento del hielo mediante la transformación de nieve en hielo [Kawamura et al., 2001]. Además del efecto sobre el hielo marino, la precipitación también afecta a las regiones circundantes. En las zonas continentales la precipitación se acumula en forma de nieve durante los meses de invierno, constituyendo la única fuente en el balance de masa de los glaciares y las superficies heladas de la región [Dowdeswell et al., 1997], así como una fuente principal para la descarga de los principales ríos árticos al acumularse en las cuencas en los meses invernales [Zhang et al., 2012]. Así la precipitación invernal se convierte en una fuente de agua dulce para el océano durante los meses de verano, cuando se produce la fusión sobre las regiones continentales, teniendo efectos sobre él, sobre todo en

los meses de máxima descarga que tiene lugar entre abril y julio [Lammers et al., 2001]. En los últimos años algunos trabajos han mostrado un efecto de esta descarga en la pérdida de hielo marino [Bauch et al., 2013; Nghiem et al., 2014; Whitefield et al., 2015].

Según algunos estudios recientes existe un incremento en la precipitación sobre la región ártica [Min et al., 2008], el cual tendrá un efecto evidente en el ciclo hidrológico. Por ejemplo, Wu et al. [2005] han relacionado el reciente aumento observado en la descarga de los ríos en el Ártico [Peterson et al., 2002; McClelland et al., 2006] con un incremento en el aporte de humedad proveniente de latitudes bajas. Además, no solo la cantidad de precipitación ha aumentado sino que también ha cambiado la forma en la que ésta se produce. Debido al calentamiento global, parte de la precipitación que se producía en forma de nieve se produce ahora en forma de lluvia. Este cambio afecta a la cobertura de nieve, apareciendo una tendencia negativa en la mayor parte de la región ártica [Callaghan et al., 2011; Linton et al., 2014; Screen and Simmonds, 2012], con la excepción de algunas zonas de Eurasia [Zhang et al. 2011] y del norte de Canadá [Liston and Hiemstra, 2011], en las cuales su incremento se ha asociado con la pérdida de hielo marino [Liu et al. 2012; Park et al., 2013].

Además de la influencia en el clima los cambios observados en la región ártica tienen un efecto observado sobre los ecosistemas que la rodean. En los últimos años diversos estudios han analizado la influencia de estos cambios en la región [Bring et al., 2016; Carmack et al., 2016; Wrona et al., 2006] y sus implicaciones sobre la ecología [Post et al., 2013; Wrona et al., 2006], como son cambios en la vegetación [Bhatt et al., 2010], o implicaciones sobre las poblaciones humanas árticas [Ford, 2009] o en la industria [Instanes et al., 2016].

En la figura 1.4 se sintetizan algunos impactos que los cambios observados en la atmósfera ártica producen en otros componentes del sistema como son la hidrología, la ecología, el océano y los recursos en la región. El estudio de la interrelación entre estos componentes resulta muy importante a la hora de analizar el cambio climático [Bring et al., 2016]. Esta figura no debe considerarse como un análisis detallado, sino que su función principal es mostrar la influencia de los cambios en la rama atmosférica del ciclo hidrológico en el Ártico. Por ejemplo, y con respecto a la hidrología, los cambios observados en la temperatura atmosférica afectarán a la temporada de nieve, mientras que los cambios en la cantidad de humedad tendrán un efecto en la descarga de los ríos. Ambas variables jugarán un papel importante en los regímenes de lluvias. Los cambios en la precipitación y en la temperatura

tendrán un efecto también sobre los recursos de la región afectando a la industria, debido a la mayor intensidad de las precipitaciones, o sobre la energía hidroeléctrica o provocando mayores inundaciones. Sobre los océanos el aumento de la temperatura atmosférica implica modificaciones en la cubierta de hielo, mientras que la humedad creciente afecta al aumento del balance de P-E y los cambios en la nubosidad tendrán un efecto en la producción primaria debido a las variaciones en la radiación solar disponible. Estos cambios en la radiación también tendrán efectos ecológicos debido a su implicación en los procesos fotosintéticos. En referencia a los factores ecológicos los cambios en la nubosidad y temperatura afectarán a los incendios forestales debido a la mayor frecuencia de las tormentas eléctricas, y el ciclo del carbono también se ve influenciado por el aumento de la temperatura y humedad atmosféricos.

Queda evidenciado pues que la rama atmosférica del ciclo hidrológico en el Ártico juega un papel clave en el comportamiento del sistema ártico y de su influencia en el clima, además de que la humedad contenida en la región y sus cambios resultan de relevancia global. Varios estudios han tratado de analizar el ciclo hidrológico en la región ártica desde la segunda mitad del siglo XX [ej. Mosby, 1962; Aagaard and Greisman, 1975]. A pesar de que algunos de los primeros trabajos relacionados con el tema ya trataban de estimar el transporte de humedad hacia el Polo Norte [Palmen and Vuorela, 1963; Starr et al., 1965], la primera estimación del balance de humedad en el Ártico fue realizada por Oort [1975] y recientemente Vihma et al. [2016] han realizado una completa revisión sobre el papel atmosférico en el ciclo hidrológico en el Ártico, los cambios observados y sus impactos. Sin embargo, y a pesar su importancia, el papel de los procesos hidrológicos atmosféricos en el Ártico está lejos de ser bien entendido.

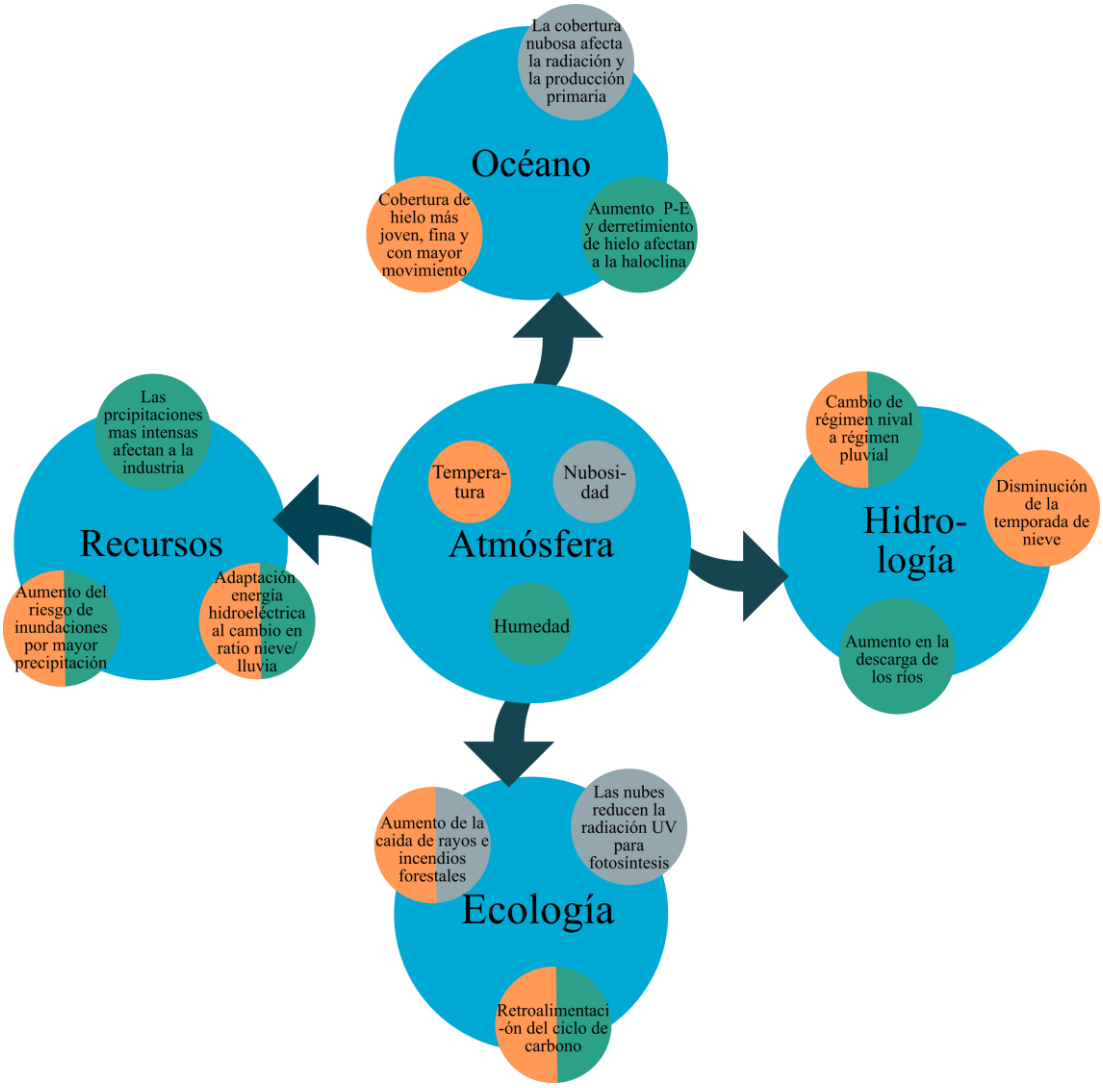

Figura 1.4. Ejemplo de los posibles impactos de los cambios atmosféricos de la región ártica en el océano, la hidrología, la ecología y los recursos, basado en la figura 7 de Vihma et al. [2016].

2

Objetivos

En la presente sección se trata de establecer los distintos objetivos a alcanzar en el desarrollo de este trabajo. Con el fin de establecer las características del transporte de humedad en la región ártica, se ha realizado un análisis climatológico tanto de las fuentes como de los sumideros para la región. Los objetivos concretos se enumeran a continuación:

1) Establecer una caracterización completa de las fuentes de humedad para la región ártica y del aporte de cada una de ellas al propio Ártico mediante una aproximación lagrangiana.

    a) Localizar las principales fuentes de humedad climatológicas de la región ártica.

    b) Estudiar la variabilidad de cada una de las fuentes principales de humedad a lo largo del año.

    c) Analizar la contribución a la precipitación sobre el sistema Ártico desde cada una de las fuentes y estudiar su variación estacional.

d) Analizar la posible influencia de la evaporación sobre las fuentes y de los principales patrones de teleconexión en el transporte de humedad desde cada una de ellas.

Este objetivo se aborda en el primero de los artículos que componen el corpus de esta tesis cuyo título es "Moisture transport into the Arctic: Source-receptor relationship and the role of atmospheric circulation" publicada en el año 2016 en la revista Journal of Geophysical Research: Atmosphere.

2) Analizar el transporte anómalo de humedad hacia la región ártica para los años que muestran valores mínimos en la extensión de hielo: 2007 y 2012.

   a) Analizar los cambios en las fuentes de humedad árticas para ambos años, tanto en extensión como en intensidad, con respecto la media climatológica.

   b) Estudiar la contribución de humedad a la precipitación desde cada una de las fuentes para ambos años y sus anomalías.

   c) Comparar el transporte de humedad a la región entre los años de máxima y mínima extensión de hielo.

   d) Analizar la contribución de humedad sobre las cuencas de los principales ríos árticos para los años de mínima extensión de hielo.

Este objetivo se aborda en el artículo "Extreme Sea Ice Loss over the Arctic: An Analysis Based on Anomalous Moisture Transport", el cual se corresponde con el segundo de los artículos que componen esta tesis y que ha sido publicado en 2017 en la revista Atmosphere.

3) Analizar el papel del transporte anómalo de humedad en algunos mecanismos hidrológicos y radiativos ligados al deshielo ártico.

   Este análisis se basa en dos publicaciones previas que sugieren un impacto de los cambios en el transporte de humedad en el deshielo ártico:

   - Mecanismo hidrológico: Zhang et al. [2012] sugieren que el transporte de humedad hacia las cuencas de los principales ríos árticos del norte de

Eurasia se ha incrementado, aumentando la descarga de estos ríos y con posibles implicaciones para el deshielo.

- Mecanismo radiativo: Kapsch et al. [2013] sugieren una relación entre un aumento en la cobertura nubosa asociado a un mayor transporte en primavera y el retroceso del hielo marino en verano sobre la región oceánica al norte de Siberia, donde se encuentran las mayores tendencias en la disminución de hielo marino en septiembre para el periodo 1979-2010.

Este objetivo se trata en detalle en el tercer artículo, que compone el cuerpo de esta tesis, cuyo título es "Atmospheric moisture transport: the bridge between ocean evaporation and Arctic ice melting", publicado en la revista Earth System Dynamics en el año 2015.

4) Analizar el transporte de humedad con origen en el océano Ártico determinando cuáles son las regiones que reciben una mayor cantidad de humedad procedente de este océano.

   a) Localizar geográficamente aquellas zonas que reciben un mayor aporte de humedad desde el océano Ártico. El análisis se realiza tanto para el Ártico en general como para cada una de las 14 regiones en las que se divide el océano Ártico.

   b) Analizar la variación estacional de los sumideros de la humedad.

   c) Estudiar la variabilidad interanual en la cantidad de humedad total aportada por cada región.

Este objetivo se aborda en el artículo "Moisture transport from the Arctic: A characterization based on a lagrangian perspective" enviado a la revista Polar Research, el cual forma parte del compendio de publicaciones que conforman esta tesis.

5) Analizar algunos de los cambios observados recientemente en la cobertura de nieve en Eurasia ligados a cambios en la cobertura de hielo en el océano Ártico.

   a) Analizar la influencia del deshielo en la cobertura de nieve en Eurasia en los meses de octubre y noviembre.

b) Establecer la diferencia del aporte de humedad sobre Eurasia, desde los mares de Barents y Kara, considerando los años con mayor y menor extensión de hielo sobre estos dos mares.

c) Comparar los resultados obtenidos con datos reales de cobertura de nieve.

d) Analizar los cambios en la captación de humedad sobre los mares de Barents y Kara según la cobertura de hielo marina sobre ellos.

Este objetivo es analizado en el quinto y último artículo de los que componen esta tesis y que lleva por título es “Arctic moisture source for Eurasian snow cover variations in autumn” publicado en el año 2015 en la revista Environmental Research Letters.

3

Metodología

3.1. Breve reseña sobre el modelo lagrangiano FLEXPART

FLEXPART es un modelo lagrangiano de dispersión de partículas inicialmente desarrollado para el estudio de la dispersión de contaminantes por Stohl et al. [1998] y posteriormente adaptado hasta convertirse en un una herramienta comprehensiva para el análisis y modelización del transporte atmosférico.

FLEXPART evoluciona desde el modelo de trayectorias FLEXTRA, el cual fue descrito y validado por Stohl et al. [1995], Baumann and Stohl [1997] y Stohl et al. [1998]. Desde su primera versión ha sufrido distintos cambios, entre ellos se ha añadido un código para la deposición (versión 2) [Stohl et al., 1998], se ha desarrollado una corrección de densidad (versión 3) [Stohl and Thomson, 1999], se ha introducido un diseño convectivo (versión 4) [Seibert et al., 2001], y así sucesivas implementaciones hasta llegar a la versión actual.

En estos momentos FLEXPART se encuentra en su versión 9, encontrándose su código fuente (desde su desarrollo inicial) disponible de manera gratuita bajo la Licencia Pública General de GNU Versión 3. A día de hoy son numerosos los grupos de investigación de distintos países que son usuarios del modelo, el cual está escrito en un código estándar de Fortran 95 y ha sido probado con varios compiladores en distintos sistemas operativos.

Una información más detallada acerca de FLEXPART se puede encontrar en la nota técnica de la versión 6.2 [Stohl et al., 2005] o en la página web https://www.flex-part.eu/wiki/FpDownloads.

3.1.1. Consideraciones físicas y computacionales

FLEXPART es un modelo off-line que usa datos meteorológicos del Centro Europeo de Predicción a Medio Plazo (ECMWF), aunque también puede ser empleado con datos del Sistema de Predicción Global (GFS) del Centro Nacional de Predicción Medioambiental (NCEP), o de otros modelos de mesoescala (e.g. WRF o COSMO) con alguna mayor dificultad.

El modelo inicialmente necesita de una serie de datos para poder ser ejecutado:

- Datos tridimensionales: componente horizontal y vertical del viento, temperatura y humedad específica.

- Datos bidimensionales: presión en superficie, cobertura nubosa total, componentes horizontales del viento a 10 metros, temperatura a 2 metros, temperatura del punto de rocío, precipitación convectiva y a larga escala, flujo de calor sensible, tensión en superficie norte/sur y este/oeste, topografía, máscara tierra-mar y desviación estándar subgrid de la topografía.

Además el modelo cuenta con una serie de parametrizaciones, como parámetros para la capa límite atmosférica (el flujo de calor o su altura), parametrizaciones de los movimientos turbulentos para las componentes del viento basados en la ecuación de Langevin, una parametrización de las fluctuaciones del viento basado en diversos parámetros de la capa límite [Hanna, 1982] con una modificación referente a la componente vertical [Ryall and Maryon, 1997], una aproximación empírica para las fluctuaciones de la velocidad del viento a mesoescala, o la parametrización de transporte convectivo, entre otras.

3.1.2. Modos forward y backward en el tiempo

El modelo FLEXPART computa las trayectorias de grandes cantidades de partículas, aproximadamente 2 millones en este trabajo, para describir el transporte y la difusión de los trazadores en la atmósfera.

El modelo puede ser ejecutado en dos formas distintas: i) las partículas pueden ser liberadas desde las zonas fuente y seguidas hacia adelante en el tiempo (modo forward) con el fin de analizar el destino de las partículas y los cambios a lo largo de las trayectorias, ii) además de este método, las partículas también pueden ser seguidas hacia atrás en el tiempo (modo backward) y en este caso las trayectorias describen el origen desde una determinada región, es decir, sirve para localizar las fuentes de las partículas. Este último modo es más eficiente a la hora de establecer relaciones fuente-receptor.

3.2. FLEXPART como herramienta para el transporte de humedad

La metodología de este trabajo está principalmente basada en el uso del modelo FLEXPART con el fin de analizar el transporte de humedad entre fuentes y sumideros en la región ártica.

Con este propósito el modelo es alimentado con datos del reanálisis de ERA-Interim, actual reanálisis atmosférico del Centro Europeo de Predicción a Medio Plazo (ECMWF) y que presenta algunas mejoras con respecto a su versión anterior, ERA-40, como una mayor resolución y cambios físicos, el uso de la asimilación de datos en cuatro dimensiones, y otros cambios diversos en la metodología del análisis [Trenberth et al., 2011], lo que supone un aumento en la calidad de predicción [Tavolato y Isaksen, 2011]. Este reanálisis atmosférico supone en general una mejor reproducción del ciclo hidrológico y del balance hídrico que otros reanálisis, como son los productos del Modern Era Retrospective Analysis for Research and Applications (MERRA) y del Climate Forecast System Reanalysis (CFSR) [Trenberth et al., 2011; Lorenz and Kunstmann, 2012]. Además ha sido validado por Jakobson et al. [2012] sobre el océano Ártico central, obteniendo los mejores resultados en comparación con el resto de reanálisis analizados. Así pues, utilizando datos de ERA-Interim de entrada en el modelo FLEXPART, las partículas son advectadas según la ecuación de movimiento:

$$\frac{dx}{dt} = v[x(t)] \qquad (3.1)$$

donde t representa el tiempo, x es el vector posición de la partícula y v es el vector del viento (que está compuesto por el viento en la escala de la rejilla, las fluctuaciones turbulentas y las fluctuaciones a mesoescala). Además los cambios en las características de las partículas son analizados a lo largo de las trayectorias. Para cada partícula se almacenan cada 6 horas (00, 06, 12, 18 UTC) las variables descritas en la tabla 3.1.

Tabla 3.1. Variables de salida del modelo lagrangiano de dispersión de partículas FLEXPART.

Variable	Símbolo	Unidad
Latitud	lat	
Longitud	lon	
Altura	H	m
Altura topográfica	TH	m
Vorticidad potencial	PV	10-6(m2K/skg)
Humedad específica	q	g/kg
Densidad del aire	ρ	kg/m3
Altura de mezcla	hmixi	m
Temperatura	T	K

Los cambios de humedad sufridos por cada partícula durante un cierto intervalo de tiempo son el resultado neto de la evaporación y la precipitación sufrida por ella. De esta manera, para cada una de las partículas consideradas se puede establecer la siguiente relación:

$$e - p = m\frac{dq}{dt} \qquad (3.2)$$

donde e y p representan la evaporación y precipitación respectivamente, m es la masa de la partícula, q representa la humedad específica y t el tiempo. De este modo las pérdidas de

humedad implicarán valores de dq/dt negativos y puede asimilarse directamente en la cantidad de precipitación, mientras que las ganancias se corresponden con valores positivos de dq/dt debidas a la incorporación de la evaporación local [James et al., 2004]. La figura 3.1 muestra una representación esquemática de los posibles cambios experimentados en la humedad específica de una partícula a lo largo de su trayectoria.

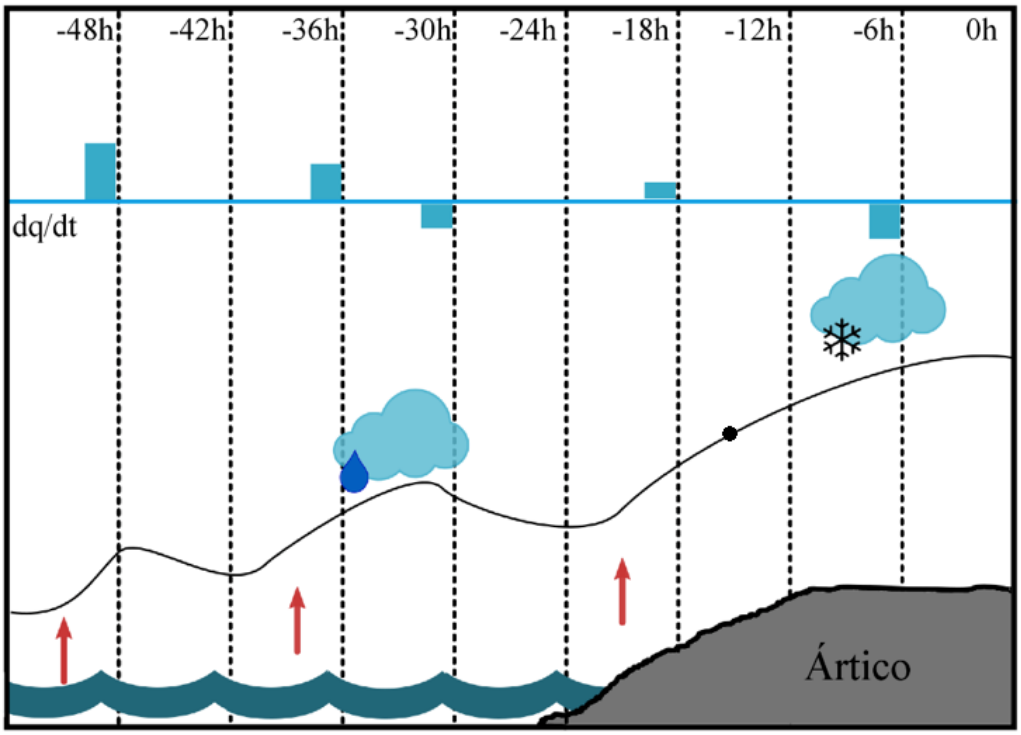

Figura 3.1. Representación esquemática de las variaciones en la humedad que sufre una partícula durante las primeras 54 horas de su trayectoria backward desde la región ártica. La línea sólida negra representa la trayectoria de la partícula y las barras azules representan las variaciones en la humedad específica. Las flechas representan las zonas en la que se produce un aumento en la humedad de la partícula. Figura adaptada de Sodemann et al. [2008]

3.2.1. Localización geográfica de las fuentes y sumideros de humedad

El modelo lagrangiano FLEXPART, por lo tanto, nos permite analizar las variaciones en la humedad específica de las partículas a lo largo de las trayectorias y ver dónde éstas ganan

o pierden humedad. Esto representa la base del presente trabajo, que tratará de analizar el transporte de humedad desde y hacia el Ártico.

Para ello se utilizan las salidas del modelo ejecutado en modo backward considerando un dominio global y alimentado con datos de ERA-Interim. La masa atmosférica completa es divida en aproximadamente 2 millones de partículas homogéneamente distribuidas. Estas partículas son advectadas por el modelo siguiendo las trayectorias del viento y para cada una de ellas se almacenan los datos que se reflejan en la tabla 3.1. A partir de estas salidas globales es posible seleccionar distintas regiones de interés y computar (e-p) para las partículas que salen o llegan a ellas en un determinado momento. Es importante resaltar que el número final de partículas consideradas en cada estudio dependerá de la región seleccionada.

Una vez delimitada la zona de estudio, las trayectorias de las partículas son analizadas durante un periodo de tiempo determinado. En el presente trabajo se consideran periodos de 33 años y de 35 años (1980-2012 y 1980-2015, respectivamente). Así a lo largo del tiempo las partículas que cada día llegan o salen de una región pueden ser seguidos hacia atrás (backward) o hacia adelante (forward) en el tiempo. Para determinar tanto fuentes como sumideros de humedad, el seguimiento de las partículas se limita a 10 días, ya que este el tiempo de residencia medio del vapor de agua en la atmósfera [Numaguti, 1999] y para el cual las trayectorias pueden ser consideradas relativamente precisas [Stohl et al., 2005].

Con el fin de localizar geográficamente las zonas donde se producen las mayores pérdidas o ganancias de humedad, para cada elemento de grid se considera el volumen total de la columna atmosférica sobre él y se suma la contribución diaria de cada una de las partículas que la atraviesa. Así podemos calcular el flujo de agua dulce en superficie (E-P) para cada elemento de grid de tamaño A:

$$E - P = \frac{\sum_{k=1}^{K}(e - p)}{A} \qquad (3.3)$$

siendo K el número total de partículas en la columna atmosférica.

Así pues, se obtiene, para cada día del periodo analizado la distribución geográfica de las pérdidas y ganancias de humedad durante los 10 días en los cuales se siguen las trayectorias

de las partículas. Posteriormente el valor de (E-P) es integrado para estos 10 días de transporte y promediado sobre todo el periodo de estudio. En el presente trabajo para el análisis de las fuentes de humedad se ha utilizado el periodo 1980-2012 y para el de los sumideros de 1980-2015.

3.3. Ventajas de un análisis lagrangiano y la visión euleriana como alternativa.

Las técnicas lagrangianas recientemente desarrolladas son una de las principales herramientas en el estudio del transporte de humedad. Sin embargo numerosas metodologías diferentes han sido empleadas también con este fin en los últimos años [Gimeno et al., 2012]. Para el estudio del transporte de humedad en el Ártico, la mayoría de los estudios hacen uso de tres métodos: modelos analíticos o de cajas, trazadores físicos y trazadores numéricos de vapor de agua. Los modelos de cajas permiten la identificación de la entrada y salida de humedad a través de límites laterales, sin embargo no ofrecen información sobre los procesos que tienen lugar dentro de la propia caja. En el caso de los trazadores físicos, estos se basan en el uso de isótopos y son especialmente útiles para la validación, ya que utiliza medidas físicas, sin embargo su uso depende de la fuerza de la señal isotópica. Por último, dentro de los trazadores numéricos podemos distinguir entre los modelos lagrangianos y los eulerianos. A diferencia de los modelos lagrangianos, que permite el seguimiento de los elementos de un fluido en el espacio y en el tiempo, los modelos eulerianos se centran en regiones específicas del espacio a través de las cuales el fluido pasa a medida que transcurre el tiempo. Esta última metodología es ampliamente utilizada debido a su simplicidad, sin embargo, con su uso no es fácil establecer la ligazón entre la precipitación que se produce en una determinada área y la región en la que esa humedad fue evaporada previamente.

A pesar de que con cada una de las metodologías mencionadas se ofrece información útil referente al transporte de humedad, la habilidad para establecer la relación entre fuentes y sumideros es la principal ventaja de los métodos lagrangianos y es el motivo por el que ha sido elegido para el desarrollo del presente trabajo. En el trabajo de Gimeno et al. [2012] se detalla la comparación entre las distintas metodologías mencionadas y se resumen en las tablas 3.2 y 3.3 las principales ventajas y desventajas de cada una de ellas.

Tabla 3.2. Resumen de las principales ventajas y desventajas de los modelos analíticos o de cajas y de los trazadores físicos de vapor de agua. Adaptada de Gimeno et al. [2012].

Tipo	Ventajas	Desventajas	Referencias (no exhaustivas)
Modelos Analítcos o de cajas	- Simplicidad, ya que necesitan de pocos parámetros	- Desprecia procesos de frontera	Budyko [1974] Brubaker et al. [1993] Eltahir and Bras [1994] Burde and Zangvil [2001a, 2001b] Dominguez et al. [2006]
Trazadores físicos de vapor de agua	- Simplicidad - Cobertura global - Incluye procesos verticales - Datos de entrada de reanálisis (con una alta resolución espaciotemporal) - Permite la combinación de modelos climático globales y modelos lagrangianos Rayleigh	- Sensibilidad de la señal isotópica - Tiempo de cálculo - Disponibilidad de datos para la validación - No considera convección y evaporación del agua de lluvia	Gat and Carmi [1970] Salati et al. [1979] Rozanski et al. [1982] Coplen et al. [2008]

Tabla 3.3. Resumen de las principales ventajas y desventajas de las metodologías que emplean trazadores numéricos de vapor de agua para el estudio del transporte de humedad. Adaptada de Gimeno et al. [2012].

Tipo		Ventajas	Desventajas	Referencias (no exhaustivas)
Trazadores numéricos de vapor de agua	**Eulerianos**	- Procesos atmosféricos detallados - Circulación atmosférica realista	- Dependen del sesgo del modelo - Se necesita forzamiento global - Pobre representación de los parámetros del ciclo hidrológico en escalas de tiempo cortas - No incluye las fuente de humedad remotas de una región	Benton and Estoque [1954] Starr and Peixoto [1958] Peixoto and Oort [1982] Joussaume et al. [1984] Koster et al. [1986] Bosilovich and Schubert [2002]
	Lagrangianos	- Alta resolución espacial en el diagnóstico de las fuentes de humedad - Interpretación cuantitativa del origen de humedad - No están limitados por un dominio específico en modelos climáticos regionales - Permiten establecer la relación fuente-sumidero de forma sencilla - El flujo de agua dulce desde una región puede ser trazado en el tiempo hacia delante o hacia atrás - Seguimiento realista de las parcelas de aire - Computacionalmente eficientes - Ofrece mayor información acerca de los campos de velocidad que las descripciones eulerianas -Permite el uso paralelo de información euleriana	- Sensibilidad computacional del flujo de humedad en periodos cortos de tiempo o regiones pequeñas - Los métodos simples no proporcionan un diagnóstico de los flujos de humedad en superficie - Sobreestimación (subestimación) de los flujos en superficie si se siguen masas de aire seco (frío) - La tasa de evaporación está basada en cálculos en lugar de en observaciones en algunos métodos - Evaporación y precipitación no son fácilmente separables en algunos métodos - El movimiento y la extracción de humedad no depende de las tendencias físicas incluídas en los datos de reanálisis	D'Abreton and Tyson [1995] Wernli [1997] Massacand et al. [1998] Dirmeyer and Brubaker [1999] Brubaker et al. [2001] Dirmeyer and Brubaker [2006] Stohl and James [2004, 2005]

A pesar de que la metodología principal seguida en este trabajo es una aproximación lagrangiana basada en el modelo de dispersión de partículas FLEXPART, en algunos casos será de utilidad el uso de una visión euleriana. Según una perspectiva euleriana el flujo de humedad en superficie aparece representado por la siguiente ecuación:

$$E - P = \frac{\partial \omega}{\partial t} + \vec{\nabla}\theta \qquad (3.4)$$

siendo ω el agua precipitable y θ el flujo de humedad integrado en la vertical representado por la siguiente ecuación:

$$\theta = \frac{1}{g}\int_0^{p_s} q\vec{v}dp \qquad (3.5)$$

donde g es la aceleración de la gravedad, p y p_s son la presión y presión en superficie respectivamente y $\vec{v}$ es el vector horizontal del viento.

Para escalas de tiempo muy largas la variación de agua precipitable puede ser despreciable, por lo tanto el flujo de agua en superficie puede ser directamente identificado con la divergencia del flujo de humedad integrado en la vertical [Trenberth and Guillemot, 1998].

En este trabajo, con el fin de analizar la divergencia de este campo se utiliza los datos de ERA-Interim correspondientes al flujo de humedad integrado en la vertical. De esta forma es posible asociar las zonas evaporativas con aquellas que presentan una divergencia en el flujo y las zonas precipitantes como las que muestran convergencia. Es importante destacar que, si bien aportan una segunda visión del flujo de humedad en la zona, los resultados obtenidos mediante esta aproximación no pueden ser directamente comparados con los obtenidos a través de la aproximación lagrangiana.

3.4. Datos suplementarios

Como ya se ha mencionado con anterioridad, el modelo FLEXPART está alimentado por datos del reanálisis ERA-Interim, entre los que cabe destacar los datos de viento y humedad específica. Sin embargo en el desarrollo del trabajo se hacen necesarios otro tipo de datos con el fin de completar los diferentes análisis. A continuación se enumeran los distintos datos empleados con este fin y cuál es su utilidad concreta dentro del trabajo.

- Datos de evaporación:

  En este trabajo se trata de analizar el transporte de humedad hacia el Ártico y estudiar los posibles cambios producidos en él en los últimos años. Los cambios en el transporte de humedad pueden tener distintas causas, entre ellas se encuentran los cambios en la evaporación. Así resultará de especial interés analizar cómo ha sido la evaporación sobre las fuentes de humedad localizadas y analizar su variación a lo largo de los años.

  Para este fin se utilizarán dos tipos de datos de evaporación en función de si ésta ocurre sobre los océanos (evaporación oceánica) o sobre los continentes (evaporación continental).

  - Evaporación oceánica: se emplean datos correspondientes al proyecto OAFlux [Yu, 2007]. Este proyecto tiene como objetivo proporcionar un análisis global multidecadal de los flujos de calor atmósfera-océano, de los flujos de agua dulce (evaporación) y del momento para su uso en estudios de recursos energéticos globales, del ciclo del agua, de la circulación atmosférica y oceánica y del clima [ver Yu et al., 2008]. Los datos se encuentran disponibles con una resolución de 1° x 1° en latitud y longitud a escala diaria para el período 1985-2016. Además dispone de los datos en escala mensual para el periodo 1958-2016 con resolución 0.25° x 0.25°. Los datos de OAFlux se pueden encontrar en la dirección web http://oaflux.whoi.edu/data.html.

  - Evaporación continental: se emplean datos de GLEAM (Global Land surface Evaporation: the Amsterdam Methodology) que utiliza datos derivados

de satélite para realizar una estimación espacial coherente del flujo evaporativo sobre regiones continentales. Los datos se encuentran disponibles en una resolución espacial de 0.25° x 0.25°, para el periodo 1980-2014, con resolución diaria. Para mayores detalles se puede consultar Miralles et al. [2011] o la página web http://www.gleam.eu/.

Datos de hielo marino:

Debido a que el presente trabajo trata de relacionar las variaciones en el transporte de humedad con la cobertura de hielo marino resulta necesario el uso de datos referentes a este campo. Los datos correspondientes a la extensión de hielo utilizados provienen de dos fuentes distintas.

- Datos basados en el conjunto de datos de hielo marino y temperatura del mar en superficie (SST) del centro Hadley en su versión 1 (HadISST1). HadISST1, en colaboración con un grupo de expertos internacionales, trata de producir un conjunto de datos homogéneos de extensión de hielo marino a través de la manipulación de los registros existentes. Trata de ofrecer un conjunto autoconsistente de datos observados de concentración de hielo marino. HadISST1 ofrece buenos registros del cambio en la extensión de hielo marino a lo largo del último siglo para el hemisferio norte. Información detallada se puede encontrar en Rayner et al. [2003].

- Datos mensuales de la extensión de hielo marino procedentes del National Snow and Sea Ice Data Center (NSIDC) mediante el conjunto de datos Sea ice Index versión 2 [Fetterer et al., 2016]. La estimación de la extensión de hielo está basada en datos de satélite y ofrece datos actualizados tanto de extensión como de concentración de hielo desde noviembre de 1978 hasta el presente con una resolución de rejilla de 25 kilómetros. Para mayor información consultar la página web del NSIDC https://nsidc.org/data/docs/noaa/g02135_seaice_index/#monthly_extent_image.

- Datos de cobertura de nieve:

  Otro de los objetivos del presente trabajo es analizar la influencia de los cambios en el transporte de humedad sobre zonas continentales. Uno de los impactos que puede tener los cambios en el transporte desde el Ártico son modificaciones en la precipitación en forma de nieve.

  Los datos de cobertura de nieve utilizados se corresponden con las observaciones regulares llevadas a cabo en las estaciones meteorológicas rusas desde 1882. Estos datos están archivados en el Instituto Ruso de Información Hidrometeorológica [Sherstyukov et al., 2007]. En este trabajo se emplea la información correspondiente a la profundidad de nieve diaria obtenida de una total de 820 estaciones meteorológicas distribuidas a través del territorio ruso. A pesar de que las estaciones se encuentran dispersas a lo largo del territorio su distribución no es del todo homogénea teniendo una mayor densidad de estaciones en la parte sur y oeste.

- Otros datos de ERA-Interim:

  Además de los datos comentados se utilizan en este trabajos los siguientes datos para el diagnóstico de la circulación atmosférica provenientes de ERA-Interim: omega (velocidad vertical del viento) en 700 hPa, viento en 700 hPa, presión media a nivel del mar, altura geopotencial en 500 hPa, transporte de vapor de agua integrado, precipitación en forma de nieve, temperatura a 2 m.

En la tabla 3.4 aparece un resumen de los principales datos suplementarios empleados.

Tabla 3.4. Resumen de los principales datos complementarios utilizados en la realización de la tesis.

Datos		Resolución	Fuente
Evaporación	**Oceánica**	0.25°×0.25° en escala diaria para el periodo 1958-2016 1°×1° en escala mensual para el periodo 1985-2016	OAFlux Project http://oaflux.whoi.edu/
	Continental	0.25°×0.25° en escala diaria para el periodo 1980-2014.	Global Land Evaporation Amsterdam Mode (GLEAM) http://www.gleam.eu/
Hielo marino	**HadISST1**	1°×1° en escala mensual desde 1871	Met Office Hadley Centre observations datasets http://www.metoffice.gov.uk/hadobs/hadisst/data/download.html
	NSIDC	Datos diarios y mensuales desde 1978 actualizados diariamente con resolución espacial de 25 km.	National Snow and Sea Ice Data Centre. https://nsidc.org/data/docs/noaa/g02135_seaice_index/
Cobertura de nieve		Datos diarios desde 1965 de 820 estaciones meteorológicas distribuidas a la largo de Rusia	Russian Institute for Hydrometeorological Information.
Otros datos (ERA-Interim)		Datos diarios y mensuales disponibles para distintos niveles en la vertical y con resolución espacial desde 0.125°×0.125° hasta 3°×3°	European Center for Medium-Range Weather Forecasts (ECMWF). http://apps.ecmwf.int/datasets/data/interim-full-daily/levtype=sfc/

3.5. Patrones de teleconexión climática

Las variaciones en el transporte de humedad puede tener distintas causas, además de los cambios en la evaporación ya mencionados, los cambios en la circulación también pueden influir en el transporte de humedad hacia la región ártica a escala interanual. Con el fin de analizar la influencia de la circulación en la contribución de humedad desde las fuentes hasta el Ártico se han utilizado las series temporales de los principales patrones de teleconexión del hemisferio norte.

Los índices de teleconexión empleados en este trabajo han sido obtenidos del Climate Prediction Center (CPC) en su página web http://www.cpc.ncep.noaa,gov/data/teledoc/telecontents.shtml, donde se ofrece una explicación detallada acerca del cálculo de sus índices.

Los patrones de teleconexión analizados son aquellos que presentan algún centro de acción sobre las fuentes de humedad localizadas para el sistema ártico y que son los enumerados a continuación:

- Oscilación del Atlántico Norte (NAO): es uno de los patrones más importantes del hemisferio norte y consiste en un dipolo de anomalías norte sur cuyos centros se encuentran sobre Groenlandia y sobre las latitudes centrales del Atlántico Norte. Su fase positiva se caracteriza por anomalías negativas de geopotencial sobre las latitudes altas de Atlántico Norte y anomalías positivas sobre el Atlántico Central, siendo la situación la contraria para su fase negativa.

- Patrón del Atlántico Este (EA): Se trata del segundo patrón más predominante del hemisferio norte y presenta una configuración similar a la NAO. Se trata de un dipolo norte-sur que se extiende a lo ancho del Atlántico Norte y cuyos centros de acción se encuentran desplazados hacia el sur con respecto a los de la NAO. A pesar de sus similitudes con la NAO se diferencia de ella en que ésta presenta una influencia subtropical.

- Patrón de Atlántico Este/Oeste de Rusia (EATL/WRUS): Este patrón tiene influencia sobre Eurasia a lo largo de todo el año y consiste en cuatro centros principales de anomalía en la altura geopotencial, estando asociada su fase negativa con anomalías positivas sobre Europa y el norte de China y anomalías negativas en el Atlántico Norte Central y el norte del mar Caspio.

- Patrón Escandinavo (SCAND): consiste principalmente en un centro de anomalía en la altura geopotencial sobre Escandinavia, con centros más débiles de signo contrario sobre el oeste de Europa y el este de Rusia/Oeste de Mongolia. Su fase positiva se asocia con anomalías positivas en la altura geopotencial sobre Escandinavia y el oeste de Rusia, siendo esta anomalía negativa en la fase contraria.

- Patrón Polar/Eurasia: este patrón aparece en todas las estaciones del año y su fase positiva se caracteriza por mostrar anomalías negativas de geopotencial sobre las regiones polares y positivas sobre el norte de China y Mongolia. El patrón se asocia con fluctuaciones en la intensidad de la circulación circumpolar.

- Patrón de Pacífico Oeste (WP): este patrón es el principal modo de variabilidad en el Pacífico Norte durante todo el año. En las estaciones de primavera e invierno el patrón consiste en un dipolo de anomalías de geopotencial norte-sur con un centro sobre la península de Kamchatka y otro centro de signo opuesto sobre el sureste de Asia y la región subtropical oeste del Pacífico Norte. Estos centros de acción aparecen desplazados al norte en el caso del verano, y además existe un tercer centro situado sobre el este del Pacífico Norte y suroeste de Estados Unidos en todas las estaciones. Las distintas fases de este patrón tiene una influencia importante sobre la corriente en chorro del Pacífico estando la fase positiva o negativa de este patrón relacionada con variaciones en la localización e intensidad de la zona de entrada en el Este de Asia.

- Patrón de Pacífico Este-Pacífico Norte (EP-NP): esta patrón aparece durante las estaciones de primavera, verano y otoño y cuenta con tres centros de acción localizados sobre Alaska/Oeste de Canadá, Pacífico Norte central y este de Norte América. La fase positiva se caracteriza por anomalías positivas de geopotencial sobre Alaska y negativas sobre los otros dos centros. Una fase positiva intensa se asocia

con una intensificación y desplazamiento hacia el sur del chorro del Pacífico, una intensificación en la circulación anticiclónica sobre el oeste de Norte América y en la circulación ciclónica en la zona este.

- Patrón de Pacífico/Norte América (PNA): La PNA es una de los modos de variabilidad más relevantes en las regiones extratropicales de Pacífico Norte. Su fase positiva presenta valores más altos de lo normal en el geopotencial en los alrededores de Hawái y el oeste de Estados Unidos y anomalías negativas a sur de las islas Aleutianas y sobre el sureste de Estados Unidos. Este patrón está asociado con fluctuaciones en la intensidad y localización del chorro del este de Asia.

- Patrón Tropical/ Hemisferio Norte (TNH): el TNH es el modo predominante durante los meses de invierno. Su fase positiva muestra anomalías positivas de geopotencial sobre el golfo de Alaska y sobre el área que va desde el golfo de México hacia el norte a través de la región oeste del Atlántico Norte y anomalías negativas en el este de Canadá. Este patrón modula significativamente el flujo de aire marino hacia Norte América y el transporte hacia el sur del aire frío desde Canadá.

- Transición de Pacífico (PT): PT es especialmente importante durante los meses de agosto y septiembre. La fase positiva se caracteriza por una altura geopotencial mayor que la media al oeste de Hawái y a través del oeste de Norte América, y altura geopotencial por debajo de la media en el golfo de Alaska y sobre el sureste de los Estados Unidos.

3.6. Análisis estadísticos.

Los análisis estadísticos son usados frecuentemente en las ciencias del clima ya que proporcionan una idea de la variabilidad climática a distintas escalas espaciales y temporales. En este trabajo se emplean análisis estadísticos de diversos tipos.

En ciertos casos será de utilidad analizar la relación entre distintas variables, con este fin en este trabajo se ha usado la correlación lineal de Pearson. Además de este análisis a continuación se describen otras herramientas estadísticas utilizadas en el desarrollo de esta investigación.

El análisis de composites supone una herramienta útil en la identificación de las condiciones observadas durante estados específicos del clima. Este análisis se basa en la selección de un subconjunto de datos en el cual algún parámetro clave puede ser identificado en el tiempo basándose en algún tipo de criterio, como puede ser la ocurrencia de eventos extremos en alguna variable determinada. Así esta técnica permite extraer señales de baja amplitud a través de la acumulación y promedio de los datos para aquellos pasos de tiempo que cumplen este criterio [Laken and Calogovic, 2013]. En nuestro caso el uso de los composites será útil para tratar de analizar las condiciones generales asociadas con los máximos y mínimos de extensión de hielo marino sobre el océano Ártico, con el fin de identificar las diferencias en el transporte de humedad asociadas a ambas situaciones extremas.

El cálculo de la media de los composites se realiza según la fórmula:

$$C_{\Gamma} = \frac{1}{n}\sum_{j=1}^{n} X_{jt} \qquad (3.6)$$

donde X representa el campo analizado condicionado por el índice t referente al criterio establecido para el número de observaciones n.

El test de significatividad estadística bootstrap es un método estadístico que permite realizar pruebas de significación estadística mediante el remuestreo de datos. El bootstrap fue contextualizado por Efron [1992] y se basa en la extracción de un número de muestras a partir de los propios datos. La principal ventaja de este método es que en él no es preciso conocer la distribución teórica a la que se ajustan los datos, como es el caso de otros test de significatividad, sino que esta se infiere a través de la propia muestra.

La técnica consiste en la extracción de nuevas muestras a través de los datos originales mediante un muestreo de reposición. Una vez obtenidas las nuevas muestras se calcula el valor de un estadístico determinado que se quiera analizar (media, coeficiente de correlación,…). Así se puede obtener una aproximación a la distribución muestral de los estadísticos de forma empírica y sin haber hecho suposiciones sobre la distribución teórica. Una explicación detallada acerca de este método puede consultarse en Efron and Tibshirani [1993].

En el caso del presente trabajo esta técnica de significatividad se ha aplicado a la diferencia entre los valores de (E-P) desde ciertas regiones árticas para las décadas 2001-2010 y 1981-1990. Para el cálculo de la significatividad se han calculado un total de 1000 muestras a partir de los valores de (E-P) del periodo de 33 años 1980-2012.

4

Conjunto de Publicaciones

La necesidad de conocer en mayor profundidad los procesos que tienen lugar en el Ártico y su influencia en el clima resulta evidente. Uno de los procesos que requiere mayor profundización es el transporte de humedad atmosférica. A lo largo de los últimos años ha crecido el número de estudios enfocados en este tema que han tratado de analizar distintas partes del globo. El reciente desarrollo de nuevas técnicas lagrangianas ha permitido no solo analizar los cambios de humedad sobre una región (posible mediante métodos eulerianos), sino también hacer un seguimiento de las partículas a lo largo de sus trayectorias. Esto permite el análisis de las fuentes y sumideros de humedad para las regiones de interés. Es decir, analizar de dónde proviene la humedad que afecta a una determinada región o cuáles son las zonas más influenciadas por ella (en términos de aportes de humedad).

En los últimos años se han realizados diversos estudios abordando el transporte de humedad hacia la región ártica. Nieto et al. [2007] han analizado las fuentes de humedad para Islandia

considerando un periodo corto de 5 años, de 2000 a 2004. Jakobson and Vihma [2010] y Rogers et al. [2001] han analizado el balance de humedad en el Ártico basándose en datos de reanálisis y Rinke et al. [2009] han estimado el vapor atmosférico total en la región. Sin embargo, a pesar del creciente uso de las aproximaciones lagrangianas y del interés que las regiones polares suscitan en la actualidad, ningún trabajo ha realizado una caracterización completa del transporte de humedad en la región, analizando de dónde proviene la humedad del Ártico, a qué áreas afecta, o cómo es el transporte desde el propio Ártico y cómo puede verse afectado por los recientes cambios en el clima ártico.

Por este motivo, en el presente trabajo se trata de realizar una caracterización del sistema ártico lo más completa posible, en lo que se refiere al transporte de humedad, a través del uso del modelo lagrangiano FLEXPART. Así, no solo se tratará de estudiar el transporte hacia el Ártico desde sus principales fuentes, sino que también se analizará el transporte desde esta región.

El estudio del Ártico como sumidero viene especialmente motivado por los recientes cambios observados sobre el sistema en los últimos años. El actual deshielo Ártico produce una mayor cantidad de océano libre de hielo durante periodos mayores de tiempo. Este hecho hace que la región ártica presente cada vez una mayor cantidad de humedad en la atmósfera potencialmente disponible para ser transportada hacia otras regiones.

En esta sección se presentan los principales resultados de la investigación, los cuales han sido publicados en cinco artículos distintos. El orden de los artículos tal y como aparecen aquí presentados no se corresponde con el orden de publicación, por lo que pueden aparecer algunas inconsistencias en los periodos analizados debido a la actualización de los datos utilizados a lo largo del desarrollo de la tesis. En términos generales se puede hablar de dos partes diferenciadas en los resultados. La primera, que es abordada en los tres primeros artículos, hace referencia a las fuentes de humedad de la región ártica. La segunda parte se refiere al transporte de humedad desde el Ártico y analiza su influencia tanto a nivel local, sobre el propio Ártico, como sobre latitudes más bajas. Esto se aborda en los dos últimos artículos presentados en esta tesis. En ambas partes se presenta un caso particular en el que se analiza el papel del deshielo ártico. El material suplementario de cada uno de los artículos se presenta en el Anexo A.

El primero de los artículos presentados tiene el título: "**Moisture transport into the Arctic: Source-receptor relationship and the role of atmospheric circulation**", por M. Vázquez, R. Nieto, A. Drumond y L. Gimeno publicado en **2016** en **Journal of Geophysical Research: Atmospheres**. En este artículo se ha realizado una caracterización climática de las fuentes para el sistema ártico y se ha analizado la influencia de la evaporación y la circulación atmosférica en el transporte desde ellas.

El segundo artículo que compone esta tesis tiene el título: "**Extreme sea ice loss over the Arctic: an analysis based on anomalous mositure transport**", por M. Vázquez, R. Nieto, A. Drumond y L. Gimeno. Este artículo ha sido publicado en la revista **Atmosphere** en el año **2017** y en él se presenta el estudio de las variaciones en el transporte de humedad hacía el Ártico para los años 2007 y 2012, años en los cuales han ocurrido los valores más bajos en la extensión de hielo marino durante las últimas décadas.

El tercer artículo de los que consta esta tesis lleva el título: "**Atmospheric moisture transport: the bridge between ocean evaporation and Arctic ice melting**", por L. Gimeno, M. Vázquez, R. Nieto y R.M. Trigo publicado en **Earth System Dynamics** en el año **2015**. En este artículo se ha tratado de asociar los cambios en el transporte desde las fuentes de humedad con el deshielo en la región ártica.

En el artículo "**Moisture transport from the Arctic: A characterization based on a lagrangian perspective**", por M. Vázquez, R. Nieto, A. Drumond y L. Gimeno y enviado para su publicación en **Polar Research**, se estudia la región ártica como fuente de humedad. En él se analiza el transporte de humedad desde el océano Ártico y cómo este varía según la estación del año y la región analizada dentro del propio océano.

Por último el artículo titulado "**Arctic moisture source for Eurasian snow cover variations**", por M. Wegmann, Y. Orsolini, M. Vázquez, L. Gimeno, R. Nieto, O. Bulygina, R. Jaiser, D. Handorf, A. Rinke, K. Dethloff, A. Sterin y S. Brönnnimann publicado en **Enviromental Research Letters** en el año **2015**, se ha estudiado el trasporte de humedad desde los mares de Barents y Kara durante los meses de octubre y noviembre para analizar el efecto del deshielo en la cobertura de nieve sobre Eurasia.

En la tabla 4.1 se muestra la posición de cada una de las revistas dentro de su categoría, mientras que en las tablas 4.2 y 4.3 se muestra la descripción, el factor de impacto y los criterios de calidad de cada una de ellas.

Tabla 4.1. Resumen de la posición de cada una de las revistas en las que se ha publicado los resultados de esta tesis doctoral dentro de su categoría.

Revista	Nombre categoría	Ranking dentro de la categoría	Quartil en la categoría
Journal of Geophysical Research-Atmosperes	Meteorología y Ciencias atmosféricas	19/85	Q1
Atmosphere	Meteorología y Ciencias atmosféricas	56/85	Q3
Earth System Dynamics	Geociencia- Multi-cisplinaria	25/188	Q1
Polar Research	Geociencia- Multi-cisplinaria	76/188	Q2
Environmental Research Letters	Meteorología y Ciencias atmosféricas	8/85	Q1

Tabla 4.2. Resumen del impacto y la calidad de cada una de las revistas, según el último-Journal Citation Reports (JCR), en las que se han publicado los resultados de esta tesis doctoral.

Revista	Descripción	Características
Journal of Geophysical Research (JGR)	Publica investigaciones científicas originales sobre los procesos físicos, químicos y biológicos que contribuyen al mejor conocimiento de la Tierra, el Sol, el Sistema Solar, y todo su medioambiente y componentes. Se organiza en 7 secciones que abordan distintas disciplinas: Atmospheres, Biogeosciences, Earth Surface, Oceans, Planets, Solid Earth y Space Physics.	Abreviatura: J. Geophys. Res. Factor de impacto: 3.454 Factor a 5 años: 3.850 Índice de inmediated: 0.668 Vida media de las citas: 9.6 Eigenfactor: 0.08665 Influencia del artículo: 1.457 ISSN: 269-897X
Atmosphere	Revista internacional de libre acceso que publica mensualmente trabajos científicos relacionados con la atmósfera de manera online a través del MDPI (Multidisciplinary Digital Publishing Institute). Entre los principales temas que aborda destacan la química y física atmosférica, la calidad del aire y la meteorología.	Abreviatura: Atmosphere-Basel Factor de impacto: 1.487 Factor a 5 años: 1.793 Índice de inmediated: 0.399 Vida media de las citas: 2.6 Eigenfactor: 0.00181 Influencia del artículo: 0.520 ISSN: 2073-4433
Earth System Dynamics (ESD)	Revista científica internacional dedicada a la publicación y discusión pública de estudios que toman una perspectiva interdisciplinar sobre el funcionamiento del sistema terrestre y el cambio global. Busca contribuciones que investiguen las interacciones entre los distintos componentes del sistema terrestre y los mecanismos subyacentes, las formas en las que estos pueden ser conceptualizados, modelados y cuantificados, predicciones del comportamiento del sistema ante cambios globales, y los impactos para su habitabilidad, humanidad y la futura gestión del sistema mediante la toma de decisiones.	Abreviatura: Earth Syst. Dynam. Factor de impacto: 3.365 Factor a 5 años: 3.869 Índice de inmediated: 0.690 Vida media de las citas: 2.9 Eigenfactor: 0.00334 Influencia del artículo: 1.690 ISSN: 2190-4979

Tabla 4.3. Continuación de la tabla 4.3

Revista	Descripción	Características
Polar Research	Revista internacional con revision por pares del Norwegian Polar Institute, institución central de Noruega para la investigación, monitoreo y mapeado medioambiental de las regiones polares. Fue creada en 1982 y en 2011 se convirtió en una revista de acceso libre.	Abreviatura: Polar Res. Factor de impacto: 2.146 Factor a 5 años: 2.404 Índice de inmediated: 0.070 Vida media de las citas: >10 Eigenfactor: 0.00248 Influencia del artículo: 0.868 ISSN: 0800-0395
Environmental Research Letters (ERL)	Revista de acceso libre con un alto impacto que trata de ser el punto de reunión para la investigación y las comunidades políticas preocupadas por el cambio medioambiental y su gestión. La cobertura de la revista refleja la naturaleza interdisciplinaria de las ciencias medioambientales. Su contenido se basa en observaciones, modelado numérico, aproximaciones teóricas y experimentales de las ciencias medioambientales, y especialmente a la ciencia relevante para la política, los impactos y toma de decisiones en temas medioambientales.	Abreviatura: Environ. Res. Lett. Factor de impacto: 4.404 Factor a 5 años: 5.221 Índice de inmediated: 0.847 Vida media de las citas: 3.7 Eigenfactor: 0.04113 Influencia del artículo: 2.025 ISSN: 1748-9326

AGU PUBLICATIONS

JGR

Journal of Geophysical Research: Atmospheres

RESEARCH ARTICLE

10.1002/2016JD025400

Special Section:
The Arctic: An AGU Joint Special Collection

Key Points:
- Main moisture sources for the Arctic domain: subtropical/southern extratropical Pacific and Atlantic Oceans, North America, and Siberia
- The moisture transport to the Arctic domain is influenced by EA, WP, and PNA interannual patterns of climate variability
- Changes in evaporation over the sources of moisture seem to be negligible to moisture transport budget in the Arctic domain

Supporting Information:
- Supporting Information S1
- Figure S1

Correspondence to:
M. Vázquez,
martavazquez@uvigo.es

Citation:
Vázquez, M., R. Nieto, A. Drumond, and L. Gimeno (2016), Moisture transport into the Arctic: Source-receptor relationships and the roles of atmospheric circulation and evaporation, *J. Geophys. Res. Atmos.*, *121*, 13,493–13,509, doi:10.1002/2016JD025400.

Received 24 MAY 2016
Accepted 9 NOV 2016
Accepted article online 11 NOV 2016
Published online 29 NOV 2016

Moisture transport into the Arctic: Source-receptor relationships and the roles of atmospheric circulation and evaporation

M. Vázquez[1], R. Nieto[1,2], A. Drumond[1], and L. Gimeno[1]

[1]Environmental Physics Laboratory, Facultade de Ciencias, Universidad de Vigo, Ourense, Spain, [2]Department of Atmospheric Sciences, Institute of Astronomy, Geophysics and Atmospheric Sciences, University of São Paulo, São Paulo, Brazil

Abstract Hydrological processes play a key role in the Arctic, as well as being an important part of the response of this region to climate change. The origin of the moisture arriving (and then precipitating) in the Arctic is a crucial question in our understanding of the Arctic hydrological cycle. In an attempt to answer this, the present study uses the Lagrangian diagnosis model FLEXPART (FLEXible PARTicle dispersion model) to localize the main sources of moisture for the Arctic region, to analyze their variability and their contribution to precipitation, and to consider the implications of any changes in the transport of moisture from particular sources within the system. From this analysis, four major moisture sources appear as the most important moisture supplies into the system: the subtropical and southern extratropical Pacific and Atlantic Oceans, North America, and Siberia. Oceanic sources play an important role throughout the year, whereas continental ones only take effect in summer. The sink areas associated with each source have been shown to be moderately influenced by changes in atmospheric circulation, mainly associated with the East Atlantic pattern for the Atlantic source and related to West Pacific and Pacific/North American (PNA) teleconnection patterns for the Pacific one. On the other hand, the variability over the sinks does not seem to be significantly related to changes in evaporation at an interannual scale.

1. Introduction

The Arctic system is often of key interest in discussions on climate change both due to its sensitivity to global warming and its possible influence in the global and regional climate [*Screen and Simmonds*, 2010]. This region is suffering from the effects of significant and rapid changes, including increasing temperatures [*Comiso*, 2006], melting sea ice [*Cavalieri and Parkinson*, 2012, *Serreze and Stroeve*, 2015], or mass loss of glaciers and ice caps [*Kaser et al.*, 2006; *Velicogna*, 2009]. All these changes make the Arctic system a focus of interest because of the possible climatic [*Maslowski et al.*, 2012] and even human implications [*Ford*, 2009; *Dodds*, 2010].

The hydrological system is not unaffected by these changes, and over the last century the Arctic has seen dramatic changes in hydrological processes, with implications not only for the ecosystem and human activities in the Arctic but also for the global ocean and cryosphere [*White et al.*, 2007; *Prowse et al.*, 2015]. At the core of the hydrological cycle, the transport of moisture from midlatitudes to the Arctic has suffered a significant change, suggesting some studies an increase over the last few decades [e.g., *Zhang et al.*, 2012], and a clear prospect of this trend continuing in under future global warming [*Kattsov et al.*, 2007].

Several studies have been undertaken in recent years to address the variability in extreme events in moisture transport into the Arctic, which is attributed by some researchers to a variety of mechanisms, including extreme events related to "atmospheric rivers" [*Woods et al.*, 2013] and Rossby wave breaking [*Liu and Barnes*, 2015]. From a general point of view, variations in moisture transport can be due to (a) changes in general circulation patterns, (b) increases or reductions in moisture supply from particular sources caused by changes in evaporation, or (c) a combination of these two effects [*Gimeno et al.*, 2012, 2013]. Several previous studies have shown the influence of circulation patterns and evaporation [e.g., *Aagaard and Greisman*, 1975; *Oort*, 1975; *Hanssen-Bauer and Førland*, 1998; *Rogers et al.*, 2001; *White et al.*, 2007; *Gimeno et al.*, 2015] on the Arctic atmospheric hydrological system. Most studies related to the transport of moisture into the Arctic region make use of three different methodologies: analytical and box models, physical water

vapor tracers (isotopes), and numerical water vapor tracers (WVT). The box model allows the identification of moisture inflow and outflow for given lateral boundaries; however, they provide no information about the physical processes that occur inside the box itself [*Gimeno et al*., 2012]. The use of isotopes [e.g., *Kurita*, 2011; *Kopec et al*., 2016] depends on the strength of the isotopic signal. Regarding WVTs, we distinguish between Eulerian and Lagrangian methods. The Eulerian methodology is widely used due to its simplicity [e.g., *Groves and Francis*, 2002a, 2002b; *Cullather et al*., 2000; *Rogers et al*., 2001], but it is not easy to extract the sink-source relationship using this method, or in other words, to define the link between the precipitation that falls over a region and the area in which the moisture previously evaporated. This ability to establish a source-receptor relationship is the principal advantage of the Lagrangian methodology, as previously described in several studies [e.g., *Nieto et al*., 2007; *Sodemann et al*., 2008]. A detailed intercomparison of all these methodologies is given in *Gimeno et al*. [2012].

All these different methodologies have previously been applied, to a greater or lesser extent, to the study of the transport of moisture into the Arctic system. A Eulerian approach was used by *Jakobson and Vihma* [2010] in an analysis of atmospheric moisture budgets in the Arctic, for example. Isotopic analysis was used to explore the origin of precipitation over Greenland by *Johnsen et al*. [1989] and to analyze the influence of sea ice on Arctic precipitation by *Kopec et al*. [2016]. In general, these previous authors identified major meridional moisture transport from the North Atlantic and the Pacific Oceans. The most recently developed Lagrangian techniques are extensively applied for evaluating the origin of the water that precipitates over a particular area [*Gimeno et al*., 2012], and their robustness has been shown in many previous studies [e.g., *Dirmeyer and Brubaker*, 2007; *Gimeno et al*., 2013]. However, there have been few Lagrangian studies of the Arctic, and none that have analyzed the complete domain.

For this purpose, the present study makes use of the Lagrangian method developed by *Stohl and James* [2004, 2005] to identify and analyze the major sources of moisture for the whole Arctic domain. This approach was successfully applied to the characterization of sources of moisture in regions close to the Arctic or within it, such as Iceland [*Nieto et al*., 2007], Norway [*Stohl et al*., 2008], and Eurasia [*Wegmann et al*., 2015; *Gimeno et al*., 2015].

The present study is furthermore an attempt to address the following specific objectives: (i) identification of moisture sources for the whole Arctic system, (ii) analysis of moisture source variability at different time scales, (iii) estimation of the moisture supply into the Arctic system from every source, and (iv) study of how changes in atmospheric circulation and evaporation affecting the sources might affect moisture supply over the Arctic.

The remainder of the paper is organized as follows. The data and methodology are described in section 2. Section 3 is devoted to the presentation of the main results, and section 4 contains a summary of the main findings.

2. Data and Methods

The Arctic domain as considered in this study was defined by *Roberts et al*. [2010] as "the geosphere and biosphere north of the boreal mean decadal 10°C sea surface isotherm, the surface air 0°C contour that encircles the North Pole, and the southern limit of terrain that drains into the High Arctic" (Figure 1). Thus, it encompasses the main terrestrial and oceanic areas affecting the Arctic environment (Arctic drainage areas, glaciers and ice sheets, permafrost areas, etc.).

The Lagrangian approach used to analyze the major oceanic and continental sources for the Arctic domain is based on the FLEXPART (FLEXible PARTicle dispersion model) v9.0 particle dispersion model [*Stohl and James*, 2004, 2005] forced by global reanalysis data ERA-Interim obtained from the European Centre for Medium-Range Weather Forecast (ECMWF). ERA-Interim is the ECMWF's current comprehensive atmospheric reanalysis, and it supposes an increase in forecast quality compared to previous ERA reanalysis versions [*Tavolato and Isaksen*, 2011]; this makes it appropriate for the reproduction of the hydrological cycle [*Trenberth et al*., 2011]. This data set is available at 6 h intervals and has a 1° × 1° spatial resolution in latitude and longitude on 61 vertical levels, from 1000 to 0.1 hPa. ERA-Interim covers the period from 1 January 1979 and continues to be extended forward in near-real time [*Dee et al*., 2011]. Here we consider a 33 year period from January 1980 to December 2012.

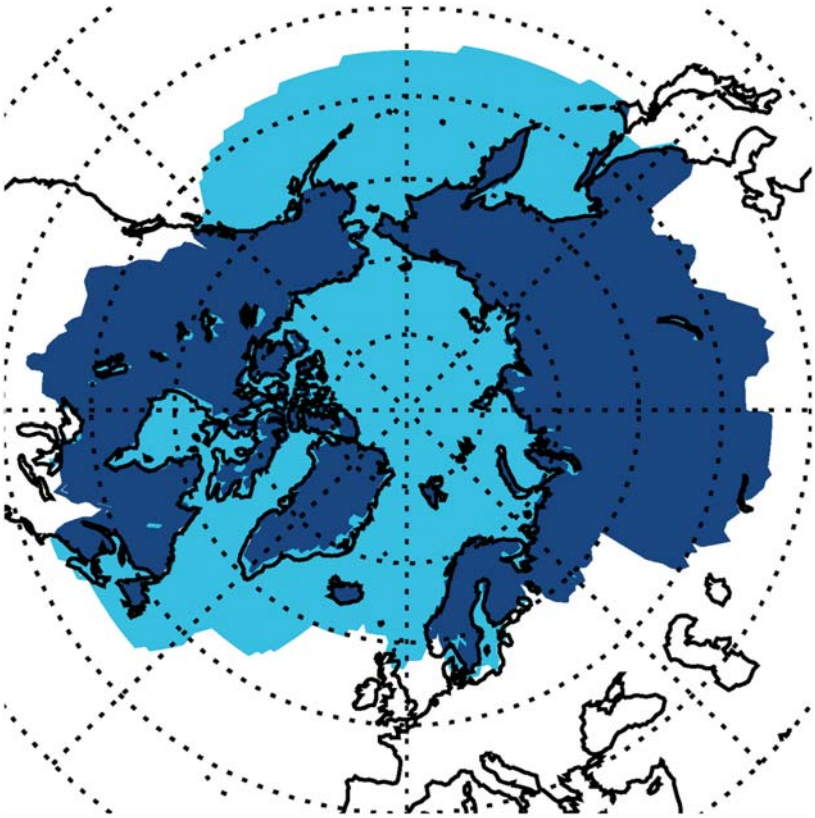

Figure 1. Arctic domain used in the present work defined as the geosphere and biosphere north of the boreal mean decadal 10°C sea surface isotherm, the surface air 0°C contour that encircles the North Pole, and the southern limit of the terrain that drains into the High Arctic, following the definition of *Roberts et al*. [2010]. Dark blue colors represent continental areas, and light blue colors represent oceanic ones.

In FLEXPART the atmosphere is homogenously divided into finite elements of volume with equal mass (hereafter "particles") to track individual 3-D trajectories representing air movement. For this study, the entire global atmosphere was divided into nearly 2.0 million particles subject to advection by the model using 3-D wind fields. The particle position (latitude, longitude, and altitude) and specific moisture (q) are stored at 6 h intervals (00:00, 06:00, 12:00, and 18:00 UTC). Time changes in specific humidity of each particle (of mass m) along its trajectory follow the equation $e - p = \mathrm{m}(\mathrm{d}q/\mathrm{d}t)$ where $(e - p)$ represents the freshwater flux associated with the particle (evaporation e minus precipitation p). By adding up $(e - p)$ for all the particles residing in the atmospheric column over a given area, it is possible to diagnose the aggregated $(E - \mathrm{P})$. It represents the surface freshwater associated with the tracked particles, where (E) and (P) are the rates of evaporation and precipitation per unit area, respectively.

FLEXPART can be used in forward mode to investigate the moisture transport of particles from their sources or backward in time to determine the sources of moisture for given areas [*Stohl et al*., 2005]. In this study, both options were applied. As a first step, moisture sources for the Arctic domain were located using the backward mode. With this in mind all particles residing over the Arctic domain (the target region) were tracked backward for 10 days to assess where the particles gained moisture. The period of tracking was limited to 10 days (i10) because this is the average residence time of water vapor in the atmosphere [*Numagati*, 1999]. The total atmospheric moisture budget $(E - P)$ integrated over the 10 days of tracking (i10) and averaged over the period of interest (seasonal or annual), hereafter the $(E - P)$i10 field, shows where the particles acquired or lost moisture before reaching the target area. For all grid points where $(E - P)\mathrm{i}10 > 0$, it is known that air parcels over that vertical column gain moisture from the atmosphere, and where $(E - P)\mathrm{i}10 < 0$ it is known that they lose moisture to the atmosphere. Therefore, the sources of moisture for the region of interest were identified as those areas with positive values in the $(E - P)$i10 fields. To define the major sources of moisture for the

Arctic domain, those areas with a moisture uptake greater than 4 mm/d were selected because this threshold represents the 95th percentile on the annual backward values of positive $(E-P)$i10. Annual and seasonal sources were selected, considering winter as December-January-February (DJF); spring as March-April-May (MAM); summer as June-July-August (JJA); and autumn as September-October-November (SON). Once we had identified the main moisture sources, a forward analysis was applied using these sources in order to analyze the moisture contribution of each source to the Arctic domain for $(E-P)$i10 <0. In this case, particles from each source region were tracked forward for 10 days to observe where they lost moisture. The procedure is analogous to backward analysis, but in this case the moisture contribution is represented by areas with $(E-P)$i10 <0. Results are shown only for the Arctic domain because this is the area where the contributions are relevant to our study. It must be stressed that this methodology cannot guarantee that the moisture gained by a particle from a source area will reach the target area. This depends on the interaction between the particles and the dynamic conditions over the area or along the trajectory [*Drumond et al*., 2014]. Moreover, FLEXPART computes the balance between evaporation and precipitation $(E-P)$, and negative values should be understood as "estimated precipitation" (as anywhere we use the term "precipitation"), because these were obtained as the total moisture lost by the particles originating from the main moisture sources during the 10 days of forward tracking. This estimated precipitation cannot be compared directly with observed precipitation over the area, but the values follow the same pattern and it can be helpful in analyzing the variability.

The influence of changes in evaporation from each moisture source was evaluated at an interannual scale. To this end, a linear Pearson correlation was calculated between the interannual forward anomalies of the $(E-P)$ i10 time series with the evaporation time series over the major sources. Evaporation data were obtained from the Objectively Analyzed air-sea Heat Fluxes (OAFlux) project [*Yu*, 2007] for oceanic sources and GLEAM (Global Land Surface Evaporation: the Amsterdam Methodology) for continental ones. The OAFlux project provides global estimates of oceanic evaporation obtained from satellite products and model reanalysis [see *Yu et al*., 2008]. The monthly data are available from 1958 on a $1°\times1°$ grid in longitude and latitude. The GLEAM data set supplies a spatially coherent estimate of the evaporative flux over land as derived from satellite observations. These data are available from 1980 to 2012 at a daily global scale with a 0.25° spatial resolution [see *Miralles et al*., 2011].

Apart from evaporation, changes in circulation can also have an influence on the transport of moisture toward the Arctic at interannual scale. The same correlation analysis was therefore applied using the main Northern Hemispheric teleconnection patterns. The indices used in this work are provided by the Climate Prediction Center in the Web page http://www.cpc.ncep.noaa.gov/data/teledoc/telecontents.shtml, where the interested reader can also find a detailed explanation of how the indexes are calculated and a description of the teleconnection patterns. Briefly, the indices are obtained through the Rotated Principal Component Analysis (RPCA) [*Barnston and Livezey*, 1987] applying Varimax rotation. This procedure isolates the primary teleconnection patterns for all months and allows time series of the patterns to be constructed. For monitoring purposes, RPCA technique is applied to monthly mean standardized 500 mb height anomalies obtained from the Climate Data Assimilation System from 20°N to 90°N, which includes all the Arctic domain. Monthly indices date back to 1950 and they are standardized by the 1981–2010 climatology. The correlation was calculated between the $(E-P)$i10 time series and the time series of the main Northern Hemispheric teleconnection patterns, namely: North Atlantic Oscillation (NAO), East Atlantic (EA), East Atlantic/Western Russia (EATL/WRUS), Scandinavian (SCAND), Polar/Eurasia, West Pacific (WP), East Pacific-North Pacific (EP-NP), Pacific/North American (PNA), Tropical/Northern Hemisphere (TNH), and Pacific Transition (PT). For each source, only those patterns with at least one of the centers of action placed over the source area were analyzed.

3. Results

3.1. Characterization of the Main Moisture Sources for the Arctic Domain

The backward analysis described above permitted us to characterize the main moisture sources for the Arctic domain as defined by *Roberts et al*. [2010]. Figure 2 (left column) shows the annual and seasonal values of the 10 day integrated atmospheric moisture budget $(E-P)$i10 obtained using the backward trajectories from our target area. From this figure it is possible to identify the main sources of moisture

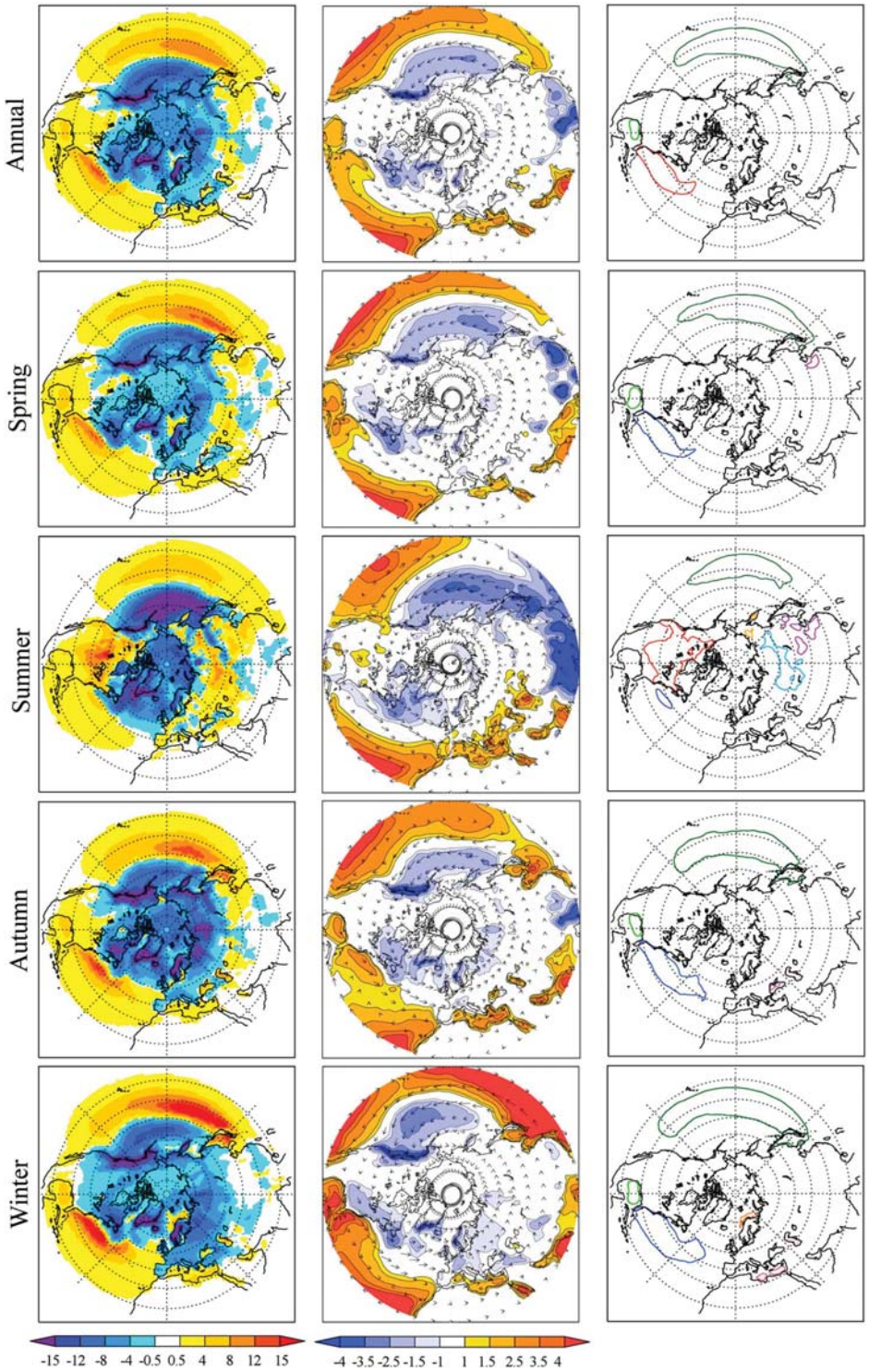

Figure 2. (left column) Climatological annual and seasonal 10 day integrated ($E - P$) values observed for the period 1979–2012, for all the particles bound for the Arctic domain, determined from backward tracking. Red (blue) colors represent moisture sources (sinks). Units are in mm d^{-1}. (middle column) Climatological annual and seasonal vertically integrated moisture flux values (vectors; measured in kg m^{-1} s^{-1}) and respective divergence (shade; measured in mm d^{-1}). Data are from ERA-Interim. (right column) Annual and seasonal moisture sources delimited only for those values of 10 day integrated ($E - P$) greater than 0.4 mm/d. Each contour color represents one source: the dark blue line represents the Atlantic source, light blue the Siberian one, dark green the Pacific, light green the Gulf of Mexico, dark pink the Black Sea, light pink the Caspian Sea, light orange the Eastern Russia source, dark orange the Norwegian and Barents Seas, purple the China source, red the North American source, and garnet the Mediterranean source.

for the 33 year period 1980–2012. The $(E-P)$i10 values both quantify the moisture gained or lost by the particles as they move toward the target area and give the locations of this gain or loss. Those areas with positive values $(E-P)\text{i}10>0$ (reddish colors) represent the uptake of moisture and may be considered sources, while areas with negative values $(E-P)\text{i}10<0$ (blueish colors) represent sinks, where particles lose moisture. The climatological annual average of $(E-P)$i10 Figure 2 (top row and right column) indicates two major sources, one over the North Pacific (dark green line) and the other over the North Atlantic (dark blue line); both show greater values along the paths of the western boundary oceanic currents. Another smaller source of moisture is evident over the Gulf of Mexico (light green line). These oceanic sources and their relative importance change by season, with continental sources also appearing during the warm season. A seasonal analysis shows that during spring (March to May) the oceanic sources are dominant, being similar to the annual pattern both in value and geographical distribution, and a continental source also appears over eastern Asia in China (purple isoline in Figure 2, right column). During summer (June to August) continental areas increase in importance compared to oceanic ones, with more sources appearing over Asia. The source in China (purple line) appearing in spring is increased in size, and two new sources appear in eastern Russia (light orange line) and Siberia (light blue line). This last source has been found previously as summer moisture source for the Arctic domain [*Serreze et al.*, 2002]. The main terrestrial source of moisture over the continents in summer, showing the greatest values of $(E-P)$ $\text{i}10>0$, appears over North America (red line), however. During summer, the Pacific (dark green line) and Atlantic (dark blue line) oceanic sources reach their minimum extension and intensity over the year, and those over the Gulf of Mexico (light green line) disappear altogether. The autumn (September–November) field of $(E-P)\text{i}10>0$ shows a reduction in the continental sources, with the oceanic sources again being dominant as in spring, but with the addition of an uptake from the Euroasiatic inner seas, especially the Caspian and Black Seas (light and dark pink lines, respectively). The intensification of the major oceanic sources continues through the winter (December to February) with a remarkable enhanced moisture uptake from the Norwegian, Barents (dark orange line), and Mediterranean Seas (garnet line), while the Black Sea (dark pink) uptake disappears. In general terms, the moisture sources identified here show good agreement with evaporative areas described in *Jakobson and Vihma* [2010], with enhanced summer evaporation over continents compared with the other seasons. For an Eulerian perspective, the ERA-Interim vertically integrated moisture flux (VIMF) and its divergence are shown in Figure 2 in the central column. The VIMF field shows acceptable agreement with the evaporative sources identified by the Lagrangian method, with areas of divergence over moisture sources, and the greatest differences over the Pacific source (displaced to the East) and over continental areas in summer, when only small areas of divergence are seen over North America and Asia. The differences between the $(E-P)$ fields obtained via the Lagrangian analysis and those obtained via the divergence of the ERA-Interim VIMF may be understood in terms of their respective methodologies. In the Lagrangian method, the calculation of the surface freshwater flux $(E-P)$ takes into account only those particles traveling along the path source-Arctic Domain, and it is obtained by summing $(e-p)$ for all the tracked particles residing in the atmospheric column over a $1°\times1°$ area. The $(E-P)$ flux calculated via VIMF considers all particles present in the atmospheric column over a given area. Thus, if all the particles present in the atmospheric column were considered in the Lagrangian approach regardless of their origin, the results would be similar to the $(E-P)$ obtained via the divergence of the VIMF [*Stohl and James*, 2004].

Figure 3 summarizes the seasonal positions and extents of the four main moisture sources, allowing comparisons to be made more easily. These major sources are the Atlantic, Pacific, North American, and Siberian. The contours plotted show values of $(E-P)$i10 greater than 4 mm/d; this threshold represents the 95th percentile of positive $(E-P)$i10 values on the annual backward tracking. Hereinafter, these four oceanic and continental sources of moisture selected using the *isoline of 4 mm/d will be considered the major sources of moisture for the Arctic Domain*. Under this criterion, other sources appear "minor," as the Euro-Asiatic inner seas, the Mediterranean, the Norwegian, and the Barents Sea, as well as the multiple minisources over eastern Asia; all have been excluded from the selection because of their limited extent. The single view of Figure 3 permits the comparison of the relative importance of the sources throughout the year and the changes occurring by season. A physical interpretation of this seasonal picture can be given in terms of the well-known importance of transients in driving mean meridional moisture transport [e.g., *Peixoto and Oort*, 1992]. As noted by *Newman et al.* [2012] the synoptic transport is maximized within the storm tracks over the western part of

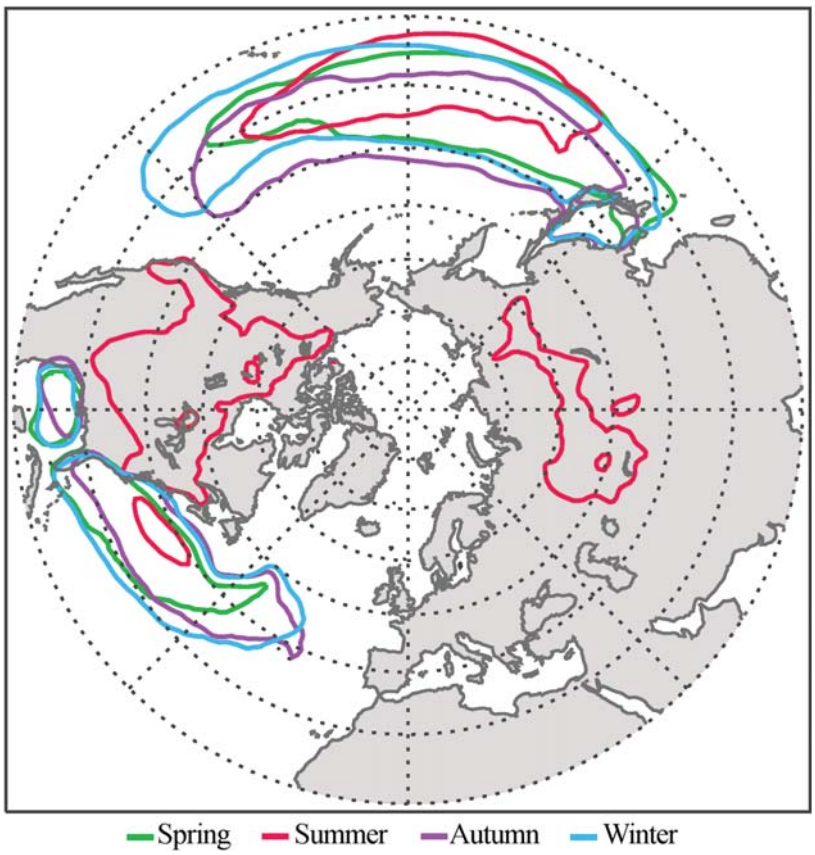

Figure 3. Seasonal variation of major moisture sources for the Arctic domain. The red contour line represents summer sources (JJA), the blue one represents winter (DJF), and green and purple represent spring (MAM) and autumn (SON), respectively. Moisture sources are defined as these areas where the 10 day integrated ($E - P$) value exceeds 4 mm/d.

both Northern Hemisphere oceans where synoptic variability is strongest [e.g., *Chang et al*., 2002]. In the winter this transport occurs primarily over the oceans, but in the summer it is dominated by poleward transport from the large land masses toward the Arctic Ocean associated to an increased frequency of blocking there during summer [e.g., *Tyrlis and Hoskins*, 2008; *Dole et al*., 2011] and an increment of the advection of moistened air by an intensification of cyclone activity in summer over northern Eurasia and Canada as shown by *Serreze et al*. [2009] and *Tilinina et al*. [2013].

Although Figure 3 shows the 10 day integrated ($E - P$) values, our methodology also allows us to compute the moisture uptake of each source for each day of the trajectory. This makes it possible to gauge at what point during the 10 days each source contributes the most moisture to the target region. The resulting temporal evolution of the uptake of different moisture sources affecting the Arctic domain is shown in Figure 4, in which the seasonal ($E - P$) values are normalized by source area. Absolute values of ($E - P$) for each day backward in time are shown in Figure S1, which reveals that the values of ($E - P$) obtained for the Pacific and Atlantic oceanic sources are higher than the others (and always in the same order), except for in summer when these oceanic sources are greatly diminished. During summer, the absolute transport from the continental North American source (Figure S1 in the supporting information) to the Arctic domain significantly exceeds the transport from the other sources, followed by the transport from Pacific source in the early days of transport (from day 10 to day 6 back) and the Siberian continental source in the last days (from day 6 back to day 0). Because the quantity of moisture transported from some sources is clearly different to others depending on the size of the source, comparison of the sources benefits from considering the area of each source (Figure 4). In general, most of the areas defined as major sources do not act as real sources during the two last days of the transport (from day 2 to day 1), with the greatest contribution of moisture uptake being from day 10 to day 5. The pattern of the major Pacific and Atlantic oceanic sources, including the

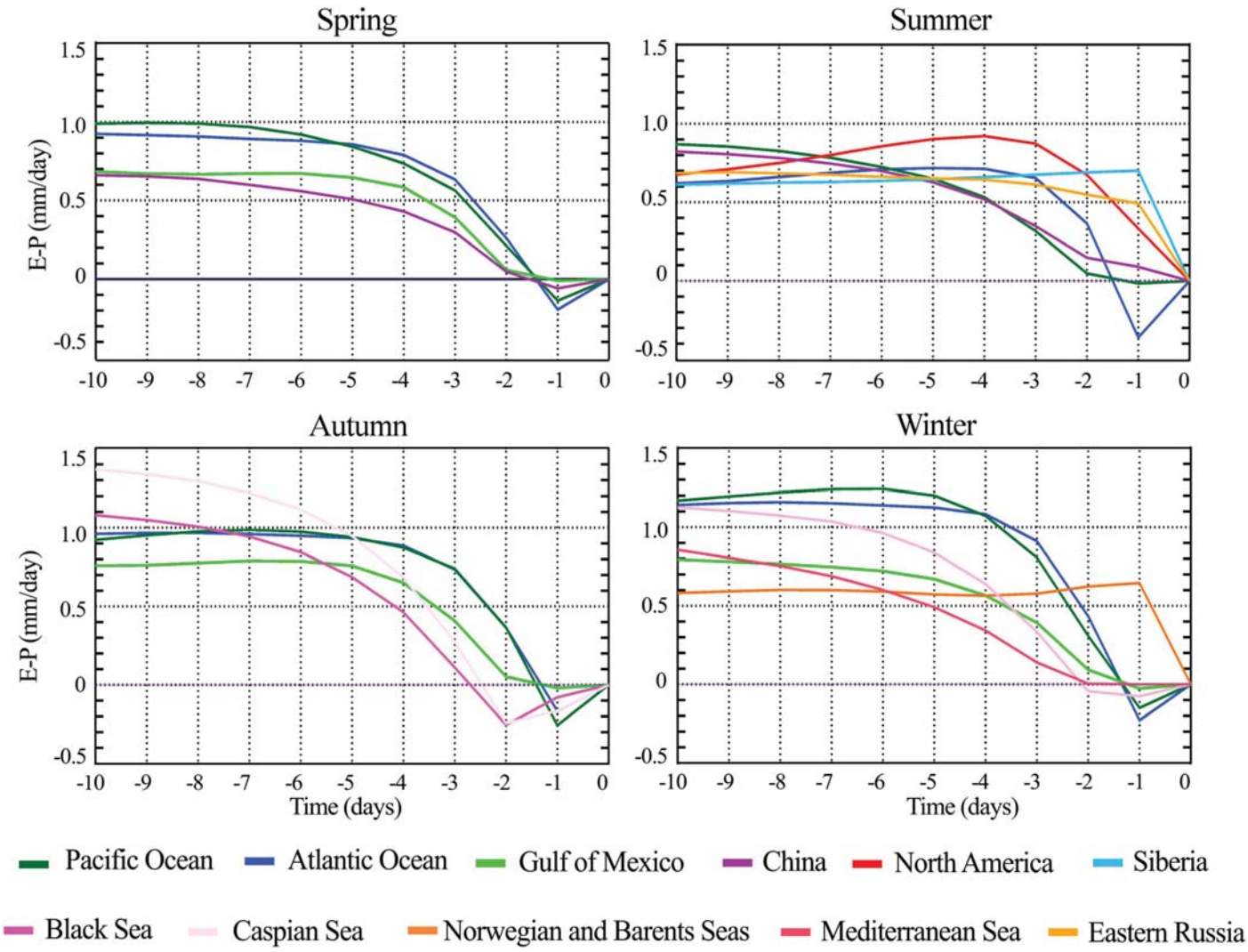

Figure 4. Ten-day ($E-P$) time series for the Arctic domain seasonally integrated over each moisture source for the period 1980–2012 relative to the area. Dark and light green lines represent the Pacific Ocean and the Gulf of Mexico, respectively; dark and light blue show the Atlantic Ocean and Siberia; purple line represents the China source; red is North America; light and dark orange represent Eastern Russia and the Norwegian and Barents Seas, respectively; garnet indicates the Mediterranean source; and the light and dark pink indicate the Caspian and Black Seas.

Gulf of Mexico, is similar for spring, autumn, and winter, with moisture supply being almost constant throughout the trajectory from day 10 to day 2, with smaller values for the Mexican Gulf source. During spring and autumn, when the China and Black and Caspian Sea sources appear, their behavior is similar to the oceanic ones. China provides moisture from day 10 to day 2, and the Black and Caspian Seas from day 10 to day 3. In summer, the pattern is rather more diverse (see also Figure S1); the continental areas gain importance as sources of moisture, especially North America and Siberia. The North American continental area appears as the most important source (Figure S1) providing the greatest moisture uptake from day 6 to day 2 (reaching a maximum value at day 4). Moisture supply from the Siberian source slowly increases along the trajectory, becoming the source that supports most moisture (in relation to its extent) during the last day of transport (Figure 4). The Pacific acts as the third most effective moisture source for the Arctic, from day 5 until day 2, and the second most effective over the first few days of transport (Figure S1). Its moisture uptake slowly decreases from the first days of transport up until day 2, when the supply becomes slight. The China source is the fourth most important during summer (Figure S1), supporting moisture throughout the time period (with a peak at 10 days). The Eastern Russia and Atlantic sources contribute the least to the Arctic during

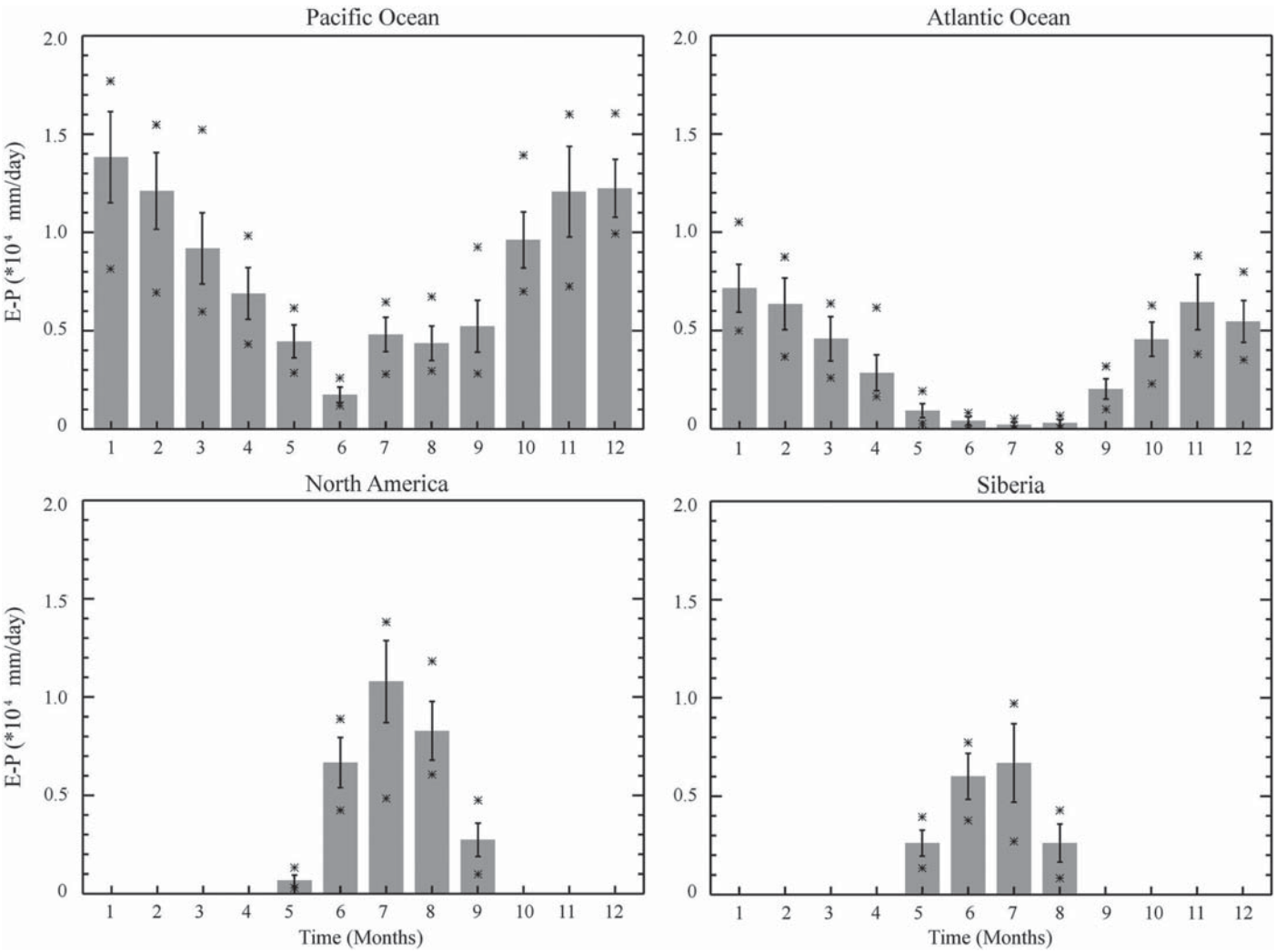

Figure 5. ($E-P$) monthly mean contribution from moisture sources (measured in mm d^{-1}) over the period 1980–2012 for the 10 day backward trajectories. The area considered for the calculation varies by month. Asterisks represent maximum and minimum values for each month, and vertical whiskers represent the standard deviation.

summer (Figure S1). The Eastern Russia moisture supply is almost constant until day 4, when the value decreases to reach a minimum on day 1. The oceanic Atlantic source provides its greatest input of moisture 4 days before the particles reach the Arctic domain. During the winter months, the Pacific is absolutely the main source of moisture for the Arctic, followed by the Atlantic, from day 10 to day 2. The day before reaching the target area, the Eastern Russia continental source is dominant, showing its higher moisture uptake, which gains in importance over the trajectory (see also Figure S1). The Mediterranean source only appears during the cold season and acts as a source from day 10 (its maximum value) to day 2.

The monthly evolution of $(E-P)i10>0$ values for the four major sources (Figure 5) confirms the remarkable differences between the oceanic and continental sources in their annual cycle. For the major oceanic sources (Pacific and Atlantic), the highest values appear during autumn and winter, reaching their maxima in January in both cases. Minimum values are detected in summer, with June the minimum for the Pacific source and July for the Atlantic one. The continental sources, however, reach maximum values in the middle of the summer. In general, there is good agreement between extent (Figure 3) and intensity (Figure 5), showing that the greater the area of the source of moisture, the higher the values of seasonal (and monthly) $(E-P)i10$ values. The only exception is in summer when despite showing a similar extent to the Siberian one (differences lower

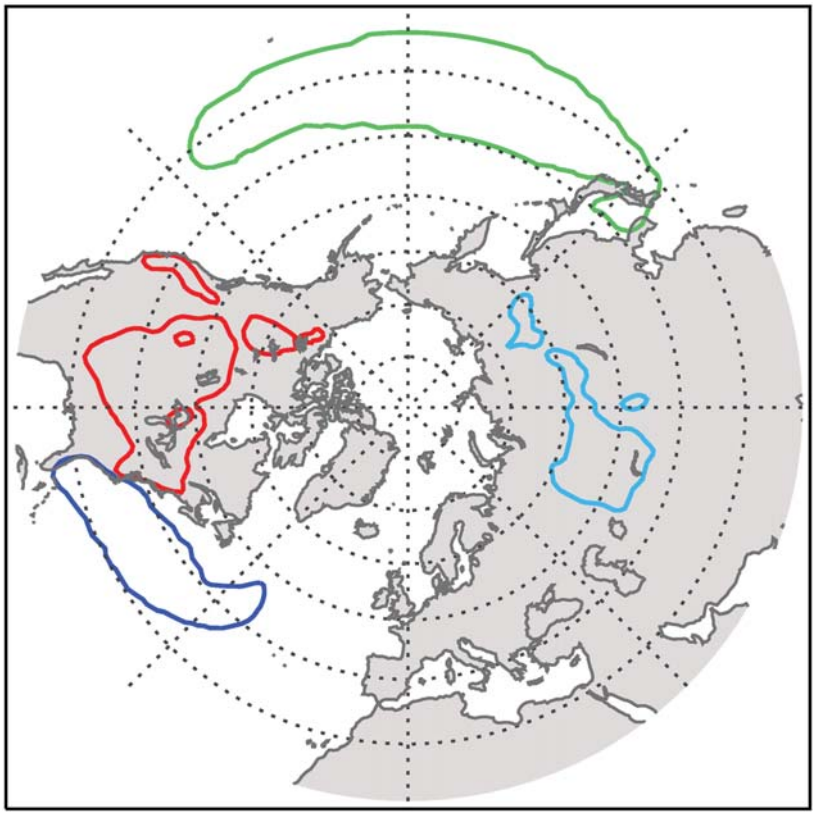

Figure 6. Moisture source contours for the forward experiment. Red contour line represents the North American moisture source, green represents the Pacific source, and light and dark blue lines represent the Siberian and Atlantic sources. North American and Siberian sources are defined as summer sources and Atlantic and Pacific Oceans as annual ones. Contour lines represent areas where the 10 day integrated ($E-P$) value is greater than 4 mm/d as a mean for the corresponding period.

than 8% on sources extension), the Pacific source is clearly less evaporative than this continental source (nearly 20% lower ($E-P$)i10 than Siberian source).

3.2. Moisture Contribution From the Main Sources of Moisture Into the Arctic Domain

Forward analysis is a useful tool for the study of the contribution of moisture from the sources to the Arctic domain. For this purpose the seasonal patterns of ($E-P$)i10 were calculated over the period 1980–2012 for the four major sources of moisture: Atlantic, Pacific, North American, and Siberian. These sources were defined taking into account only those months when they appear, i.e., the whole year for the oceanic sources and just the summer for the continental ones (Figure 6).

Because we are interested in the moisture loss over the region from each source, only ($E-P$)i10 with negative values (($E-P$)i10 <0) were computed over the Arctic domain. Hereafter, we denote the moisture that comes from the sources to the Arctic as PFLEX. The positive values of the balance of ($E-P$)i10 were subtracted at the end of the computation, following the methodology of *Castillo et al.* [2014b], who demonstrated that in this way the general net ($E-P$)i10 <0 is unaffected.

Table 1 shows the total ($E-P$)i10 <0 contribution (PFLEX) over the Arctic domain from the major sources. In summer, most of the PFLEX contribution comes from Pacific Ocean (40%), followed by the continental sources over North America (30%) and Siberia (18%), while the oceanic Atlantic source represents the lowest contribution (12%) during this season. The Pacific Ocean appears as the source with the maximum PFLEX contribution over the Arctic domain for all seasons, showing its maximum values in summer and minimum in winter. The Atlantic source reaches a maximum during autumn. The North American source far exceeds the Siberian one in importance.

Table 1. Seasonal PFLEX (10 day Integrated $(E-P)<0$) Total Value Calculated as the Total Contribution to the Arctic Domain From the Atlantic Ocean (Atl), Pacific Ocean (Pac), North America (NA), and Siberia (Sib)[a]

	Spring	Summer	Autumn	Winter
ATL	3154.95	3478.37	4071.99	3140.18
PAC	7081.58	11774.80	7906.81	6363.84
NA		8794.73		
SIB		5378.51		

[a]Units are in mm d^{-1}.

Figure 7 shows the plot for the main moisture PFLEX sinks that come from the four main sources. The general pattern is similar for all seasons for the two oceanic sources, which follow a similar pattern: the major sink is located in the corresponding ocean within the Arctic domain and positioned to the northeast of its respective source. The Pacific Ocean appears to be the source with a PFLEX contribution that is spread more widely in the cold season. During summer and focusing on the continental sources, for the North American source the main sinks are over Eastern Canada with an expansion toward the Atlantic Ocean, and for the Siberian source the sink is located over the Russian part of the Arctic domain, to the north and south of the source. Siberian moisture contribution north of the source agrees with previous results which found an important influence of Siberia in precipitation over the Eurasian Arctic watersheds [*Serreze et al.*, 2002; *Serreze and Etringer*, 2003].

3.3. Changes in the Transport of Moisture: The Influence of Evaporation in the Sources and Teleconnection Patterns

Changes in the transport of moisture and its related PFLEX may be related either to alterations in the moisture sources due to changes in circulation patterns or to changes in the intensity of the moisture sources due to enhanced evaporation, or to a combination of these two mechanisms.

At interannual scales, changes in both the intensity of the source [*Seager et al.*, 2010; *Gimeno et al.*, 2013] and in the circulation [*Nieto et al.*, 2014; *Castillo et al.*, 2014a] could be relevant. The former is addressed here by analyzing how differences in evaporation over the sources are also linked with patterns of climate variability, while the latter is addressed by considering the influence of the major teleconnection patterns on the Arctic domain moisture supply related to each source (PFLEX).

To address the influence of precipitation on PFLEX over the Arctic domain, we compare the behavior of the time series of the anomalous supply of moisture over the Arctic (($E-P$)i10 <0) that comes from each source calculated from FLEXPART (PFLEX) with the time series of the anomalous evaporation over the sources. Evaporation data were obtained for oceanic sources from OAFlux data product (annual and seasonal) and, in the case of continental sources, from GLEAM data (only for summer, when these sources are important).

To quantify the relationship between moisture supply and evaporation, Table 2 shows the correlations between PFLEX with the anomaly evaporation time series (only significant values at 90% are shown). For the oceanic sources, positive significant correlations appear only for the Pacific source in summer and autumn (therefore, the PFLEX contribution changes in the same sense as the evaporation), but negative values appear during winter. For the continental sources, North America shows a positive correlation of 0.46, but no relationship is detected for the Siberian time series.

Correlations between the PFLEX time series and the major teleconnection patterns are also shown in Table 2 for each source. On this analysis positive correlations suggest that PFLEX varies in the same way that the teleconnection indices, being the positive (negative) phase of the index associated with increased (decreased) contribution. The opposite interpretation is valid for negative correlations. In this case, correlations were only calculated with those patterns that had some relevant fingerprint over the area of influence. For the *Atlantic moisture source* significant negative correlations appear with the EA pattern for summer and winter, and during autumn with EATL/WRUS. The PFLEX time series from the *Pacific source* shows a significant negative correlation with PNA for all seasons and a positive one with WP in spring and summer and with TNH in winter. When *North America* is analyzed (only for summer), a negative correlation with moisture supply appears for EP-NP and WP. For the moisture supply from the *Siberian* source, negative significant correlations appear with EP-NP and PT. It is important to highlight that, despite significant correlations, they are relatively low being in most of the cases lower than 0.5.

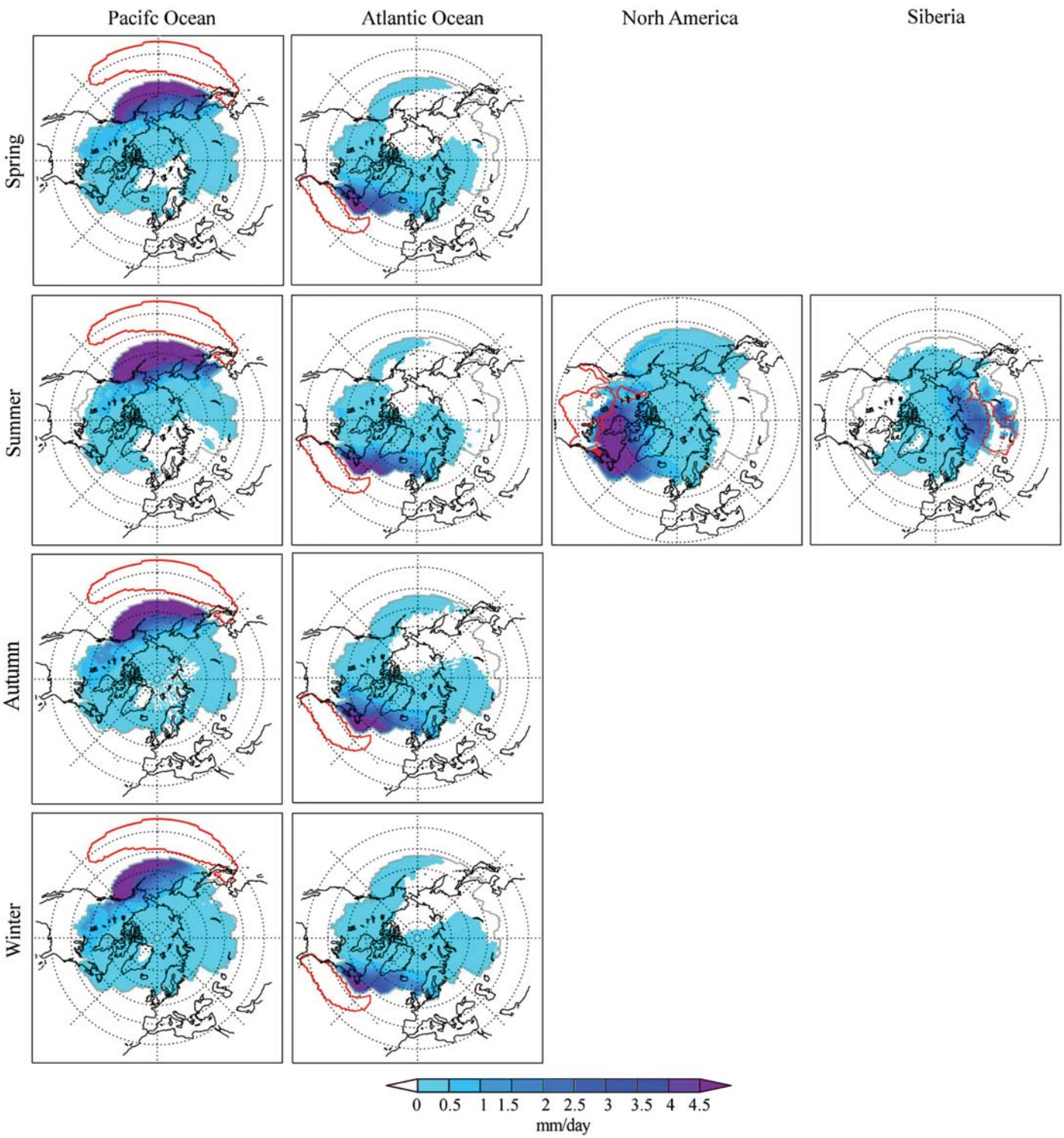

Figure 7. Climatological seasonal PFLEX fields (10 day integrated $(E - P) < 0$), measured in mm d^{-1}, from major moisture sources for the period 1980–2012. Red contour line represents moisture sources as defined in Figure 6, and the grey contour lines represent the Arctic domain.

Table 2. Linear Pearson Correlation of PFLEX (10 day Integrated $(E-P)<0$) Interannual Contribution Time Series With Evaporation (Calculated From OAFlux and GLEAM) and Principal Northern Hemisphere Teleconnection Index Time Series[a]

		Spring	Summer	Autumn	Winter
ATL	EA		−0.382		−0.456
	EATL/WRUS			−0.478	
PAC	EVAP		0.327	0.347	−0.323
	PNA	−0.544	−0.493	−0.319	−0.676
	WP	0.500	0.317		
	TNH				0.653
NA	EVAP		0.462		
	EP-NP		−0.328		
	WP		−0.455		
SIB	EP-NP		−0.343		
	PT		−0.346		

[a]The correlation was calculated seasonally for every source for the period 1980–2012. Correlation results are only shown when the correlation is significant at 90%.

These results reflect the dynamics related to the patterns of variability over the regions. To illustrate the coherence of these correlations, in Figure 8 we show those loading patterns which have some of their action center affecting one of the main sources. In this figure, at every grid point the correlation between the teleconnection pattern time series and the monthly standardized height anomalies (in 500 mb) is represented as defined by NOAA (http://www.cpc.ncep.noaa.gov). Maps presented show the positive phase of teleconnection patterns (showing significant correlation), related with decreased PFLEX contribution from Atlantic, North America, and Siberia moisture sources. For the Pacific moisture source, PNA positive phase is related with decreased contribution and the opposite relation occurs for the remaining patterns. For the Atlantic moisture source, during the positive phase of EA, a positive anomaly in the geopotential field dominates over the mid-North Atlantic, and negative anomalies appear to the north. In summer (July) the Atlantic moisture source (blue contour in Figure 8) is positioned under the influence of the high anomaly center, so the moisture that comes from it remains at midlatitudes forced by the anticyclonic circulation (or it moves eastward), resulting in a lower amount of moisture into the Arctic domain. During winter (January) the intensification of the dipole in EA acts to favor a zonal circulation, avoiding the northward transport of moisture from the Atlantic source. For EATL/WRUS in autumn (October) the influence of a low anomaly center over the eastern part of the source increases the loss of moisture outside the Arctic domain and makes difficult the northward transport.

For the case of PNA, and analyzing only the influence of the pattern over the Pacific Ocean, the teleconnection consists of a dipole with high positive anomalies to the south and below-average values to the north; this configuration leads to a more zonal flow that prevents moisture from arriving in the Arctic system from the Pacific source. The positive correlation of Pacific PFLEX contribution with WP might be related with the lower height values over eastern Russia and the intensification of height values over the source. This pattern produces a stronger north-south gradient that brings moisture to the Bering Strait. This increased precipitation associated with positive values in WP index is in agreement with results obtained by NOAA (http://www.cpc.ncep.noaa.gov/data/teledoc/wp_pmap.shtml). In the case of TNH, the positive phase of the pattern is associated with higher height values over the Gulf of Alaska in winter. This can reduce the loss of moisture over the coast and produce a more efficient transport into the domain.

For EP-NP and WP in relation to North American source, the intensification of Pacific High (west of the source) and lower than normal height values on the east part of the source may increase the southeastward transport and produce higher loss of moisture outside of the domain.

And finally, for the moisture supply from Siberian source, significant correlation has not been found with any of the teleconnection patterns affecting the source.

4. Summary and Concluding Remarks

In this study, the Lagrangian model FLEXPART was used to analyze moisture sources for the Arctic domain, and their contribution to the Arctic moisture availability at seasonal and annual scales over the 33 year

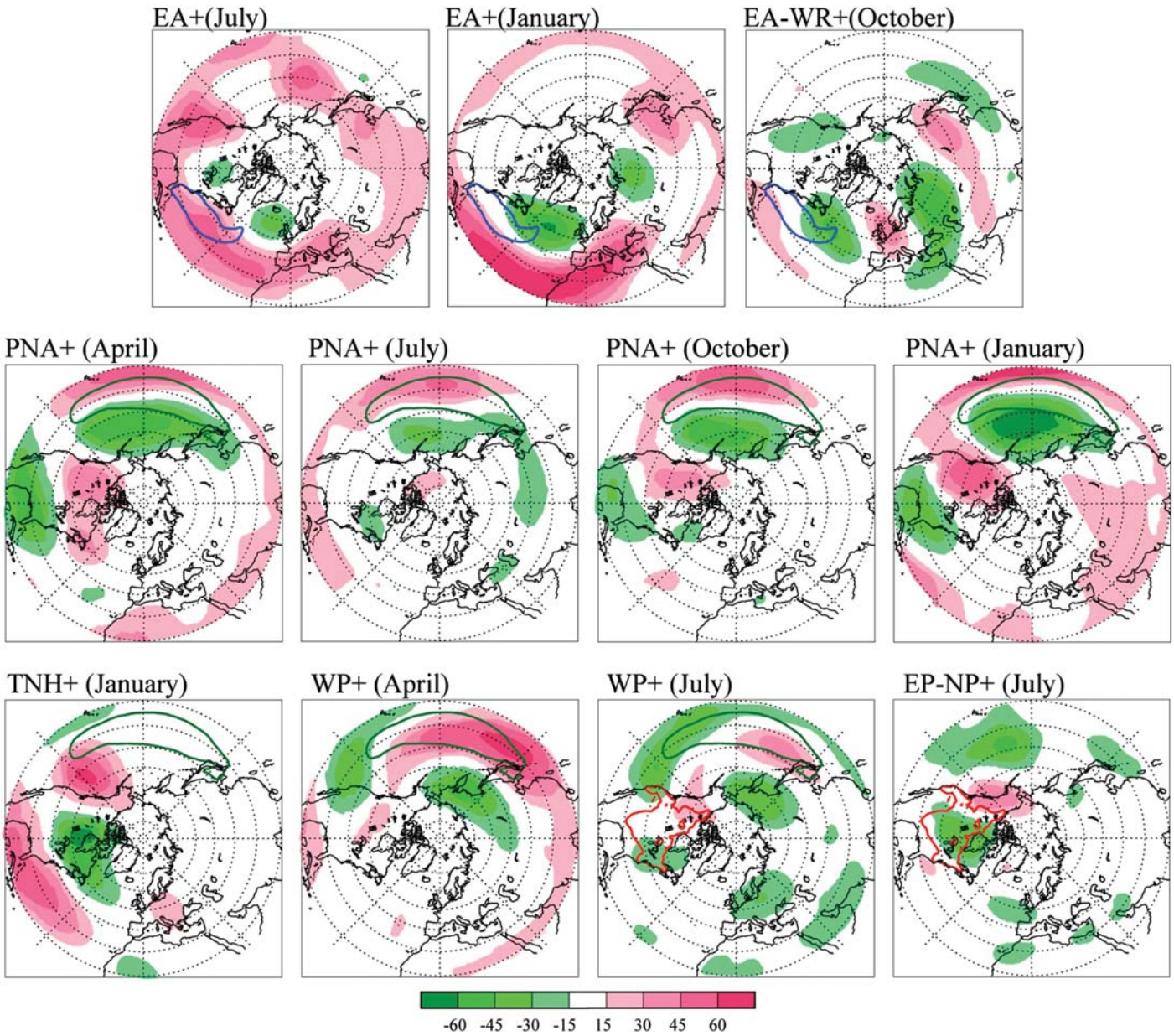

Figure 8. The positive phase of the teleconnection patterns defined by NOAA as the correlation between teleconnection index time series and 500 mb height anomalies at every grid point. Pinkish colors represent that areas with a positive correlation and greenish colors a negative correlation. Only those patterns presenting significant correlations with moisture supply time series (at 90%) and with at least one the action centers affecting the source area are shown. Black contour lines represent the sources as defined for the forward experiment.

period 1980–2012. This long temporal domain has allowed an accurate and meaningful determination of Arctic sources and their contribution to moisture input into the system, together with an assessment of their variability.

The results thus obtained have allowed us to identify four major sources for the Arctic region: subtropical and southern extratropical Atlantic and Pacific Oceans, North America, and Siberia. The Atlantic and particularly the Pacific Oceans appear as dominant sources with an influence throughout the year. These sources show maximum values in winter both in extent and intensity; however, in summer they appear weakened and the continental sources (North America and Siberia) gain in importance. In general terms, these results for the location and seasonal variability of moisture sources show good agreement with previous work such

as the origins of precipitable water flux in *Groves and Francis* [2002b] and areas of positive meridional moisture flux in *Jakobson and Vihma* [2010]. Each moisture source has been shown to have a different area of influence over the system. In general, the major sources contribute to a moisture supply mostly to the northeast of the source itself.

Despite the seasonal variability of the evaporation from the oceanic moisture sources, showing maximum values in winter, their moisture supply is greater during summer, and this discrepancy supports the findings of a previous study [*Jakobson and Vihma*, 2010]. The estimation of the total moisture input into the system shows higher values in summer too, with lowest values in winter. Similar results have been observed by different authors [*Jakobson and Vihma*, 2010; *Dickson et al*., 2000; *Sorteberg and Walsh*, 2008]. *Sorteberg and Walsh* [2008] suggested the abundance of moisture in the summer as the cause of the amplified moisture transport.

Moisture supply over the Arctic has been shown to be slightly influenced by teleconnection patterns. However, the relationship is not strong enough to confirm the findings of previous studies. *Rogers et al*. [2001] found a positive significant correlation between NAO index and moisture budget over the system for winter. In the present study such a clear relationship cannot be seen, in the sense that no significant positive correlation was found for this season with any. Our results suggest a generally greater influence of EA for the Atlantic source and of WP or PNA for the Pacific one. Changes in the evaporation over the sources do not seem to have a significant relationship with the variability of the moisture supply into the Arctic at an interannual scale.

Despite the important advantages of this Lagrangian methodology compared with other approaches, it also has some limitations. The concept of a net uptake of moisture is restricted by the ability of FLEXPART to track those regions where particles have absorbed or expelled moisture before reaching the Arctic. In regard to moisture characterization, the method follows air parcels backward from the Arctic domain and computes the uptake of moisture. However, the uptake of moisture does not necessarily imply that the moisture will contribute to precipitation. An overestimate of the moisture sources is therefore possible.

Finally, the present study points toward some interesting perspectives on future investigations. Of primary interest might be a more detailed study of the Arctic domain, taking into account separately subareas and periods such as regions of high ice-melt or regions with trends in moisture transport, together with an analysis of any mechanisms of moisture transport affecting these regions such as atmospheric rivers or cyclones. The investigation of how the sources might change in future in the context of a changing climate represents a considerable challenge and could also be the subject of a future paper.

Acknowledgments
The authors acknowledge funding by the European ERA.Net RUS programme, within the project ACPCA, by Salvador Madariaga program under grant PR2015/00011 and by the Spanish government within the EVOCAR (CGL2015-65141-R) project, which is also funded by FEDER (European Regional Development Fund). Raquel Nieto was also supported by the Brazilian government through the CNPq grant 314734/2014-7. We would like to acknowledge the three anonymous reviewers whose comments helped us to improve the manuscript. The data used are available in the following Web pages: Era-Interim data are provided by the ECMWF on http://apps.ecmwf.int/datasets/data/interim-full-daily/levtype=sfc/, GLEAM data are available under request at http://www.gleam.eu/, OAFlux data can be found at http://oaflux.whoi.edu/data.html, and teleconnection pattern indices can be found at http://www.cpc.ncep.noaa.gov/.

References

Aagaard, K., and P. Greisman (1975), Toward new mass and heat budgets for the Arctic Ocean, *J. Geophys. Res.*, *80*(27), 3821–3827, doi:10.1029/JC080i027p03821.

Barnston, A. G., and R. E. Livezey (1987), Classification, seasonality and persistence of low-frequency atmospheric circulation patterns, *Mon. Weather Rev.*, *115*, 1083–1126.

Castillo, R., R. Nieto, A. Drumond, and L. Gimeno (2014a), The role of the ENSO cycle in the modulation of moisture transport from major oceanic moisture sources, *Water Resour. Res.*, *50*, 1046–1058, doi:10.1002/2013WR013900.

Castillo, R., R. Nieto, A. Drumond, and L. Gimeno (2014b), Estimating the temporal domain when the discount of the net evaporation term affects the resulting net precipitation pattern in the moisture budget using a 3-D Lagrangian approach, *PLoS One*, *9*(6), e99046, doi:10.1371/journal.pone.0099046.

Cavalieri, D. J., and C. L. Parkinson (2012), Arctic sea ice variability and trends, 1979–2010, *Cryosphere*, *6*, 881–889, doi:10.5194/tc-6-881-2012.

Chang, E. K. M., S. Lee, and K. L. Swanson (2002), Storm track dynamics, *J. Clim.*, *15*, 2163–2183.

Comiso, J. C. (2006), Arctic warming signals from satellite observations, *Weather*, *61*, 70–76, doi:10.1256/wea.222.05.

Cullather, R. I., D. H. Bromwich, and M. C. Serreze (2000), The atmospheric hydrologic cycle over the Arctic Basin from reanalyses. Part I: Comparison with observations and previous studies, *J. Clim.*, *13*, 923–937, doi:10.1175/1520-0442(2000)013<0923:TAHCOT>2.0.CO;2.

Dee, D. P., et al. (2011), The ERA-Interim reanalysis: Configuration and performance of the data assimilation system, *Q. J. R. Meteorol. Soc.*, *137*, 553–597, doi:10.1002/qj.828.

Dickson, R. R., T. J. Osborn, J. W. Hurrell, J. Meincke, J. Blindheim, B. Adlandsvik, T. Vinje, G. Alekseev, and W. Maslowski (2000), The Arctic Ocean response to the North Atlantic Oscillation, *J. Clim.*, *13*, 2671–2696, doi:10.1175/1520-0442(2000)013<2671:TAORTT>2.0.CO;2.

Dirmeyer, P. A., and K. L. Brubaker (2007), Characterization of the global hydrologic cycle from a back-trajectory analysis of atmospheric water vapor, *J. Hydrometeorol.*, *8*, 20–37, doi:10.1175/JHM557.1.

Dodds, K. (2010), Flag planting and finger pointing: The Law of the Sea, the Arctic and the political geographies of the outer continental shelf, *Political Geogr.*, *29*(2), 63–73.

Dole, R., M. Hoerling, J. Perlwitz, J. Eischeid, P. Pegion, T. Zhang, X.-W. Quan, T. Xu, and D. Murray (2011), Was there a basis for anticipating the 2010 Russian heat wave?, *Geophys. Res. Lett.*, *38*, L06702, doi:10.1029/2010GL046582.

Drumond, A., J. Marengo, T. Ambrizzi, R. Nieto, L. Moreira, and L. Gimeno (2014), The role of the Amazon Basin moisture in the atmospheric branch of the hydrological cycle: A Lagrangian analysis, *Hydrol. Earth Syst. Sci.*, *18*, 2577–2598, doi:10.5194/hess-18-2577-2014.

Ford, J. D. (2009), Dangerous climate change and the importance of adaptation for the Arctic's Inuit population, *Environ. Res. Lett.*, *4*(2), 024006, doi:10.1088/1748-9326/4/2/024006.

Gimeno, L., A. Stohl, R. M. Trigo, F. Dominguez, K. Yoshimura, L. Yu, A. Drumond, A. M. Durán-Quesada, and R. Nieto (2012), Oceanic and terrestrial sources of continental precipitation, *Rev. Geophys.*, *50*, RG4003, doi:10.1029/2012RG000389.

Gimeno, L., R. Nieto, A. Drumond, R. Castillo, and R. M. Trigo (2013), Influence of the intensification of the major oceanic moisture sources on continental precipitation, *Geophys. Res. Lett.*, *40*, 1443–1450, doi:10.1002/grl.50338.

Gimeno, L., M. Vázquez, R. Nieto, and R. M. Trigo (2015), Atmospheric moisture transport: The bridge between ocean evaporation and Arctic ice melting, *Earth Syst. Dyn.*, *6*, 583–589, doi:10.5194/esd-6-583-2015.

Groves, D. G., and J. A. Francis (2002a), Moisture budget of the Arctic atmosphere from TOVS satellite data, *J. Geophys. Res.*, *107*(D19), 4391, doi:10.1029/2001JD001191.

Groves, D. G., and J. A. Francis (2002b), Variability of the Arctic atmospheric moisture budget from TOVS satellite data, *J. Geophys. Res.*, *107*(D24), 4785, doi:10.1029/2002JD002285.

Hanssen-Bauer, I., and E. J. Førland (1998), Long-term trends in precipitation and temperature in the Norwegian Arctic: Can they be explained by changes in atmospheric circulation patterns?, *Clim. Res.*, *10*, 143–153.

Jakobson, E., and T. Vihma (2010), Atmospheric moisture budget in the Arctic based on the ERA-40 reanalysis, *Int. J. Climatol.*, *30*, 2175–2194, doi:10.1002/joc.2039.

Johnsen, S. J., W. Dansgaard, and J. W. C. White (1989), The origin of Arctic precipitation under present and glacial conditions, *Tellus, Ser. B.*, *41*(4), 452–468.

Kaser, G., J. G. Cogley, M. B. Dyurgerov, M. F. Meier, and A. Ohmura (2006), Mass balance of glaciers and ice caps: Consensus estimates for 1961–2004, *Geophys. Res. Lett.*, *33*, L19501, doi:10.1029/2006GL027511.

Kattsov, V. M., J. E. Walsh, W. L. Chapman, V. A. Govorkova, T. V. Pavlova, and X. Zhang (2007), Simulation and projection of Arctic freshwater budget components by the IPCC AR4 global climate models, *J. Hydrometeorol.*, *8*, 571–589.

Kopec, B. G., X. Feng, F. A. Michel, and E. S. Posmentier (2016), Influence of sea ice on Arctic precipitation, *Proc. Natl. Acad. Sci. U.S.A.*, *113*, 46–51, doi:10.1073/pnas.1504633113.

Kurita, N. (2011), Origin of Arctic water vapor during the ice-growth season, *Geophys. Res. Lett.*, *38*, L02709, doi:10.1029/2010GL046064.

Liu, C., and E. A. Barnes (2015), Extreme moisture transport into the Arctic linked to Rossby wave breaking, *J. Geophys. Res. Atmos.*, *120*, 3774–3788, doi:10.1002/2014JD022796.

Maslowski, W., J. C. Kinney, M. Higgins, and A. Roberts (2012), The future of Arctic Sea ice, *Annu. Rev. Earth Planet. Sci.*, *40*, 625–654, doi:10.1146/annurev-earth-042711-105345.

Miralles, D. G., T. R. H. Holmes, R. A. M. De Jeu, J. H. Gash, A. G. C. A. Meesters, and A. J. Dolman (2011), Global land-surface evaporation estimated from satellite-based observations, *Hydrol. Earth Syst. Sci.*, *15*, 453–469, doi:10.5194/hess-15-453-2011.

Newman, M., G. N. Kiladis, K. M. Weickmann, F. M. Ralph, and P. D. Sardeshmukh (2012), Relative contributions of synoptic and low-frequency eddies to time-mean atmospheric moisture transport, including the role of atmospheric rivers, *J. Clim.*, *25*(21), 7341–7361.

Nieto, R., L. Gimeno, D. Gallego, and R. Trigo (2007), Contributions to the moisture budget of airmasses over Iceland, *Meteorol. Z.*, *16*, 37–44.

Nieto, R., R. Castillo, and A. Drumond (2014), The modulation of oceanic moisture transport by the hemispheric annular modes, *Front. Earth Sci.*, *2*, 1–12, doi:10.3389/feart.2014.00011.

Numagati, A. (1999), Origin and recycling processes of precipitation water over the Eurasian continent: Experiments using an atmospheric general circulation model, *J. Geophys. Res.*, *104*, 1957–1972, doi:10.1029/1998JD200026.

Oort, A. H. (1975), Year-to-year variations in the energy balance of the Arctic atmosphere, *J. Geophys. Res.*, *79*, 1253–1260, doi:10.1029/JC079i009p01253.

Peixoto, J. P., and H. Oort (1992), *Physics of Climate*, pp. 520, American Institute of Physics, New York.

Prowse, T., A. Bring, J. Mård, E. Carmack, M. Holland, A. Instanes, T. Vihma, and F. J. Wrona (2015), Arctic freshwater synthesis: Summary of key emerging issues, *J. Geophys. Res. Biogeosci.*, *120*, 1887–1893, doi:10.1002/2015JG003128.

Roberts, A., et al. (2010), A science plan for Regional Arctic System Modeling: A report to the National Science Foundation from the International Arctic Science Community International Arctic Research Center Technical Papers 10-0001.

Rogers, A. N., D. H. Bromwich, E. N. Sinclair, and R. I. Cullather (2001), The atmospheric hydrologic cycle over the Arctic Basin from Reanalyses. Part II: Interannual variability, *J. Clim.*, *14*, 2414–2429, doi:10.1175/1520-0442(2001)014<2414:TAHCOT>2.0.CO;2.

Screen, J. A., and I. Simmonds (2010), The central role of diminishing sea ice in recent Arctic temperature amplification, *Nature*, *464*, 1334–1337, doi:10.1038/nature09051.

Seager, R., N. Naik, and G. A. Vecchi (2010), Thermodynamic and dynamic mechanisms for large-scale changes in the hydrological cycle in response to global warming, *J. Clim.*, *23*, 4651–4668, doi:10.1175/2010JCLI3655.1.

Serreze, M. C., and A. J. Etringer (2003), Precipitation characteristics of the Eurasian Arctic drainage system, *Int. J. Climatol.*, *23*, 1267–1291, doi:10.1002/joc.941.

Serreze, M. C., and J. Stroeve (2015), Arctic sea ice trends, variability and implications for seasonal ice forecasting, *Philos. Trans. R. Soc., A*, *373*(2045), 20140159, doi:10.1098/rsta.2014.0159.

Serreze, M. C., D. H. Bromwich, M. P. Clark, A. J. Ertringer, T. Zhang, and R. Lammers (2002), Large-scale hydro-climatology of the terrestrial Arctic drainage system, *J. Geophys. Res.*, *108*(D2), 8160, doi:10.1029/2001JD000919.

Serreze, M. C., A. Barrett, J. Stroeve, D. Kindig, and M. Holland (2009), The emergence of surface-based Arctic amplification, *Cryosphere*, *3*, 11–19, doi:10.5194/tc-3-11-2009.

Sodemann, H., C. Schwierz, and H. Wernli (2008), Interannual variability of Greenland winter precipitation sources: Lagrangian moisture diagnostic and North Atlantic Oscillation influence, *J. Geophys. Res.*, *113*, D03107, doi:10.1029/2007JD008503.

Sorteberg, A., and J. E. Walsh (2008), Seasonal cyclone variability at 70 N and its impact on moisture transport into the Arctic, *Tellus, Ser. A*, *60*, 570–586.

Stohl, A., and P. A. James (2005), A Lagrangian analysis of the atmospheric branch of the global water cycle. Part II: Moisture transports between Earth's ocean basins and river catchments, *J. Hydrometeorol.*, *6*, 961–984, doi:10.1175/JHM470.1.

Stohl, A., and P. James (2004), A Lagrangian analysis of the atmospheric branch of the global water cycle. Part I: Method description, validation, and demonstration for the August 2002 flooding in central Europe, *J. Hydrometeorol.*, *5*, 656–678, doi:10.1175/1525-7541(2004)005<0656:ALAOTA>2.0.CO;2.

Stohl, A., C. Forster, A. Frank, P. Seibert, and G. Wotawa (2005), Technical note: The Lagrangian particle dispersion model FLEXPART version 6.2, *Atmos. Chem. Phys.*, *5*, 2461–2474, doi:10.5194/acp-5-2461-2005.

Stohl, A., C. Forster, and H. Sodemann (2008), Remote sources of water vapor forming precipitation on the Norwegian west coast at 60 N—A tale of hurricanes and an atmospheric river, *J. Geophys. Res.*, *113*, D05102, doi:10.1029/2007JD009006.

Tavolato, C., and L. Isaksen (2011), *Data Usage and Quality Control for ERA-40, ERA-Interim, and the Operational ECMWF Data Assimilation System*, *ERA Rep. Ser.*, vol. 7, European Centre for Medium Range Weather Forecasts, Shinfield Park, Reading, Berkshire, U. K.

Tilinina, N., S. K. Gulev, I. Rudeva, and P. Koltermann (2013), Comparing cyclone life cycle characteristics and their interannual variability in different reanalyses, *J. Clim.*, *26*, 6419–6438, doi:10.1175/JCLI-D-12-00777.1.

Trenberth, K. E., J. T. Fasullo, and J. Mackaro (2011), Atmospheric moisture transports from ocean to land and global energy flows in reanalyses, *J. Clim.*, *24*, 4907–4924, doi:10.1175/2011JCLI4171.1.

Tyrlis, E., and B. J. Hoskins (2008), Aspects of a Northern Hemisphere atmospheric blocking climatology, *J. Atmos. Sci.*, *65*, 1638–1652.

Velicogna, I. (2009), Increasing rates of ice mass loss form the Greenland and Antarctic ice sheets revealed by GRACE, *Geophys. Res. Lett.*, *36*, L19503, doi:10.1029/2009GL040222.

Wegmann, M., Y. Orsolini, M. Vázquez, L. Gimeno, R. Nieto, O. Bulygina, R. Jaiser, D. Handorf, A. Rinke, and K. Dethloff (2015), Arctic moisture source for Eurasian snow cover variations in autumn, *Environ. Res. Lett.*, *10*, 5.

White, D., et al. (2007), The Arctic freshwater system: Changes and impacts, *J. Geophys. Res.*, *112*, G04S54, doi:10.1029/2006JG000353.

Woods, C., R. Caballero, and G. Svensson (2013), Large-scale circulation associated with moisture intrusions into the Arctic during winter, *Geophys. Res. Lett.*, *40*, 4717–4721, doi:10.1002/grl.50912.

Yu, L. (2007), Global variations in oceanic evaporation (1958–2005): The role of the changing wind speed, *J. Clim.*, *20*, 5376–5390.

Yu, L., X. Jin, and R. A. Weller (2008), Multidecade global flux datasets from the objectively analyzed air-sea fluxes (OAFlux) Project: Latent and sensible heat fluxes, ocean evaporation, and related surface meteorological variables OAFlux Project Tech. Rep. OA-2008-01, 64 pp., Woods Hole Oceanographic Institution, Woods Hole, Mass.

Zhang, X., J. He, J. Zhang, I. Polyakov, R. Gerdes, J. Inoue, and P. Wu (2012), Enhanced poleward moisture transport and amplified northern high-latitude wetting trend, *Nat. Clim. Change*, *3*, 47–51, doi:10.1038/nclimate1631.

atmosphere

MDPI

Article

Extreme Sea Ice Loss over the Arctic: An Analysis Based on Anomalous Moisture Transport

Marta Vázquez [1,*], Raquel Nieto [1,2], Anita Drumond [1] and Luis Gimeno [1]

[1] Environmental Physics Laboratory (EPhysLab), Facultade de Ciencias, Universidad de Vigo, Ourense 32004, Spain; rnieto@uvigo.es (R.N.); anitadru@uvigo.es (A.D.); l.gimeno@uvigo.es (L.G.)

[2] Department of Atmospheric Sciences, Institute of Astronomy, Geophysics and Atmospheric Sciences, University of São Paulo, São Paulo 05508-090, Brazil

* Correspondence: martavazquez@uvigo.es

Academic Editor: Anthony R. Lupo

Received: 18 November 2016; Accepted: 3 February 2017; Published: 7 February 2017

Abstract: The Arctic system has experienced in recent times an extreme reduction in the extent of its sea ice. The years 2007 and 2012 in particular showed maxima in the loss of sea ice. It has been suggested that such a rapid decrease has important implications for climate not only over the system itself but also globally. Understanding the causes of this sea ice loss is key to analysing how future changes related to climate change can affect the Arctic system. For this purpose, we applied the Lagrangian FLEXible PARTicle dispersion (FLEXPART) model to study the anomalous transport of moisture for 2006/2007 and 2011/2012 in order to assess the implications for the sea ice. We used the model results to analyse the variation in the sources of moisture for the system (backward analysis), as well as how the moisture supply from these sources differs (forward analysis) during these years. The results indicate an anomalous transport of moisture for both years. However, the pattern differs between events, and the anomalous moisture supply varies both in intensity and spatial distribution for all sources.

Keywords: Arctic system; moisture supply; Lagrangian method

1. Introduction

The Arctic system has been experiencing strong reductions in sea ice over the past few decades [1–4], and the decrease is expected to continue under global warming [5,6]. The observed decreases have affected not only the extent but also the thickness and the volume of the ice [7]. For the period 1979–2010, the annual mean extent of sea ice showed a decrease of more than 4% per decade [8]. While a decreasing trend for the total extent of Arctic sea ice is apparent for all months [8,9], the trend is greatest in summer [1,10], when the sea ice extent is at its lowest annual value [11–14]. The month showing the minimum sea ice is September, with a downward trend of more than 12% per decade for the period 1979–2010 [1,10]. Reductions in sea ice have important implications locally, affecting heat budgets [15] and precipitation [16], but the effects are also external and global. Some authors suggest that sea ice reductions have implications for atmospheric circulation by affecting mid-latitudinal winter snowfall [17] or summer precipitation [18]. A detailed review of sea ice reductions and their effects is available in Vihma [19].

The years 2007 and 2012 had the minima September sea ice extent over recent decades, with anomalies of −1.6 and −2.3 million km^2 respectively compared with the 1981–2010 climatological mean [19]. The sea ice data from the National Snow and Ice Data Center (NSIDC) [20] shown in Figure 1 reveal the reduction in September sea ice extent in 2007 (green) and 2012 (dark blue) compared to the 1981–2010 mean (red line). Major reductions have been seen north of the Bering Strait, over the Laptev, East Siberian, Chukchi and Beaufort Seas. Especially remarkable are the reductions north of

Eurasia in 2007 and north of Alaska in 2012. Some reductions also appear over the Barents and Kara Seas and over the Canadian Arctic Archipelago, especially in 2012. A number of studies have recently been undertaken to assess the possible causes of the sea ice reduction. These causes were summarised by Meier et al. [9], Stroeve et al. [14], and Polyakov et al. [21]. The recent change in the perennial sea ice [22,23] is considered one of the most important reasons for the decrease in sea ice volume by several authors. However, variations in the hydrological cycle can affect sea ice too, and in some reports the reduction in sea ice has been related to increased river discharge [24–26] or storm activity [27,28].

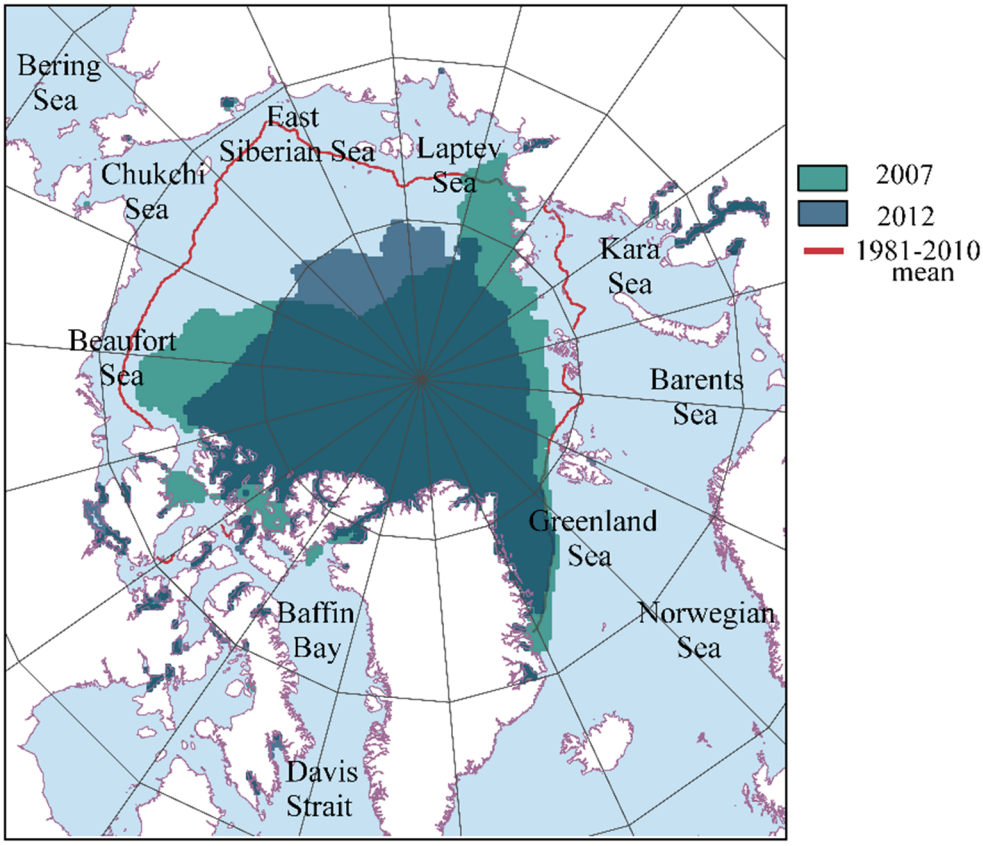

Figure 1. September minimum sea ice extent for the years 2007 (green) and 2012 (dark blue), with climatological 1981–2010 mean (red contour). Data obtained from National Snow and Ice Data Center (NSIDC).

Atmospheric moisture transport has an important role in sea ice extent variations. The increase in cloud cover or water vapour over the Arctic have been suggested as one of the main causes of the downwelling longwave flux [29,30], which is considered to be closely related with sea ice extent [29,31]. The relation between the amplified moisture transport toward norther latitudes and its influence on river discharge was demonstrated by Zhang et al. [32]. Several authors have discussed the recent increase in river discharge over the Arctic (e.g., [33,34]), and it was determined that the river discharge has an influence over the Arctic system in different ways [24]. Although its influence on sea ice extent remains unclear, several studies have suggested a link between river runoff and summer ice melt or early freezing [25,26,35].

Moisture transport is a key component of the hydrological cycle and its study could be helpful in the analysis of changes observed in the climate system [36]. In the present study, we analyse anomalous moisture transport into the Arctic system for the years of observed minimum sea ice extent: 2007 and 2012. For this purpose, we employed the Lagrangian FLEXible PARTicle dispersion (FLEXPART) model [37,38] to assess variations in arctic moisture sources, and to observe how the

moisture contribution from these sources into the Arctic varied for 2007 and 2012, as a means of investigating the possible relationship between variations in moisture supply over the main arctic river basins and any reductions in sea ice. Lagrangian techniques have been widely applied for evaluating moisture transport (e.g., [39,40]). The main advantages and disadvantages of this methodology were addressed by Gimeno et al. [41], and an intercomparision was made between the different methodologies applied with this purpose.

2. Experiments

In order to analyse anomalous moisture transport into the Arctic linked to sea ice retreat, a Lagrangian methodology based on the FLEXPART v9.0 particle dispersion model [37,38] was applied. The Arctic domain used for this work was defined by Roberts et al. [42] as "the geosphere and biosphere north of the boreal mean decadal 10 °C sea surface isotherm, the surface air 0 °C contour that encircles the North Pole, and the southern limit of terrain that drains into the High Arctic". This appears in Figure 2 in the light and dark blue, red and dark pink filled regions. The FLEXPART model employs the global reanalysis data from ERA-Interim with a 1° regular grid and 61 vertical levels, obtained from the European Centre for Medium-Range Weather Forecast (ECMWF) [43], and tracks atmospheric moisture along trajectories. The 3-D wind field is used to move many (near 2 million) so-called particles (air parcels) that result from the homogeneous division of the atmosphere. For each air parcel, the specific humidity (q) and position (latitude, longitude, and altitude) are stored at 6-h intervals.

Changes in the specific humidity of the particle are related to increases (e) and decreases in moisture (p) by the equation:

$$e - p = m(dq/dt),$$

where m is the mass of the particle and t is the time. The total surface freshwater flux (E–P) is obtained at each grid position by adding (e–p) from all the air parcels observed over it. (E) and (P) are the rates of evaporation and precipitation per unit area, respectively.

The trajectory of the particles can be followed both backwards in time with the aim of identifying sources of moisture for a specific area, and forwards in time to analyse the sinks of the moisture transported from a given source (e.g., Gimeno et al. [40,44] for backward analysis, and Gimeno et al. [45] for forward analysis). Both approaches were used in the present study. First, the trajectories for particles reaching the Arctic system every day were obtained by backward tracking for the whole year prior to the 2007 and 2012 minimum sea ice extents. Particles were tracked for a period of 10 days as it represents the average time of residence of water vapour in the atmosphere [46]. From this analysis, we were able to analyse where particles gained (and lost) moisture on their trajectories towards the Arctic. By considering at each grid point the total freshwater flux resulting from all particles tracked backwards from it, we obtained the sources of moisture for the Arctic for those areas where evaporation exceeded precipitation (E–P) > 0. In addition to the years 2007 and 2012, the sources for the period 1980–2012 were used to provide the climatological mean in order to allow comparisons to be made. Climatological sources as used in this study were previously calculated by Vázquez et al. [47], in which sources were defined as those areas where (E–P) exceeded 4 mm/day for the backward experiment; they are represented by the yellow contours in Figure 2. Only the Pacific and Atlantic Ocean, North America, and Siberia were considered in the analysis to represent those continental and oceanic sources with major seasonal importance [47]. Secondly, in addition to backward tracking, trajectories were tracked forwards in time from the climatological Arctic sources (yellow contours in Figure 2) in order to analyse the variation in moisture supply into the Arctic. An area is considered to be a moisture receptor from a source when, taking the contributions of all the particles crossing the region, it is revealed that precipitation exceeds evaporation (E–P) < 0.

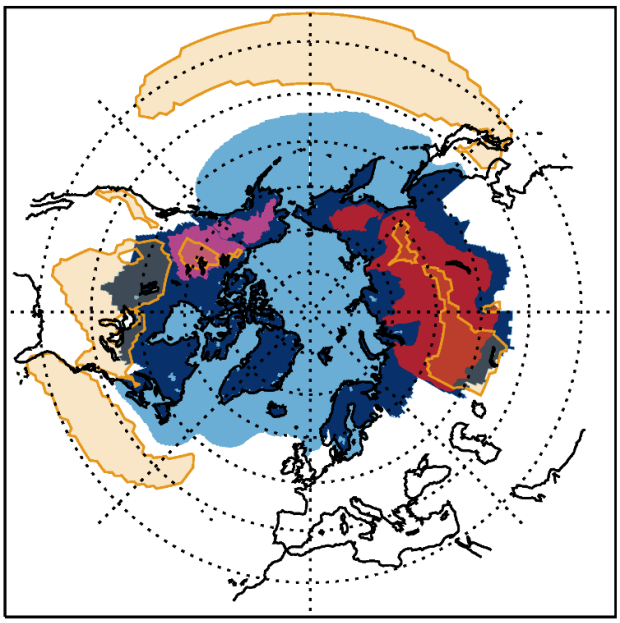

Figure 2. Main regions of study. The total solid colour-filled area (dark and light blue, red and pink) represents the Arctic domain as defined by Roberts et al. [42]. The red and pink regions represent the Eurasian and Canadian river basins respectively as considered in this study. Yellow contour areas represent the sources of moisture for the Arctic system used in the forward experiment developed by Vázquez et al. [47] in annual climatology from 1980–2012.

The analysis for both the sources and their contribution to the Arctic, for years showing minimum sea ice extents (2007 and 2012), was achieved by calculating anomalous (E–P) with reference to the climatology for 1980–2012. For the backward analysis only the (E–P) > 0 values were considered, and for the forward analysis we considered only those areas where (E–P) < 0.

To assess the possible implications for sea ice extent as affected by river discharge, in addition to the total system, the moisture contribution from the main Arctic river basins was also investigated. We consider the Eurasian and Canadian basins separately because of their influence over the different regions of the Arctic Ocean. The Eurasian river basins considered herein are Lena, Ob, Yenisey and Kolyma (the red-coloured areas in Figure 2); the main Canadian basins are McKenzie and Yukon (pink areas in Figure 2). For both areas, we calculated the mean moisture supply for each period of interest (2007, 2012) and climatology separately, which we then integrated over the basin areas.

The analysis described above was applied on both a seasonal and an annual basis. Because the minimum sea ice extent occurs in September, we considered the period from September to August 2006–2007 and the same period in 2011–2012. Hereinafter these periods are denoted 2006/2007 and 2011/2012. Seasons were defined as autumn (September to November; SON), winter (December to February; DJF), spring (March to May; MAM), and summer (June to August; JJA).

3. Results

3.1. Changes in Moisture Sources

Figure 3 shows the seasonal anomalies for 2006/2007 and 2011/2012 in moisture uptake (E–P) > 0 for backward analysis from the Arctic system. Positive anomalies (reddish colours) represent those areas where the particles took more moisture during these years on their transport to the Arctic compared to climatological mean. The opposite is valid for negative anomalies (bluish colours). Contour magenta lines represent the climatological seasonal moisture sources as defined previously [47]. From this figure, we observed variations in the moisture sources for those years with minimum sea ice extent. To facilitate the interpretation of this figure, Figure 4 shows (E–P)

climatological seasonal values for both years. Climatological sources for the period 1980–2012 can be found in Vázquez et al. [47].

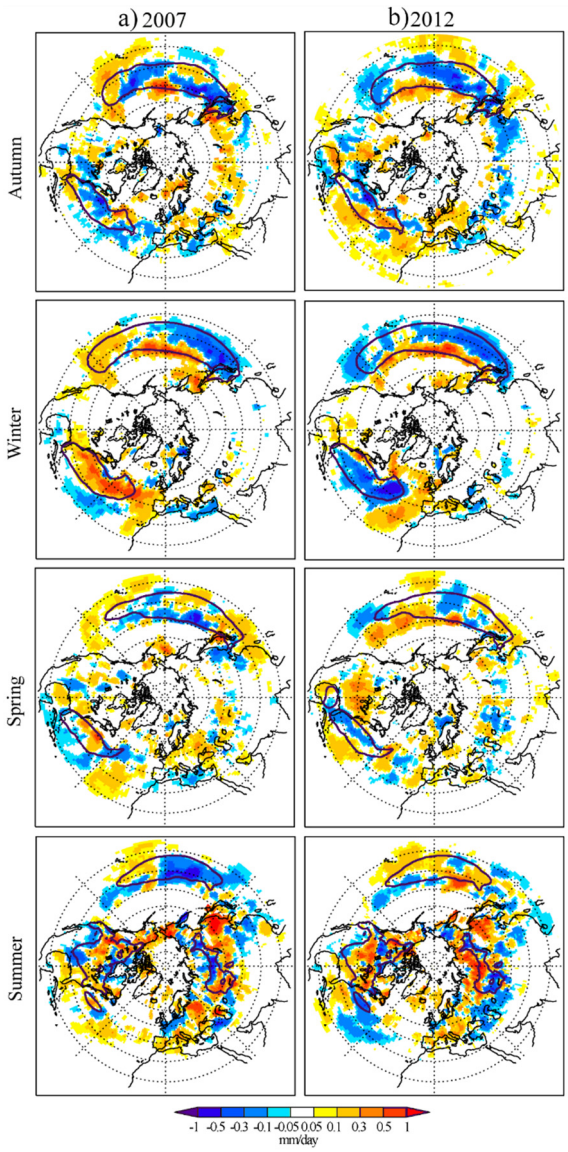

Figure 3. Seasonal evaporation–precipitation (E–P) > 0 anomalies for (**a**) 2006/2007 and (**b**) 2011/2012 compared with the 1980–2012 climatology. The reddish colours represent areas over which moisture uptake is greater that year (positive anomalies) and the bluish colours represent areas where moisture uptake is lower that year (negative anomalies). Contour magenta lines represent the main climatological moisture sources for the Arctic system based on the results of Vázquez et al. [47].

As found by Vazquez et al. [47], Atlantic and Pacific Oceans represent main moisture sources for the Arctic Ocean for the entire year, and North America and Siberia become relevant sources only in summer. In general, it can be seen from Figure 3 that the Atlantic source increases its moisture uptake over the climatological source area for 2006/2007, with the exception of autumn. Meanwhile for 2011/2012, in general the moisture uptake from Atlantic Ocean shows an increase around climatological area and a decrease over the climatological source itself. For the Pacific source, major differences between both years appear in spring and especially in summer; for these seasons, moisture uptake shows an increase for 2012, which does not appear in 2007. Finally, relating to continental summer sources, both years show a general increase in moisture uptake from North America. From the Siberian

source, it seems to be displaced northward for 2012, however only the south part of the source shows positive anomalies in 2007.

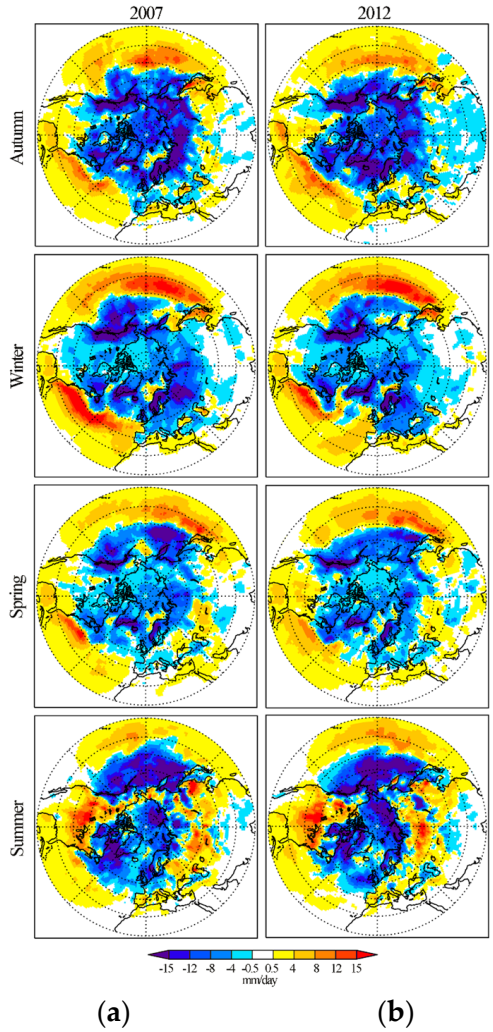

Figure 4. Climatological seasonal 10-day integrated (E–P) values observed for the period 2006/2007 (**a**) and for the period 2011/2012 (**b**), for all the particles bound for the Arctic domain, determined from backward tracking. Red colours represent moisture sources and blue colours represent moisture sinks.

For 2006/2007 (Figure 3a), and considering autumn, it appears that the uptake of moisture from the Atlantic source was reduced. For the Pacific Ocean in general, the moisture uptake became weaker over the climatological source area (contoured area); however, evaporation increased over some areas around this region. Especially remarkable is the increase in E–P that occurred over the eastern Pacific. In Figure 4a it can be seen that this source appears separated into two different areas. Despite not being the main source, in autumn the Norwegian and Barents Seas showed an increase in their potential moisture contribution to the system, and some Eurasian continental areas gained in importance as well. In winter the Atlantic moisture source clearly increased its moisture uptake and expanded eastwards (see also Figure 4a). Meanwhile, the Pacific Ocean seems to have gained in importance as a source northwards and eastwards and have decreased its moisture uptake in a southwest direction. In this season, an important increase in moisture uptake is also observed over the Okhotsk Sea (to the north of Japan and delimited to the east by the Kamchatka Peninsula). In spring, the Atlantic source seems to have a reduced eastward extent compared with the climatological source and an intensification can be seen over its central area. A slight increase in moisture uptake can be observed over the eastern

Atlantic Ocean. The Pacific source shows an uneven pattern, with negative anomalies over most of the source and positive ones over the southeastern climatological source area and over Japan and the East China Sea. Positive anomalies higher than 0.3 mm/day can be seen over the Bering Sea and Europe. Finally, in summer the North American source increased its moisture uptake over most of its area. Over Eurasia, positive anomalies generally appear around the latitudinal 50° N band, and China gains importance as a source with greater (E–P) values than Siberia (Figure 4a). For the Atlantic Ocean, moisture uptake increased over most of the area despite the fact that this source is not that important in this season. The Pacific source showed negative anomalies over most of its area, indeed this source was somewhat limited to the eastern Pacific this year, as shown in Figure 4a.

For 2011/2012 (Figure 3b), in autumn the moisture uptake over the Pacific moisture source was considerably reduced. The Atlantic moisture source seems to be displaced southwards and, in general, evaporation increased over the ocean below 40° N and the Gulf of Mexico. The positive anomalies seen over Europe for this season are also remarkable. In winter, the Atlantic source weakened over the climatological source area and the ocean to the north and east. In Figure 4b, it can be seen that two different evaporative areas appear over the Atlantic Ocean. The first coincides approximately with the climatological source and the second is located over the eastern Atlantic. The Pacific Ocean showed negative anomalies over most of its area, with the exception of a band of positive anomalies between 30° and 40° N. Positive anomalies appeared too over the Okhotsk Sea and the western Bering Sea. In spring, over the Atlantic climatological source area the moisture uptake was considerably lower, with slight increases observed mainly to the south of the climatological source. Over the Pacific Ocean, positive anomalies are seen to the northeast of the source, suggesting an expansion of the moisture source in this direction. It is important to highlight the positive anomalies over the North American source, suggesting an earlier development of this source, which usually only appears in summer. Finally, in summer the Atlantic Ocean generally shows negative anomalies over most of the western Atlantic Ocean. However, positive anomalies also appear to the east of Florida suggesting a southward displacement of the source, which can be observed in Figure 4b. The Pacific Ocean mainly shows an increase in moisture uptake. For the continental moisture sources, North America seems to have a higher moisture uptake over most of its area. Moreover, Alaska gained in importance as a source for this season. The Siberian source was displaced northwards (see Figure 4b), showing very strong positive anomalies to the north of the source. China and Europe also show a higher moisture uptake.

All the available data are brought together in Figure 5, which shows the total seasonal moisture uptake (E–P) > 0 for each source for both years (2006/2007 and 2011/2012) and for the climatology mean (1980–2012). Following the same methodology as that employed by Vázquez et al. [47], sources for 2006/2007 and 2011/2012 were defined as those areas showing values greater than 4 mm/day over the Pacific and Atlantic Ocean, North America, and Siberia (see Figure 4). For each of the four sources, the total (E–P) value was calculated. An increase in moisture uptake may be seen for almost every source and season. The only exception is over the Pacific area, which shows decreases in moisture uptake in winter, and especially in autumn of 2006/2007 and during summer of 2011/2012. Especially relevant also are the increase in spring and summer for 2011/2012 over this source. Over the Atlantic area, some reduction appeared for autumn 2006/2007, and there was a notable increase in moisture uptake occurring in winter for this year. In 2011/2012 the total (E–P) increased for every season, with higher values appearing in autumn and a negligible increase in summer. As for the continental sources in summer, these intensified in moisture uptake in both years. However, the total (E–P) was greater for 2011/2012, which could justify the increased sea ice retreat in 2012 compared to 2007.

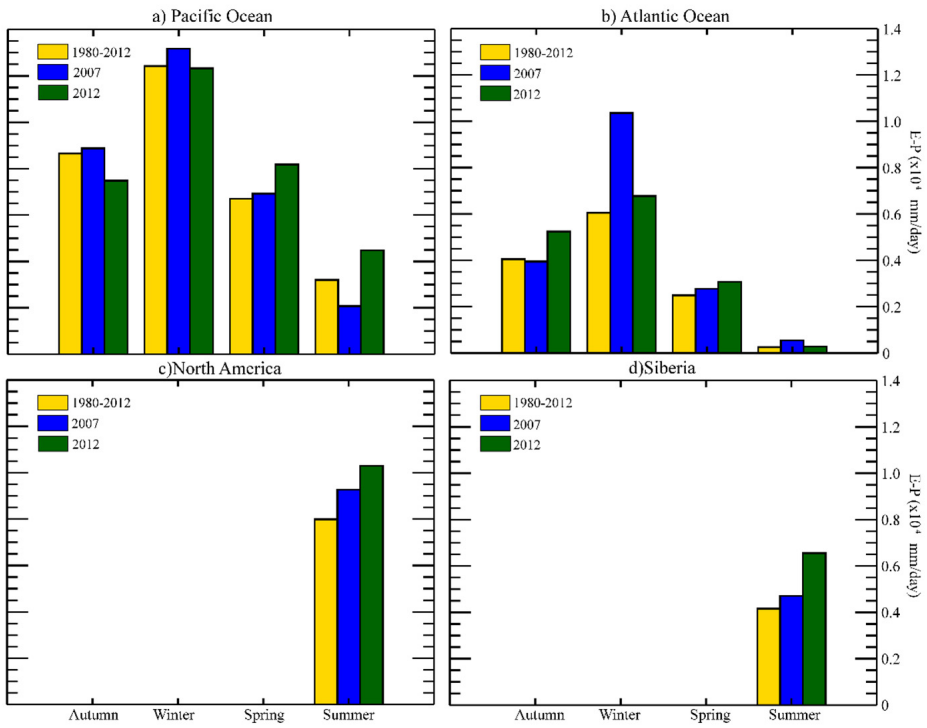

Figure 5. Total seasonal moisture uptake (E–P) > 0 for 1980–2012 (yellow bar), 2006/2007 (blue bar) and 2011/2012 (green bar) over each source of moisture: (**a**) Pacific Ocean; (**b**) Atlantic Ocean; (**c**) North America and (**d**) Siberia.

3.2. Anomalous Moisture Contribution from Each Moisture Source

The forward analysis allows us to analyse anomalous transport of moisture from the main climatological moisture sources (yellow contour lines in Figure 2) into the Arctic system for those years showing minimum sea ice extent. To analyse the geographical variations in moisture transport, Figures 6 and 7 show the seasonal moisture contribution anomalies for each of the main sources for 2006/2007 and 2011/2012, respectively. In order to link moisture transport and sea ice retreat, the purple contour indicates the sea ice extent at the end of every season.

For the Pacific moisture source (Figure 6a) we observed important differences in the (E–P) < 0 anomaly by season. Focusing the analysis on those areas showing major sea ice retreat, for this moisture source we observed an important increased moisture contribution north of the Bering Strait in autumn, affecting the area where the maximum September ice retreat was observed (see Figure 1). In spring and summer, some increases are observed north of Siberia, where sea ice loss is especially important. Figure 6b shows the (E–P) < 0 anomaly for the Atlantic moisture source. An amplification of the moisture contribution from the Atlantic moisture source can be observed to the northeast of the source for winter, spring, and summer affecting the Barents and Kara Seas, where sea ice retreat was observed over this period. In autumn, however, there was no important increase in moisture contribution over this area, in fact the transport from the Atlantic source was amplified mainly to the west of Greenland. This region is also affected by an amplified moisture transport from the North American source in summer (Figure 6c). Increased moisture contribution from both sources could have affected the sea ice retreat over the Canadian Arctic archipelago observed in 2006/2007. The contribution of the Siberian moisture source (Figure 6d) showed a strong increase to the north of the source, with an amplified contribution over the Pacific Ocean, Scandinavia, and the Atlantic Ocean. Increased moisture contribution appeared over the Arctic Ocean between the Laptev Sea and the East Siberian Sea.

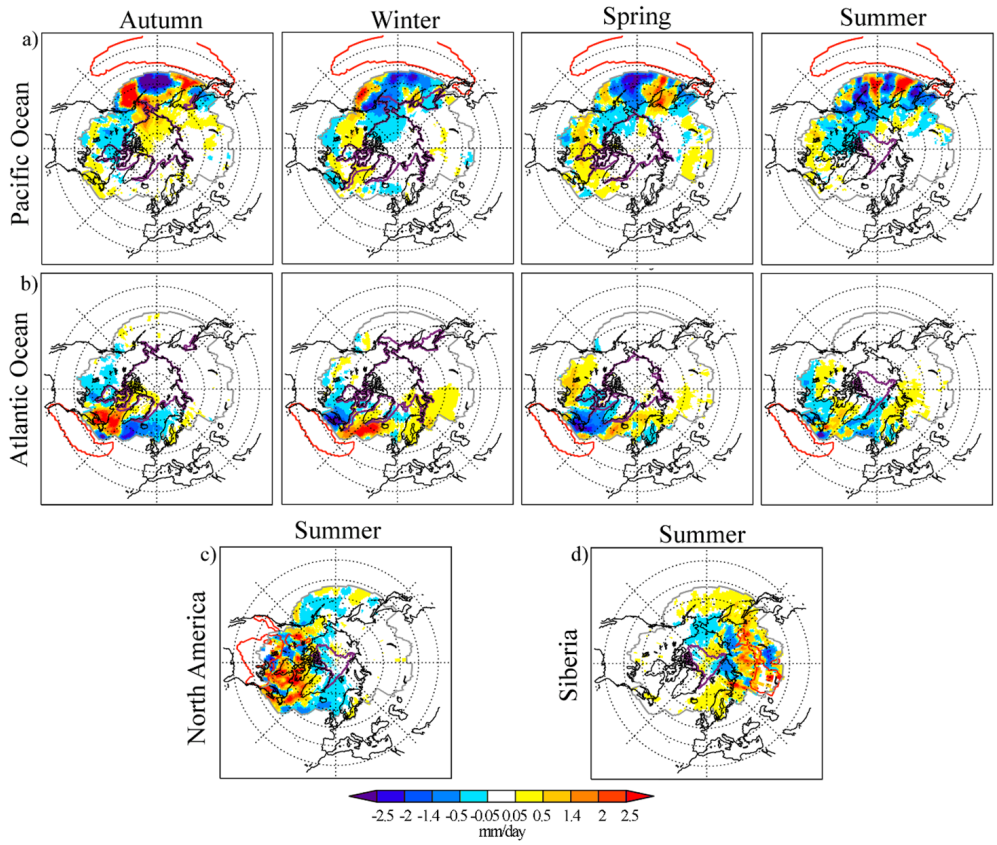

Figure 6. Seasonal (E–P) < 0 anomalies for 2006/2007 in the forward experiment from (**a**) the Pacific Ocean (**b**) the Atlantic Ocean (**c**) North America and (**d**) Siberia. Reddish colours represent areas over which the moisture supply is greater that year from the selected source (positive anomalies) and bluish colours represent areas where the moisture uptake is lower that year (negative anomalies). Red contour lines represent climatological moisture sources for the Arctic system. Purple contour lines represent the sea ice extent at the end of every season.

As far as the geographical variations in moisture supply for 2011/2012 are concerned (Figure 7), for the Pacific source (Figure 7a) negative anomalies in moisture contribution (E–P) < 0 are generally seen over the East Siberian, Chukchi, and Beaufort Seas between autumn and spring. Positive anomalies, however, are observed over the East Siberian Sea in summer. This area suffered an unusual sea ice retreat during this season (see also Figure 1). For 2011/2012 the Pacific source seems to show an increased moisture contribution over the Barents and Kara seas in autumn, and the Norwegian Sea in autumn and winter. For the Atlantic Ocean (Figure 7b), as in 2006/2007, the moisture contribution increased northeast of the source. In this case, the increase occurred in autumn, winter, and spring, affecting the Barents and Kara Seas. In summer, however positive anomalies over these seas can be only observed from North American source, In this season, some increases in moisture transport can be observed over the Canadian Arctic archipelago, from both the Atlantic and North American (Figure 7c) sources. The variation in moisture supply over this area is negligible for the remaining sources and seasons. Finally, for the Siberian moisture source (Figure 7d) the anomalies in moisture contribution over the Arctic Ocean are mainly negative. Positive anomalies can be seen over the East Siberian and Chucki Seas and over the Kara Sea.

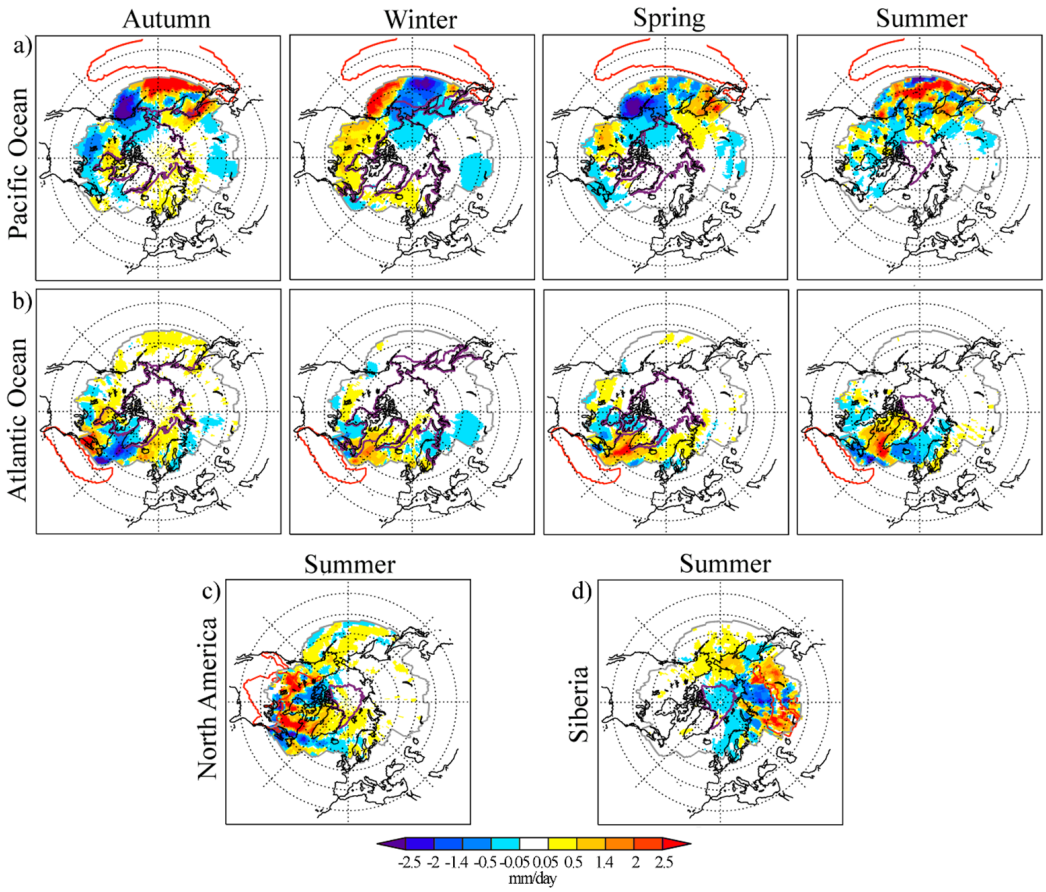

Figure 7. Seasonal (E–P) < 0 anomalies for 2011/2012 in the forward experiment from (**a**) the Pacific Ocean (**b**) the Atlantic Ocean (**c**) North America and (**d**) Siberia. Reddish colours represent areas over which the moisture supply is greater in that year from the selected source (positive anomalies) and bluish colours represent areas where the moisture uptake is lower (negative anomalies). Red contour lines represent climatological moisture sources for the Arctic system. Purple contour lines represent the sea ice extent at the end of every season.

With the aim of analysing the net variation in (E–P) over the system as a whole, Figure 8 shows the total seasonal moisture contribution from each moisture source, computed by integrating (E–P) for each grid cell and considering only values where (E–P) < 0. For the year 2006/2007, for the Pacific source the moisture contribution was generally lower compared with the mean contribution for 1980–2012. The only exception occurred in the autumn when the moisture contribution showed a slight increase. The Atlantic moisture contribution increased in autumn and winter; meanwhile, it showed similar values to the climatology for spring and summer. Finally, from both the continental sources, North America and Siberia, moisture transport over the Arctic was considerably greater.

The total seasonal contribution for 2011/2012 (green bar in Figure 8) shows that moisture transport from the Pacific moisture source was greater for autumn and summer, and decreased in the other seasons. The Atlantic moisture contribution increased in all seasons, as did the North American contribution in summer. Finally, the contribution of the Siberian source showed a slight decrease this year compared with the climatology.

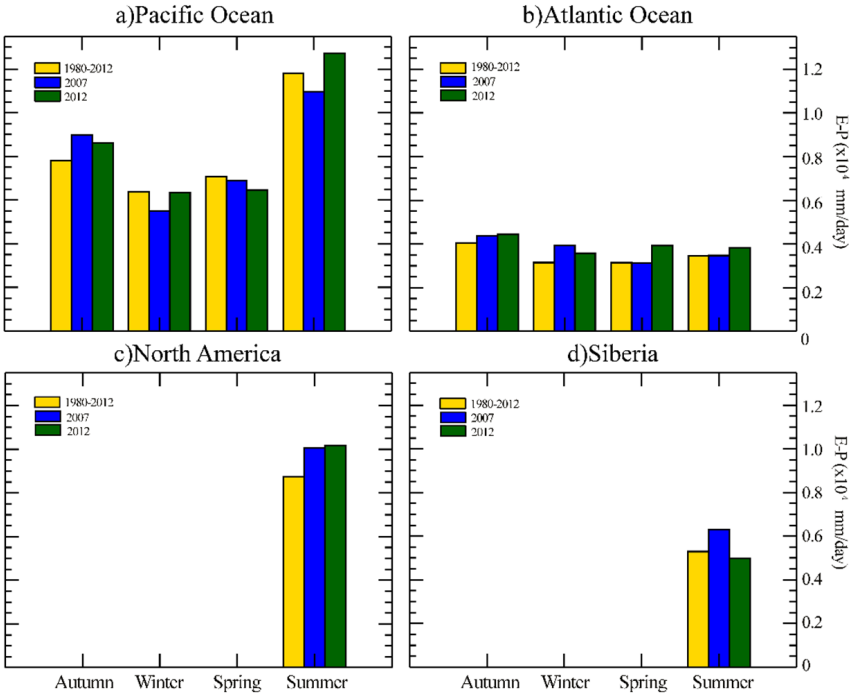

Figure 8. Seasonal mean moisture contribution over the total Arctic domain for 1980–2012 (yellow bar), 2006/2007 (blue bar) and 2011/2012 (green bar) from (**a**) Pacific Ocean; (**b**) Atlantic Ocean; (**c**) North America and (**d**) Siberia.

3.3. Contrasting Analysis: Maximum September Sea Ice Extent

To analyse the influence of moisture transport on sea ice extent it is interesting to investigate not only the situation for minimum sea ice extent but also for those years showing maximum coverage during September. The maximum September sea ice extent occurred during September 1996 (see Figure 9). With the purpose of analysing variations in moisture supply associated with maximum and minimum sea ice extent in September, and taking in mind that the behaviour of the previous summer is important in the moisture supply to the Arctic system related with the minimum, the summer contribution was analysed for 1996, and then it was compared with the 2007 situation. Figure 10 shows the anomalous moisture contribution for the year 1996 from the four climatological sources.

If the sea ice extent during 2007 (Figure 1) is observed, it can be seen that major differences occurred over the Laptev and East Siberian seas, the Barents and Kara Sea and the Canadian Arctic Archipelago. Analysing moisture contribution over those areas, it is observed that the opposite situation with respect to moisture contribution occurred over those areas in 1996 (Figure 11) and 2007 (Figure 6). In the case of Laptev and East Siberian Seas, a decreased moisture contribution is observed in 1996 from the Pacific Ocean and Siberia, however an increased contribution occurred over those areas in 2007 from the same sources. With reference to the Barents and Kara Sea, an increased contribution is observed over this area from the Atlantic Ocean and Siberia in 2007. However, any anomalous contribution appears to be from the Atlantic source in 1996 and decreased supply can be observed from the Siberian source. Finally, over the Canadian Archipelago, major differences can be found with respect to the North American source. The North American contribution increased in 2007 over this area and decreased in 1996.

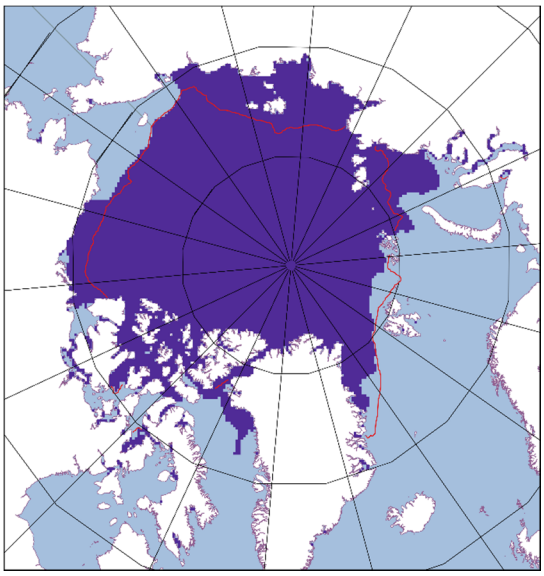

Figure 9. September minimum sea ice extent for 1996 and the climatological 1981–2010 mean (red contour). Data obtained from National Snow and Ice Data Center (NSIDC).

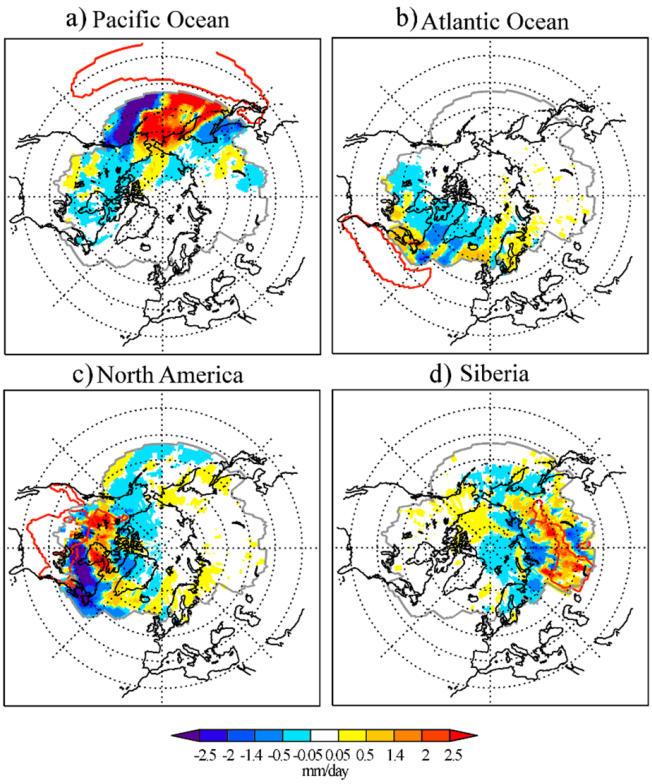

Figure 10. Summer (E–P) < 0 anomalies for 1996 in the forward experiment from (**a**) the Pacific Ocean (**b**) the Atlantic Ocean (**c**) North America and (**d**) Siberia. Reddish colours represent areas over which the moisture supply is greater that year from the selected source (positive anomalies) and bluish colours represent areas where the moisture uptake is lower that year (negative anomalies). Contour red lines represent climatological moisture sources for the Arctic system.

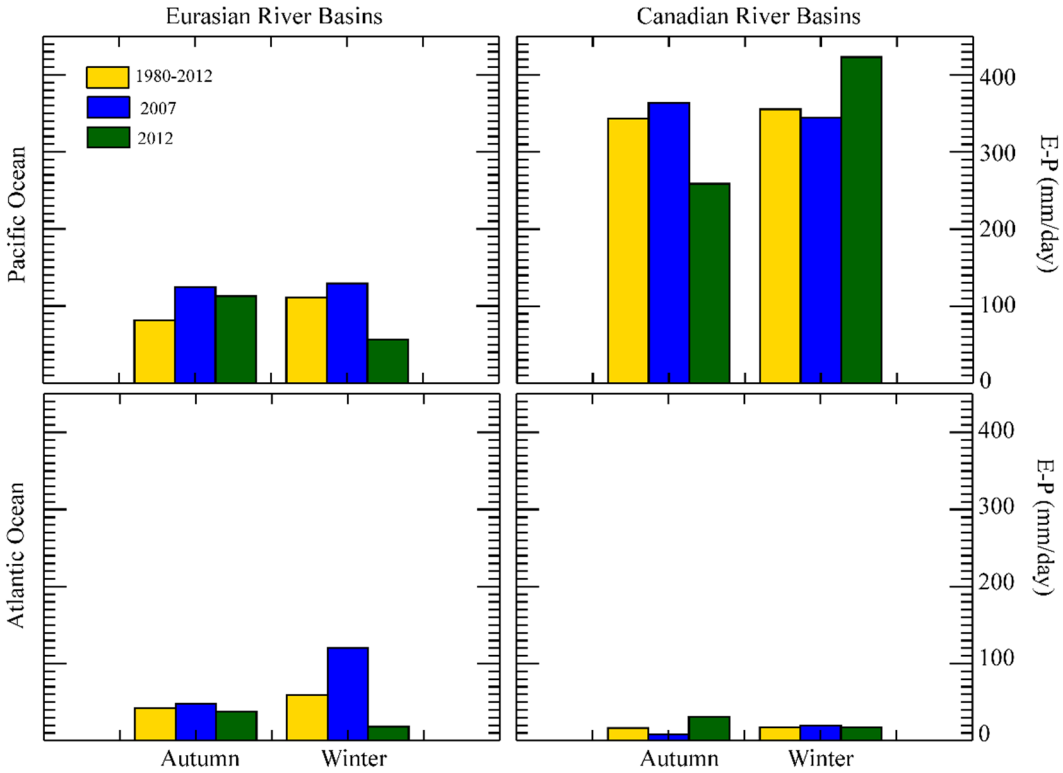

Figure 11. Mean moisture contribution over Eurasian (left-hand column) and Canadian (right-hand column) river basins from Pacific Ocean (first row) and Atlantic Ocean (second row) for 1980–2012 (yellow bar), 2007 (blue bar) and 2012 (green bar).

3.4. River Basins

With the aim of investigating how moisture variations over the major Arctic river basins affect the extent of the sea ice, we analysed the moisture contribution over the Lena, Ob, Yenisey and Kolyma (Eurasian rivers that flow to the Arctic system, red coloured in Figure 2) together, and over McKenzie and Yukon river basins (Canadian rivers, marked in pink in Figure 2). Figure 11 shows the seasonal moisture contribution from each moisture source over the main Eurasian (left-hand column) and Canadian Arctic river basins (right-hand column). These contributions were calculated for the complete climatology (yellow bar) and for the individual periods 2006/2007 and 2011/2012 (blue and green bars, respectively) in order to assess the possible variations. As the snowpack most related with summer Arctic river discharge occurred during the period October–March [32], in this work only the autumn and winter seasons were analysed (continental sources of moisture were not analysed). In this section we assume that amplified moisture transport into the river basins leads to larger river discharge into the Arctic Ocean, however changes in river discharge were not analysed in this paper.

For 2006/2007 (blue bar), the Pacific moisture sources supplied a greater amount of moisture to the Eurasian river basin in both seasons, with the increase in moisture supply being greater in autumn compared with the climatology mean. Over the Canadian river basins, the moisture contribution only increased during autumn, showing some decrease in the winter compared with the 1980–2012 mean contribution. In general terms, the moisture contribution from the Pacific source is greater over the Canadian basins than over the Eurasian ones. In the case of the Atlantic Ocean, during 2006/2007 its contribution over the Eurasian basins increased for both seasons, as occurred for the Pacific source over these basins. Of special note is the case in winter, when the moisture contribution is more than twice the climatological mean contribution. For the Canadian basins for the same year, its contribution was also increased in winter and decreased in autumn; however, variations are small compared with the Eurasian basins.

In 2011/2012 (green bar), the Pacific moisture contribution over the Eurasian River basins showed an increase in autumn and a decrease in winter. The situation for this source is the opposite over Canadian basins. Variations are more important over these watersheds than over the Eurasian ones, showing variations of around 100 mm/day in both seasons. Moisture supply from the Atlantic Ocean decreased over the Eurasian basins during autumn and winter, with the contribution for the latter being less than half the climatological mean contribution. Over the Canadian basins, this source showed an increase in autumn, the supply in winter being almost the same as the 1980–2012 climatology mean.

4. Discussion

Moisture transport shows some important variations for those years experiencing minimum sea ice extents compared with the 1980–2012 climatology; however, the situation differs between the two years considered here.

In 2006/2007, the Pacific Ocean seems to have gained importance as a moisture source in autumn, winter, and spring; however, in summer the moisture uptake (E–P) > 0 was less than the 1980–2012 mean value (Figure 5). Its contribution to precipitation (Figure 6a) increased over some areas of major sea ice retreat north of the Bering Strait, especially in autumn but also in spring and summer over the East Siberian Sea. Kapch et al. [48] suggested a relationship between increased humidity over an area and an intensification of the sea ice retreat there. Moisture uptake (Figure 3) increased over continental areas in North America and Asia, and the Siberian moisture contribution was greater than average to the north of the climatological source. Especially remarkable is the intensification of the Atlantic Ocean as a moisture source in winter (Figure 5), showing an increase in moisture uptake greater than 4000 mm/day over the complete source. Except for during autumn 2006, this source showed positive anomalies over most of its areas for all seasons (Figure 3). This amplification of the moisture source resulted in an increased moisture contribution in every season (Figure 8), which was geographically localised over oceanic areas around Greenland and Eurasia and affecting some areas of major ice retreat such as the Barents and Kara Seas (Figure 6b). The increase in moisture supply over Eurasia produced an increase in moisture contribution over the main Arctic river basins (Figure 11) of more than 100% on an annual basis (result not shown). This increased supply can be related with the intensification in the Atlantic moisture source found for this year in winter (Figure 3). Gimeno et al. [49] have previously demonstrated the relation between intensification of this moisture source and increased moisture contribution over the Eurasian river basins. This finding is especially relevant because the Atlantic Ocean was previously found to be one of the most important sources for the Eurasian river basins [50]. In agreement with our result, Zhang et al. [32] observed an increased moisture transport into the Eurasian river basins, and Shiklomanov and Lammers [50] described a peak river discharge in 2007. Some authors have suggested a link between increased Eurasian river discharge and sea ice decline [25,26]. This relationship is in accordance with our own results, given the important sea ice retreat that occurred to the north of the main Eurasian Arctic river estuaries in 2006/2007 (Figure 1).

In 2011/2012, the continental areas showed an important intensification of the moisture uptake (Figure 3). The North American moisture contribution increased considerably for this period too, however the Siberian moisture contribution remains similar to the climatological mean (Figure 8). The Atlantic source experienced a remarkable decrease in moisture uptake over the climatological evaporative area, especially in winter (Figure 3). However, positive anomalies were found over the surrounding areas, resulting in an intensification of the ocean as a source (Figure 5). The total moisture contribution over the Arctic from this source showed increased values with respect to 1980–2012 (Figure 8). Positive anomalies in moisture uptake to the north of the climatological source (Figure 3) suggest an intensification of the moisture uptake from particles on their way to the Arctic domain, which could produce an intensification of the final moisture contribution. For the Pacific moisture source, an increased moisture contribution appears over the system in autumn and summer, producing an increased moisture supply over the Barents and Kara Seas, and over the East Siberian and Chucki

Seas, respectively. In this year, important reductions occurred to the north of Russia (Figure 1). Some authors have related the sea ice reduction over this area to the occurrence of a great cyclone originating in Siberia in August of that year [51–53].

Despite seasonal variations in moisture contribution; it seems like summer conditions are crucial for the variability of sea ice extent for both years, as it is in this season when major retreats were observed. In the case of 2007 increased moisture contribution was observed, in general, over the Laptev and East Siberian Seas, Barents and Kara Seas and the Canadian Arctic archipelago (those areas of major retreat). In the case of 2012 such a clear relation cannot be addressed. For this year positive anomalies in moisture contribution appeared north of the Bering Strait, where ice retreat was especially high. However, most of the sources decreased moisture contribution over the Barents and Kara seas for this year, where the retreat was even higher than for 2007.

Finally, if we compare the sea ice extent over the Barents and Kara seas (Figure 1) an important difference can be observed between the two years. This difference seems to be related to the path of the moisture transport associated with the Atlantic moisture source. In Figure 6b we note that moisture transport from the Atlantic moisture source showed an eastward movement into Eurasia in 2006/2007, meanwhile, in 2011/2012 (Figure 7b) the moisture contribution showed a major northeastward trend. An important amount of moisture from the Atlantic Ocean is transported into the Arctic by cyclones [54], especially in winter [55]. Storms play an important role in sea ice reduction [19] and have been proven to affect the sea ice extent over this area [56].

5. Conclusions

We have analysed the variation in moisture transport occurring in the years 2006/2007 and 2011/2012 and have attempted to relate this to the minimum Arctic sea ice extent observed in these years.

Important variations in moisture transport over the Arctic have become apparent for those years with minimum sea ice extents. For the year 2006/2007, for example, an increase in moisture contribution over the Arctic domain was observed from continental sources in summer and from the Atlantic source in autumn and winter. In the case of the 2011/2012 minimum extent, increases in moisture supply were observed from every source with the exception of Siberia in summer, and the Pacific Ocean in winter and spring. From our results, it seems increased summer moisture contribution may be related with sea ice retreat. In general, positive anomalies were found over areas of major retreat for this season.

From our results, increased moisture transport over the main Arctic river basins seems to have some implications for the sea ice reductions observed over the Arctic Ocean. Moisture transport over these basins was not the same for both years. In 2006/2007 the Atlantic moisture contribution increased by more than 100% over the Eurasian river basins. In the same year, anomalous sea ice reductions occurred over the Arctic Ocean to the north of the basins. Despite the observed moisture increase and the importance of Atlantic Ocean as a source for this watershed, further analysis should be undertaken in order to assess the strength of the relationship between river discharge and sea ice extent.

The Atlantic moisture source seems to be especially related to the sea ice extent over the Barents and Kara Sea regions. Over these areas, greater sea ice reductions were observed in 2011/2012, when the moisture transport from the Atlantic source had a northward component, bringing moisture into the area of major retreat.

Acknowledgments: The authors acknowledge funding by the Spanish government within the EVOCAR (CGL2015-65141-R) project, which is also funded by FEDER (European Regional Development Fund). Raquel Nieto was also supported by the Brazilian government through a CNPq grant 314734/2014-7.

Author Contributions: Raquel Nieto and Luis Gimeno designed, proposed and conducted the research; Marta Vazquez performed the experiments and analysed the data; Marta Vazquez, Raquel Nieto, Luis Gimeno, and Anita Drumond wrote the paper.

Conflicts of Interest: The authors declare no conflict of interest. The founding sponsors had no role in the design of the study; in the collection, analyses, or interpretation of data; in the writing of the manuscript, or in the decision to publish the results.

References

1. Stroeve, J.C.; Kattsov, V.; Barrett, A.; Serreze, M.; Pavlova, T.; Holland, M.; Meier, W.N. Trends in Arctic sea ice extent from CMIP5, CMIP3, and observations. *Geophys. Res. Lett.* **2012**, *39*, L16502. [CrossRef]
2. Stroeve, J.; Holland, M.M.; Meier, W.; Scambos, T.; Serreze, M. Arctic sea ice decline: Faster than forecast. *Geophys. Res. Lett.* **2007**, *34*, L09501. [CrossRef]
3. Comiso, J.C.; Parkinson, C.L.; Gersten, R.; Stock, L. Accelerated decline in the Arctic sea-ice cover. *Geophys. Res. Lett.* **2008**, *35*, L01703. [CrossRef]
4. Parkinson, C.L.; DiGirolamo, N.E. New visualizations highlight new information on the contrasting Arctic and Antarctic sea-ice trends since the late 1970s. *Remote Sens. Environ.* **2016**, *183*, 198–204. [CrossRef]
5. Holland, M.M.; Bitz, C.M.; Tremblay, B. Future abrupt reductions in the summer Arctic sea ice. *Geophys. Res. Lett.* **2006**, *33*, L23503. [CrossRef]
6. Gregory, J.M.; Stott, P.A.; Cresswell, D.J.; Rayner, N.A.; Gordon, C.; Sexton, D.M.H. Recent and future changes in Arctic sea ice simulated by the HadCM3 AOGCM. *Geophys. Res. Lett.* **2002**, *29*, 2175. [CrossRef]
7. Laxon, S.W.; Giles, K.A.; Ridout, A.L.; Wingham, D.J.; Willatt, R.; Cullen, R.; Kwok, R.; Schweiger, A.; Zhang, J.; Haas, C.; et al. CryoSat-2 estimates of Arctic sea ice thickness and volume. *Geophys. Res. Lett.* **2013**, *40*, 732–737. [CrossRef]
8. Cavalieri, D.J.; Parkinson, C.L. Arctic sea ice variability and trends, 1979–2010. *Cryosphere* **2012**, *6*, 881–889. [CrossRef]
9. Meier, W.N.; Gerland, S.; Granskog, M.A.; Key, J.R.; Haas, C.; Hovelsrud, G.K.; Kovacs, K.; Makshtas, A.; Michel, C.; Perovich, D.; et al. Sea ice. In *AMAP (2011) Snow, Water, Ice and Permafrost in the Arctic (SWIPA): Climate Change and the Cryosphere*; Arctic Monitoring and Assesment Programme (AMAP): Oslo, Norway, 2011; Chapter 9.
10. Serreze, M.C.; Holland, M.M.; Stroeve, J. Perspectives on the Arctic's Shrinking Sea-Ice Cover. *Science* **2007**, *315*, 1533–1536. [CrossRef] [PubMed]
11. Gloersen, P.; Campbell, W.J.; Cavalieri, D.J.; Comiso, J.C.; Parkinson, C.L.; Zwalley, H.J. Satellite passive microwave observations and analysis of Arctic and Antarctic sea ice, 1978–1987. *Ann. Glaciol.* **1993**, *17*, 149–154.
12. Parkinson, C.L.; Cavalieri, D.J.; Gloersen, P.; Zwally, H.J.; Comiso, J.C. Arctic sea ice extents, areas, and trends, 1978–1996. *J. Geophys. Res.* **1999**, *104*, 20837–20856. [CrossRef]
13. Parkinson, C.L. Global Sea Ice Coverage from Satellite Data: Annual Cycle and 35-Yr Trends. *J. Clim.* **2014**, *27*, 9377–9382. [CrossRef]
14. Stroeve, J.; Serreze, M.C.; Holland, M.M.; Kay, J.E.; Malik, J.; Barrett, A.P. The Arctic's rapidly shrinking sea ice cover: A research synthesis. *Clim. Chang.* **2012**, *110*, 1005. [CrossRef]
15. Screen, J.A.; Simmonds, I. The central role of diminishing sea ice in recent Arctic temperature amplification. *Nature* **2010**, *464*, 1334–1337. [CrossRef] [PubMed]
16. Kopec, B.G.; Feng, X.; Michel, F.A.; Posmentier, E.S. Influence of sea ice on Arctic precipitation. *Proc. Natl. Aacd. Sci. USA* **2016**, *113*, 46–51. [CrossRef] [PubMed]
17. Tang, Q.; Zhang, X.; Yang, X.; Francis, J.A. Cold winter extremes in northern continents linked to Arctic sea ice loss. *Environ. Res. Lett.* **2013**, *8*, 014036. [CrossRef]
18. Screen, J.A. Influence of Arctic sea ice on European summer precipitation. *Environ. Res. Lett.* **2013**, *8*, 044015. [CrossRef]
19. Vihma, T. Effects of Arctic Sea Ice Decline on Weather and Climate: A Review. *Surv. Geophys.* **2014**, *35*, 1175–1214. [CrossRef]
20. Fetterer, F.; Knowles, K.; Meier, W.; Savoie, M. *Sea Ice Index*; National Snow and Ice Data Center: Boulder, CO, USA, 2002.
21. Polyakov, I.V.; Walsh, J.E.; Kwok, R. Recent changes in the Arctic multiyear sea ice coverage and its likely causes. *Bull. Am. Meteorol. Soc.* **2012**, *96*, 145–151. [CrossRef]
22. Nghiem, S.V.; Rigor, I.G.; Perovich, D.K.; Clemente-Colón, P.; Weatherly, J.W.; Neumann, G. Rapid reduction of Arctic perennial sea ice. *Geophys. Res. Lett.* **2007**, *34*, L19504. [CrossRef]

23. Maslanik, J.; Fowler, C.; Stroeve, J.; Drobot, S.; Zwally, J.; Yi, D.; Emery, W. A younger, thinner Arctic ice cover: Increased potential for rapid, extensive sea-ice loss. *Geophys. Res. Lett.* **2007**, *34*, L24501. [CrossRef]
24. Nummelin, A.; Ilicak, M.; Li, C.; Smedsrud, L.H. Consequences of future increased Arctic runoff on Arctic Ocean stratification, circulation, and sea ice cover. *J. Geophys. Res. Oceans* **2016**, *121*, 617–637. [CrossRef]
25. Bauch, D.; Hölemann, J.A.; Nikulina, A.; Wegner, C.; Janout, M.A.; Timokhov, L.A.; Kassens, H. Correlation of river water and local sea-ice melting on the Laptev Sea shelf (Siberian Arctic). *J. Geophys. Res. Oceans* **2013**, *118*, 550–561. [CrossRef]
26. Nghiem, S.V.; Hall, D.K.; Rigor, I.G.; Li, P.; Neumann, G. Effects of Mackenzie River discharge and bathymetry on sea ice in the Beaufort Sea. *Geophys. Res. Lett.* **2014**, *41*, 873–879. [CrossRef]
27. Simmonds, I.; Keay, K. Extraordinary September Arctic sea ice reductions and their relationships with storm behavior over 1979–2008. *Geophys. Res. Lett.* **2009**, *36*, L19715. [CrossRef]
28. Mesquita, M.; Hodges, K.I.; Atkinson, D.E.; Bader, J. Sea-ice anomalies in the Sea of Okhotsk and the relationship with storm tracks in the Northern Hemisphere during winter. *Tellus A* **2011**, *63*, 313–323. [CrossRef]
29. Francis, J.A.; Hunter, E. New insight into the disappearing Arctic Sea ice. *Eos Trans. Am. Geophys. Union AGU* **2006**, *87*, 509–511. [CrossRef]
30. Francis, J.A.; Hunter, E. Changes in the fabric of the Arctic's greenhouse blanket. *Environ. Res. Lett.* **2007**, *2*, 045011. [CrossRef]
31. Mortin, J.; Svensson, G.; Graversen, R.G.; Kapsch, M.L.; Stroeve, J.C.; Boisvert, L.N. Melt onset over Arctic sea ice controlled by atmospheric moisture transport. *Geophys. Res. Lett.* **2016**, *43*, 6636–6642. [CrossRef]
32. Zhang, X.; He, J.; Zhang, J.; Polyakov, I.; Gerdes, R.; Inoue, J.; Wu, P. Enhanced poleward moisture transport and amplified northern high-latitude wetting trend. *Nat. Clim. Chang.* **2012**, *3*, 47–51. [CrossRef]
33. Peterson, B.J.; Holmes, R.M.; McClelland, J.W.; Vörösmarty, C.J.; Lammers, R.B.; Shiklomanov, A.I.; Shiklomanov, I.A.; Rahmstorf, S. Increasing river discharge to the Arctic Ocean. *Science* **2002**, *98*, 2171–2173. [CrossRef] [PubMed]
34. McClelland, J.W.; Déry, S.J.; Peterson, B.J.; Holmes, R.M.; Wood, E.F. A pan-arctic evaluation of changes in river discharge during the latter half of the 20th century. *Geophys. Res. Lett.* **2006**, *33*, L06715. [CrossRef]
35. Whitefield, J.; Winsor, P.; McClelland, J.; Menemenlis, D. A new river discharge and river temperature climatology data set for the pan-Arctic region. *Ocean Model.* **2015**, *88*, 1–15. [CrossRef]
36. Gimeno, L.; Dominguez, F.; Nieto, R.; Trigo, R.M.; Drumond, A.; Reason, C.; Taschetto, A.S.; Ramos, A.M.; Kumar, R.; Marengo, J. Major Mechanisms of Atmospheric Moisture Transport and Their Role in Extreme Precipitation Events. *Annu. Rev. Environ. Resour.* **2016**, *41*, 117–141. [CrossRef]
37. Stohl, A.; James, P.A. A Lagrangian Analysis of the Atmospheric Branch of the Global Water Cycle. Part I: Method Description, Validation, and Demonstration for the August 2002 Flooding in Central Europe. *J. Hydrometeorol.* **2004**, *5*, 656–678. [CrossRef]
38. Stohl, A.; James, P.A. A Lagrangian Analysis of the Atmospheric Branch of the Global Water Cycle. Part II: Moisture Transports between Earth's Ocean Basins and River Catchments. *J. Hydrometeorol.* **2005**, *6*, 961–984. [CrossRef]
39. Dirmeyer, P.A.; Brubaker, K.L. Characterization of the Global Hydrologic Cycle from a Back-Trajectory Analysis of Atmospheric Water Vapor. *J. Hydrometeorol.* **2007**, *8*, 20–37. [CrossRef]
40. Gimeno, L.; Nieto, R.; Drumond, A.; Castillo, R.; Trigo, R.M. Influence of the intensification of the major oceanic moisture sources on continental precipitation. *Geophys. Res. Lett.* **2013**, *40*, 1443–1450. [CrossRef]
41. Gimeno, L.; Stohl, A.; Trigo, R.M.; Domínguez, F.; Yoshimura, K.; Yu, L.; Drumond, A.; Durán-Quesada, A.M.; Nieto, R. Oceanic and Terrestrial Sources of Continental Precipitation. *Rev. Geophys.* **2012**, *50*, RG4003. [CrossRef]
42. Roberts, A.; Cassano, J.; Döscher, R.; Hinzman, L.; Holland, M.; Mitsudera, H.; Sumi, A.; Walsh, J.E.; Alessa, L.; Alexeev, V.; et al. *A Science Plan for Regional Arctic System Modeling: A Report to the National Science Foundation from the International Arctic Science Community*; International Arctic Research Center (IARC): University of Alaska, Fairbanks, AK, USA, 2010.
43. Dee, D.P.; Uppala, S.M.; Simmons, A.J.; Berrisford, P.; Poli, P.; Kobayashi, S.; Andrae, U.; Balmaseda, M.A.; Balsamo, G.; Bauer, P.; et al. The ERA-Interim reanalysis: Configuration and performance of the data assimilation system. *Q. J. R. Meteorol. Soc.* **2011**, *137*, 553–597. [CrossRef]

44. Gimeno, L.; Nieto, R.; Trigo, R.M.; Vicente, S.; Lopez-Moreno, J.I. Where does the Iberian Peninsula moisture come from? An answer based on a Largrangian approach. *J. Hydrometeorol.* **2010**, *11*, 421–436. [CrossRef]
45. Gimeno, L.; Drumond, A.; Nieto, R.; Trigo, R.M.; Stohl, A. On the origin of continental precipitation. *Geophys. Res. Lett.* **2010**, *37*. [CrossRef]
46. Numagati, A. Origin and recycling processes of precipitation water over the Eurasian continent: Experiments using an atmospheric general circulation model. *J. Geophys. Res.* **1999**, *104*, 1957–1972. [CrossRef]
47. Vazquez, M.; Nieto, R.; Drumond, A.; Gimeno, L. Moisture transport into the Arctic: Source-receptor relationships and the roles of atmospheric circulation and evaporation. *J. Geophys. Res. Atmos.* **2016**, *121*. [CrossRef]
48. Kapsch, M.L.; Graversen, R.G.; Tjernström, M. Springtime atmospheric energy transport and the control of Arctic summer sea-ice extent. *Nat. Clim. Chang.* **2013**, *3*, 744–748. [CrossRef]
49. Gimeno, L.; Vázquez, M.; Nieto, R.; Trigo, R.M. Atmospheric moisture transport: The bridge between ocean evaporation and Arctic ice melting. *Earth Syst. Dyn.* **2015**, *6*, 583–589. [CrossRef]
50. Shiklomanov, A.I.; Lammers, R.B. Record Russian river discharge in 2007 and the limits of analysis. *Environ. Res. Lett.* **2009**, *4*, 045015. [CrossRef]
51. Parkinson, C.L.; Comiso, J.C. On the 2012 record low Arctic sea ice cover: Combined impact of preconditioning and an August storm. *Geophys. Res. Lett.* **2013**, *40*, 1356–1361. [CrossRef]
52. Zhang, J.; Lindsay, R.; Schweiger, A.; Steele, M. The impact of an intense summer cyclone on 2012 Arctic sea ice retreat. *Geophys. Res. Lett.* **2013**, *40*, 720–726. [CrossRef]
53. Simmonds, I.; Rudeva, I. The great Arctic cyclone of August 2012. *Geophys. Res. Lett.* **2012**, *39*, L23709. [CrossRef]
54. Sorteberg, A.; Walsh, J.E. Seasonal cyclone variability at 70°N and its impact on moisture transport into the Arctic. *Tellus A* **2008**, *60*, 570–586. [CrossRef]
55. Zhang, X.; Walsh, J.E.; Zhang, J.; Bhatt, U.S.; Ikeda, M. Climatology and interannual variability of Arctic cyclone activity: 1948–2002. *J. Clim.* **2004**, *17*, 2300–2317. [CrossRef]
56. Boisvert, L.N.; Petty, A.A.; Stroeve, J.C. The Impact of the Extreme Winter 2015/16 Arctic Cyclone on the Barents–Kara Seas. *Mon. Weather Rev.* **2016**, *144*, 4279–4287. [CrossRef]

Earth Syst. Dynam., 6, 583–589, 2015
www.earth-syst-dynam.net/6/583/2015/
doi:10.5194/esd-6-583-2015

Earth System Dynamics
Open Access

Atmospheric moisture transport: the bridge between ocean evaporation and Arctic ice melting

L. Gimeno[1], M. Vázquez[1], R. Nieto[1], and R. M. Trigo[2]

[1]EPhysLab (Environmental Physics Laboratory), Universidad de Vigo, Facultad de Ciencias, Ourense, Spain
[2]University of Lisbon, CGUL, IDL, Lisbon, Portugal

Correspondence to: L. Gimeno (l.gimeno@uvigo.es)

Abstract. Changes in the atmospheric moisture transport have been proposed as a vehicle for interpreting some of the most significant changes in the Arctic region. The increasing moisture over the Arctic during the last decades is not strongly associated with the evaporation that takes place within the Arctic area itself, despite the fact that the sea ice cover is decreasing. Such an increment is consistent and is more dependent on the transport of moisture from the extratropical regions to the Arctic that has increased in recent decades and is expected to increase within a warming climate. This increase could be due either to changes in circulation patterns which have altered the moisture sources, or to changes in the intensity of the moisture sources because of enhanced evaporation, or a combination of these two mechanisms. In this short communication we focus on the more objective assessment of the strong link between ocean evaporation trends and Arctic Sea ice melting. We will critically analyse several recent results suggesting links between moisture transport and the extent of sea ice in the Arctic, this being one of the most distinct indicators of continuous climate change both in the Arctic and on a global scale. To do this we will use a sophisticated Lagrangian approach to develop a more robust framework on some of these previous disconnecting results, using new information and insights. Results reached in this study stress the connection between two climate change indicators, namely an increase in evaporation over source regions (mainly the Mediterranean Sea, the North Atlantic Ocean and the North Pacific Ocean in the paths of the global western boundary currents and their extensions) and Arctic ice melting precursors.

1 The outstanding role of Arctic climate within the global climate system

The last IPCC Assessment Report has confirmed that the main components of the climate system have been warming (atmosphere, oceans) or shrinking (cryosphere) since the 1970s, as a result of global warming induced by the significant increment in concentration of greenhouse gases of anthropogenic origin (AR5, IPCC, 2013). The so-called hiatus in the rise of global air temperature since the late 1990s is observed neither in the relentless decadal shift of temperature distributions in both hemispheres (Hansen et al., 2012) nor in the frequency of extreme hot events over the continents (Seneviratne et al., 2014). The much larger capacity of the oceans to store heat, with respect to the atmosphere, has played a fundamental role in storing the excessive heat retained in the climate system in the Pacific (Kosaka and Xie, 2013) and the Atlantic (Chen and Tung, 2014) oceans.

However, global warming is a very uneven phenomenon impossible to be encapsulated by a single indicator relative to one subsystem, such as the global average of near-surface atmospheric temperature. The spatial pattern of observed temperature trends is very asymmetrical and regionalized, with continents warming more than oceans, and with high latitudes also presenting considerably higher warming rates than midlatitude and tropical regions. In particular, several authors have shown that the rise in Arctic near-surface temperature (AST) has been twice as large as the global average throughout most of the year (e.g. Screen and Simmonds, 2010; Tang et al., 2014; Cohen et al., 2014). Additionally, the evolution of the climate in the Arctic region is often associated with two important indicators – the summer and autumn sea ice extent (SIE) and the spring and summer snow cover extent (SCE) – both characterized by a very significant decline since the 1970s and widely recognized as some of the

Published by Copernicus Publications on behalf of the European Geosciences Union.

most undeniable indicators of continuous climate change affecting the climate system (Tang et al., 2014; IPCC, 2013).

Nevertheless, the opposite evolution of AST and SIE indices in recent decades emphasizes that both phenomena are not independent and, actually, are known to reinforce each other (Tang et al., 2014), as changes in surface albedo (associated with melting snow and ice) tend to enhance warming in the Arctic (Serreze and Francis, 2006) as shown in the recent review paper by Cohen et al. (2014). Nevertheless both indicators (AST and SIE) may also respond to other mechanisms including changes in atmospheric circulation patterns (Graversen et al., 2008), ocean circulation (Comiso et al., 2008), and changes in radiative fluxes associated with cloud cover and water vapour content in the atmosphere (Schweiger et al., 2008; Kapsch et al., 2013), through the absorption of the outgoing long-wave radiation from the surface by the increased atmospheric moisture and then remitted toward the Arctic surface, resulting in the surface warming and sea ice decline (Kapsch et al., 2013). In particular, changes in the atmospheric moisture have been proposed as a vehicle for interpreting the most significant changes in the Arctic region either due to increased transport from middle latitudes (Lucarini and Ragone, 2011; Zanhg et al., 2012) or via enhanced local evaporation (Bintanja and Selten, 2014). However, some recent studies have shown that the evaporation from the Arctic surface appears not to be an important moisture source (e.g. Graversen et al., 2008; Park et al., 2015).

According to some authors, the recent rise on the incidence of summer extreme weather events over Northern Hemisphere continental land masses (Coumou and Rahmstorf, 2012; Seneviratne et al., 2014) is probably driven by the accelerated decline of summer SIE and SCE observed in recent decades (Francis and Vavrus, 2012; Tang et al., 2014). According to this hypothesis, the observed weakening of poleward temperature gradient triggered changes in atmospheric circulation, namely slower progression of Rossby waves (Francis and Vavrus, 2012) and the existence of a planetary-scale wave life cycle (Bagget and Lee, 2015) that is highly amplified (blocking) despite a reduced meridional temperature gradient (consistent with Francis and Vavrus, 2012). These mechanisms have favoured more persistent weather conditions that are often associated with extreme weather events, such as the mega heatwave in Russia in 2010 (Barriopedro et al., 2011) or the long drought in central USA (Coumou and Rahmstorf, 2012). However, there is currently much debate on the nature of mechanism(s) responsible for this increment of persistent weather patterns associated with such extreme climatic events (Cohen et al., 2014), with some authors suggesting other drivers (albeit equally exacerbated by global warming), such as the role of drying soils associated with earlier SCE melting (Tang et al., 2014) or simply related to tropical extratropical interactions (Palmer, 2014). According to Cohen et al. (2014) there are three major dynamical frameworks to propagate the anomalous climate signals originating in the Arctic (namely changes in SIE and SCE) toward midlatitudes: (1) changes in storm tracks, (2) changes in the characteristics of the jet stream, and (3) anomalous planetary wave configurations triggered by regional changes in the tropospheric circulation. Tang et al. (2014) compared the role played by both SIE and SCE in what concerns their capacity to change atmospheric circulation and inducing extreme summer extremes in northern midlatitudes. These authors have found that despite the stronger decrease in SCE compared to SIE, the latter provides a stronger response in terms of atmospheric circulation anomalies. Often related with climatic extremes, Tang et al. (2014) provide evidence that the combined reductions of SIE and SCE are associated with "widespread upper-level height increases, weaker upper-level zonal winds at high latitudes, a more amplified upper-level pattern, and a general northward shift in the jet stream".

Considering all the above reasons the Arctic sector emerges as the most sensitive region of the climate system to the effects of global warming, but it also represents an area where current and future changes are bound to affect the climate at a much larger scale (Screen and Simmonds, 2010; Tang et al., 2014; Cohen et al., 2014).

2 Main mechanisms relating sea ice decline and increased moisture transport

The atmospheric branch of the hydrological cycle plays a fundamental role in establishing the link between the Arctic system and the global climate. However, to the best of our knowledge, this role has not been fully accounted for objectively, although the transport of moisture from the extratropical regions to the Arctic has increased in recent decades (Zhang et al., 2012), and it is expected to further increase under global warming, independently of the climate change scenario considered (Kattsov et al., 2007). Some works try to explain extreme events of atmospheric moisture transport to the Arctic through the occurrence of atmospheric rivers (Woods et al., 2013) and Rossby wave breaking events (Liu and Barnes, 2015). The general increase of moisture could be due to changes in circulation patterns, which have altered the location of the most important moisture sources, or it could be the result of changes in the magnitude of the existing moisture sources as a consequence of enhanced evaporation, or a combination of these two mechanisms (Gimeno et al., 2012, 2013).

Most studies of changes on moisture transport towards the Arctic climate make use of one of three possible techniques, namely (1) Eulerian approaches (e.g. Jakobson and Vihma, 2010), which can be used to estimate the ratio of advected-to-recycled moisture and to calculate the moisture transport between predetermined source and sink regions; (2) isotope analysis (e.g. Kurita, 2011), but neither this nor the Eulerian techniques are capable of a proper geographical identifica-

tion of the sources; or (3) more complex Lagrangian computational techniques that are able to infer the sources of the precipitation that falls in a target region and thus overcome the limitations of (1) and (2). An analysis of the performance of these Lagrangian techniques and their advantages over Eulerian and isotope analysis was recently given by Gimeno et al. (2012). Here we will critically analyse some of the previous assessments that have established the link between moisture transport from midlatitudes towards the Arctic region and changes in Arctic SIE. In addition, we will use a sophisticated Lagrangian approach to contrast these existing results using new information and insights.

In recent years a number of mechanisms have been put forward relating the strength of moisture transport and Arctic SIE. These mechanisms vary significantly in the nature of their main driver, including the following: (i) hydrological drivers, such as increments in Arctic river discharges (Zhang et al., 2012) or increments in precipitation due to enhanced local evaporation due to less SIE (Bintanja and Selten, 2014); (ii) radiative drivers, particularly through rises in cloud cover and water vapour (Kapsch et al., 2013); and (iii) dynamical drivers, namely more summer storms with unusual characteristics crossing the Arctic (Simmonds and Rudeva, 2012). Most likely these different mechanisms coexist to a certain extent and are not necessarily mutually exclusive. For instance the autumn and early positive trend is SCE (Estilow et al., 2015), which can be closely related to positive trends in Eurasian rivers (Yang et al., 2007). In particular, two of these works (Zhang et al., 2012; Kapsch et al., 2013) provide novel insight on the role played by the transport of moisture and the melting of sea ice or snow cover. Their main findings are summarized below:

1. According to Zhang et al. (2012) in their work entitled "Enhanced poleward moisture transport and amplified northern high-latitude wetting trend", the authors provide strong evidence to support (i) that there is a trend in the net poleward atmospheric moisture transport (AMT) towards the Eurasian Arctic river basins, (ii) that this net AMT is captured in 98 % of the gauged climatological river discharges, and (iii) that the upward trend of 2.6 % net AMT per decade is in good agreement with the 1.8 % increase per decade in the gauged discharges.

   The increase in Arctic river discharge is a possible cause of sea ice melting in agreement with several studies realized over the Canadian Arctic region that support these results (e.g. Dean et al., 1994; Nghiem et al., 2014). Thus, AMT can be seen to have an important role to play in this process. Nevertheless, Zhang et al. (2012) used a very simple analysis of integrated moisture fluxes, in which they calculated moisture transport from predetermined source and sink regions, and they were unable to identify the moisture source regions directly.

2. Using a very different methodology Kapsch et al. (2013), in the paper entitled "Springtime atmospheric energy transport and the control of Arctic summer sea-ice extent", demonstrated that in areas of summer ice retreat, a significantly enhanced transport of humid air is evident during spring, producing increased cloudiness and humidity resulting in an enhanced greenhouse effect.

   As for Kapsch et al. (2013), global balances of atmospheric moisture flux were used, which allowed neither the identification of the moisture sources nor any assessment of their role in the variability of the moisture transport.

3 Identifying objectively the main sources of moisture for large Eurasian river basins

The analysis adopted here to discuss existing results is mostly based on the Lagrangian particle dispersion model FLEXPART (Bintanja and Selten, 2014; Stohl and James, 2004), using data from 1979 to 2013 obtained from the ERA-Interim reanalysis of the ECMWF (Dee et al., 2011), which can be considered the state-of-the-art reanalysis in terms of the hydrological cycle (Trenberth et al., 2011; Lorenz and Kunstmann, 2012). The analysis will be restricted to years after 1979 in order to avoid working with results obtained prior to the incorporation of satellite data in the reanalysis. Using a horizontal resolution of 1° in latitude and longitude and a resolution of 61 vertical levels, the algorithm tracks atmospheric moisture along trajectories. A 3-D wind field moves a large number of so-called particles (air parcels) resulting from the homogeneous division of the atmosphere. The specific humidity (q) and the position (latitude, longitude and altitude) of all the particles are recorded at 6 h intervals. The model then calculates increases (e) and decreases (p) in moisture along each trajectory at each time step by means of variations in q with respect to time (i.e. $e - p = m\,\mathrm{d}q/\mathrm{d}t$). The quantity ($E - P$) is calculated for a given area of interest by summing $e - p$ for all particles crossing a 1° grid column of the atmosphere, where E and P are the rates of evaporation and precipitation, respectively. The particles are tracked and a database is created with values of $E - P$ averaged and integrated over 10 days of transport, this being the average residence time of water vapour in the atmosphere (Numaguti, 1999). The main sources of moisture for the target area (in terms of when and where the air masses that reach the target area acquire or lose moisture) are shown through the analysis of the 10-day integrated $E - P$ field. For a comprehensive review see Gimeno et al. (2012), which provides details of the limitations of this Lagrangian approach, its uncertainty and significance, and its advantages and disadvantages with respect to other methods of estimating moisture sources. For further information on FLEXPART model see Stohl et al. (2004).

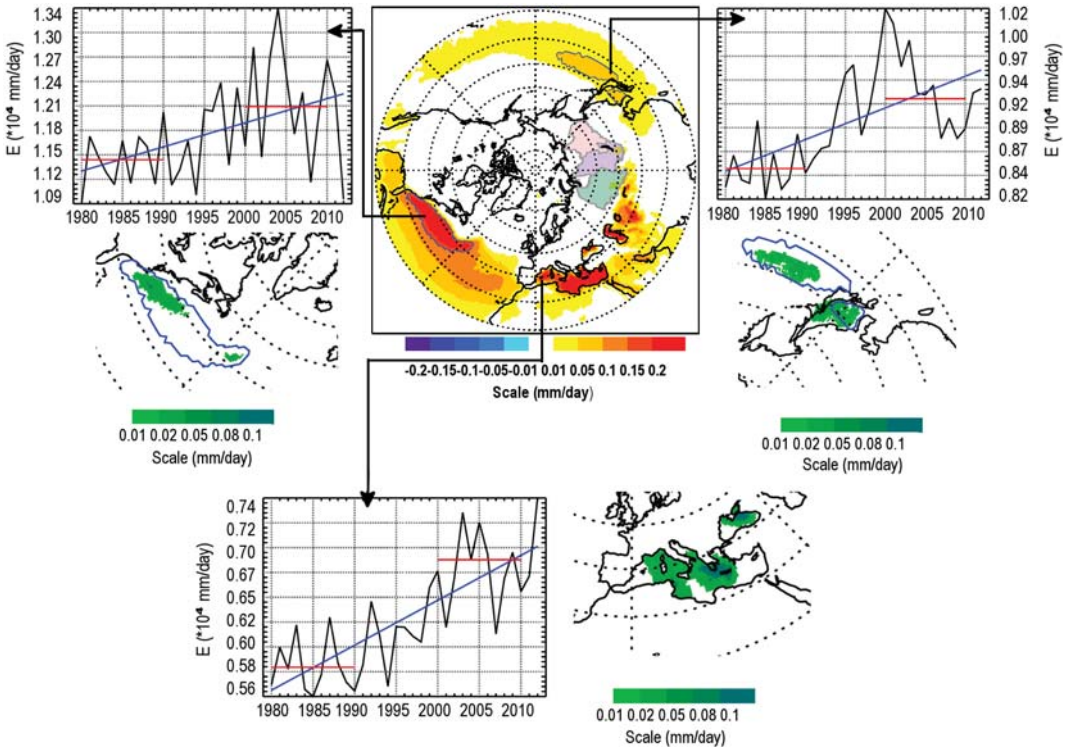

Figure 1. Centre panel: climatological October–March 10-day integrated ($E - P$) values observed for the period 1979–2012, for all the particles bound for the Ob, Yenisei and Lena river basins (green, purple and pink areas respectively indicate the basin area), determined from backward tracking. Warm colours represent regions acting as moisture sources for the tracked particles. Plots in green show the significant positive differences at the 95 % level after bootstrap test (1000 interactions) in the composites of the moisture sources of the Arctic river basins between the decades 2001–2010 and 1981–1990. Temporal series show the evolution of the average evaporation derived from OAFlux data set for the main moisture sources for the Arctic river basins (the Atlantic and Pacific sources, those circled with a blue line in the central figure, and for the whole Mediterranean Sea basin). The blue lines are the linear trend and the red ones denote the 10-year periods used on composites.

According to Zhang et al. (2012), temporal lags must be considered when linking AMT from lower latitudes with snowpack accumulation and also between this and Arctic river discharges. Thus, summer Arctic river discharge can be related to the result of the melting of the snowpack that accumulated during the preceding months, while the AMT most related to the summer river discharge corresponds to that resulting from snowpack accumulation during the period October–March. We therefore choose this period to estimate the moisture sources for the target region formed by the Ob, Yenisei and Lena river basins, as in the work of Zhang et al. (2012). The central panel of Fig. 1 shows that the main moisture sources are located over the Mediterranean Sea, and the smaller Caspian and Black seas, as well as the North Atlantic Ocean and to a somewhat lesser degree the North Pacific Ocean in the paths of the global western boundary currents and their extensions. This result is striking because these source regions seem to match those areas with the highest trends in terms of evaporation in the past few decades.

4 Trends in evaporation from main sources: possible consequences

Using some of the best estimates of evaporation, namely those derived from the OAFlux data (Yu and Weller, 2007), strong increasing trends can be seen in evaporation from the oceans since 1978, with the upward trend being most pronounced during the 1990s. The spatial distribution of these trends (Yu, 2007) shows that while the increase in evaporation has occurred globally, it has primarily been observed during the hemispheric winter and is strongest along the paths of the global western boundary currents and any inner seas with wind forcing playing a dominant role. According to Yu (2007) and after performing an empirical orthogonal function (EOF) analysis of evaporation and its related variables (wind speed and air–sea humidity differences), the wind forcing is mainly responsible for the decadal change through two mechanisms: one direct – "greater wind speed induces more evaporation by carrying water vapour away from the evaporating surface to allow the air–sea humidity gradients to be reestablished at a faster pace" – and a

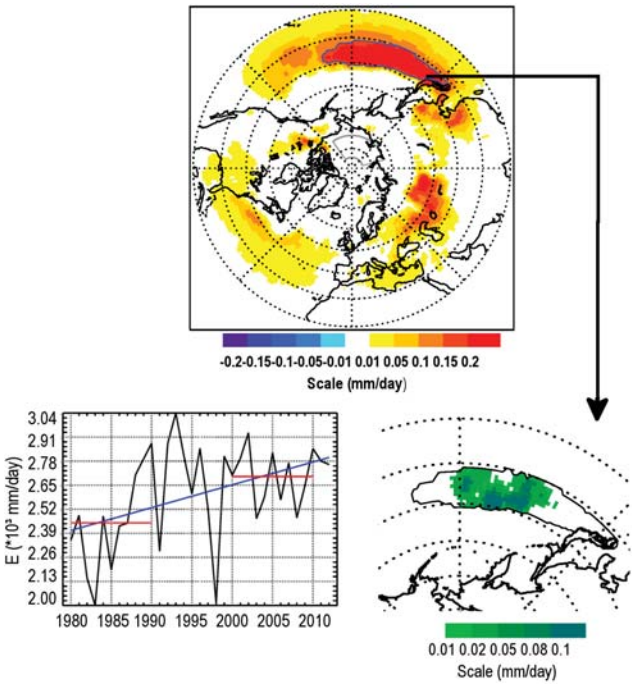

Figure 2. As Fig. 1 but for the Kapsch area (75–85° N, 115–215° E), denoted with the grey contour in the bottom panel.

second one indirect – "the enhanced surface wind strengthens the wind-driven subtropical gyre, which in turn drives a greater heat transport by the western boundary currents, warms up SST along the paths of the currents and extensions, and causes more evaporation by enlarging the air–sea humidity gradients". The EOF analysis also showed that the interannual variability of evaporation occurred on similar timescales to those of the El Niño–Southern Oscillation. Figure 1a–c also show the evolution of the average evaporation derived from OAFlux for the main moisture sources for the Arctic river basins (those circled with a blue line and the entire Mediterranean Sea basin). Although important, interannual variability superimposed to a pronounced decadal-scale variability previously commented, trends are significant in most of the grid points encircled and are especially clear for the Atlantic, Pacific and Mediterranean sources. Similar results were reached when evaporation taken from ERA-Interim was used (not shown). The differences in the composites of the moisture sources of the Arctic river basins between the decade 2001–2010 and the decade 1981–1990 are also shown in Fig. 1, with greenish colours indicating regions where their contribution as a source intensified over these years. From these results it seems clear that there is an enhanced moisture contribution from those moisture regions where the evaporation increased.

We have repeated the procedure considering the region analysed by Kapsch et al. (2013). That is, in this case, the late spring (April and May) moisture sources detected are related to the area where the September sea ice anomaly is encountered. Overall results (Fig. 2) are quite similar to those presented for the Arctic river basins, and the main moisture sources are also placed in the paths of the global western boundary currents in both the North Atlantic and the North Pacific oceans (the main one in this case) and in the Mediterranean basins (more moderate in this case).

In this regard the intensification of evaporation in these source regions could have a dual effect on the reduction of September Arctic ice, through (1) intensification of summer river discharge and (2) enhancement of the greenhouse effect due to an increase in cloudiness and humidity over the ice-melting regions.

5 Summary and conclusions

We have made a critical assessment of the results obtained in two important recent works that offer new understanding of the role played by the transport of moisture and the melting of sea ice or snow cover (Zhang et al., 2012; Kapsch et al., 2013). The Lagrangian analysis adopted in our approach stresses the connection between two climate change indicators, namely an increase in evaporation over source regions and Arctic ice melting. We are confident that our results provide the necessary link between these two realms and suggest an intricate chain of events related to (1) positive trends in evaporation in specific ocean areas that correspond to the main moisture source regions of Eurasian rivers, (2) upward trends in atmospheric transport from these regions to the Arctic river basins/regions where ice-melting occurs, and (3) trends in river discharges/moisture and cloud cover. These developments merit further and more comprehensive study in terms of their effects on present and future climates.

Acknowledgements. The authors acknowledge funding by the European ERA.Net RUS programme, within the project ACPCA and by the Spanish MINECO and FEDER within the project TRAMO.

Edited by: C. Franzke

References

Baggett, C. and Lee, S.: Arctic warming induced by tropically forced tapping of available potential energy by planetary scale waves, J. Atmos. Sci., 72, 1562–1568, 2015.

Barriopedro D., Fischer E. M., Luterbacher L., Trigo R. M., and García-Herrera R.: The hot summer of 2010: redrawing the temperature record map of Europe, Science, 332, 220–224, doi:10.1126/science.1201224, 2011.

Bintanja, R. and Selten, F. M.: Future increases in Arctic precipitation linked to local evaporation and sea-ice retreat, Nature, 509, 480–482, 2014.

Chen, X. and Tung, K. K.: Varying planetary heat sink led to global-warming slowdown and acceleration, Science, 345, 897–903, doi:10.1126/science.1254937, 2014.

Cohen, J., Screen, J. A., Furtado, J. C., Barlow, M., Whittleston, D., Coumou, D., Francis, J., Dethloff, K., Entekhabi, D., Overland, J., and Jones, J.: Recent Arctic amplification and extreme mid-latitude weather, Nat. Geosci., 7, 627–637, doi:10.1038/ngeo2234, 2014.

Comiso, J. C., Parkinson, C. L., Gersten, R., and Stock, L.: Accelerated decline in the Arctic sea ice cover, Geophys. Res. Lett., 35, L01703, doi:10.1029/2007GL031972, 2008.

Coumou, D. and Rahmstorf, S.: A decade of weather extremes, Nat. Clim. Chang., 2, 491–496, 2012.

Dean, K. G., Stringer, W. J., Ahlnas, K., Searcy, C., and Weingartner, T.: The influence of river discharge on the thawing of sea ice, Mackenzie River Delta: albedo and temperature analyses, Polar Res., 13, 83–94, doi:10.1111/j.1751-8369.1994.tb00439.x, 1994.

Dee, D, Uppala, S. M., Simmons, A. J., Berrisford, P., Poli, P., Kobayashi, S., Andrae, U., Balmaseda, M. A., Balsamo, G., Bauer, P., Bechtold, P., Beljaars, A. C. M., van de Berg, L., Bidlot, J., Bormann, N., Delsol, C., Dragani, R., Fuentes, M., Geer, A. J., Haimberger, L., Healy, S. B., Hersbach, H., Hólm, E. V., Isaksen, L., Kållberg, P., Köhler, M., Matricardi, M., McNally, A. P., Monge-Sanz, B. M., Morcrette, J. J., Park, B. K., Peubey, C., de Rosnay, P., Tavolato, C., Thépaut, N., and Vitart, F.: The ERA Interim reanalysis: Configuration and performance of the data assimilation system, Q. J. Roy. Meteorol. Soc., 137, 553–597, doi:10.1002/qj.828, 2011.

Estilow, T. W., Young, A. H., and Robinson, D. A.: A long-term Northern Hemisphere snow cover extent data record for climate studies and monitoring, Earth Syst. Sci. Data, 7, 137-142, doi:10.5194/essd-7-137-2015, 2015.

Francis, J. A. and Vavrus, S. J.: Evidence linking Arctic amplification to extreme weather in mid-latitudes, Geophys. Res. Lett., 39, L06801, doi:10.1029/2012GL051000, 2012.

Gimeno, L., Stohl, A., Trigo, R. M., Dominguez, F., Yoshimura, K., Yu, L., Drumond, A., Duran-Quesada, A. M., and Nieto, R.: Oceanic and Terrestrial Sources of Continental Precipitation, Rev. Geophys., 50, RG4003, doi:10.1029/2012RG000389, 2012.

Gimeno, L., Nieto, R., Drumond, A., Castillo, R., and Trigo, R. M.: Influence of the intensification of the major oceanic moisture sources on continental precipitation, Geophys. Res. Lett., 40, 1443–1450, doi:10.1002/grl.50338, 2013.

Graversen, R. G., Mauritsen, T., Tjernstrom, M., Källen, E., and Svensson, G.: Vertical structure of recent Arctic warming, Nature, 451, 53–56, doi:10.1038/nature06502, 2008.

Hansen, J., Sato, M., and Ruedy, R.: Perception of climate change, P. Natl. Acad. Sci., 109, 14726–14727, doi:10.1073/pnas.1205276109, 2012.

IPCC: Climate Change 2013: The physical science basis, in: Contribution of working group 1 to the fifth assessment report of the intergovernmental panel on climate change, edited by: Stocker, T. F., Qin, D., Planttner, G. K., Tignor, M., Allen, S. K., Boschung, J., Nauels, A., Xia, Y., Bex, V., and Midgley, P. M., Cambridge University Press, Cambridge, UK and New York, NY, USA, 2013.

Jakobson, E. and Vihma, T.: Atmospheric moisture budget in the Arctic based on the ERA-40 reanalysis, Int. J. Climatol., 30, 2175–2194, doi:10.1002/joc.2039, 2010.

Kapsch, M. L., Graversen, R. G., and Tjernström, M.: Springtime atmospheric energy transport and the control of Arctic summer sea-ice extent, Nat. Clim. Change, 3, 744–748, doi:10.1038/nclimate1884, 2013.

Kattsov, V. M., Walsh, J. E., Chapman, W. L., Govorkova, V. A., Pavlova, T. V., and Zhang, X.: Simulation and projection of Arctic freshwater bedget components by the IPCC AR4 global climate models, J. Hydrometeorol., 8, 571–589, 2007.

Kosaka, Y. and Xie, S. P.: Recent global-warming hiatus tied to equatorial Pacific surface cooling, Nature, 501, 403–407, doi:10.1038/nature12534, 2013.

Kurita, N.: Origin of Arctic water vapor during the ice-growth season, Geophys. Res. Lett., 38, L02709, doi:10.1029/2010GL046064, 2011.

Liu, C. and Barnes, E. A.: Extreme moisture transport into the Arctic linked to Rossby wave breaking, J. Geophys. Res.-Atmos., 120, 3774–3788, doi:10.1002/2014JD022796, 2015.

Lorenz, C. and Kunstmann, H.: The hydrological cycle in three state-of-the-art reanalyses: Intercomparison and performance analysis, J. Hydrometeorol., 13, 1397–1420, 2012.

Lucarini, V. and Ragone, F.: Energetics of climate models: Net energy balance and meridional enthalpy transport, Rev. Geophys., 49, RG1001, doi:10.1029/2009RG000323, 2011.

Nghiem, S. V., Hall, D. K., Rigor, I. G., Li, P., and Neumann, G.: Effects of Mackenzie River discharge and bathymetry on sea ice in the Beaufort Sea, Geophys. Res. Lett., 41, 873–879, doi:10.1002/2013GL058956, 2014.

Numaguti, A.: Origin and recycling processes of precipitating water over the Eurasian continent: Experiments using an atmospheric general circulation model, J. Geophys. Res., 104, 1957–1972, 1999.

Palmer T.: Record-breaking winters and global climate change, Science, 344, 803–804, doi:10.1126/science.1255147, 2014.

Park, D. S. R., Lee, S., and Feldstein, S. B.: Attribution of the Recent Winter Sea Ice Decline over the Atlantic Sector of the Arctic Ocean, J. Climate, 28, 4027–4033, 2015.

Schweiger, A. J., Lindsay, R. W., Vavrus, S., and Francis, J. A.: Relationships between Arctic sea ice and clouds during autumn, J. Climate, 21, 4799–4810, 2008.

Screen, J. A. and Simmonds, I.: The central role of diminishing sea ice in recent Arctic temperature amplification, Nature, 464, 1334-1337, doi:10.1038/nature09051, 2010.

Seneviratne, S., Donat, M. G., Mueller, B., and Alexander, L. V.: No pause in the increase of hot temperature extremes, Nat. Clim. Change, 4, 161–163, 2014.

Serreze, M. C. and Francis, J. A.: The Arctic amplification debate, Climatic Change, 76, 241–264, 2006.

Simmonds, I. and Rudeva, I.: The great Arctic cyclone of August 2012, Geophys. Res. Lett., 39, L23709, doi:10.1029/2012GL054259, 2012.

Stohl, A. and James, P. A.: Lagrangian analysis of the atmospheric branch of the global water cycle: Part I. Method description, validation, and demonstration for the August 2002 flooding in central Europe, J. Hydrometeorol., 5, 656–678, 2004.

Tang, Q., Zhang, X., and Francis, J. A.: Extreme summer weather in northern mid-latitudes linked to a vanishing cryosphere, Nat. Clim. Change, 4, 45–50, doi:10.1038/nclimate2065, 2014.

Trenberth, K. E., Fasullo, J. T., and Mackaro, J.: Atmospheric moisture transports from ocean to land and global energy flows in reanalyses, J. Climate, 24, 4907–4924, 2011.

Woods, C., Caballero, R., and Svensson, G.: Large-scale circulation associated with moisture intrusions into the Arctic during winter, Geophys. Res. Lett., 40, 4717–4721, doi:10.1002/grl.50912, 2013.

Yang, D., Zhao, Y., Armstrong, R., Robinson, D., and Brodzik, M.-J.: Streamflow response to seasonal snow cover mass changes over large Siberian watersheds, J. Geophys. Res., 112, F02S22, doi:10.1029/2006JF000518, 2007.

Yu, L.: Global variations in oceanic evaporation (1958–2005): The role of the changing wind speed, J. Climate, 20, 5376–5390, 2007.

Yu, L. and Weller, R. A.: Objectively analyzed air–sea heat fluxes for the global ice-free oceans (1981–2005), B. Am. Meteorol. Soc., 88, 527–539, 2007.

Zhang, X., He, J., Zhang, J., Polyakov, I., Gerdes, R., Inoue, J., and Wu, P.: Enhanced poleward moisture transport and amplified northern high-latitude wetting trend, Nat. Clim. Change, 3, 47–51, doi:10.1038/nclimate1631, 2012.

Moisture transport from the Arctic: A characterization from a Lagrangian perspective

M. Vázquez[1], R. Nieto[1,2], A. Drumond[1] and L. Gimeno[1]

[1] Environmental Physics Laboratory (EPhysLab), Facultade de Ciencias, Universidad de Vigo, Ourense, Spain
[2] Department of Atmospheric Sciences, Institute of Astronomy, Geophysics and Atmospheric Sciences, University of São Paulo, São Paulo, Brazil

*Correspondence: martavazquez@uvigo.es

Abstract- The Arctic Ocean has suffered extreme reductions in sea ice in recent decades, and the changes observed suggest implications in terms of moisture transport. The analysis of those areas affected by Arctic moisture transport is important for establishing those areas vulnerable to change. To this end, the Lagrangian model FLEXPART was used in this work to establish the main sinks for the Arctic Ocean, focusing on the moisture transport from this region. Our results suggest that most of the moisture loss occurs locally over the Arctic Ocean, especially in summer. However, the contribution of moisture from the Arctic Ocean to continental areas in North America and Eurasia in autumn and winter is also noted.

Keywords- Arctic sinks; moisture transport; Lagrangian model

I. INTRODUCTION

The Arctic region is currently experiencing extreme changes. The extent of sea ice has shown a downward trend in the last few decades for all seasons (Cavaliery and Parkinson, 2012; Polyakov et al., 2012; Comiso and Hall, 2014; Comiso et al. 2008; Parkinson and DiGirolamo, 2016), reaching its lowest recorded September value in 2012 according to the satellite record (Fetterer et al., 2016). Moreover, the melt season is lengthening (Stroeve et al., 2016), producing ever longer periods without any sea ice at all. This situation is expected to increase under global warming (Holland et al. 2006; Wang and Overland, 2009; Overland et al., 2013).

This reduction in sea ice and its possible implications have been the subject of wide-ranging investigations in recent years. The effects of sea-ice decline on the climate system has been of particular interest, and a detailed review of its local and remote effects was undertaken by Vihma (2014). Any reduction in sea ice has a direct influence on moisture uptake, and increased evaporation over the region has already been observed for the period 2003-2013 (Boisvert et al., 2015). Many previous authors have analysed the effect of decreasing sea ice on atmospheric circulation. Overland and Wang (2010) for example showed the influence of sea-ice decrease on patterns of atmospheric circulation. Furthermore, reduced sea ice has been proven to affect mid-latitude weather. Recent results point to a link between sea-ice reduction and extreme winter weather conditions in Eurasia (Wegmann et al., 2015; Cohen et al., 2014; Liu et al., 2012), and a number of authors have highlighted a relationship between the decrease in sea ice and an increase in winter snowfall over Siberia (Wegmann et al., 2015; Liu et al. 2012; Park et al., 2012), but with the opposite relationship applying over North America, and in general at the hemispheric scale (Park et al., 2012).

Several studies have analysed the moisture budget for the Arctic region (eg. Groves and Francis, 2002; Serreze et al. 2006). From this studies the Arctic region can be considered as a

net sink of moisture being specially relevant on the moisture input precipitation from lower latitudes or river discharge (Serreze et al., 2006). Despite this fact, and as commented before, the recent changes suffered on the Arctic and the intensification on the hydrological cycle in this region could have influences beyond the Arctic too (eg. Cohen et al., 2014; Vihma 2014). As far as we know, no complete analysis of moisture transport from the Arctic has yet been undertaken. The recent increase in the amount of open water in the Arctic Ocean means that it is of crucial importance to analyse how this change can affect the moisture transport from the region, in order to identify those areas affected by the Arctic contribution of moisture, and to establish those regions most vulnerable to possible changes in moisture transported from the Arctic. For this purpose, the Lagrangian model FLEXPART was used in this study to establish the main sinks for moisture originating in the Arctic Ocean. Lagrangian models have previously been shown to be useful for investigating source-sink relationships (Gimeno et al., 2012), and have been widely applied to this end in a number of previous studies (e.g., Nieto et al., 2007; Sodemann, 2008; Vazquez et al., 2016).

II. METHODS

The Arctic Ocean was divided into different areas as shown in Figure 1; these are considered "source" regions (those regions from where particles were followed). It is important to notice that the use of the term "source" in this work is referred to those regions form where particles were follow. This division follows the approach of Boisvert et al. (2015) in separating the Arctic Ocean into its more relevant areas.

A Lagrangian approach was used to analyse moisture transport from the Arctic, based on the particle dispersion model FLEXPART v9.0 (i.e., the FLEXible PARTicle dispersion model of Stohl and James (2004, 2005)) and forced by ERA-Interim reanalysis data from the European Centre for Medium-Range Weather Forecasts (ECMWF). Data from this reanalysis cover the period from January 1979 and continue to be used, extending forwards in near-real time (Dee et al., 2011). The data are available at six-hour intervals at a 1°x1° spatial resolution in latitude and longitude on 61 vertical levels (1000 to 0.1 hPa).

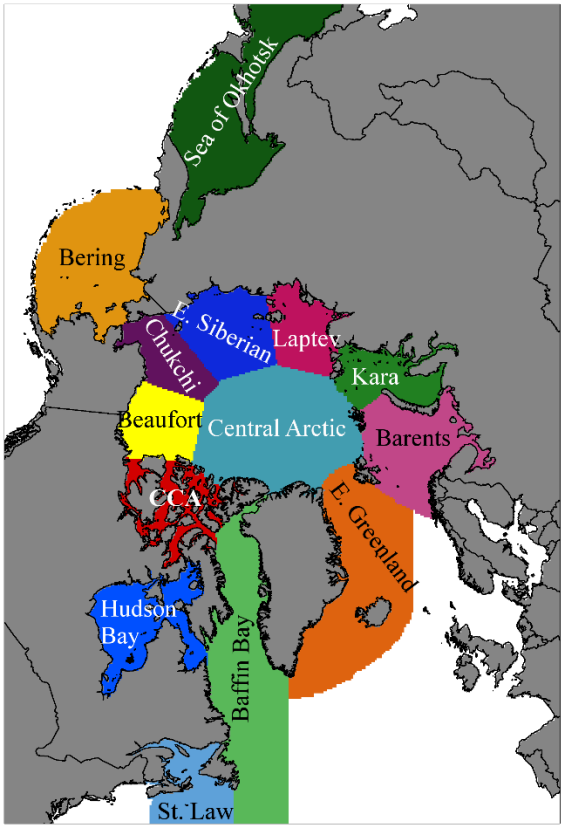

Figure 1. Division of the Arctic as used in this study.

The FLEXPART model divides the atmosphere into finite elements of volume with equal mass (hereafter "particles") and, as used herein, it follows the air movement by tracking individual 3-D trajectories forwards in time for 10 days, this being the period representing the average residence time of water vapour in the atmosphere (Numagati, 1999). This tracking allows us to identify the main sinks for the Arctic Ocean by analysing changes in specific humidity (q). Taking into account the changes in (q) it is possible to obtain the net rate of change of water vapour $(e-p)$ for every particle (of mass m) along its trajectory using the expression $(e-p)=m(dq/dt)$, where e and p represent evaporation and precipitation, respectively. The total atmospheric moisture budget $(E-P)$ is obtained by adding up $(e-p)$ for all the particles over a given area at each time step used in the analysis. It is important to

clarify that the $(E-P)$ value as calculated here do not represent the total $(E-P)$ balance over and specific region and cannot be compared with the result obtained via a eulerian perspective. In our approach the $(E-P)$ value represent only the moisture change of particles which come from the Arctic region. For further details on lagrangian methodologies and their comparison with another methodologies for moisture transport analysis can be found on Gimeno et al. (2012).

Despite being a useful tool on moisture transport analyses and to be widely used for this purpose (eg. Stohl et al., 2008; Nieto et al., 2007; Gimeno et al., 2013), FLEXPART model have some limitations. The limited resolution of input data, as well as their uncertainties and interpolation is an important source of error, especially in areas of low data coverage (Schlosser et al., 2008; Scharchilli et al. 2011). Moreover there are numerical errors related with the temporal variation of the particles' moisture which produce miscalculation on the moisture transport (Stohl and James, 2004). However, according to Stohl and James (2004), those errors may cancel each other due to the huge amount of particles considered in the experiment.

In this study we consider the 36-year period 1980-2015 for the tracking of particles from the Arctic Ocean as a whole and the individual regions described previously. Because the tracking is undertaken for 10 days, the moisture budget $(E-P)$ over each grid cell was integrated for the whole period and hereinafter denoted as $(E-P)i10$, this amount showing those areas where particles acquire or lose moisture along their trajectories. The aim of this work is to analyse the moisture transport from the Artic region and for that purpose the particles from the ocean were followed along their trajectories. As we are interested in those areas with a net moisture contribution from the Arctic, only those regions showing negative values of $(E-P)i10$ were selected. However it is important to highlight that the moisture lost on the transport did not necessary come from Arctic evaporation. Despite the model take into account this process, at the initial step of the simulation all the moisture availability is considered; some of which should proceed from external areas.

III. RESULTS

The analysis described above allowed us to identify sinks for the moisture from the Arctic Ocean. Figure 2 represents the moisture contribution from the whole of the Arctic Ocean (all the regions in Fig. 1 taken together) on an annual and seasonal basis (Figure 2a and 2b-e, respectively). In general, it can be observed that most of the moisture contribution from the Arctic Ocean occurs over the region itself, especially over the Central Arctic and East Greenland Seas, with the contribution over the Gulf of Alaska and the western coast of Greenland also notable. An important moisture contribution occurs over the Eurasian seas (from Barents to the Chukchi Sea), the Beaufort Sea, and the Sea of Okhotsk. In seasonal terms, the spatial distribution of moisture contribution also shows some variations. In spring (Figure 2b,), a major contribution can be seen over the East Greenland Sea, on the southeastern coast of Greenland, and also over the Gulf of Alaska where an important contribution can be seen. Over the Central Arctic and especially over its surrounding seas, the moisture contribution shows lower values than the annual mean. In general, the contribution in spring is seen over oceanic areas, although some contribution occurs over northeastern Russia, the west coast of North America, and northern Canada (values lower than 0.8 mm/day). In summer (Figure 2c) the moisture contribution increases considerably and is especially important over the Central Arctic, the East Greenland Sea, and Baffin Bay, although some high values (greater than 4.8 mm/day) appear over most of the Arctic Ocean. A generally less important contribution occurs over continental areas during summer. In autumn (Figure 2d) the moisture contribution from the Arctic Ocean shows a similar distribution to the annual mean. The contribution occurs in general over the whole of the Arctic Ocean, with the exception of the Bering Sea and most of the Norwegian and Barents Seas. Maximum moisture input is observed over the Central Arctic, the East Greenland Sea, the West Coast of Greenland, the Norwegian coast, and the Gulf of Alaska.

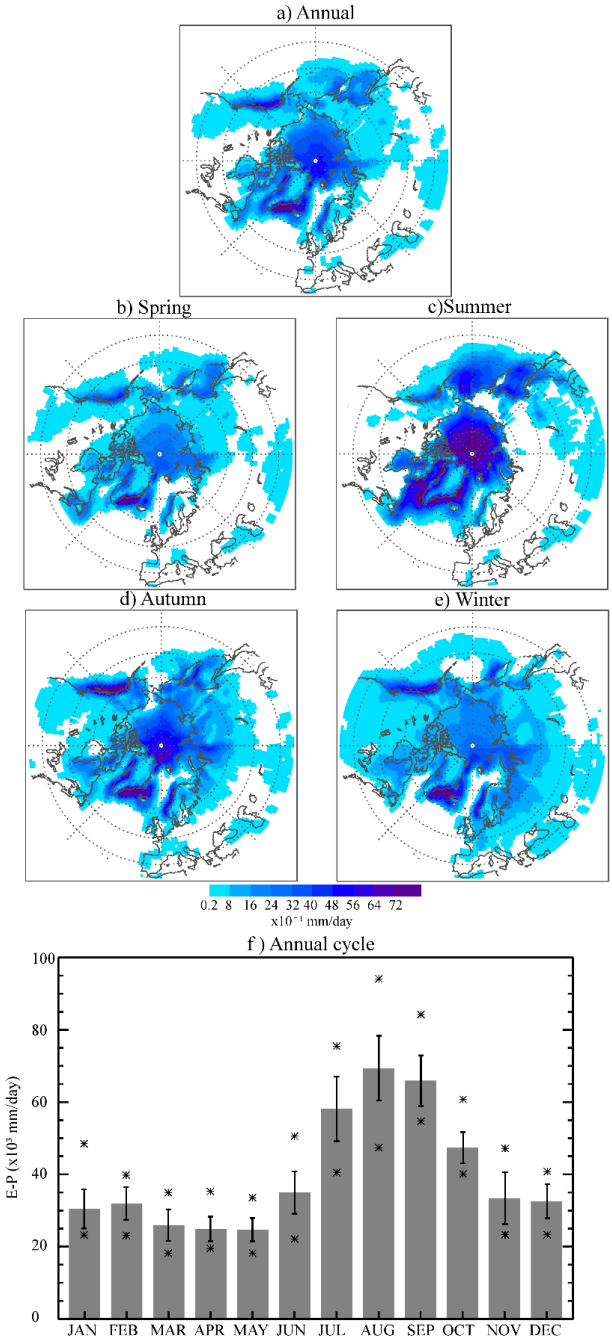

Figure 2. Geographical (E-P)<0 distribution from the whole Arctic Ocean annually (a) and seasonally (b-e) and seasonal cycle (f). Asterisks represent maximum and minimum values for each month and vertical whiskers represent the standard deviation.

During this season the moisture contribution is increased over the continental areas, especially over North Eurasia, North America, and Canada. Finally, in winter (Figure 2e) the moisture contribution is more evenly distributed, affecting the oceanic areas in general, but also revealing some contribution over the continents of North America and northern Asia. The most important contribution occurs over the East Greenland Sea, the Gulf of Alaska, and the Norwegian coast.

In order to show the annual variability of the moisture supplied by the Arctic Ocean, Figure 2f shows the monthly contributions. It can be seen that these are at their highest levels from June to October, with a maximum contribution in August, followed by September. For the remaining months the contribution does not show important variations, with a total contribution of around 10000 mm/day. In general, the seasonal cycle seems to be influenced by the extent of the sea ice, which shows minimum values in late summer and early autumn, providing a greater amount of moisture available for precipitation at these times.

In order to assess the contributions of different parts of the Arctic Ocean, Figure 3 shows the values of (E-P)i10 <0 for each of the areas indicated in Figure 1. In general, the contributions occur over the area itself in each case, especially for the Central Arctic and surrounding seas (regions 2 to 9). The exceptions are the Barents Sea and Baffin Bay, which provide moisture to the regions around them, rather than to the source itself. For the Barents Sea, its contribution affects mainly the central Arctic to the north of the source, the Kara Sea, the East Greenland Sea, and the Norwegian coast. The moisture contribution from Baffin Bay mainly affects the surrounding coastal areas and to a lesser degree the East Greenland Sea and the Norwegian coast, the Canadian Archipelago, Hudson Bay, and the Gulf of Alaska. Both these regions were previously identified as moisture sources for the Arctic: Baffin Bay represents an important moisture source for the Canadian Archipelago (Koerner and Russel, 1979) and the Barents Sea was recently discovered to provide a significant amount of moisture for the Arctic system in winter (Vazquez et al., 2016). This suggests that these regions could be considered evaporative areas for moisture entering the Arctic domain. For the remaining regions, the Canadian seas (the Canadian Archipelago, and the Beaufort and Chukchi Seas) provide some moisture contribution for the Gulf of Alaska,

and the Eurasian ones show some influence over northern Russia, especially the East Siberian Sea. For those areas situated at lower latitudes, the moisture contributions are more widespread. The East Greenland Sea mainly provides moisture for the oceanic regions around Greenland, and some contribution can be observed too over Hudson Bay and the Gulf

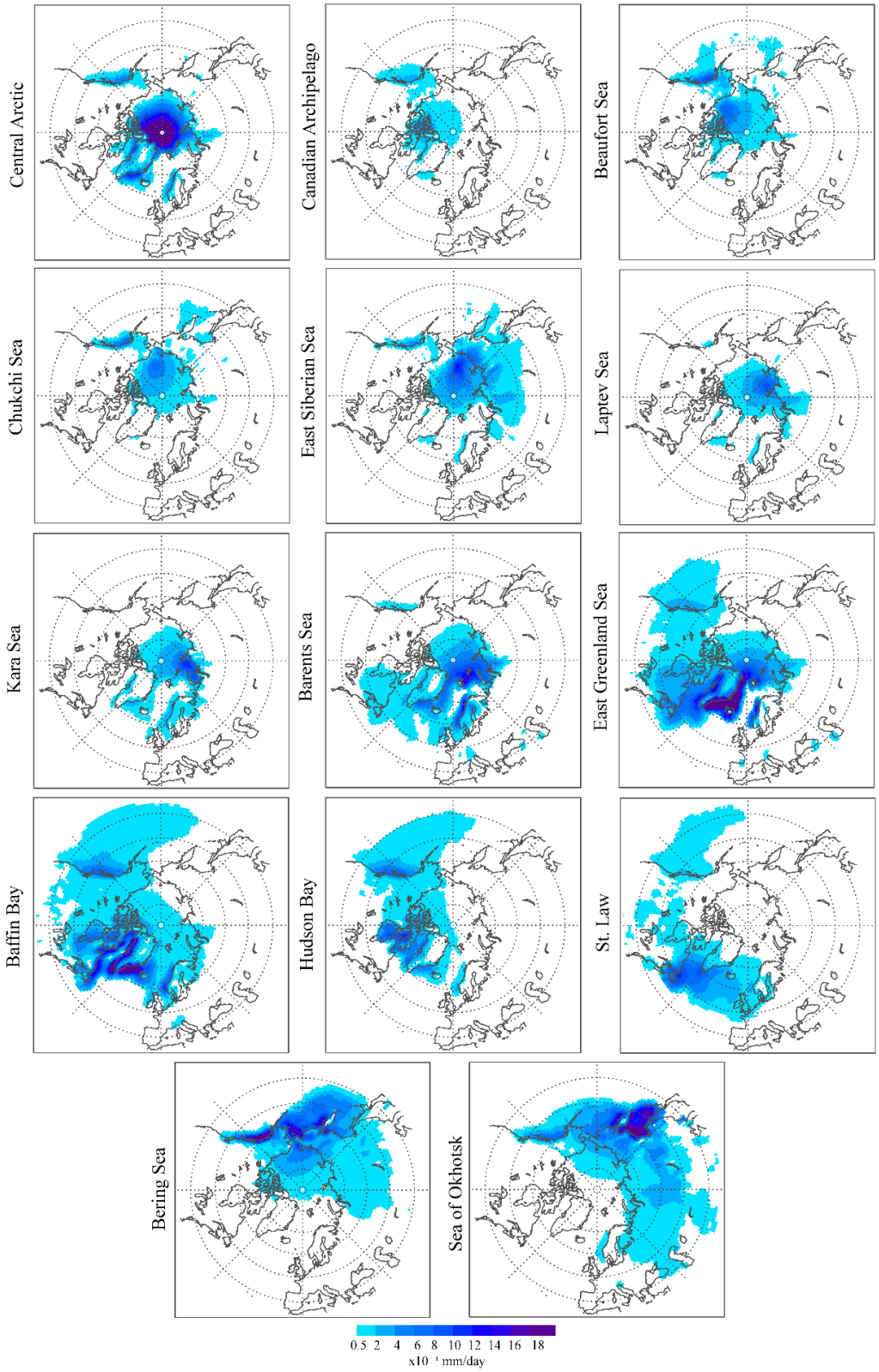

Figure 3. Geographical distribution of (E-P)<0 analysed annually from each of the source areas described in Figure 1.

of Alaska. The contribution of Hudson Bay is similar to that of Baffin Bay, but it has less of an influence over the East Greenland Sea and the Norwegian Coast. The St. Law contribution mainly affects the south of Greenland. The Bering Sea provides moisture over and around itself, affecting mainly the Chukchi, East Siberian and Laptev Seas, the Gulf of Alaska, and the Sea of Okhotsk. The moisture contribution from this last sea, the Sea of Okhotsk, affects north Pacific oceanic areas and some continental regions over Eastern and Central Russia.

The complete analysis for all the regions that constitute the Arctic Sea is shown in Figures S1 to S14. These figures show the seasonal moisture contribution of each, together with the annual cycle. In general terms, it is possible to see that the maximum moisture contribution occurs between July and September and the minimum between March and May for all regions (panel b in each Figure). Spring represents not only the season with the lowest contribution (panel b) but also with the lowest spatial distribution (panel a). Despite the highest contribution being in summer or autumn, in general the greatest geographical spread is in autumn and/or winter, the exception being the Beaufort and Chukchi Seas (Figure S4a and S5a). For both these sources, the moisture contribution in summer shows not only the highest values, it also affects the greatest area due to the increase in moisture contribution over the Bering Sea. Some regions show an increase in moisture contribution over Eurasia in autumn and winter, including the Central Arctic (Figure S2a), Baffin Bay (Figure S10a), East Siberian (Figure S5a), Laptev (Figure S6a), Kara (Figure S7a), Barents (Figure S8a) and East Greenland Seas (Figure S9a). This increase can be observed in autumn for the Beaufort (Figure S3a) and Chukchi (Figure S4a) Seas, and in summer and autumn for the Bering Sea (Figure S13a) and the Sea of Okhotsk (Figure S14a).

IV. CONCLUSIONS

Characterization of the moisture contribution from the Arctic region was performed using a Lagrangian approach for the period 1980 – 2015.

In general, the moisture contribution from the Arctic occurs over the region itself, taking into account both the complete Arctic and its more relevant individual areas. Despite this local contribution, some influence on the surrounding areas was observed, affecting mainly North America and Eurasia during fall and winter, mainly from the central Arctic, the East Siberian Sea, the Laptev, Kara, Barents, East Greenland, and Bering Seas, and the Sea of Okhotsk.

The annual cycle of moisture contribution shows maximum values for late summer and early fall, when the sea ice is at a minimum. Despite high values of total moisture contribution during summer, its distribution is mainly over the Arctic itself, having little contribution over the continental areas of Alaska and Eastern Asia.

This work is a first step in the analysis of the Arctic as a moisture source and forms part of the investigation of the possible implications of changes in the Arctic in respect of the global climate. Of particular interest may be the analysis of the changes in moisture contribution associated with maximum and minimum sea ice extents, which could form the basis of future work.

ACKNOWLEDGMENT

The authors acknowledge funding by the Spanish government within the EVOCAR (CGL2015-65141-R) project, which is also funded by FEDER (European Regional Development Fund). Raquel Nieto was also supported by the Brazilian government through a CNPq grant 314734/2014-7

REFERENCES

[1] Boisvert L. N., Wu D. L. & Shie C.-L. 2015. Increasing evaporation amounts seen in the Arctic between 2003 and 2013 from AIRS data. J. Geophys. Res. Atmos. 120, 6865–6881, doi: 10.1002/2015JD023258.

[2] Cavalieri D. J. & Parkinson C. L. 2012. Arctic sea ice variability and trends, 1979–2010, The Cryosphere 6, 881-889, doi:10.5194/tc-6-881-2012.

[3] Cohen J., Screen J. A., Furtado J. C., Barlow M., Whittleston D., Coumou D., Francis J., Dethloff K., Entekhabi D., Overland J. & Jones J. 2014. Recent Arctic amplification and extreme mid-latitude weather. Nat. Geosci. 7, 627–637.

[4] Comiso J. C. & Hall D. K. 2014. Climate trends in the Arctic as observed from space. WIREs Clim Change 5: 389–409, doi:10.1002/wcc.277

[5] Comiso J. C., Parkinson C. L., Gersten R. & Stock L. 2008. Accelerated decline in the Arctic sea ice cover. Geophys. Res. Lett. 35, L01703, doi:10.1029/2007GL031972.

[6] Dee D.P., Uppala S.M., Simmons A.J., Berrisford P., Poli P., Kobayashi S., Andrae U., Balmaseda M.A., Balsamo G., Bauer P., Bechtold P., Beljaars A.C.M., van de Berg L., Bidlot J., Bormann N., Delsol C., Dragani R., Fuentes M., Geer A.J., Haimberger L., Healy S.B., Hersbach H., Hólm E.V., Isaksen L., Kallberg P., Köhler M., Matricardi M., McNally A.P., Monge-Sanz B.M., Morcrette J.-J.,. Park B.-K, Peubey C., de Rosnay P., Tavolato C., Thépaut J.-N. & Vitart F. 2011. The ERA-Interim reanalysis: configuration and performance of the data assimilation system. Q.J.R. Meteorol. Soc. 137, 553–597, doi: 10.1002/qj.828

[7] Fetterer F., Knowles K., Meier W. & Savoie M. 2016, updated daily. Sea Ice Index, Version 2. Boulder, Colorado USA. NSIDC: National Snow and Ice Data Center. doi: http://dx.doi.org/10.7265/N5736NV7.

[8] Gimeno L., Stohl A., Trigo R.M., Dominguez F., Yoshimura K., Yu L., Drumond A., Durán-Quesada A.M. & Nieto R. 2012. Oceanic and terrestrial sources of continental precipitation. Rev. Geophys. 50, RG4003, doi:10.1029/2012RG000389

[9] Gimeno L., Nieto R., Drumond A., Castillo R., Trigo R.M. 2013. Influence of the intensification of the major oceanic moisture sources on continental precipitation. Geophysical Research Letters 40, 1443-1450, doi:10.1002/grl.50338.

[10] Groves D.G. & Francis J.A. 2002. Moisture budget of the Arctic atmosphere from TOVS satellite data, J. Geophys. Res. 107(D19), 4391, doi:10.1029/2001JD001191.

[11] Holland M.M., Bitz C.M. & Tremblay B. 2006. Future abrupt reductions in the summer Arctic sea ice. Geophys. Res. Lett. 33, L23503, doi:10.1029/2006GL028024

[12] Koerner R & Russell R.D. 1979. Delta-O-18 variations in snow on the Devon Island Ice Cap, Northwest-Territories, Canada. Can J Earth Sci. 16(7), 1419–1427.

[13] Liu J.P., Curry J.A., Wang H.J., Song M.R. & Horton R.M. 2012. Impact of declining Arctic sea ice on winter snowfall. Proc. Nat. Acad. Sci. USA 109, 4074–4079, doi: (2012).10.1073/pnas.1114910109

[14] Nieto R., Gimeno L., Gallego D. & Trigo R. 2007. Contributions to the moisture budget of airmasses over Iceland, Meteorologische Zeitschrift 16, 37-44.

[15] Numagati A. 1999. Origin and recycling processes of precipitation water over the Eurasian continent: Experiments using an atmospheric general circulation model. J. Geophys. Res. 104, 1957-1972.

[16] Overlan J.E. & Wang M. 2010. Large-scale atmospheric circulation changes are associated with the recent loss of Arctic sea ice. Tellus A 62, 1–9, doi:10.1111/j.1600-0870.2009.00421.x

[17] Overland J.E., Wang M., Walsh J.E. & Stroeve J.C. 2014. Future Arctic climate changes: Adaptation and mitigation time scales. Earth's Future 2: 68–74.

[18] Park H, Walsh J.E, Kim Y, Nakai T & Ohata T. 2013. The role of declining Arctic sea ice in recent decreasing terrestrial Arctic snow depths. Polar Sci. 7, 174– 187.

[19] Polyakov I.V., Walsh J.E. & Kwok R. 2012. Recent Changes of Arctic Multiyear Sea Ice Coverage and the Likely Causes.

Bull. Amer. Meteor. Soc., 93, 145–151, doi: 10.1175/BAMS-D-11-00070.1.

[20] Scarchilli C., Frezzotti M. & Ruti P.M. 2011. Snow precipitation at four ice core sites in East Antarctica: provenance, seasonality and blocking factors. Clim. Dyn. 37: 2107, doi:10.1007/s00382-010-0946-4.

[21] Schlosser E., Oerter, H., Masson-Delmotte V., Reijmer C.H. 2008. Atmospheric influence on the deuterium excess signal in polar firn - implications for ice core interpretation. Journal of Glaciology 54(184), 117 – 124, doi: https://doi.org/10.3189/002214308784408991.

[22] Serreze M.C., Barrett A.P., Slater A.G., Woodgate R.A., Aagaard K., Lammers R.B., Steele M., Moritz R., Meredith M. & Lee C.M. 2006. The large-scale freshwater cycle of the Arctic. J. Geophys. Res. 11, C11010, doi:10.1029/2005JC003424.

[23] Stohl A. & James P. 2004. A Lagrangian Analysis of the Atmospheric Branch of the Global Water Cycle. Part I: Method Description, Validation, and Demonstration for the August 2002 Flooding in Central Europe. J. Hydrometeor 5, 656–678, doi: http://dx.doi.org/10.1175/1525-7541(2004)005<0656:ALAOTA>2.0.CO;2

[24] Stohl, A. & James P.A. 2005. A Lagrangian Analysis of the Atmospheric Branch of the Global Water Cycle. Part II: Moisture Transports between Earth's Ocean Basins and River Catchments. J. Hydrometeorol. 6, 961–984, doi: http://dx.doi.org/10.1175/JHM470.1

[25] Stohl A., Forster C. & Sodemann H. 2008. Remote sources of water vapor forming precipitation on the Norwegian west coast at 60 N—A tale of hurricanes and an atmospheric river. J. Geophys. Res. 113, D05102, doi:10.1029/2007JD009006

[26] Stroeve J.C., Markus T., Boisvert L., Miller J. & Barrett A. 2014. Changes in Arctic melt season and implications for sea ice loss. Geophys. Res. Lett. 41, 1216–1225, doi:10.1002/2013GL058951.

[27] Vázquez M., Nieto R., Drumond A. & Gimeno L. 2016. Moisture transport into the Arctic: Source-receptor relationships and the roles of atmospheric circulation and evaporation. J. Geophys. Res. Atmos. 121, 13,493–13,509, doi:10.1002/2016JD025400.

[28] Vihma T. 2014. Effects of Arctic Sea Ice Decline on Weather and Climate: A Review. Surv. Geophys. 35: 1175, doi:10.1007/s10712-014-9284-0

[29] Vihma T., Screen J., Tjernström M., Newton B., Zhang X., Popova V., Deser C., Holland M. & Prowse T. 2016. The atmospheric role in the Arctic water cycle: A review on processes, past and future changes, and their impacts. J. Geophys. Res. Biogeosci. 121, 586–620, doi:10.1002/2015JG003132.

[30] Wang M. & Overland J. E. 2009. A sea ice free summer Arctic within 30 years? Geophys. Res. Lett. 36, L07502, doi:10.1029/2009GL037820.

[31] Wegmann M., Orsolini Y., Vázquez M., Gimeno L., Nieto R., Bulygina O., Jaiser R., Handorf D., Rinke A., Dethloff K., Sterin A. & Brönnimann S. 2015. Arctic moisture source for Eurasian snow cover variation in autumn. Environ Res Lett 10:054015 S. Zhang, C. Zhu, J. K. O. Sin, and P. K. T. Mok, "A novel ultrathin elevated channel low-temperature poly-Si TFT," *IEEE Electron Device Lett.*, vol. 20, pp. 569–571, Nov. 1999

Environmental Research Letters

OPEN ACCESS

RECEIVED
7 February 2015

REVISED
27 April 2015

ACCEPTED FOR PUBLICATION
28 April 2015

PUBLISHED
15 May 2015

LETTER

Arctic moisture source for Eurasian snow cover variations in autumn

Martin Wegmann[1], Yvan Orsolini[2], Marta Vázquez[3], Luis Gimeno[3], Raquel Nieto[3], Olga Bulygina[4], Ralf Jaiser[5], Dörthe Handorf[5], Annette Rinke[5], Klaus Dethloff[5], Alexander Sterin[4] and Stefan Brönnimann[1]

[1] Oeschger Centre for Climate Change Research and Institute of Geography, University of Bern, Switzerland
[2] NILU—Norwegian Institute for Air Research, Kjeller, Norway
[3] EPhysLab, Facultade de Ciencias, Universidade de Vigo, Ourense, Spain
[4] All-Russian Research Institute of Hydrometeorological Information—World Data Centre, Obninsk, Russian Federation
[5] Alfred Wegener Institute, Helmholtz Centre for Polar and Marine Research, Research Unit Potsdam, Germany

E-mail: martin.wegmann@giub.unibe.ch

Keywords: snow depth, Arctic warming, global change, global warming, sea ice, Siberia

Supplementary material for this article is available online

Abstract

Eurasian fall snow cover changes have been suggested as a driver for changes in the Arctic Oscillation and might provide a link between sea-ice decline in the Arctic during summer and atmospheric circulation in the following winter. However, the mechanism connecting snow cover in Eurasia to sea-ice decline in autumn is still under debate. Our analysis is based on snow observations from 820 Russian land stations, moisture transport using a Lagrangian approach derived from meteorological re-analyses. We show that declining sea-ice in the Barents and Kara Seas (BKS) acts as moisture source for the enhanced Western Siberian snow depth as a result of changed tropospheric moisture transport. Transient disturbances enter the continent from the BKS region related to anomalies in the planetary wave pattern and move southward along the Ural mountains where they merge into the extension of the Mediterranean storm track.

1. Introduction

Arctic summer sea-ice extent has declined by more than 10% per decade since the start of the satellite era (e.g. Stroeve *et al* 2011), culminating in a record low in September 2012, with the long-term trend largely attributed to anthropogenic global warming.

This results in an increasing autumn surface heat flux from the open waters to the cooler atmosphere with anomalous warming of the lower Arctic atmosphere (e.g. Overland and Wang 2010, Screen and Simmonds 2010) and important consequences for mid-latitude climate. Various mechanisms have been suggested as to how the atmosphere responds to this heat flux anomaly, starting in fall, and then into the subsequent winter season (see Vihma 2014 for a review). Honda *et al* 2009 used observations and numerical experiments to investigate the influence of Arctic sea-ice decrease on cold Eurasian winters. They argued that an October heat low over the Barents-Kara Seas (BKS) triggers a dynamical feedback, leading to increased November SLP and amplified cold advection over Central Siberia. Recently, Mori *et al* 2014 used an ensemble model approach to compare high and low sea-ice conditions and found that sea-ice reduction leads to more severe winters in central Eurasia, due to increased European blockings and resulting cold-air advection. In simulations Orsolini *et al* 2012 showed that, by December intensified surface highs were found on the American and Eurasian continents, associated with anomalous southward advection of cold polar air on their eastern sides. Contrasting the 1990–2000 and the 2001–2010 decades in re-analysis, Jaiser *et al* 2012 showed that low September sea-ice extent is associated with earlier onset of baroclinic wave activity at high latitudes, and later influenced planetary-scale wave trains extending over the North Pacific.

However, the sign and magnitude of the large-scale response is highly sensitive to the amount of sea-ice reduction and its location (Petoukhov and Semenov 2010, Rinke *et al* 2013). For example, the BKS has been suggested to be a key source region for anomalous heat fluxes and large-scale wave trains across Eurasia in winter (Inoue *et al* 2012).

Contrary to this Arctic Sea warming, North America, Europe, and East Asia have experienced anomalously cold winters with record high snowfalls and cold air outbreaks during recent winters. Such conditions have had a large impact on society and understanding the causes of such extreme events is therefore of large societal importance. While not being the only mechanism proposed, reduced summer and autumn Arctic sea-ice has been linked to atmospheric circulation changes that caused these extreme winter conditions (Honda *et al* 2009, Cohen *et al* 2014).

Francis *et al* 2009 and then Liu *et al* 2012 associated the low autumn sea-ice extent to blocking, jet stream meandering and enhanced moisture transport and snowfall in winter. Francis and Vavrus 2012 argued, based on observational evidence, for increased planetary wave amplitudes during autumn and winter in low Arctic sea-ice years, which might support the occurrence of weather extremes in mid-latitudes. Hence, the reduction in Arctic summer sea-ice could potentially increase the Eurasian autumn snowpack.

Moreover, observational as well as model studies have shown that the Eurasian autumn snowpack influences the propagation of planetary waves and the phase of the winter NAO, leading to an intensification and westward expansion of the Siberian High (Cohen *et al* 2007, Orsolini and Kvamst\o 2009, Peings *et al* 2012, Zhang *et al* 2013). Cold advection from the Arctic to Western Siberia has been shown to strengthen the Siberian high (Takaya and Nakamura 2005). Furthermore, recent studies demonstrate that initialization of snow has an impact on sub-seasonal autumn and winter forecasts (Jeong *et al* 2013, Orsolini *et al* 2013).

Finnis *et al* 2007 and more recently Stroeve *et al* 2011 linked low Arctic sea-ice in autumn to enhanced Arctic precipitation and cyclone activity, especially in the Atlantic sector. Ghatak *et al* 2012 further used a suite of dedicated model simulations with varying forcings to attribute the increase in modelled snow depth and cover over northeastern Siberia to the decreasing trend in sea-ice. Cohen *et al* 2012 qualitatively linked sea-ice loss to additional surface evaporation and earlier snowfall over high-latitude lands, consistent with estimated trends in Arctic moisture content from radiosondes and in Eurasian snow cover extent. Using a land surface model forced by observational data, Park *et al* 2013 showed increased precipitation and snow depths over northeastern Siberia in particular, associated with low autumn sea-ice extent analysed from satellite data.

However, so far no empirical, statistical or model study clearly attributed the snow increase over high-latitude land to moisture transport following specific circulation pathways originating over the ice-free parts of the Arctic Ocean. Furthermore some of these statistical studies of the sea-ice influence on winter climate are still strongly debated (e.g. Barnes 2013, Screen and Simmonds 2013). Hence, uncertainties remain in how different sea-ice anomalies influence the atmospheric circulation, either directly or through enhanced moisture. Furthermore, identifying this response is an intricate issue given the large natural variability in the cold season (i.e. Deser *et al* 2012) and inherent uncertainties arising from deficiencies in large-scale snow observations.

The goal of this study is to demonstrate the consistency between *in situ* observations of the snow pack variability over parts of Siberian and Russian Arctic regions in the early snow fall season (October, November), and sea-ice variability in the BKS region. We focus on the Siberian and Russian Arctic regions since we are using a new set of homogeneised snow observations over Russia. We calculate composites for low and high September sea-ice over the BKS of snow depths, forward trajectories out of the BKS region, and backward trajectories from high snowfall regions.

The paper is organised as follows. Section 2 describes the data and methods used. Section 3 presents the results separately for October and November. Results are discussed in section 4. Conclusions are then drawn in section 5.

2. Data and methods

2.1. Analysis framework and atmospheric circulation diagnostics

Based on HadISST sea-ice data (Rayner *et al* 2003) we defined years with high or low sea-ice in the BKS region (65–85°N, 30–90°E) in September (figure 1). In September, sea-ice reaches its annual minimum and open waters provide a strong moisture source for the cold Arctic atmosphere (Bintanja and Selten 2014). High and low ice years are defined by exceeding one standard deviation of the normalized sea-ice concentration for the timeframe of ERA-Interim 1979–2013 (see supplementary material available at stacks.iop.org/ERL/10/054015/mmedia). This results in six high sea-ice years (1980, 1981, 1989, 1998, 2002, 2003) and four low sea-ice years (1979, 1984, 1985, 2012). We then analyse snow depth, moisture transport and atmospheric circulation diagnostics for the selected years in October and November. In the following, we show the differences for low minus high September sea-ice; the significance of the differences was calculated using a t-test.

The following atmospheric circulation diagnostics were calculated from ERA-Interim (Dee *et al* 2011): Omega (vertical wind speed) at 700 hPa, wind at 700 hPa, mean sea level pressure (SLP), 500 hPa geopotential height, integrated water vapour transport, snowfall, 2 m temperatures, variance of 2–7 day band-passed daily SLP.

2.2. Snow cover data

Regular snow observations have been conducted at Russian meteorological stations since 1882. Daily

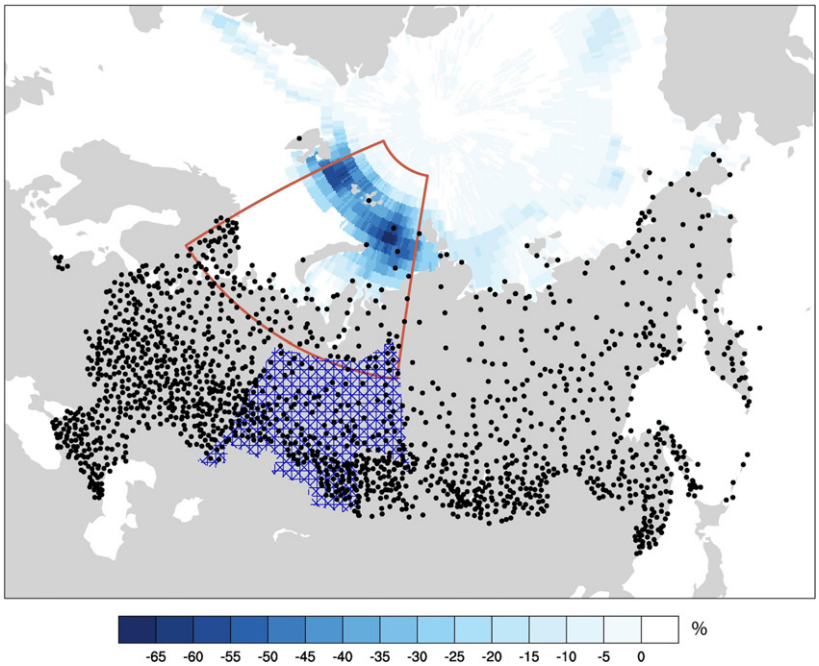

Figure 1. Map showing the positions of the 820 snow cover stations (black dots), with the Barents/Kara Sea (BKS) and the 'southwestern Siberia' regions highlighted (red frame and blue crossing, respectively). Blue shading shows the composite of HadISST October and November sea-ice concentration anomalies of low minus high sea-ice years.

snow observations at meteorological stations include snow depth measurements, determination of the snow cover in an area around a meteorological station and determination of the snow cover characteristics. This study uses time series of daily snow depths for 820 Russian meteorological stations, distributed as shown on figure 1. The time series are prepared by RIHMI-WDC. Meteorological data sets are automatically checked for quality control. Since the procedure of snow observations changed in the past, particular attention was given to the removal of all possible sources of inhomogeneity in the data. However, there have been no changes in the observation procedures since 1965. Only the period 1979–2012 was used in the study.

For definition of snow covered regions in this paper, we used as a primary step Russian national climate monitoring regions as defined by Alisov 1956 and by Bulygina *et al* 2010. The primary division to regions considers 18 regions over all the territory of Russia, which describe all the variety of climate conditions and, within the region, have similar environmental conditions. This includes similar landscapes, meteorological conditions, vegetation types and more. Based on an analysis of spatial distributions of a number of climate characteristics, including snow cover characteristics, that involved sets of more than 600 meteorological stations, these 18 primary regions were then merged into nine quasi-homogeneous regions of Russian territory. Here we chose one of those regions as the main region of interest, namely the '*southwestern Siberia*', *hereafter SW-Siberia,* region (highlighted in blue crossing in figure 1).

We use monthly maximum snow depth instead of mean values because it reflects the process of snow accumulation (snow depth is a cumulative and highly inertial characteristic of climate system). It is especially essential for autumn months when the main processes of snow accumulation occurs over the territories of Russia.

2.3. Lagrangian modeling

The Lagrangian analyses in this work has been developed using the model FLEXPART V9.0 and is based on the method developed by Stohl and James 2004, 2005. This model uses ERA-Interim reanalysis data to track changes in atmospheric moisture along trajectories. The model considers the atmosphere divided into a large number of particles, which are advected using the three dimensional wind data. The increases (evaporation e) and decreases (precipitation p) in moisture along any trajectory can be calculated through changes in (specific humidity q) with time (e-$p = m\mathrm{d}q/\mathrm{d}t$), with ($m$) being the mass of the particle. By summing (e-p) for all particles residing in the atmospheric column over an area we can obtain the total (E-P) field. The number of particles reaching a target area from a source can be different for different periods. However, the global amount of particles stays the same at all times.

In this work we first try to establish a relation between the retreat of sea-ice in the BKS region and

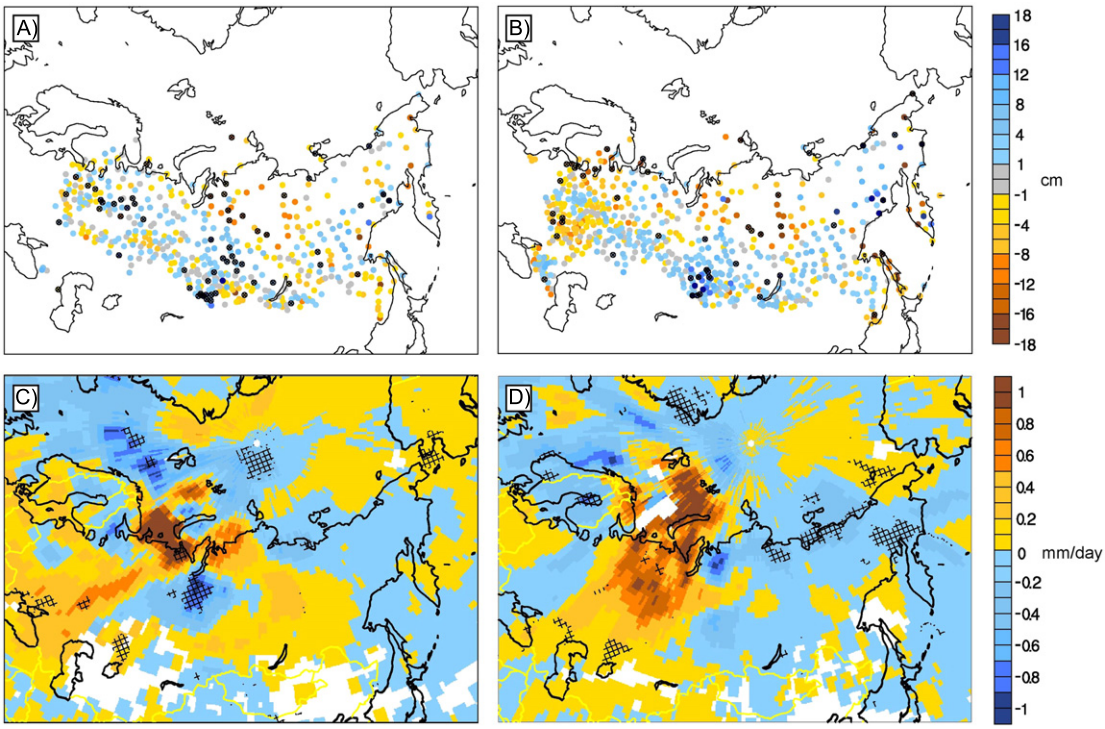

Figure 2. Differences between low and high BKS September sea-ice in station snow depth (cm) for (A) October and (B) November. *E-P* differences (mm day^{-1}) from forward trajectories starting in the BKS region for (C) October and (D) November. Cross hatched areas and crossed stations represent 90% Student's t-test significance level.

the precipitation over the region 'southwestern Siberia' (figure 1). This is done by a forward analysis considering only particles starting in the BKS region and following the particles over a period of three days. Areas where particles from this region lose moisture are represented by a negative value on *E-P* field. Furthermore, a backward trajectory analysis is carried out where particles arriving over 'southwestern Siberia' are tracked backwards to their region of origin over a period of three days. In this way we determine the regions where particles arriving in 'southwestern Siberia' have picked up moisture. In this case, the grid points where $E\text{-}P > 0$ represent areas where particles gain moisture.

Full details on the methods in the forward or backward modes can be found in Nieto *et al* 2008 or Gimeno *et al* 2010 respectively, and a comparison of the Lagrangian technique with other methods for derivation of moisture sources can be found in Gimeno *et al* 2012.

3. Results

3.1. October

The composite difference of *in situ* snow observations in figure 2 shows that Octobers in years with low BKS sea-ice have significantly higher snow depths in Southern Siberia, and also in some coastal areas of the Far East and Northern Volga, with the first being the most striking region of positive anomalies. Forward trajectories composite difference also indicate, that during low ice years, air parcels which start over the BKS tend to lose more moisture over the Urals and the Far East. The maximum loss difference is located in an area with its western boundary over the Urals and continuing to south-west Siberia, whereas moisture loss minima are found at the coastal areas of the Northwest and at the western Russian border (figure 2).

We now consider composite differences of a variety of dynamical diagnostics derived from ERA-Interim (figure 3). We can see in figure 3 (second row) that the region of the loss maximum is located at the northern edge of a strong negative SLP anomaly, which is bound to the north and west by anti-cyclonic anomalies, the latter centered south of Scandinavia. Positive 2 m temperature anomalies are found over the open waters of the BKS while there are only weak temperature anomalies over continental Russia (also figure 3, second row). At the south-eastern flank of the negative SLP anomaly an increase of vertical uplift can be observed (figure 3, first row). The opposite is true for areas of positive SLP anomalies. Regions with strongly enhanced (decreased) vertical uplift fit very well with positive (negative) snow depth from the independent *in situ* measurements (figure 2) and with the snowfall anomalies from re-analyses (figure 3, first row).

The composite difference of 500 hPa geopotential height and SLP (figure 3) reveals a northern

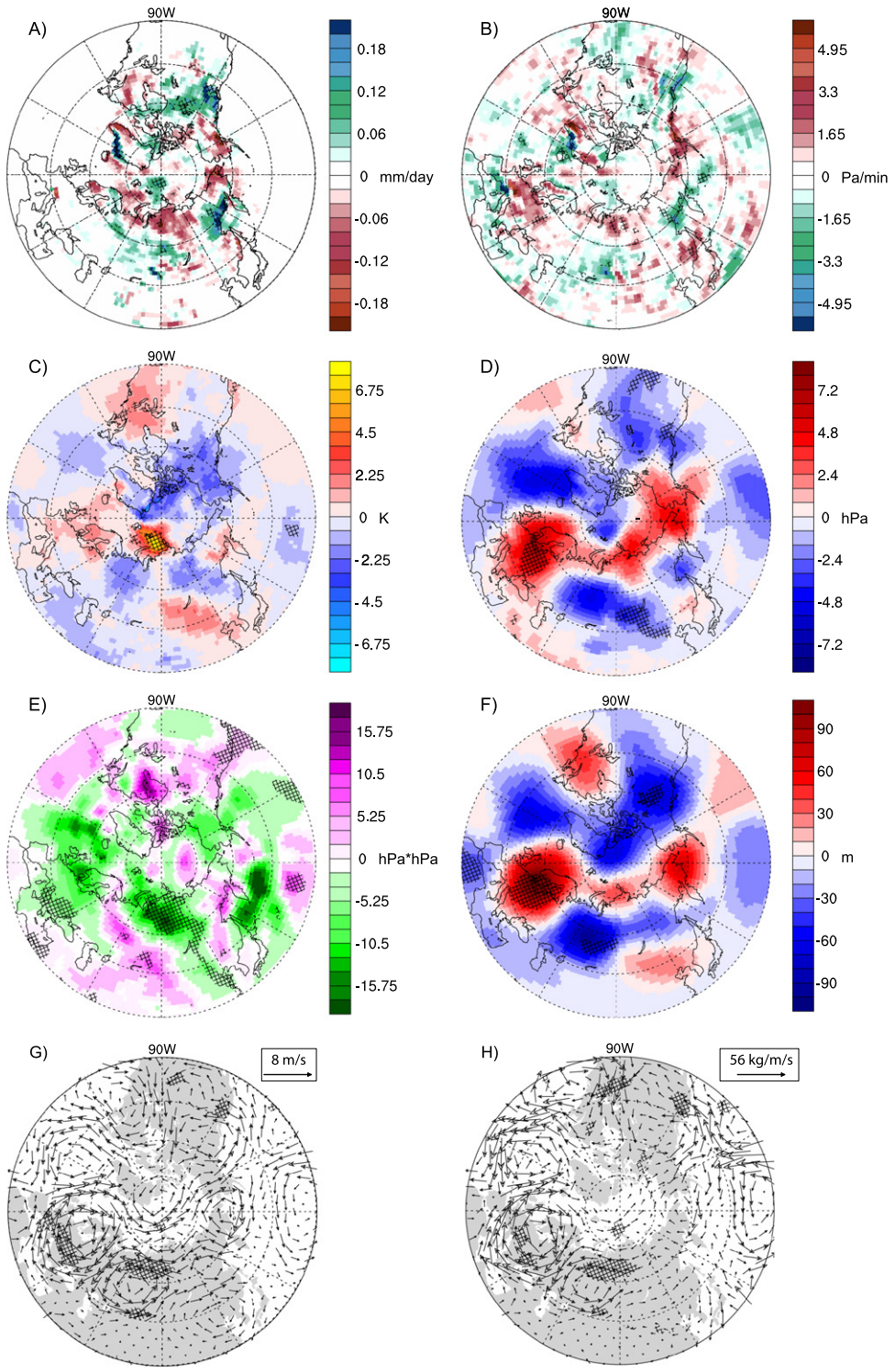

Figure 3. Difference between low and high sea-ice years in the Barents Kara Sea region for (A) snow fall (mm day^{-1}), (B) 700 hPa Omega (Pa min^{-1}), (C) 2 m temperature (K), (D) SLP (hPa), (E) and 2–7 day 247 bandpassed SLP variance (hPa^2), (F) geopotential height at 500 hPa (m), (G) 700 hPa wind (m s^{-1}), (H) integrated water vapour transport (kg m^{-1} s^{-1}) for October. Cross hatched areas represent 90% Student´s t-test significance level.

hemispheric barotropic wavetrain pattern in October. While both low and high sea-ice years show a circumpolar wave train, the low sea-ice wavetrain has a higher wavenumber (see supplementary material available at stacks.iop.org/ERL/10/054015/mmedia). Strong blocking is found over northern Europe and negative geopotential height anomalies dominate over the Ural Mountains and Western Siberia. Moisture and air mass transport over Central Russia is influenced by the cyclonic SLP anomaly to the west. The atmosphere *E-P* anomalies are positive over the warmer, open sea at the western flank of the cyclonic anomaly, as well as

over the eastern flank due to the dry, continental origin of the airmasses. Bandpassed SLP variance (figure 3) shows increased storm activity entering the Central Russia land areas through a small sector from the BKS. Hence storm are veering abruptly southward along the Urals, and areas with maximum bandpassed SLP variance fit very well with positive snow depth and snowfall anomalies.

The source of moisture can be addressed by means of the backward trajectory analysis. Backward trajectories arriving in SW-Siberia show that there are several main climatological moisture source regions for the snow falling in that region (figure 5, top row): first and foremost the large open water areas to the West, namely the Mediterranean and the North Atlantic. Furthermore, the Black Sea, Caspian Sea and the BKS region act as climatological moisture source. During low sea-ice years (figure 5, bottom row), it appears that air parcels arriving in SW-Siberia have picked up more moisture over the BKS region as opposed to high sea-ice years. This is consistent with enhanced evaporation over the low sea-ice areas (assuming no precipitation changes). A third moisture source during low sea-ice years is the Balkan region. Conversely, a region east of the southern Urals appears as a more important moisture source for high sea-ice years (figure 5). However, the importance of moisture sources can only be stated in relative terms for backward trajectory anomalies.

3.2. November

For November, the analysis of snow observations reveals similar anomalies as for October. Strong positive anomalies in Southern Siberia between Lake Balkash and Lake Baikal, positive anomalies in the Far East, now more inland than in October, coexist with significant decrease of snow depth mainly between Lake Baikal and the Arctic coast as well as towards the western border of Russia (figure 2).

Forward trajectories in FLEXPART indicate that air parcels starting over the Barents/Kara Seas tend to loose less moisture over Western Russia than during high ice years. The anticyclonic pressure anomaly over this region shuffles more continental airmasses around its core causing the atmosphere to loose less moisture along the northern and eastern flank (figure 4). Over most of Siberia and the Far East, air parcels lose more moisture in low sea-ice years. A very strong moisture loss is found at the Arctic Coast in Northern Siberia, a region where SLP is low and vertical uplift is increased, but snow anomalies are (still) negative. Moreover, positive 2 m temperature anomalies reach from the BKS inland and cover the Siberian and Far East Arctic coast. However, ERA-INTERIM indicates increased snowfall in this area (figure 4). Increased uplift and positive snowfall anomalies fit in general very well over the plotted domain.

Large-scale circulation wise, composites of 500 hPa geopotential height and SLP for low minus high sea-ice in the Barents/Kara Seas show a baroclinic pattern (figure 4). A weaker blocking occurs over European Russia and negative SLP anomalies over the northern North Atlantic appear. Both, at the surface and in the middle troposphere, the positive pressure anomalies along the Russian Arctic coast in October vanish, and more cylonic systems prevail. This opens an entry passage for a direct storm track coming from the BKS passing east of the Urals to Central Siberia and Asia. Again, areas of maximum bandpassed SLP variance match regions of positive snowfall, negative omega as well as positive snow depth anomalies from *in situ* observations. In this case, Central and Southern Siberia is pinched between an anti-cyclonic anomaly to the west and and cyclonic anomaly to the east. In the Far East, storm systems are shifted from the Pacific to Arctic areas north of Kamchatka, a region with increased moisture loss and snowfall (figure 4).

The November composite difference of backward trajectories for SW-Siberia shows again two relatively enhanced moisture source regions in low sea-ice years: the Kara Sea and the northern surroundings of the Caspian Sea. Compared to October, the Black Sea and the Balkan region no longer appear as significantly enhanced sources (figure 5).

4. Discussion

Although small in sample size, our results indicate a significant increase of observed Siberian snow depth during low sea-ice years.

Our analysis focuses on moisture transport resulting from Hori *et al* (2011) sea-ice decline in the BKS, which allows us to specify regions of interest for the FLEXPART trajectories and snow depth observations. Open waters in the BKS have been shown to increase the diabatic heating of the atmosphere (Sato *et al* 2014), which amplifies baroclinic cyclones and might induce a remote atmospheric response by triggering stationary Rossby waves (Honda *et al* 2009).

Consistent with the results, our analysis shows increased cold air advection from the north from the BKS region over western Russia and the Urals in October in low sea-ice years. This cold air convection persists in November, but is located further to the East. Snow cover anomalies then may further amplify the Siberian high through radiative and thermodynamic effects (Cohen *et al* 2012, Orsolini *et al* 2013). In fact, similar composited plots for December and January show a strengthening of the Siberian high following low sea-ice conditions during fall (see supplementary material available at stacks.iop.org/ERL/10/054015/mmedia), indicating that the anomalous northerly advection continues to build a negative 2 m temperature anomaly, in agreement with Hori *et al* 2011.

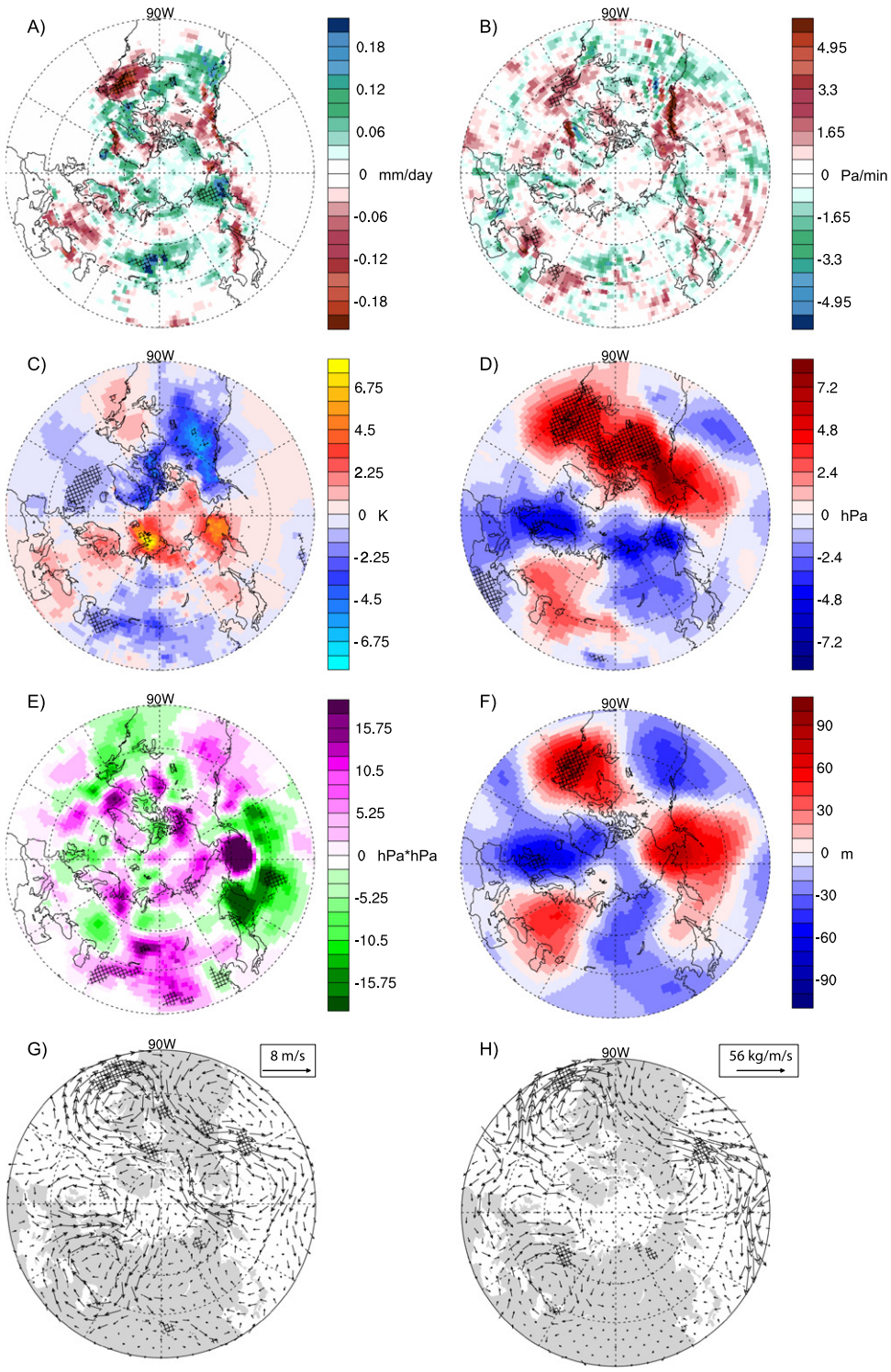

Figure 4. Difference between low and high sea-ice years in the Barents Kara Sea region for (A) snow fall (mm day^{-1}), (B) 700 hPa Omega (Pa min^{-1}), (C) 2 m temperature (K), (D) SLP (hPa), (E) and 2–7 day bandpassed SLP variance (hPa^2), (F) geopotential height at 500 hPa (m), (G) 700 hPa wind (m s^{-1}), (H) integrated water vapour transport (kg m^{-1} s^{-1}) for November. Cross hatched areas represent 90% Student´s t-test significance level.

In agreement with these studies, we found strengthened European blocking and increased wave numbers at 500 hPa. Moreover, our results show enhanced storm activity originating in the BKS with disturbances entering the continent through a small sector over the BKS, steered in October by a Scandinavia block and a low to the East and extending to Central Russia. In case of the strong snow depth increase during October in SW-Siberia, enhanced frontal activity on the southeastern flank of the cyclonic anomaly is a possible trigger for the increased vertical uplift. Maxima in storm activity trigger increasing

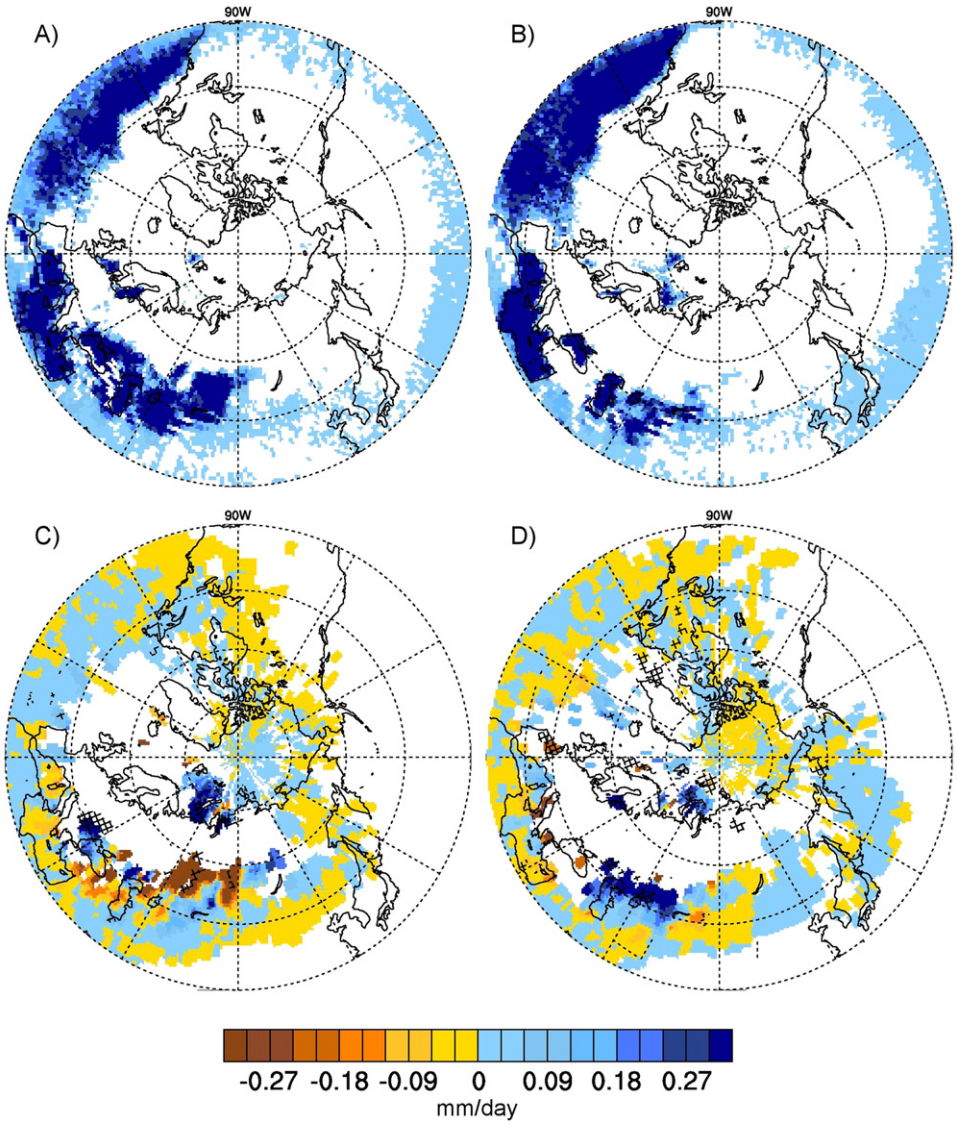

Figure 5. (A) Climatological (1980–2012) moisture sources and (C) composite differences in the moisture gain for backward trajectories starting in southwestern Siberia' (region of relatively high snow depth in low ice years) for October. B and D show the same for November. Cross hatched areas represent 90% Student´s test significance level for anomaly plots.

uplift, often accompanied by positive snowfall and snow depth anomalies. Forward and backward FLEXPART analysis support the idea that decreasing Arctic sea-ice cover in the BKS region is a main source and an important factor for continental snow accumulation, especially so in SW-Siberia. Over other areas, like the Pacific coast of the Far East., a combination of frontal activity and coastal convergence causes upward vertical wind anomalies and snow accumulation. This initial snowpack anomaly is then influencing the evolution of the November snow pack.

However, no direct link between Lagrangian moisture loss and snow accumulation in observations can be made. FLEXPART computes moisture loss in a diverse way, including cloud evolution and related processes. Additionally, surface temperature conditions impacts on snowmelt and snow depth cannot be accounted for in the FLEXPART analysis. We needed to use a combination of Lagrangian and Eularian approaches to analyse snow depth evolution.

In this study, focused on early autumn, we were not able to determine the circulation response to BKS sea-ice anomalies, as it appears masked or embedded in the circumglobal wavetrain (see supplementary material available at stacks.iop.org/ERL/10/054015/mmedia). Kim *et al* 2014 recently looked at BKS sea-ice retreat influence on the atmosphere in re-analyses and model data. They found that the response in the mid-tropospheric circulation becomes apparent only by December, inducing cold wintertime anomalies over northern Eurasia. Our paper complements their study in that we investigated the leading season to that signal.

Future studies are needed to investigate further the links and impacts of the rapidly changing Arctic climate. Ensemble model simulations for past and current conditions may increase the statistical

significance of the proposed physical links, connecting reduced sea-ice and Eurasian surface conditions. Future climate model simulations (Deser *et al* 2010, Callaghan *et al* 2011) indicate an increase in snow water equivalent over Siberia due to decreasing Arctic sea-ice.

5. Summary

An extensive, dense snow depth observation dataset was analyzed to examine autumn snow depth evolution in Russia during the recent Arctic warming period. Evidence was found for an increase of SW-Siberian snow depth in years of low sea-ice in the BKS region. Backward trajectories from FLEXPART originating in that region indicate the BKS as an important moisture source.

Eulerian diagnostics from ERA-INTERIM show an increased atmospheric wavenumber and meridional circulation during low sea-ice years. Besides promoting cold air advection from the Arctic Ocean into the Eurasian continent, these circulation changes are accompanied by an intensified storm track into SW-Siberia. Anomalies in snowfall generally agree well with snow depth observations and are often found over regions with strong changes in atmospheric lift. Both the southeastern flanks of cyclonic anomalies and the coastal sea breeze convergence are major triggers for such upward vertical motions. However, surface conditions are critical for the conversion of snowfall into snow depth. Reversely, the SW-Siberian snow depth increase is subsequently influences temperature and positive pressure tendency later in the cold season.

These findings are consistent with several former studies and consequently underline the importance of Arctic climate change for lower latitude regions. The question remains open if future sea-ice melting will lead to the same results, however modeling studies point towards a similar mechanism. To further quantify the impacts of those environmental changes, it is critical to continue a dense, high quality snow depth observation network in the coming decades. Moreover, extending the study to other sea-ice loss areas and to other continental areas of the Northern Hemisphere might give insight into the regional differences of the 'warm Arctic, cold continent' model.

Acknowledgements

The authors acknowledge funding by the European ERAnet.RUS programme, especially within the project ACPCA. The EPhysLab acknowledges the funding of the TRAMO project by the Spanish MINECO and FEDER.

References

Alisov B P 1956 *Climate of the USSR* (Moscow: Moscow University)
Barnes E A 2013 Revisiting the evidence linking Arctic amplification to extreme weather in midlatitudes *Geophys. Res. Lett.* **40** 4734–9
Bintanja R and Selten F M 2014 Future increases in Arctic precipitation linked to local evaporation and sea-ice retreat *Nature* **509** 479–82
Bulygina O N, Groisman P Y, Razuvaev V N and Radionov V F 2010 Snow cover basal ice layer changes over Northern Eurasia since 1966 *Environ. Res. Lett.* **5** 015004
Callaghan T V, Johansson M, Prowse T D, Olsen M S and Reiersen L O 2011 Arctic cryosphere: changes and impacts *Ambio* **40** 3–5
Cohen J, Barlow M, Kushner P J and Saito K 2007 Stratosphere–troposphere coupling and links with Eurasian land surface variability *J. Clim.* **20** 5335–43
Cohen J, Screen J A, Furtado J C, Barlow M, Whittleston D, Coumou D, Francis J, Dethloff K, Entekhabi D and Overland J 2014 Recent Arctic amplification and extreme mid-latitude weather *Nat. Geosci.* **7** 627–37
Cohen J L, Furtado J C, Barlow M A, Alexeev V A and Cherry J E 2012 Arctic warming, increasing snow cover and widespread boreal winter cooling *Environ. Res. Lett.* **7** 014007
Dee D P *et al* 2011 The ERA-Interim reanalysis: configuration and performance of the data assimilation system *Q. J. R. Meteorol. Soc.* **137** 553–97
Deser C, Phillips A, Bourdette V and Teng H 2012 Uncertainty in climate change projections: the role of internal variability *Clim. Dyn.* **38** 527–46
Deser C, Tomas R, Alexander M and Lawrence D 2010 The seasonal atmospheric response to projected Arctic sea ice loss in the late twenty-first century *J. Clim.* **23** 333–51
Finnis J, Holland M M, Serreze M C and Cassano J J 2007 Response of Northern Hemisphere extratropical cyclone activity and associated precipitation to climate change, as represented by the Community Climate System Model *J. Geophys. Res.: Biogeosci.* **112** G04S42
Francis J A, Chan W, Leathers D J, Miller J R and Veron D E 2009 Winter Northern Hemisphere weather patterns remember summer Arctic sea-ice extent *Geophys. Res. Lett.* **36** L07503
Francis J A and Vavrus S J 2012 Evidence linking Arctic amplification to extreme weather in mid-latitudes *Geophys. Res. Lett.* **39** L06801
Ghatak D, Deser C, Frei A, Gong G, Phillips A, Robinson D A and Stroeve J 2012 Simulated Siberian snow cover response to observed Arctic sea ice loss, 1979–2008 *J. Geophys. Res.: Atmos.* **117** D23108
Gimeno L, Drumond A, Nieto R, Trigo R M and Stohl A 2010 On the origin of continental precipitation *Geophys. Res. Lett.* **37** L13804
Gimeno L, Stohl A, Trigo R M, Dominguez F, Yoshimura K, Yu L, Drumond A, n.-Q. A. M. i. a. Dur\'a and Nieto R 2012 Oceanic and terrestrial sources of continental precipitation *Rev. Geophys.* **50** RG4003
Honda M, Inoue J and Yamane S 2009 Influence of low Arctic sea-ice minima on anomalously cold Eurasian winters *Geophys. Res. Lett.* **36** L08707
Hori M E, Inoue J, Kikuchi T, Honda M and Tachibana Y 2011 Recurrence of intraseasonal cold air outbreak during the 2009/2010 winter in Japan and its ties to the atmospheric condition over the Barents-Kara Sea *SOLA* **7** 25–8
Inoue J, Hori M E and Takaya K 2012 The role of Barents Sea ice in the wintertime cyclone track and emergence of a warm-Arctic cold-Siberian anomaly *J. Clim.* **25** 2561–8
Jaiser R, Dethloff K, Handorf D O R, Rinke A and Cohen J 2012 Impact of sea ice cover changes on the Northern Hemisphere atmospheric winter circulation *Tellus* A **64** 11595
Jeong S-J, Ho C-H, Kim B-M, Feng S and Medvigy D 2013 Non-linear response of vegetation to coherent warming over northern high latitudes *Remote Sens. Lett.* **4** 123–30

Kim B M, Son S W, Min S K, Jeong J H, Kim S J, Zhang X D, Shim T and Yoon J H 2014 Weakening of the stratospheric polar vortex by Arctic sea-ice loss *Nat. Commun.* **5** 4646

Liu J, Curry J A, Wang H, Song M and Horton R M 2012 Impact of declining Arctic sea ice on winter snowfall *Proc. Natl Acad. Sci. USA* **109** 4074–9

Mori M, Watanabe M, Shiogama H, Inoue J and Kimoto M 2014 Robust Arctic sea-ice influence on the frequent Eurasian cold winters in past decades *Nat. Geosci.* **7** 869–73

Nieto R, Gallego D, Trigo R, Ribera P and Gimeno L 2008 Dynamic identification of moisture sources in the Orinoco basin in equatorial South America *Hydrol. Sci. J.* **53** 602–17

Orsolini Y J and Kvamst\o N G 2009 Role of Eurasian snow cover in wintertime circulation: decadal simulations forced with satellite observations *J. Geophys. Res.: Atmos.* **114** D19108

Orsolini Y J, Senan R, Balsamo G, Doblas-Reyes F J, Vitart F, Weisheimer A, Carrasco A and Benestad R E 2013 Impact of snow initialization on sub-seasonal forecasts *Clim. Dyn.* **41** 1969–82

Orsolini Y J, Senan R, Benestad R E and Melsom A 2012 Autumn atmospheric response to the 2007 low Arctic sea ice extent in coupled ocean–atmosphere hindcasts *Clim. Dyn.* **38** 2437–48

Overland J E and Wang M 2010 Large-scale atmospheric circulation changes are associated with the recent loss of Arctic sea ice *Tellus* A **62** 1–9

Park H, Walsh J E, Kim Y, Nakai T and Ohata T 2013 The role of declining Arctic sea ice in recent decreasing terrestrial Arctic snow depths *Polar Sci.* **7** 174–87

Peings Y, Saint-Martin D and Douville H 2012 A numerical sensitivity study of the influence of Siberian snow on the northern annular mode *J. Clim.* **25** 592–607

Petoukhov V and Semenov V A 2010 A link between reduced Barents-Kara sea ice and cold winter extremes over northern continents *J. Geophys. Res.: Atmos.* **115** D21111

Rayner N A, Parker D E, Horton E B, Folland C K, Alexander L V, Rowell D P, Kent E C and Kaplan A 2003 Global analyses of sea surface temperature, sea ice, and night marine air temperature since the late nineteenth century *J. Geophys. Res.: Atmos.* **108** 4407

Rinke A, Dethloff K, Dorn W, Handorf D and Moore J C 2013 Simulated Arctic atmospheric feedbacks associated with late summer sea ice anomalies *J. Geophys. Res.: Atmos.* **118** 7698–714

Sato K, Inoue J and Watanabe M 2014 Influence of the Gulf stream on the Barents Sea ice retreat and Eurasian coldness during early winter *Environ. Res. Lett.* **9** 084009

Screen J A and Simmonds I 2010 Increasing fall-winter energy loss from the Arctic Ocean and its role in Arctic temperature amplification *Geophys. Res. Lett.* **37** L16707

Screen J A and Simmonds I 2013 Exploring links between Arctic amplification and mid-latitude weather *Geophys. Res. Lett.* **40** 959–64

Stohl A and James P 2004 A Lagrangian analysis of the atmospheric branch of the global water cycle: I. Method description, validation, and demonstration for the August 2002 flooding in central Europe *J. Hydrometeorol.* **5** 656–78

Stohl A and James P 2005 A Lagrangian analysis of the atmospheric branch of the global water cycle: II. Moisture transports between Earth's ocean basins and river catchments *J. Hydrometeorol.* **6** 961–84

Stroeve J C, Maslanik J, Serreze M C, Rigor I, Meier W and Fowler C 2011 Sea ice response to an extreme negative phase of the Arctic Oscillation during winter 2009/2010 *Geophys. Res. Lett.* **38** L02502

Takaya K and Nakamura H 2005 Mechanisms of intraseasonal amplification of the cold Siberian high *J. Atmos. Sci.* **62** 4423–40

Vihma T 2014 Effects of Arctic Sea ice decline on weather and climate: a review *Surv. Geophys.* **35** 1175–214

Zhang X, He J, Zhang J, Polyakov I, Gerdes R U D, Inoue J and Wu P 2013 Enhanced poleward moisture transport and amplified northern high-latitude wetting trend *Nat. Clim. Change* **3** 47–51

5

Conclusiones

En esta tesis se ha tratado de analizar el transporte de humedad en la región ártica. Este transporte ha sido estudiado en dos sentidos: tanto hacía el Ártico desde sus principales fuentes como desde él hacia sus principales sumideros. Se han localizado las principales fuentes de humedad para el sistema ártico y se ha estudiado la contribución de cada una de ellas a la región, analizando además el efecto de los patrones de teleconexión en el transporte. Asimismo se han identificado los principales sumideros de humedad del océano Ártico y se ha abordado la posible relación de la anomalía en el transporte de humedad con el deshielo observado en el ártico.

Las principales conclusiones que se pueden extraer de este trabajo se enuncian a continuación:

Localización de las principales fuentes de humedad para el sistema ártico

- Las principales fuentes de humedad localizadas a escala anual son el océano Atlántico, el océano Pacífico y el golfo de México.
- A escala estacional el origen de la humedad es distinto según la época de año:
    - En general las fuentes oceánicas dominan en otoño (septiembre, octubre, noviembre) e invierno (diciembre, enero, febrero), apareciendo como fuentes, además de las ya mencionadas a escala anual, el mar Caspio y mar Negro en ambas estaciones, y el Mediterráneo y los mares de Noruega y Barents para el invierno.
    - En primavera las fuentes oceánicas continúan dominando, sin embargo en esta estación solo aparecen el Atlántico, Pacífico y golfo de México. Comienza a aparecer influencia continental sobre la región de China.
    - En verano las fuentes continentales ganan importancia, apareciendo éstas sobre Norte América y distintas regiones Euroasiáticas como Siberia, Rusia Oriental o China. Las fuentes oceánicas del Atlántico y del Pacífico se ven reducidas en su extensión, especialmente la del océano Atlántico.

En general los resultados obtenidos en la localización y variación estacional de las fuentes de humedad concuerdan con resultados de trabajos anteriores.

Contribución de cada una de las fuentes principales a la región ártica

- Para la fuente oceánica del Pacífico su contribución a la precipitación sobre el Ártico se localiza principalmente al norte de la propia fuente, con una relativa influencia sobre Canadá y la región norte de Estados Unidos.
- La fuente oceánica del Atlántico tiene una especial contribución al noreste de ella misma, principalmente sobre el propio Atlántico norte, el mar de Labrador, el mar de Groenlandia y el de Noruega.
- La fuente continental sobre Norte América influye principalmente sobre la región este de Canadá, especialmente sobre la bahía de Hudson, Quebec y también llega a

mostrar una cierta influencia sobre el Atlántico Norte que se extiende hacia el mar de Groenlandia y la bahía de Baffin.

- La fuente continental sobre Siberia tiene una mayor influencia sobre todo en el continente, ocurriendo su mayor contribución alrededor de la propia fuente.
- En general las fuentes continentales son las únicas que muestran una contribución a lo largo de todo el océano Ártico, aunque su influencia es pequeña con valores en general menores a 0.5 mm/día.
- La fuente del Pacífico contribuye a la precipitación invernal sobre el sistema ártico completo tal cual lo consideramos en este análisis.
- Para las fuentes oceánicas, la contribución mínima se produce en invierno para ambas fuentes. La contribución máxima por el contrario se produce en otoño para la fuente atlántica y en verano para la fuente pacífica.
- Teniendo en cuenta las estimaciones de la contribución total de las cuatro fuentes principales de humedad la contribución máxima se produce en verano y la mínima en inverno, coincidiendo con resultados de trabajos previos obtenidos a través de diferentes metodologías.

Influencia de la evaporación sobre las fuentes y la circulación en el transporte de humedad hacia el Ártico

- En general la evaporación no parece tener una influencia clara en la contribución de humedad. Solo aparecen correlaciones positivas (significativas al 90%) para la fuente de humedad de Norte América y del Pacífico en verano y otoño. Además, para esta última fuente aparece una correlación negativa en inverno.
- Con respecto a los principales patrones de teleconexión climática que afectan a la región se ha encontrado relación con la contribución desde algunas fuentes.
    - La contribución desde la fuente del Atlántico muestra correlaciones negativas significativas al 90% con el patrón del Atlántico Este en verano y en inverno, y con el patrón de Atlántico Este/Oeste de Rusia en otoño.

- La contribución desde la fuente del Pacífico muestra correlaciones negativas significativas con el patrón de Pacífico/Norte América en todas las estaciones del año, y son especialmente importantes durante los meses de primavera e invierno con correlaciones mayores a 0.5. La contribución desde esta fuente muestra también correlación significativa positiva con el patrón del Pacífico Oeste en primavera y verano, y con el patrón Tropical/Hemisferio Norte en invierno.

- Las fuentes continentales muestran correlación negativa con el patrón de Pacífico Este-Pacífico Norte. Además también aparece una correlación negativa con el patrón del Pacífico Oeste para la fuente de Norte América y con la transición del Pacífico para la fuente sobre Siberia.

- A pesar de que los resultados obtenidos muestran cierta relación entre los patrones de teleconexión climática y la contribución de humedad desde las fuentes, los resultados no son los suficientemente fuertes como para confirmar los resultados de trabajos previos en los que se encontraron correlaciones positivas estadísticamente significativas entre el índice NAO y el balance de humedad en el sistema ártico.

Localización de los principales sumideros para la humedad procedente del océano Ártico.

- En general el transporte de humedad desde el océano Ártico tiene una influencia local sobre el propio océano, considerando tanto el aporte del océano completo como el de las regiones individuales en las que se ha dividido.

- Existe cierta influencia sobre Eurasia y Norte América, especialmente en otoño e invierno desde el Ártico central, el mar de Siberia oriental, los mares de Laptev, Barents y Kara, el mar de Groenlandia oriental, el mar de Bering y el mar de Okhotsk.

- La contribución de humedad muestra valores máximos entre los últimos meses de verano y principios de otoño. Este periodo coincide con los valores mínimos en la extensión de hielo ártico.

- En otoño e invierno la contribución de humedad desde la región del Ártico muestra una mayor distribución geográfica.

Relación entre el transporte de humedad y la disminución en la cobertura de hielo marino en el Ártico.

- Las principales fuentes oceánicas, tanto para los principales ríos árticos de Eurasia como para la región con mayores variaciones en la extensión de hielo marino, se han localizado sobre los océanos Atlántico y Pacífico y en el mar Mediterráneo (de menos importancia en el caso de la segunda región).

- Sobre cada una de esas fuentes se ha observado una tendencia positiva en la evaporación durante el periodo 1980-2012.

- En general sobre gran parte de esas fuentes se ha observado un incremento significativo en la evaporación en la década 2001-2010 con respecto a 1981-1990.

- Se han observado variaciones en la contribución de humedad desde las principales fuentes del sistema ártico completo en los años de mínima extensión de hielo.

    - Durante el periodo 2006/2007 se ha observado un incremento en la contribución de humedad en verano desde las fuentes continentales y en otoño e invierno desde la fuente del Atlántico.

    - En el periodo 2011/2012 se ha mostrado un incremento en la contribución de humedad de todas las fuentes menos la siberiana en verano y desde la fuente del Pacífico en invierno y primavera.

- En general se han observado anomalías positivas en la contribución de humedad en verano sobre las áreas de mayor retroceso de hielo, sugiriendo una relación entre el transporte de humedad en esta estación y la disminución del hielo marino.

- Parece existir cierta relación en el transporte de humedad hacia las principales cuencas de los ríos árticos y el retroceso del hielo marino. En el periodo 2006/2007 la contribución atlántica sobre las principales cuencas Euroasiáticas aumentó en más

de un 100%, coincidiendo con un importante retroceso del hielo marino al norte de las mismas.

- La fuente del Atlántico parece estar especialmente relacionada con el deshielo sobre los mares de Barents y Kara. Para el periodo 2011/2012 se ha observado un importante retroceso de la capa de hielo sobre estas áreas coincidiendo con un aumento en el transporte de humedad desde la fuente atlántica hacia esos mares

Influencia del deshielo en la cobertura de nieve en Eurasia

- Se han encontrado evidencias de un aumento en la cobertura de nieve sobre la región suroeste de Siberia para los años en los que los mares de Barents y Kara muestra valores mínimos en su extensión de hielo.

- Se ha observado un aumento de la cobertura de nieve en la región suroeste de Siberia al tiempo que ocurre una intensificación de los mares de Barents y Kara como fuente de humedad en los años en los que la extensión de hielo es mínima.

- Se ha mostrado un aumento en la pérdida de humedad sobre el extremo oriente ruso, los montes Urales en octubre, o la mayor parte de Siberia en el mes de noviembre; mostrando algunas de estas regiones un aumento en la cobertura de nieve.

- En los años de mínima extensión de hielo se ha observado un aumento en advección de aire frío desde el océano Ártico hacia el continente euroasiático.

- Se ha observado una intensificación en la trayectoria de las tormentas sobre el suroeste de Siberia desde los mares de Barents y Kara, coincidiendo con un aumento en la precipitación en forma de nieve y la cobertura de nieve.

- Las anomalías en la precipitación en forma de nieve, en general aparecen en concordancia con los datos de cobertura observados y aparecen asociados a zonas con cambios importantes en el movimiento vertical atmosférico.

A

Material suplementario

En este apartado se presenta el material suplementario de los artículos que componen el cuerpo de esta tesis. Este material está disponible para su consulta en las plataformas online de cada una de las revistas.

A.1. Moisture transport into the Arctic: Source-receptor relationships and the roles of atmospheric circulation and evaporation (2016), JGR

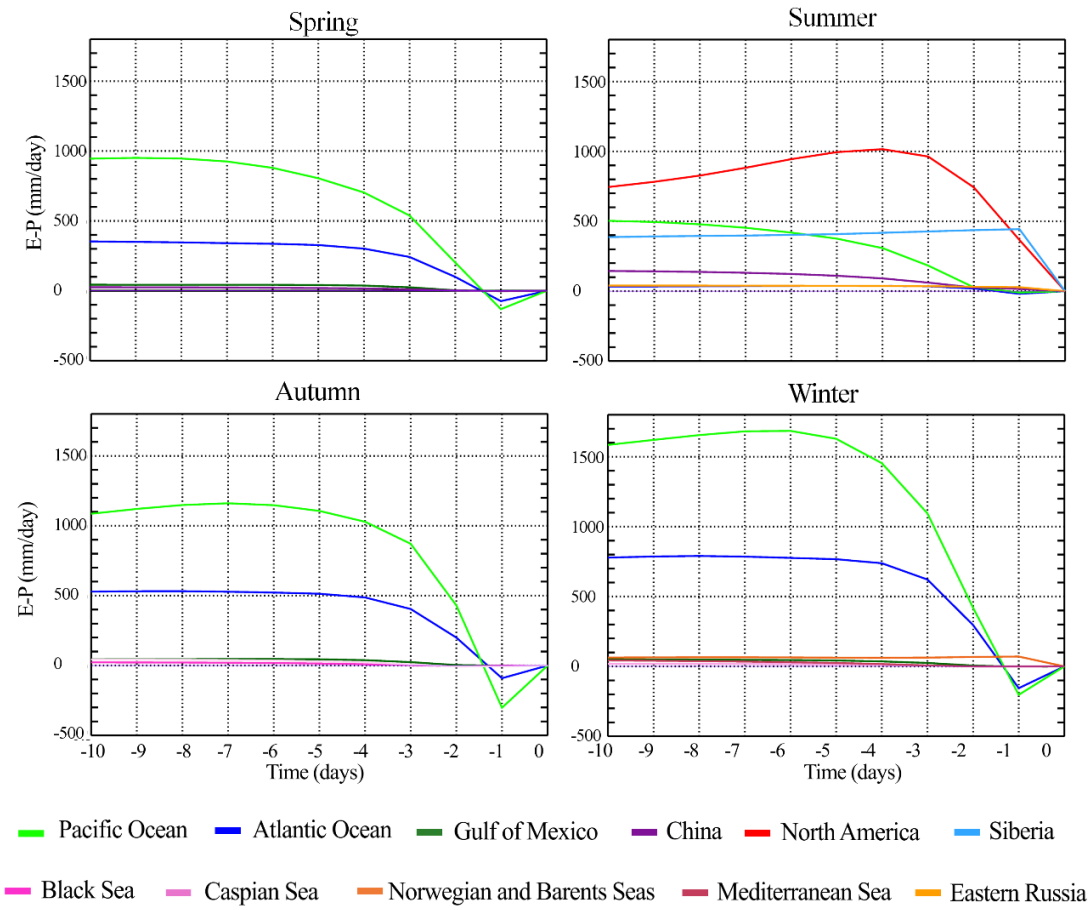

Figura A.1. Series temporales de E-P para los 10 días que se siguen las trayectorias desde el sistema ártico. Los resultados están integrados estacionalmente sobre cada una de las fuentes de humedad durante el período 1980-2012. Las líneas verde oscuro y claro representan el océano Pacífico y el golfo de México respectivamente, las azul oscuro y claro el océano Atlántico y Siberia, la línea morada representa la fuente de China, la roja de Norte América, la líneas naranja claro y oscuro son Rusia Oriental y los mares de Noruega y Barents respectivamente, el color granate representa la fuente del mar Mediterráneo y el rosa claro y oscuro el mar Caspio y mar Negro, respectivamente.

A.2. Moisture transport from the Arctic: A characterization from a Lagrangian perspective (2017), Polar Research.

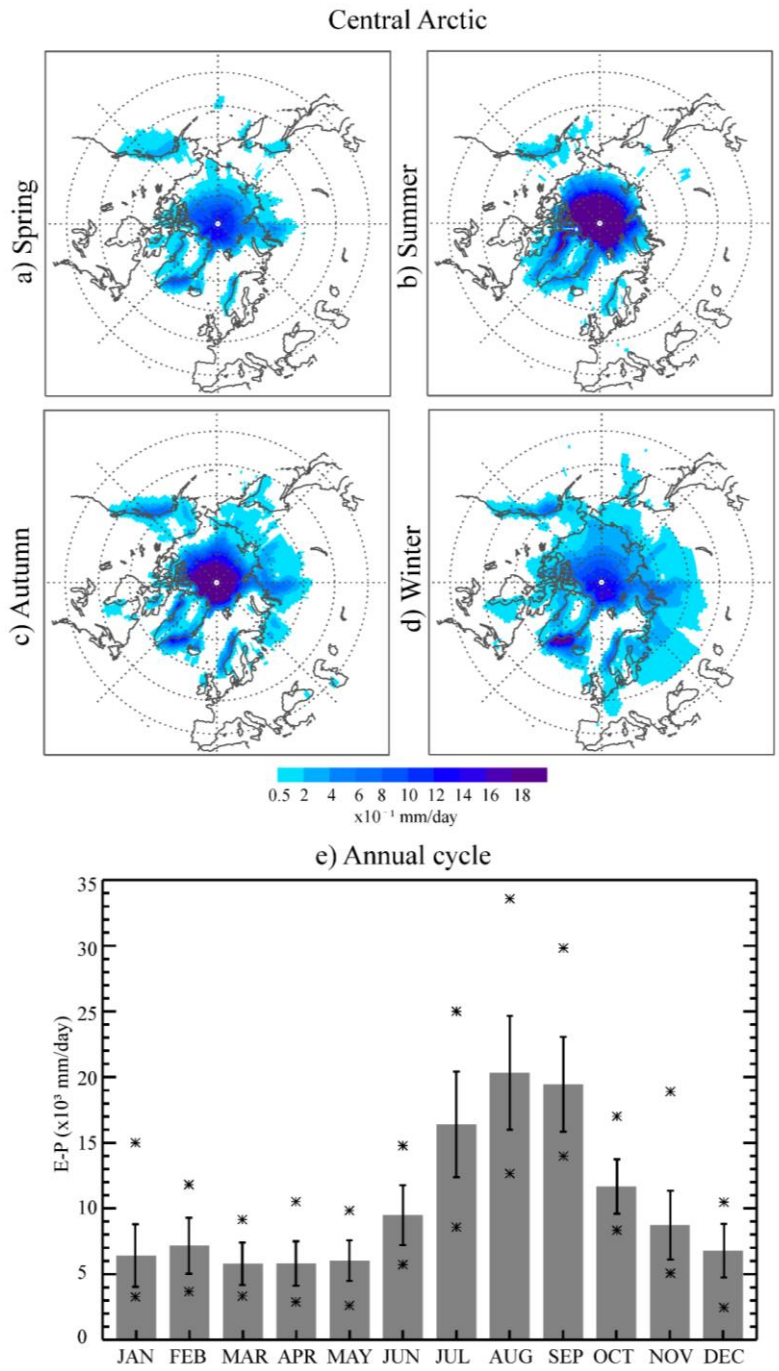

Figura A.2.1. Distribución geográfica de los valores (E-P)<0 desde el Ártico Central calculados estacionalmente (a-d) y su ciclo estacional (f). Los asteriscos representan los valores máximos y mínimos para cada mes y las líneas verticales la desviación estándar.

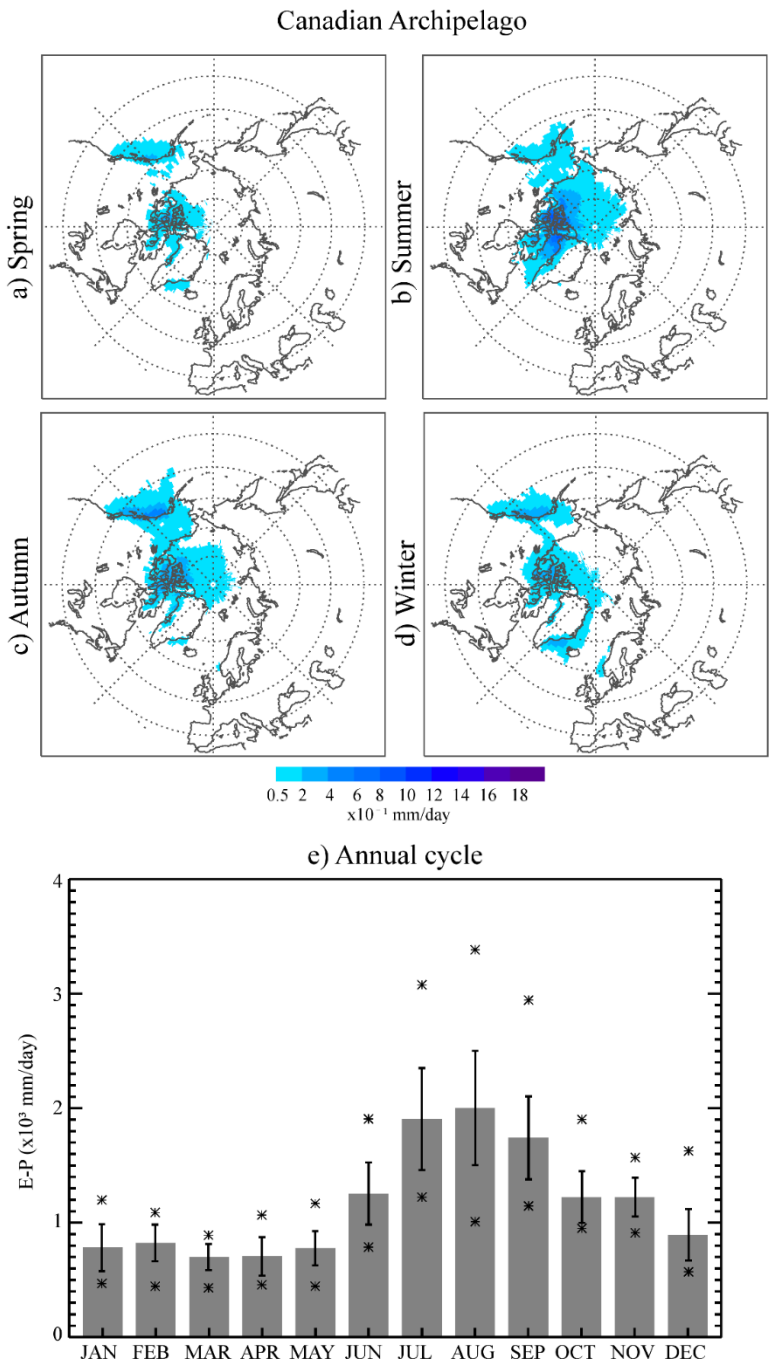

Figura A.2.2. Idem figura A.2.1 para el archipiélago canadiense

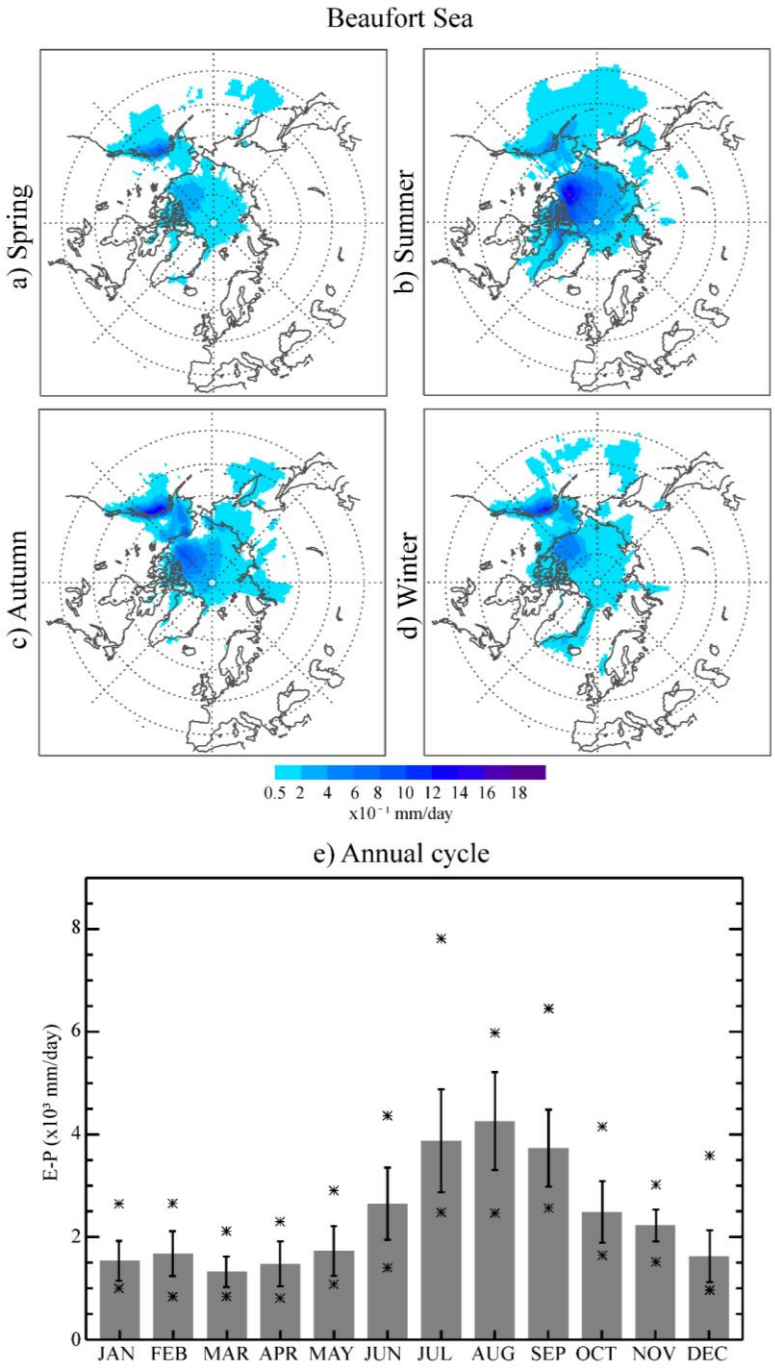

Figura A.2.3. Idem figura A.2.1 para el mar de Beaufort.

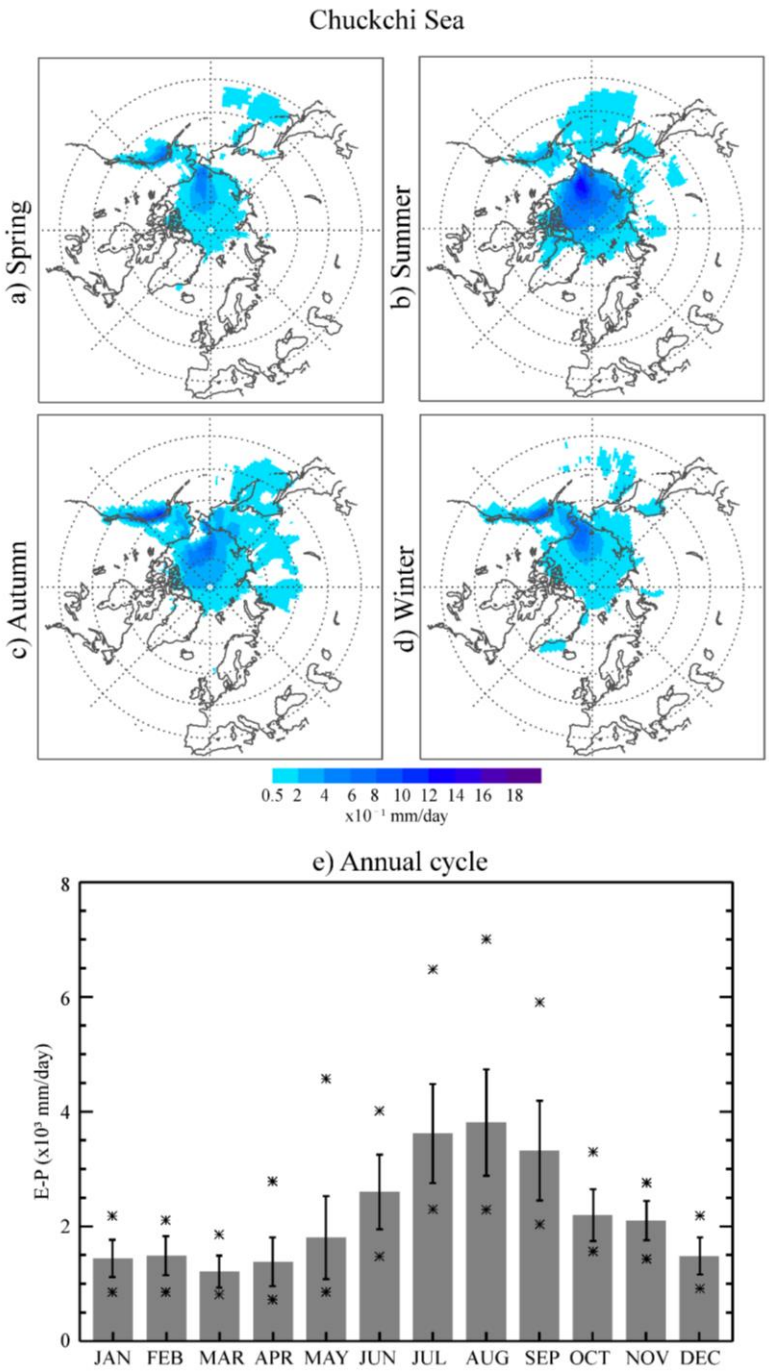

Figura A.2.4. Idem figura A.2.1 para el mar de Chuckchi

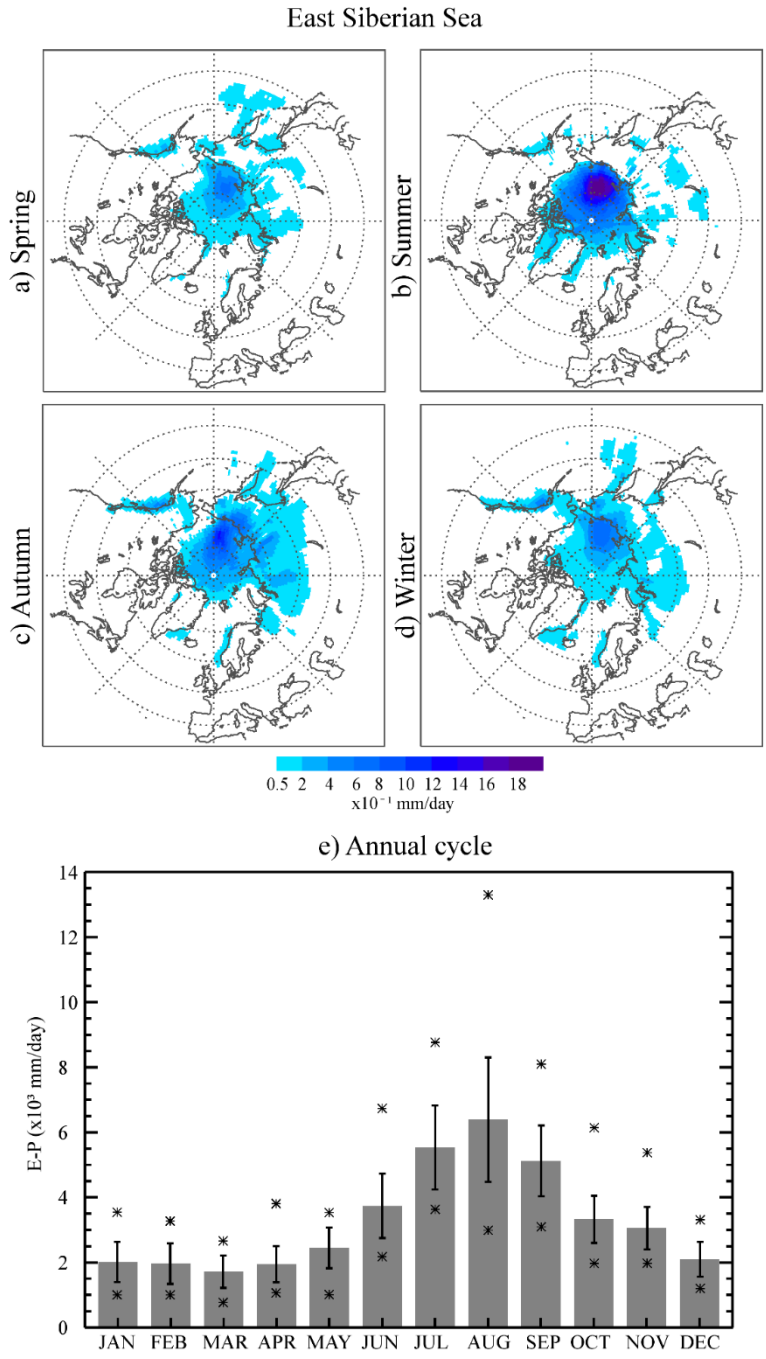

Figura A.2.5. Idem figura A.2.1 para el mar de Siberia Oriental

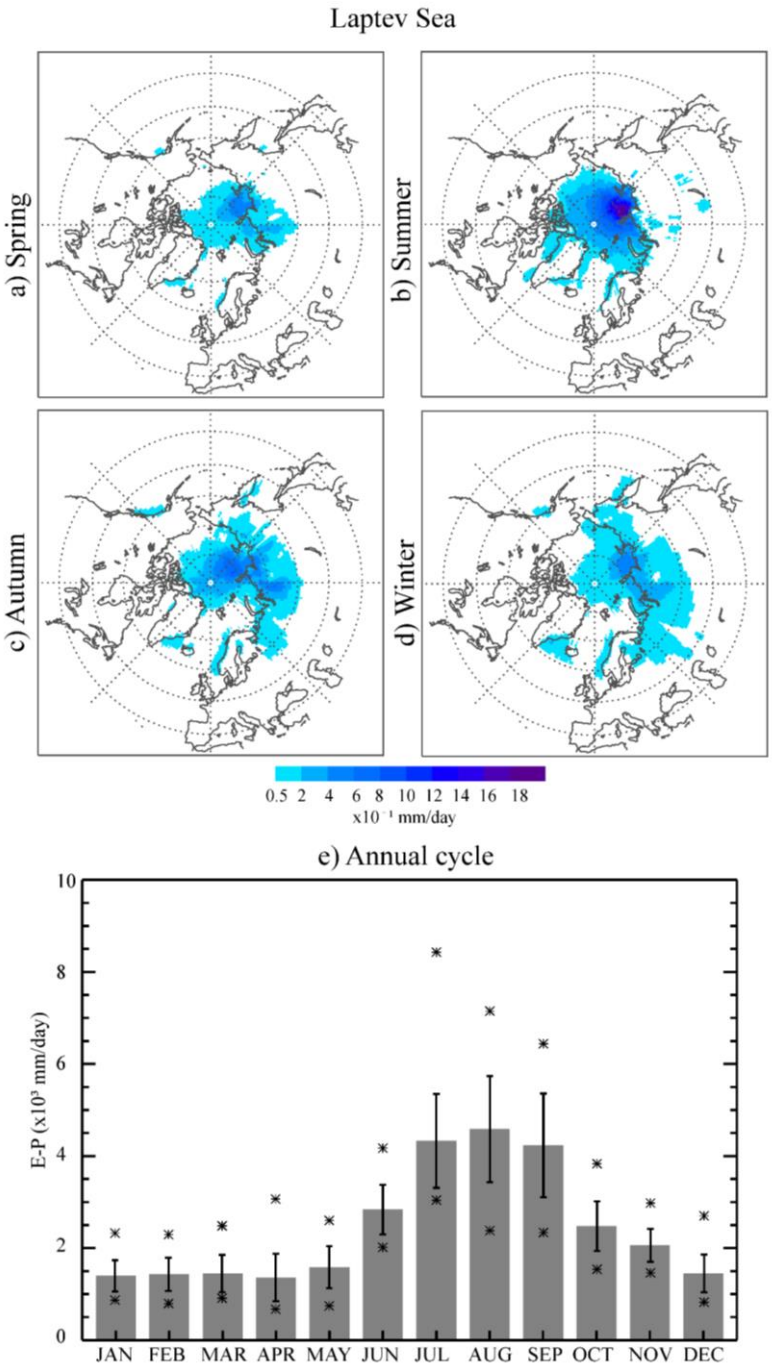

Figura A.2.6. Idem figura A.2.1 para el mar de Laptev

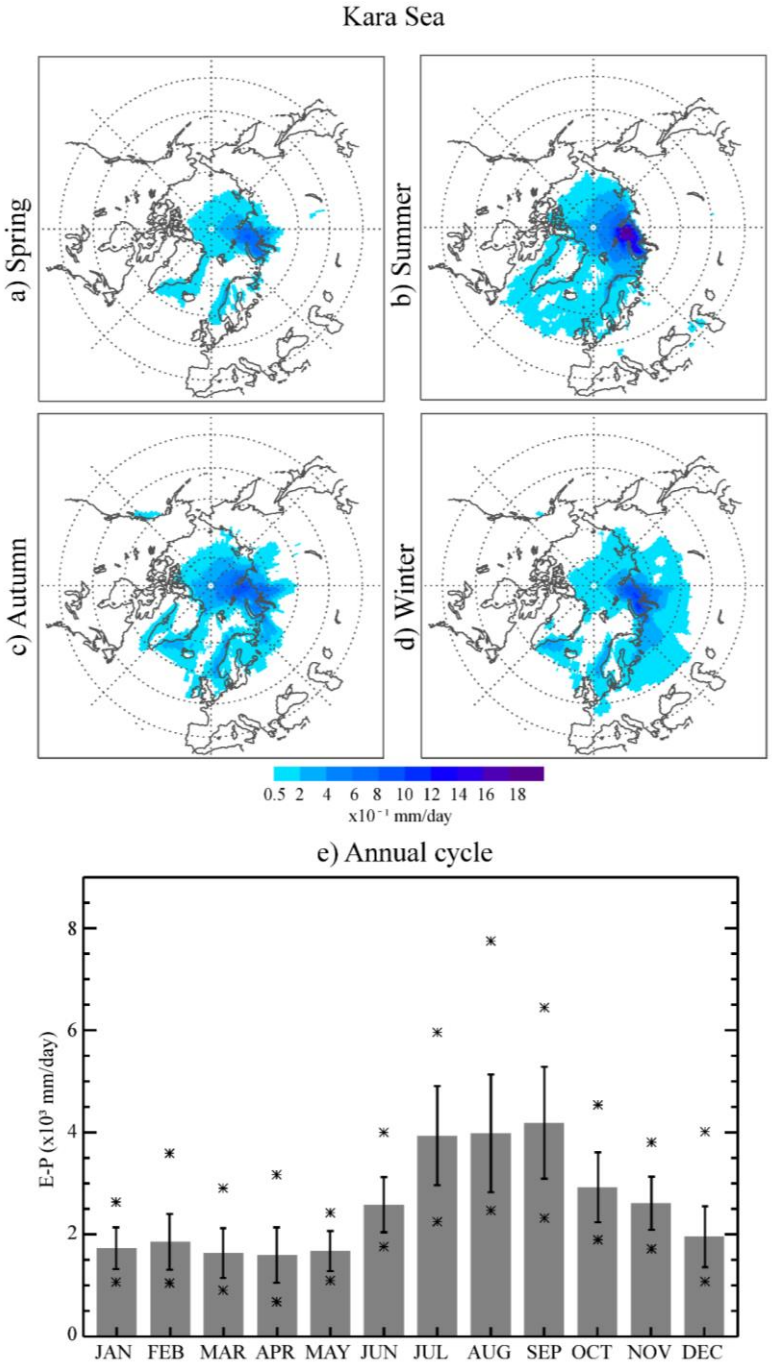

Figura A.2.7. Idem figura A.2.1 para el mar de Kara

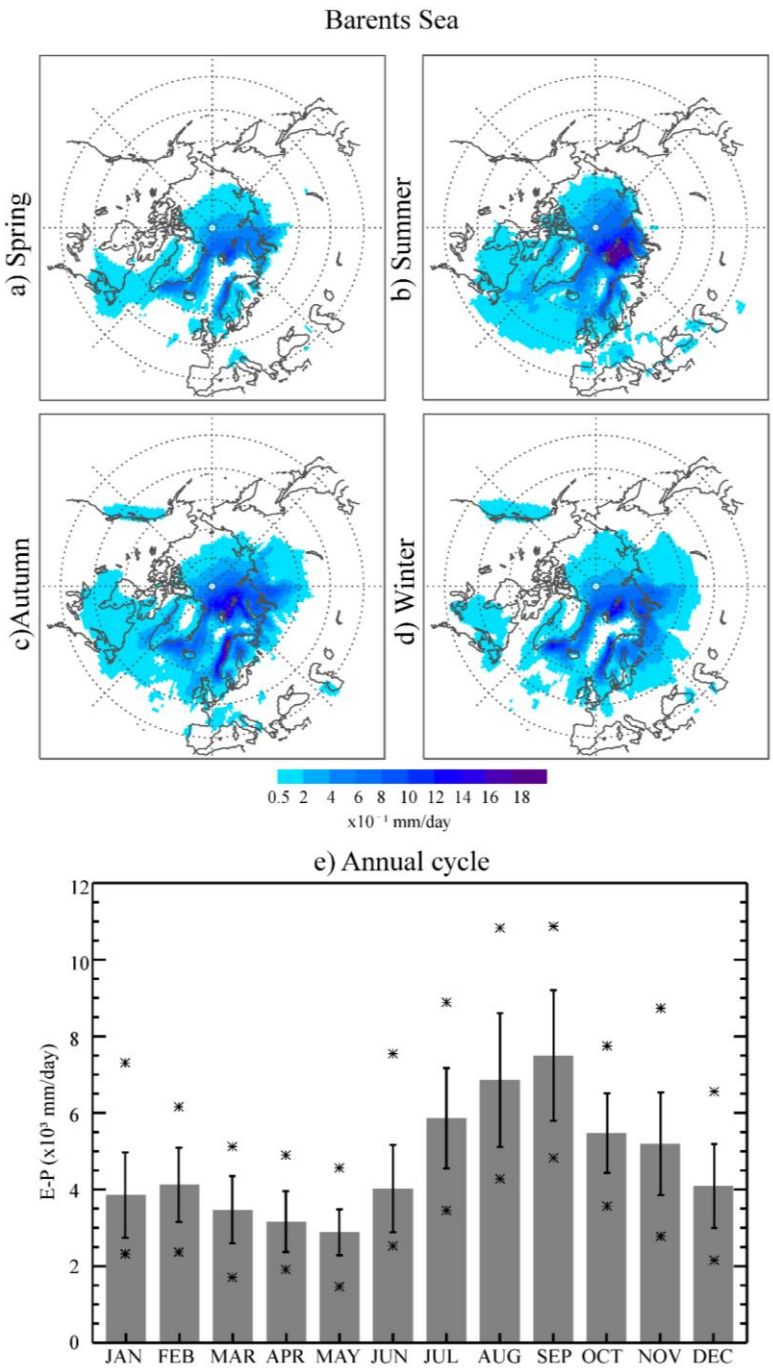

Figura A.2.8. Idem figura A.2.1 para el mar de Barents

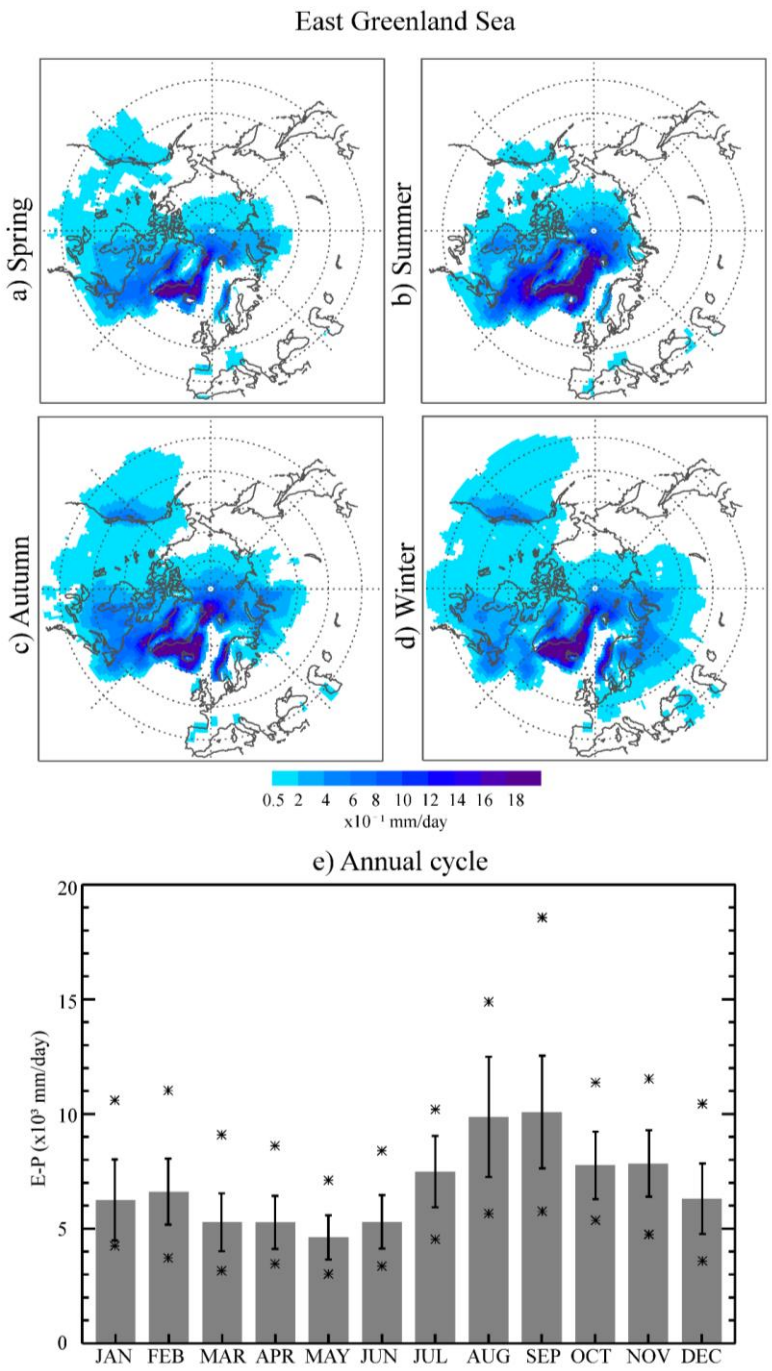

Figura A.2.9. Idem figura A.2.1 para el mar de Groenlandia

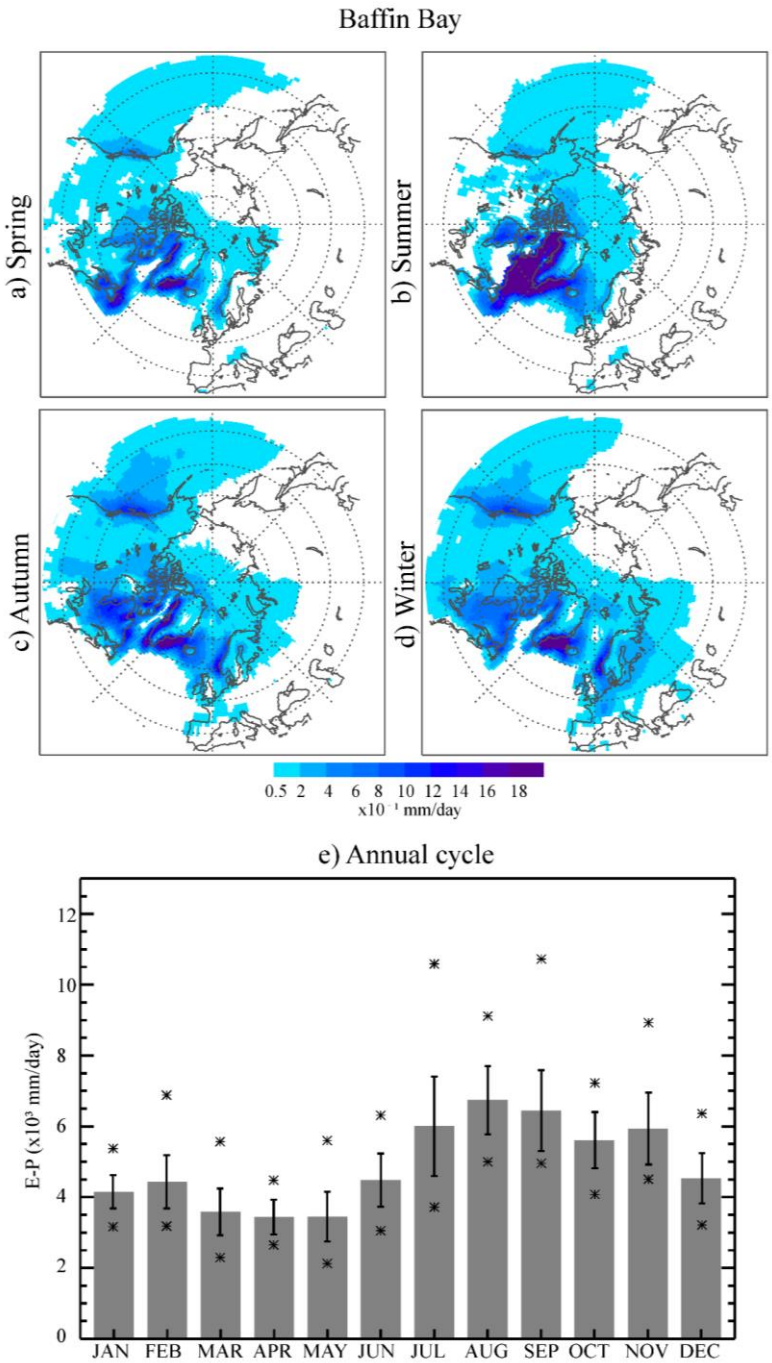

Figura A.2.10. Idem figura A.2.1 para la bahía de Baffin.

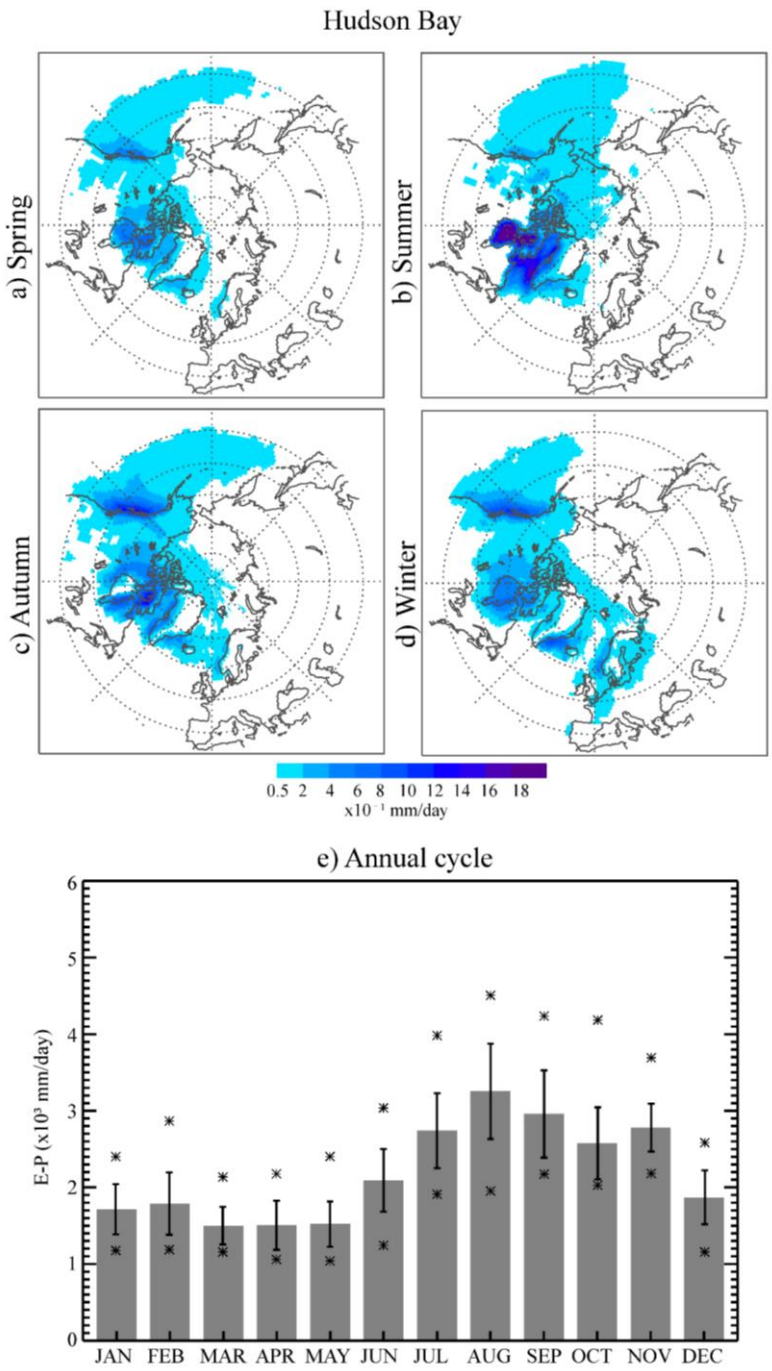

Figura A.2.11. Idem figura A.2.1 para la bahía de Hudson.

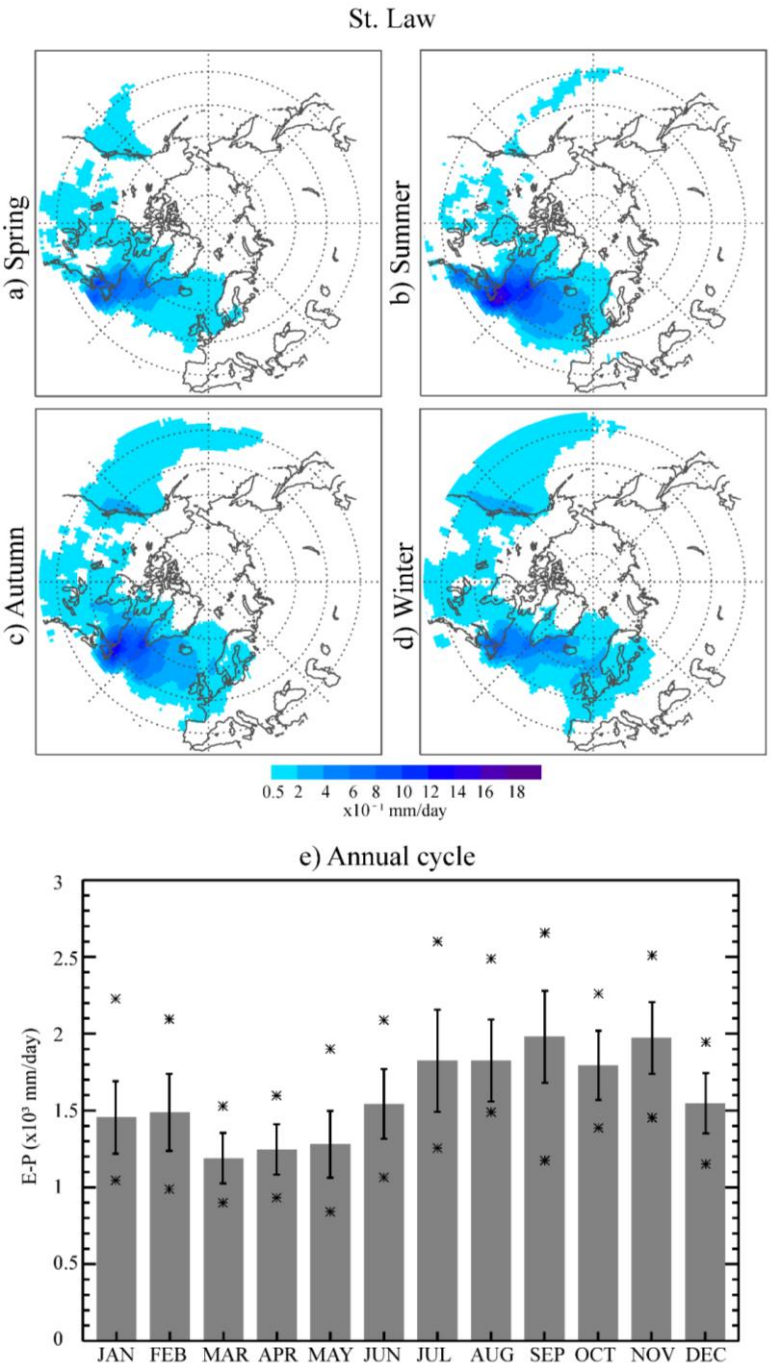

Figura A.2.12. Idem figura A.2.1 para St. Law.

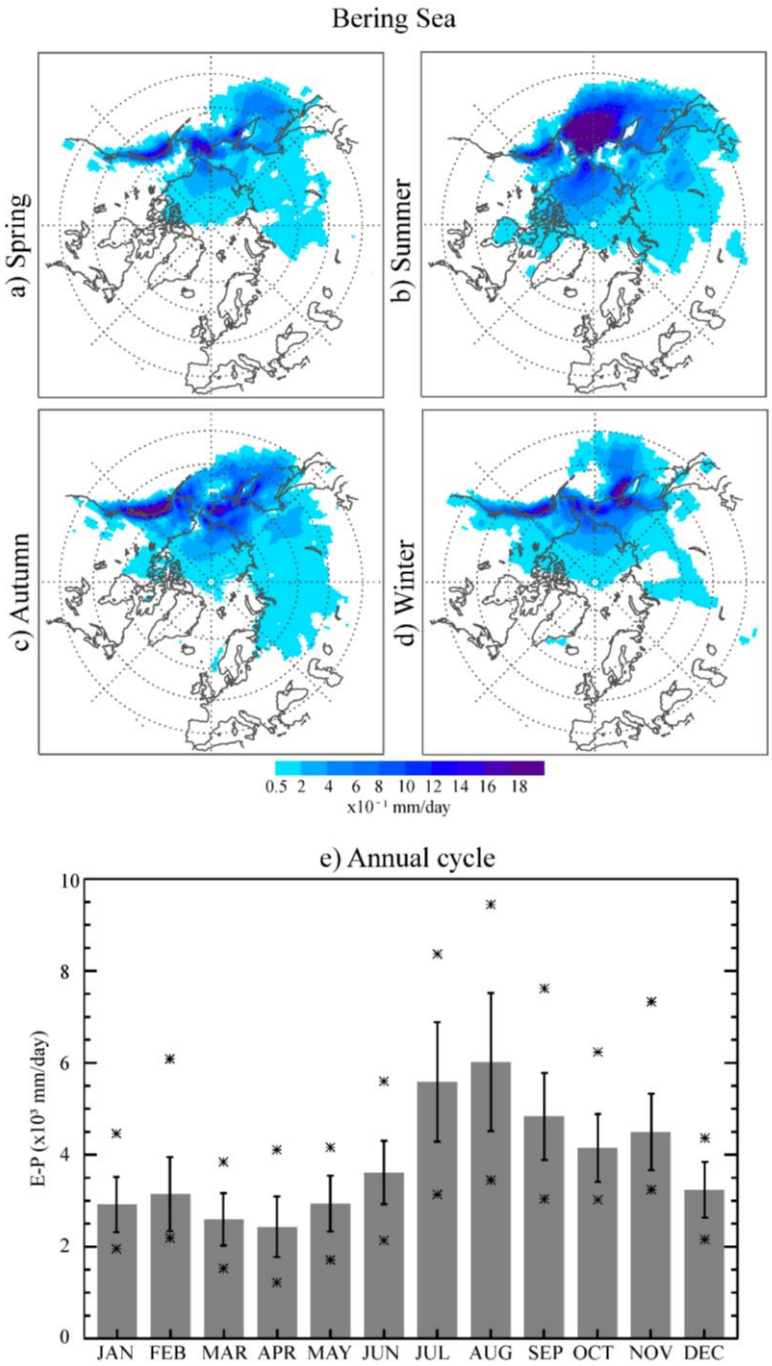

Figura A.2.13. Idem figura A.2.1 para el mar de Bering.

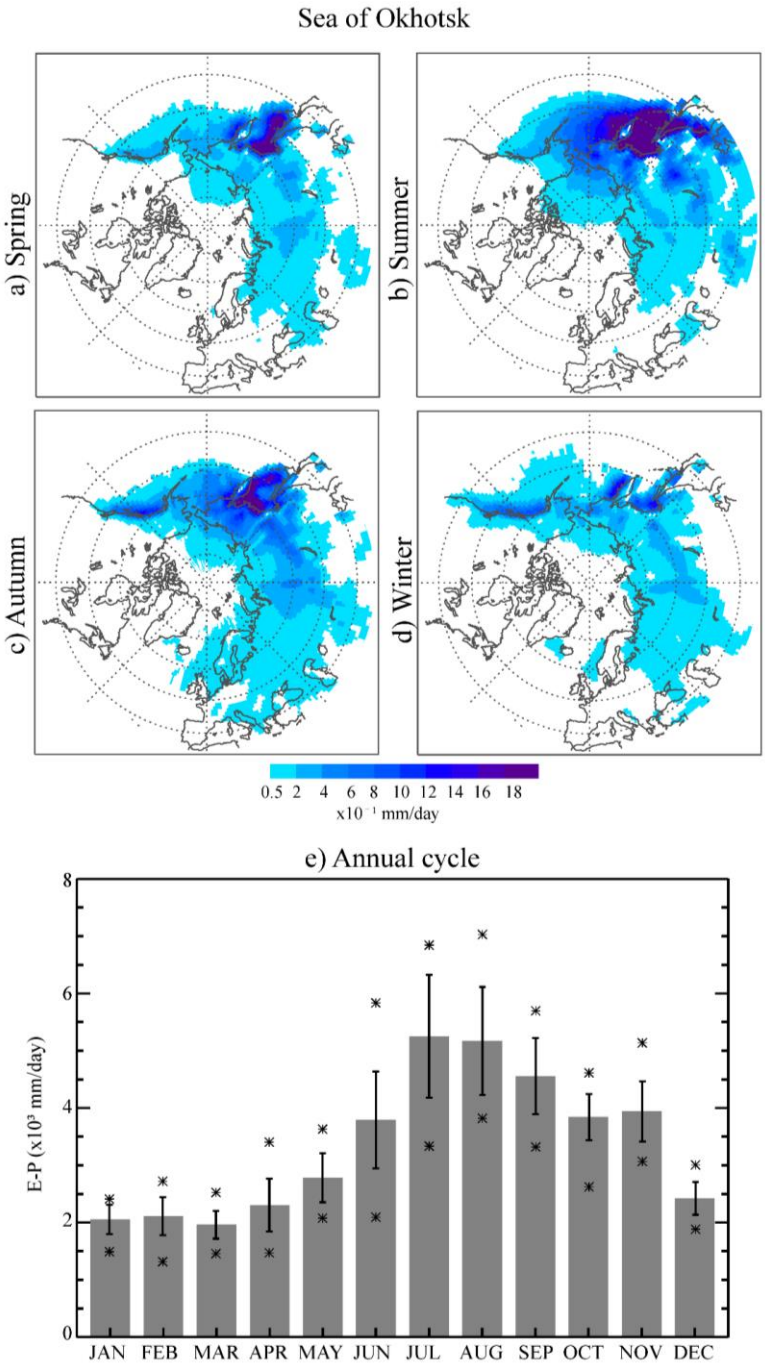

Figura A.2.14. Idem figura A.2.1 para el mar de Okhotsk.

A.3. Arctic moisture source for Eurasian snow cover variations in autumn (2015), ERL

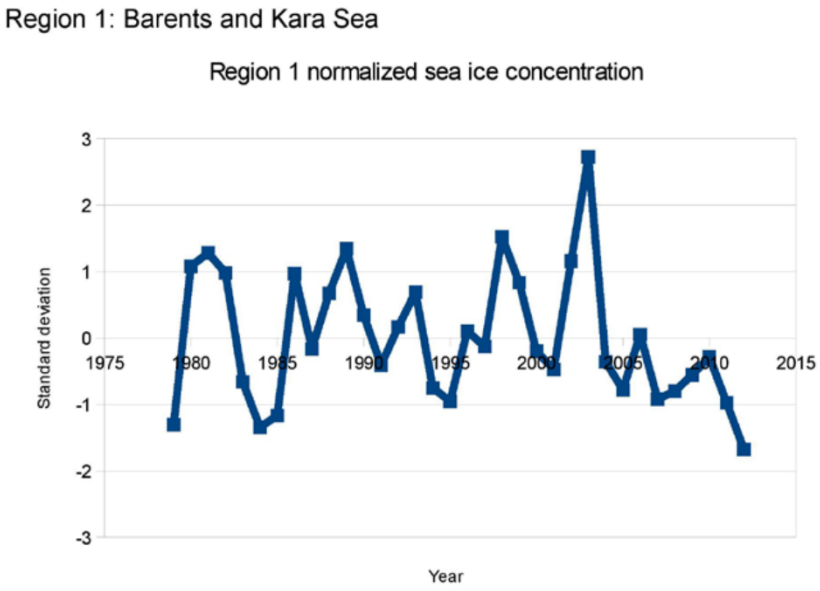

High ice	Low ice
1980	1979
1981	1984
1989	1985
1998	2012
2002	
2003	

Figura A.3.1. Desviación estándar normalizada de la concentración de hielo marino en sep-tiembre para el periodo 1979-2012. La concentración de hielo marino ha sido obtenida de la base de datos HadISST. La tabla representa los años con una concentración de hielo marino mayor/menor que una desviación estándar.

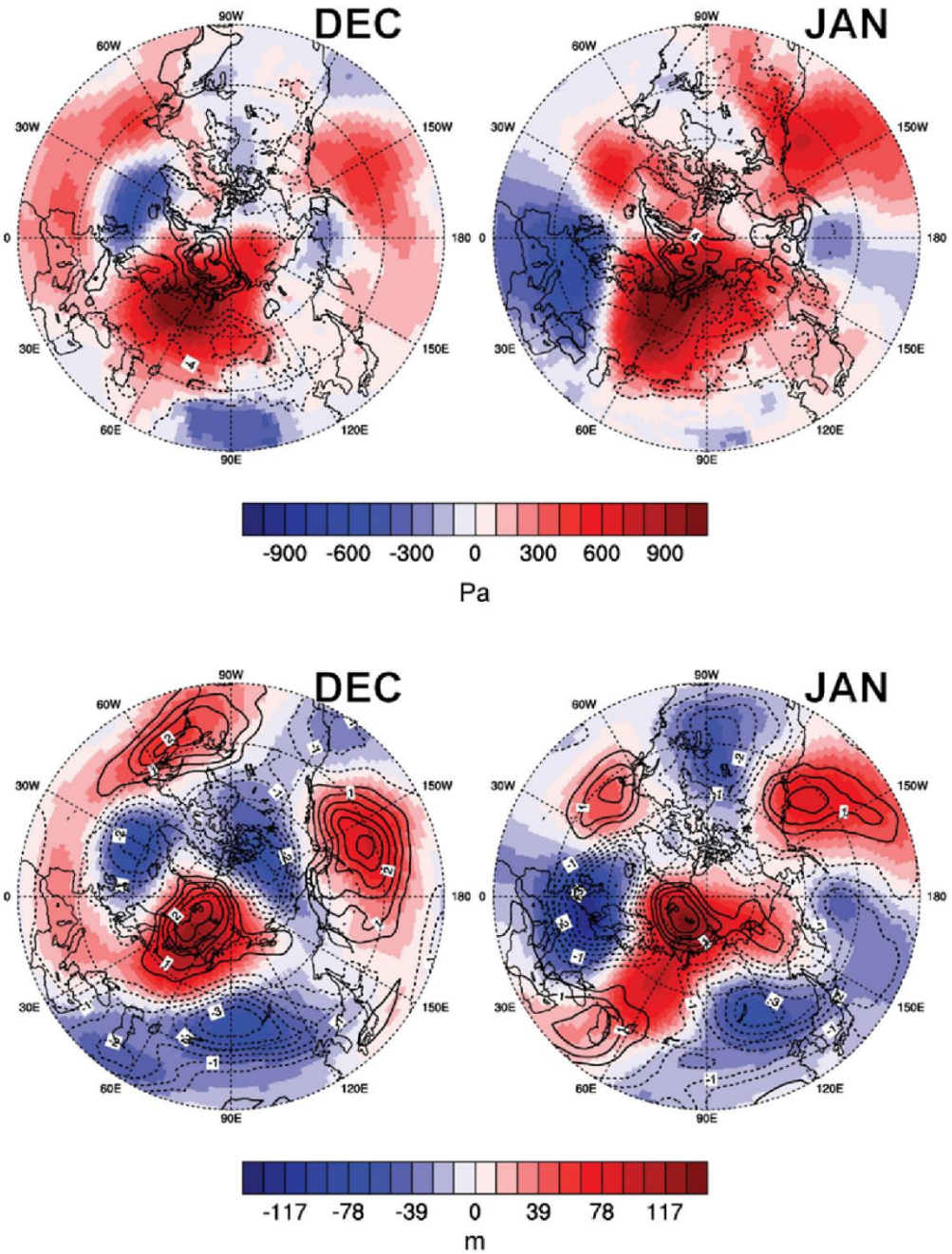

Figura A.3.2. Diferencia entre los años de alta y baja concentración de hielo marino para diciembre y enero para los datos de ERA-Interim. Superior: Presión a nivel del mar (colores) y temperatura a 2 metros (contorno desde -8 hasta 8 cada 2 K). Inferior: Altura geopotencial en 500 hPa (colores) y temperatura a 500 hPa (contornos de -3 a 3 cada 0.5 K).

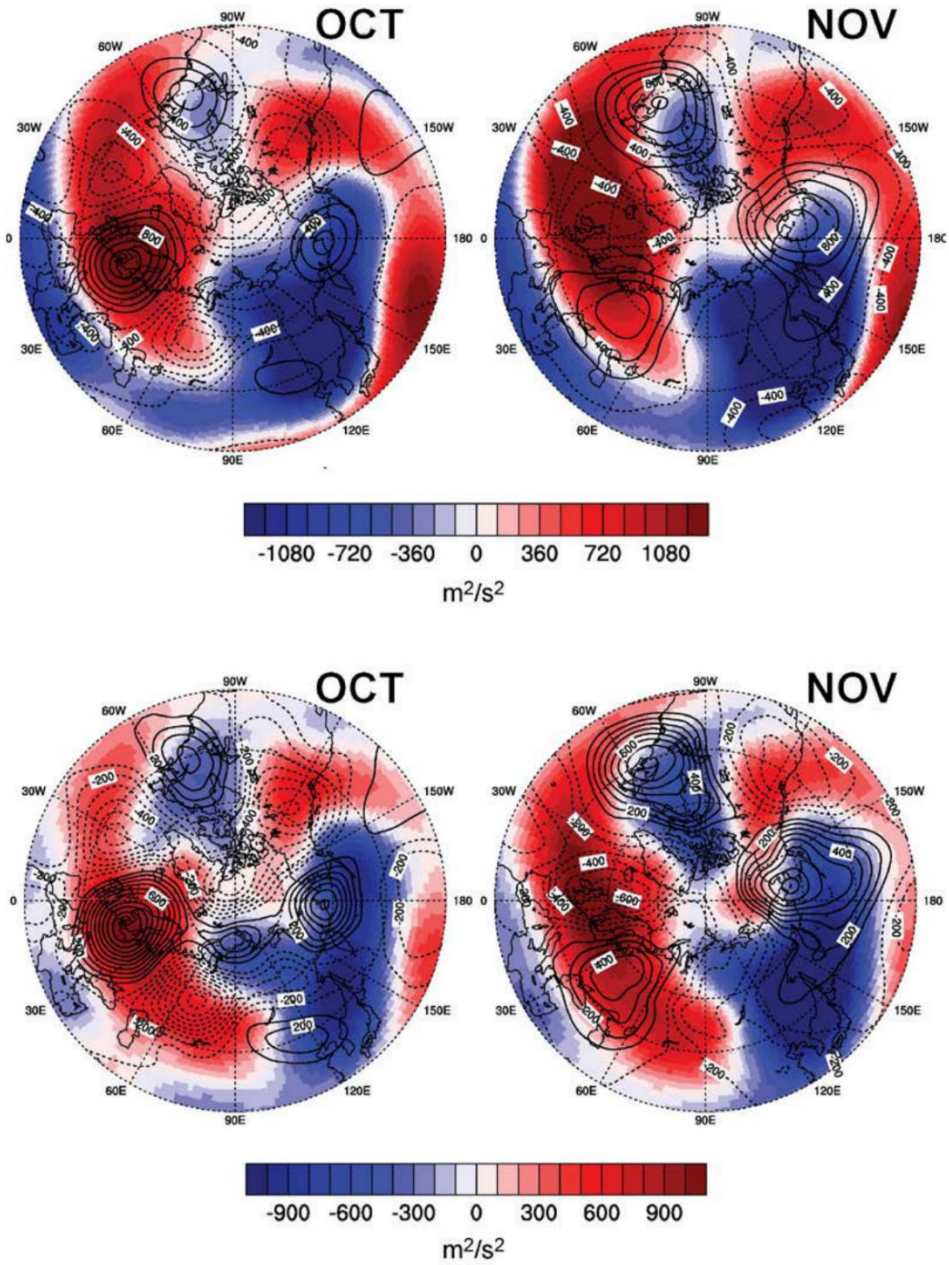

Figura A.3.3. Superior: Climatología (1979-2012) del geopotencial en 200 hPa para octubre y noviembre mostrado como la anomalía con respecto a la media anual (colores) y como la diferencia entre los años de máxima y mínima extensión de hielo para la misma variable (contornos desde -2000 hasta 2000 a intervalos de 200 m^2/s^2). Inferior: Idem para 500 hPa (contornos desde -1000 hasta 1000 a intervalos de 100 m^2/s^2). Datos de ERA-Interim.

Referencias

Aagaard K. and P. Greisman (1975), Toward new mass and heat budgets for the Arctic Ocean. J. Geophys. Res., 80, 3821–3827, doi:10.1029/JC080i027p03821.

Bales, RC (2003), Hydrology, Overview, Encyclopedia of Atmospheric Sciences 2nd Edition, Elsevier: 968-973, doi:10.1016/j.physletb.2003.10.071.Bordi, 2007.

Bauch D., J.A. Hölemann, A. Nikulina, C. Wegner, M.A. Janout, L.A. Timokhov, H. Kassens (2013), Correlation of river water and local sea-ice melting on the Laptev Sea shelf (Siberian Arctic). J. Geophys. Res. Oceans, 118, 550–561, doi:10.1002/jgrc.20076.

Baumann K. and A. Stohl (1997), Validation of a long-range trajectory model using gas balloon tracks from the Gordon Bennett Cup 95. J. Appl. Meteor., 36, 711–720, doi: 10.1175/1520-0450-36.6.711

Benton G.S. and M.A. Estoque (1954), Water vapor transfer over the North American continent. Journal of Meteorology, 11(6), 462–477, doi: 10.1175/1520-0469(1954)011h0462:WVTOTNi2.0.CO;2.

Bhatt, U.S., D.A. Walker, M.K. Raynolds, J.C. Comiso, H.E. Epstein, G. Jia, R. Gens, J.E. Pinzon, C.J. Tucker, C.E. Tweedie, and P.J. Webber (2010), Circumpolar Arctic Tundra Vegetation Change Is Linked to Sea Ice Decline. Earth Interact., 14, 1–20, doi: 10.1175/2010EI315.1.

Bintanja, R. and F.M. Selten (2014), Future increases in Arctic precipitation linked to local evaporation and sea-ice retreat. Nature, 509, 479–82, doi: 10.1038/nature13259.

Boisvert L.N. and J.C. Stroeve (2015), The Arctic is becoming warmer and wetter as revealed by the Atmospheric Infrared Sounder. Geophys. Res. Lett., 42, 4439–4446, doi:10.1002/2015GL063775.

Boisvert L.N., D.L. Wu and C.-L. Shie (2015), Increasing evaporation amounts seen in the Arctic between 2003 and 2013 from AIRS data. J. Geophys. Res. Atmos., 120, 6865–6881, doi: 10.1002/2015JD023258.

Bosilovich M.G. and S.D. Schubert (2002), Water vapor tracers as diagnostics of the regional hydrologic cycle. Journal of Hydrometeorology, 3(2), 149–165, doi: 10.1175/1525-7541(2002)003h0149:WVTADOi2.0.CO;2.

Bring A., I. Fedorova, Y. Dibike, L. Hinzman, J. Mård, S.H. Mernild, T. Prowse, O. Semenova, S.L. Stuefer, and M.-K. Woo (2016), Arctic terrestrial hydrology: A synthesis of processes, regional effects, and research challenges. J. Geophys. Res. Biogeosci., 121, doi:10.1002/2015JG003131.

Brubaker K. L., D. Entekhabi and P. Eagleson (1993), Estimation of continental precipitation recycling. Journal of Climate, 6(6), 1077–1089, doi:10.1175/1520-0442(1993)006h1077:EOCPRi2.0.CO;2.

Brubaker K L., P.A. Dirmeyer, A. Sudradjat, B.S. Levy and F. Bernal (2001), A 36-yr climatological description of the evaporative sources of warm-season precipitation in the Mississippi River basin. Journal of Hydrometeorology, 2(6), 537–557, doi: 10.1175/1525-7541(2001)002h0537:AYCDOTi2.0.CO;2.

Budyko M.I. (1974), Climate and Life, 508 pp., Academic, New York.

Burde G. and A. Zangvil (2001a), The estimation of regional precipitation recycling. Part I: Review of recycling models. Journal of Climate, 14(12), 2497–2508, doi: 10.1175/1520-0442(2001)014h2497:TEORPRi2.0.CO;2.

Burde G. and A. Zangvil (2001b), The estimation of regional precipitation recycling. Part II: A new recycling model. Journal of Climate, 14(12), 2509–2527, doi: 10.1175/1520-0442(2001)014h2509:TEORPRi2.0.CO;2.

Callaghan T., M. Johansson, R.D. Brown, P.Y. Groisman, N. Labba, V. Radionov, R.G. Barry, O.N. Bulygina, R.L.H. Essery, D.M. Frolov, V.N. Golubev, T.C. Grenfell,

M.N. Petrushina, V.N. Razuvaev, D.A. Robinson, P. Romanov, D. Shindell, A.B. Shmakin, S.A. Sokratov, S. Warren and D. Yang (2011), The changing face of Arctic snow cover: A synthesis of observed and projected changes. Ambio, 40, 17–31, doi: 10.1007/s13280-011-0212-y

Carmack E. C., M. Yamamoto-Kawai, T.W. N. Haine, S. Bacon, B.A. Bluhm, C. Lique, H. Melling, I.V. Polyakov, F. Straneo, M.-L. Timmermansand W.J. Williams (2016), Freshwater and its role in the Arctic Marine System: Sources, disposition, storage, export, and physical and biogeochemical consequences in the Arctic and global oceans. J. Geophys. Res. Biogeosci., 121, 675–717, doi:10.1002/2015JG003140.

Cavalieri D.J. and C.L. Parkinson (2012), Arctic sea ice variability and trends, 1979–2010. Cryosphere, 6, 881–889, doi:10.5194/tc-6-881-2012.

Cheng B., Z. Zhang, T. Vihma, M. Johansson, L. Bian, Z. Li, and H. Wu (2008), Model experiments on snow and ice thermodynamics in the Arctic Ocean with CHINARE2003 data. J. Geophys. Res., 113, C09020, doi:10.1029/2007JC004654.

Cohen J., J.A. Screen, J.C. Furtado, M. Barlow, D. Whittleston, D. Coumou, J. Francis, K. Dethloff, D. Entekhabi, J. Overland and J. Jones (2014), Recent Arctic amplification and extreme mid-latitude weather, Nat. Geosci., 7, 627–637, doi: 10.1038/ngeo2234

Comiso J.C. and D.K. Hall (2014), Climate trends in the Arctic as observed from space. WIREs Clim Change, 5: 389–409. doi:10.1002/wcc.277.

Comiso J.C., C.L. Parkinson, R. Gersten and L. Stock (2008), Accelerated decline in the Arctic sea ice cover. Geophys. Res. Lett., 35, L01703, doi:10.1029/2007GL031972.

Coplen T.B., P.J. Neiman, A.B. White, J.M. Landwehr, F.M. Ralph and M.D. Dettinger (2008), Extreme changes in stable hydrogen isotopes and precipitation characteristics in a landfalling Pacific storm. Geophysical Research Letters, 35(L21808), doi:10.1029/2008GL035481.

D'Abreton P. and P. Tyson (1995), Divergent and non-divergent water vapour transport over southern Africa during wet and dry conditions. Meteorology and Atmospheric Physics, 55(1-2), 47–59, doi:10.1007/BF01029601.

Devasthale A., J. Sedlar and M. Tjernström (2011), Characteristics of water-vapour inversions observed over the Arctic by Atmospheric Infrared Sounder (AIRS) and radiosondes. Atmos. Chem. Phys., 11, 9813–9823, doi:10.5194/acp-11-9813-2011.

Dirmeyer P.A. and K.L. Brubaker (1999), Contrasting evaporative moisture sources during the drought of 1988 and the flood of 1993. Journal of Geophysical Research, 104(D16), 19383–19397, doi:10.1029/1999JD900222.

Dirmeyer P.A. and K.L. Brubaker (2006), Evidence for trends in the Northern Hemisphere water cycle. Geophysical Research Letters, 33(L14712), doi:10.1029/2006GL026359.

Dominguez F., P. Kumar, X.-Z. Liang and M. Ting (2006), Impact of atmospheric moisture storage on precipitation recycling. Journal of Climate, 19(8), 1513–1530, doi: 10.1175/JCLI3691.1.

Dowdeswell, J.A., J.O. Hagen, H. Björnsson, A.F. Glazovsky, W.D. Harrison, P. Holmlund, J. Jania, R.M. Koerner, B. Lefauconnier, C.S.L. Ommanney and R.H. Thomas (1997), The Mass Balance of Circum-Arctic Glaciers and Recent Climate Change. Quaternary Research, 48, 1-14, doi: 10.1006/qres.1997.1900

Efron, B. (1992). “Bootstrap methods: another look at the jackknife,” in Breakthroughs in Statistics: Methodology and Distribution, eds S. Kotz and N. L. Johnson (New York, NY: Springer), 569–593. doi: 10.1007/978-1-4612-4380-9_41

Efron B. and R.J. Tibshirani (1993), An introduction to the bootstrap. Boca Raton, FL: Chapman & Hall.

Eltahir E.A. and R.L. Bras (1994), Precipitation recycling in the Amazon basin. Quarterly Journal of the Royal Meteorological Society, 120(518), 861–880, doi:10.1002/qj.49712051806.

Fetterer F., K. Knowles, W. Meier and M. Savoie (2016), updated daily. Sea Ice Index, Version 2. Boulder, Colorado USA. NSIDC: National Snow and Ice Data Center. doi: http://dx.doi.org/10.7265/N5736NV7.

Ford J.D. (2009), Dangerous climate change and the importance of adaptation for the Arctic's Inuit population. Environ. Res. Lett., 4(2), 024006, doi:10.1088/1748-9326/4/2/024006.

Francis J.A. and S.J. Vavrus, (2012), Evidence linking Arctic amplification to extreme weather in mid-latitudes, Geophys. Res. Lett., 39, L06801, doi:10.1029/2012GL051000.

Gat J. and I. Carmi (1970), Evolution of the isotopic composition of atmospheric waters in the Mediterranean Sea area. Journal of Geophysical Research, 75(15), 3039–3048, doi:10.1029/JC075i015p03039.

Gimeno L., A. Stohl, R. M. Trigo, F. Dominguez, K. Yoshimura, L. Yu, A. Drumond, A. M. Durán-Quesada, and R. Nieto (2012), Oceanic and terrestrial sources of continental precipitation. Rev. Geophys., 50, RG4003, doi:10.1029/2012RG000389.

Gimeno L., R. Nieto, A. Drumond, R. Castillo, and R. M. Trigo (2013), Influence of the intensification of the major oceanic moisture sources on continental precipitation. Geophys. Res. Lett., 40, 1443–1450, doi:10.1002/grl.50338.

Gimeno L., R. Nieto, M. Vázquez and D. Lavers (2014), Atmospheric rivers: a mini-review. Frontiers in Earth Science, 2, 2, doi: 10.3389/feart.2014.00002

Graversen R.G. and M. Wang (2009), Polar amplification in a coupled climate model with locked albedo. Climate Dyn., 33, 629–643, doi: 10.1007/s00382-009-0535-6.

Groves D.G. and J.A. Francis (2002), Variability of the Arctic atmospheric moisture budget from TOVS satellite data. J. Geophys. Res., 107(D24), 4785, doi:10.1029/2002JD002285.

Hanna, S.R. (1982), Applications in Air Pollution Modeling, in F. T. M. Nieuwstadt and H. van Dop (eds.), Atmospheric Turbulence and Air Pollution Modelling. D. Reidel Publishing Company, Dordrecht.

Holland M.M., C.M. Bitz and B. Tremblay (2006), Future abrupt reductions in the summer Arctic sea ice. Geophys. Res. Lett., 33, L23503, doi:10.1029/2006GL028024.

Honda M., J. Inoue and S. Yamane (2009), Influence of low Arctic sea-ice minima on anomalously cold Eurasian winters. Geophys. Res. Lett., 36, L08707, doi:10.1029/2008GL037079.

Instanes A., V. Kokorev, R. Janowicz, O. Bruland, K. Sand and T. Prowse (2016), Changes to freshwater systems affecting Arctic infrastructure and natural resources. J. Geophys. Res. Biogeosci., 121, doi:10.1002/2015JG003125.

Intrieri J.M., M.D. Shupe, T. Uttal, and B.J. McCarty (2002), An annual cycle of Arctic cloud characteristics observed by radar and lidar at SHEBA. J. Geophys. Res., 107(C10), 8030, doi:10.1029/2000JC000423.

IPCC (2013), Climate Change 2013: The physical science basis, in: Contribution of working group 1 to the fifth assessment report of the intergovernmental panel on climate change, edited by: Stocker, T. F., Qin, D., Planttner, G. K., Tignor, M., Allen, S. K., Boschung, J., Nauels, A., Xia, Y., Bex, V., and Midgley, P. M., Cambridge University Press, Cambridge, UK and New York, NY, USA.

Jakobson E. and T. Vihma (2010), Atmospheric moisture budget in the Arctic based on the ERA-40 reanalysis. Int. J. Climatol., 30, 2175–2194, doi:10.1002/joc.2039.

Jakobson, E., T. Vihma, T. Palo, L. Jakobson, H. Keernik, and J. Jaagus (2012), Validation of atmospheric reanalyses over the central Arctic Ocean. Geophys. Res. Lett., 39, L10802, doi:10.1029/2012GL051591.

James P., A. Stohl, N. Spichtinger, S. Eckhardt and C. Forster (2004), Climatological aspects of the extreme European rainfall of August 2002 and a trajectory method for estimating the associated evaporative source regions. Nat. Hazards Earth Syst. Sci., 4, 733-746, doi:10.5194/nhess-4-733-2004

Joussaume S., R. Sadourny and J. Jouzel (1984), A general circulation model of water isotope cycles in the atmosphere. Nature, 311(5981), 24–29, doi:10.1038/311024a0.

Kapsch M.L., R.G. Graversen and M. Tjernström (2013) Springtime atmospheric energy transport and the control of Arctic summer sea-ice extent. Nat. Clim. Change, 3, 744–748, doi:10.1038/nclimate1884

Kawamura T., K. Shirasawa, N. Ishikawa, A. Lindfors, K. Rasmus, M.A. Granskog, J. Ehn, M. Leppäranta, T. Martma, and R. Vaikmäe (2001), Time-series observations of the structure and properties of brackish ice in the Gulf of Finland. Ann. Glaciol., 33, 1–4.

Koenigk T., L. Brodeau, R.G. Graversen, J. Karlsson, G. Svensson, M. Tjernström, , U. Willén and K. Wyser (2013), Arctic climate change in 21st century CMIP5 simulations with EC-Earth. Clim Dyn, 40: 2719, doi:10.1007/s00382-012-1505-y.

Kopec B.G., X. Feng, F.A. Michel and E. S. Posmentier (2016), Influence of sea ice on Arctic precipitation. Proc. Natl. Acad. Sci. U.S.A., 113, 46–51, doi:10.1073/pnas.1504633113.

Koster R., J. Jouzel, R. Suozzo, G. Russell, W. Broecker, D. Rind and P. Eagleson (1986). Global sources of local precipitation as determined by the NASA/GISS GCM. Geophysical Research Letters, 13(2), 121–124, doi:10.1029/GL013i002p00121.

Kug J.S., D.H. Choi, F.F. Jin, W.T. Kwon, and H.L. Ren (2010), Role of synoptic eddy feedback on polar climate responses to the anthropogenic forcing. Geophys. Res. Lett., 37, L14704, doi:10.1029/2010GL043673.

Kwok R. and D.A. Rothrock (2009), Decline in Arctic sea ice thickness from submarine and ICESat records: 1958-2008. Geophys. Res. Lett., 36, L15501, doi:10.1029/2009GL028737.

Laken B.A. and J. Čalogović (2013), Composite analysis with Monte Carlo methods: an example with cosmic rays and clouds. J. Space Weather Space Clim., 3, doi: 10.1051/swsc/2013051

Lammers R.B., A.I. Shiklomanov, C.J. Vörösmarty, B.M. Fekete, and B.J. Peterson (2001), Assessment of contemporary Arctic river runoff based on observational discharge records. J. Geophys. Res., 106, 3321–34, doi:10.1029/2000JD900444.

Lindsay R.W and J. Zhang (2005), The thinning of Arctic sea ice, 1988–2003: have we passed a tipping point? J. Climate, 18:4879–4894, doi: 10.1175/JCLI3587.1.

Lindsay R.W., J. Zhang, A. Schweiger, M. Steele and H. Stern (2009), Arctic sea ice retreat in 2007 follows thinning trend. J. Climate, 22, 165–176, doi:10.1175/2008JCLI2521.1

Linton H.C., T.D. Prowse, Y.B. Dibike and B.R. Bonsal (2014), Spatial and temporal variations in hydroclimatic variables affecting streamflow across western Canada. MSc thesis, Univ. of Victoria, BC, Canada.

Liston G.E. and C.A. Hiemstra (2011), The changing cryosphere: Pan-Arctic snow trends (1979–2009). J. Clim., 24, 5691–5712, doi:10.1175/JCLI-D-11-00081.1.

Liu C. and E.A. Barnes (2015), Extreme moisture transport into the Arctic linked to Rossby wave breaking. J. Geophys. Res. Atmos., 120, 3774–3788, doi:10.1002/2014JD022796.

Liu J.P., J.A. Curry, H.J. Wang, M.R. Song and R.M. Horton (2012), Impact of declining Arctic sea ice on winter snowfall. Proc. Nat. Acad. Sci. USA, 109, 4074–4079, doi: (2012).10.1073/pnas.1114910109

Lorenz C. and H. Kunstmann (2012), The hydrological cycle in three state-of-the-art reanalyses: intercomparison and performance analysis. J. Hydrometeorol. 13, 1397–1420, doi: 10.1175/jhm-d-11–088.1.

Lucarini V. and F. Ragone (2011), Energetics of climate models: Net energy balance and meridional enthalpy transport, Rev. Geophys., 49, RG1001, doi:10.1029/2009RG000323.

Massacand A.C., H. Wernli and H.C. Davies (1998), Heavy precipitation on the alpine southside: An upper-level precursor. Geophysical Research Letters, 25(9), 1435–1438, doi:10.1029/98GL50869.

McClelland, J.W., S.J. Déry, B.J. Peterson, R.M. Holmes and E.F. Wood (2006), A pan-arctic evaluation of changes in river discharge during the latter half of the 20th century. Geophys. Res. Lett., 33, L06715, doi:10.1029/2006GL025753.

Min S.K., X.B. Zhang, and F. Zwiers (2008), Human-induced Arctic moistening. Science, 320, 518–520, doi: 10.1126/science.1153468

Miralles D.G., T.R.H. Holmes, R.A.M. De Jeu, J.H. Gash, A.G.C.A. Meesters, and A.J. Dolman (2011), Global land-surface evaporation estimated from satellite-based observations. Hydrol. Earth Syst. Sci., 15, 453–469, doi:10.5194/hess-15-453-2011.

Mosby H. (1962), Water, salt and heat balance of the north Polar Sea and of the Norwegian Sea. Geofys. Publ., 24, 289–313.

Mundhenk, B.D., E.A. Barnes, E.D. Maloney and K. M. Nardi (2016), Modulation of atmospheric rivers near Alaska and the U.S. West Coast by northeast Pacific height anomalies. J. Geophys. Res. Atmos., 121, 12,751–12,765, doi:10.1002/2016JD025350.

Neff, W., G.P. Compo, F.M. Ralph and M.D. Shupe (2014), Continental heat anomalies and the extreme melting of the Greenland ice surface in 2012 and 1889. J. Geophys. Res. Atmos., 119, 6520–6536, doi:10.1002/2014JD021470.

Nghiem S.V., D.K. Hall, , I.G. Rigor, P. Li and G. Neumann (2014), Effects of Mackenzie River discharge and bathymetry on sea ice in the Beaufort Sea. Geophys. Res. Lett., 41, 873–879, doi:10.1002/2013GL058956.

Nieto R., L. Gimeno, D. Gallego, and R. Trigo (2007), Contributions to the moisture budget of airmasses over Iceland. Meteorol. Z., 16, 37–44, doi: 10.1127/0941-2948/2007/0176

Numaguti A. (1999), Origin and recycling processes of precipitation water over the Eurasian continent: Experiments using an atmospheric general circulation model. J. Geophys. Res., 104, 1957–1972, doi:10.1029/1998JD200026.

Ohmura, A. (2001), Physical Basis for the Temperature-Based Melt-Index Method. J. Appl. Meteorol., 40, 753–761, doi: 10.1175/1520-0450(2001)040<0753:PBFTTB>2.0.CO;2

Oort A.H. (1975), Year-to-year variations in the energy balance of the Arctic atmosphere. J. Geophys. Res., 79, 1253–1260, doi:10.1029/JC079i009p01253.

Overland J.E. and M. Wang (2010), Large-scale atmospheric circulation changes are associated with the recent loss of Arctic sea ice. Tellus A., 62, 1–9, doi:10.1111/j.1600-0870.2009.00421.x

Overland J.E. and M. Wang (2013), When will the summer Arctic be nearly sea ice free? Geophys. Res. Lett., 40, 2097–2101, doi:10.1002/grl.50316.

Overland J.E., M. Wang, J.E. Walsh and J.C. Stroeve, (2014), Future Arctic climate changes: Adaptation and mitigation time scales. Earth's Future, 2: 68–74. doi:10.1002/2013EF000162

Palmen E., and L.A. Vuorela (1963), On the mean meridional circulations in the Northern Hemisphere during the winter season, Q. J. R. Meteorol. Soc., 89, 131–138.

Park H., J.E. Walsh, Y. Kim, T. Nakai and T. Ohata (2013), The role of declining Arctic sea ice in recent decreasing terrestrial Arctic snow depths. Polar Sci. 7, 174– 187, doi: 10.1016/j.polar.2012.10.002

Parkinson C.L. and J.C. Comiso (2013) On the 2012 record low Arctic sea ice cover: Combined impact of preconditioning and an August storm. Geophys. Res. Lett., 40, 1356–1361, doi:10.1002/grl.50349

Peixoto J.P. and A.H. Oort (1992), Physics of climate, 520 pp., American Institute of Physics, New York.

Peterson B.J., R.M. Holmes, J.W. McClelland, C.J. Vörösmarty, R.B. Lammers, A.I. Shiklomanov, I.A. Shiklomanov, S. Rahmstorf (2002), Increasing river discharge to the Arctic Ocean, Science, 98(5601):2171-3, doi: 10.1126/science.1077445

Polyakov I.V., J. E. Walsh and R. Kwok (2012), Recent changes of Arctic multiyear sea ice coverage and the likely causes. Bull. Am. Meteorol. Soc., 93, 145–151, doi: http://dx.doi.org/10.1175/BAMS-D-11-00070.1.

Post, E., U.S. Bhatt, C.M. Bitz, J.F. Brodie, T.L. Fulton, M. Hebblewhite, J. Kerby, S.J. Kutz, I. Stirling, D.A. Walker (2013), Ecological Consequences of Sea-Ice Decline. Science, 341 (6145), 519-524, doi: 10.1126/science.1235225

Rayner N.A, D.E. Parker, E.B. Horton, C.K. Folland, L.V. Alexander, D.P. Rowell, E.C. Kent and A. Kaplan (2003), Global analyses of sea surface temperature, sea ice, and night marine air temperature since the late nineteenth century. J. Geophys. Res.: Atmos., 108, 4407, doi:10.1029/2002JD002670, D14.

Rinke A., C. Melsheimer, K. Dethloff and G. Heygster (2009), Arctic Total Water Vapor: Comparison of Regional Climate Simulations with Observations, and Simulated Decadal Trends. J. Hydrometeor., 10, 113–129, doi: 10.1175/2008JHM970.1.

Roberts A., et al. (2010), A science plan for Regional Arctic System Modeling: A report to the National Science Foundation from the International Arctic Science Community International Arctic Research Center Technical Papers 10-0001.

Rogers A.N., D.H. Bromwich, E.N. Sinclair and R.I. Cullather (2001), The atmospheric hydrologic cycle over the Arctic Basin from Reanalyses. Part II: Interannual variability. J. Clim., 14, 2414–2429, doi:10.1175/1520-0442(2001)014<2414:TAHCOT>2.0.CO;2.

Rozanski K., C. Sonntag and K. Munnich (1982), Factors controlling stable isotope composition of European precipitation. Tellus, 34(2), 142–150, doi:10.1111/j.2153-3490.1982.tb01801.x.

Ryall D.B. and R. H. Maryon (1997), Validation of the UK Met Oce name model against the ETEX dataset. In: Model Verication and Emergency Response, edited by: Nodop, K., ETEX Symposium on Long-Range Atmospheric Transport, 151-154.

Salati E., A. Dall'Olio, E. Matsui and J.R. Gat (1979), Recycling of water in the Amazon basin: An isotopic study. Water Resources Research, 15(5), 1250–1258, doi:10.1029/WR015i005p01250.

Screen J.A. and I. Simmonds (2010), The central role of diminishing sea ice in recent Arctic temperature amplification. Nature, 464, 1334–1337, doi:10.1038/nature09051.

Screen J.A. and I. Simmonds (2012), Declining summer snowfall in the Arctic: Causes, impacts and feedbacks. Clim. Dyn., 38, 2243–2256, doi:10.1007/s00382-011-1105-2.

Sedlar J., M. Tjernström, T. Mauritsen, M. Shupe, I. Brooks, P.O. Persson, C. Birch, C. Leck, A. Sirevaag, and M. Nicolaus (2011), A transitioning Arctic surface energy budget: The impacts of solar zenith angle, surface albedo and cloud radiative forcing. Clim. Dyn., 37, 1643–1660, doi:10.1007/s00382-010-0937-5.

Seibert P., B. Kruger and A. Frank (2001), Parametrisation of convective mixing in a Lagrangian particle dispersion model, Proceedings of the 5th GLOREAM Workshop, Wengen, Switzerland, 24–26.

Sepp M. and J. Jaagus (2011), Changes in the activity and tracks of Arctic cyclones. Clim. Change, 105, 577–595, doi: 10.1007/s10584-010-9893-7

Sherstyukov B.G, V.N Razuvaev, O.N Bulygina and P.Y. Groisman (2007), NEESPI Science and Data Support Center for Hydrometeorological Information in Obninsk, Russia Environ. Res. Lett. 2 045010

Shupe M.D. and J.M. Intrieri (2004), Cloud radiative forcing of the Arctic surface: The influence of cloud properties, surface albedo, and solar zenith angle. J. Clim., 17, 616–628, doi: 10.1175/1520-0442(2004)017<0616:CRFOTA>2.0.CO;2.

Singarayer J.S., J.L. Bamber and P.J. Valdes (2006), Twenty-first-century climate impacts from a declining Arctic sea ice cover. J Clim., 19, 1109–1125, doi: 10.1175/JCLI3649.1

Smedsrud L.H., A. Sorteberg and K. Kloster (2008), Recent and future changes of the Arctic sea-ice cover. Geophys. Res. Lett., 35, L20503, doi:10.1029/2008GL034813.

Sodemann, H., C. Schwierz and H. Wernli (2008), Interannual variability of Greenland winter precipitation sources: Lagrangian moisture diagnostic and North Atlantic Oscillation influence. J. Geophys. Res., 113, D03107, doi:10.1029/2007JD008503.

Sorteberg A. and J.E. Walsh (2008), Seasonal cyclone variability at 70°N and its impact on moisture transport into the Arctic. Tellus A, 60, 570–586, doi: 10.1111/j.1600-0870.2008.00314.x

Starr V.P. and J.P. Peixoto (1958), On the global balance of water vapor and the hydrology of deserts. Tellus, 10(2), 188–194, doi:10.1111/j.2153-3490.1958.tb02004.x.

Starr V.P., J.P. Peixoto and A.R. Chrsti (1965), Hemispheric water balance for the IGY, Tellus, 17, 463–472.

Stohl A. and D.J. Thomson (1999), A density correction for Lagrangian particle dispersion models. Bound.-Layer Met., 90, 155–167, doi: 10.1023/A:1001741110696

Stohl A. and P. James (2004), A Lagrangian analysis of the atmospheric branch of the global water cycle. Part I: Method description, validation, and demonstration for the August 2002 flooding in central Europe. J. Hydrometeorol., 5, 656–678, doi:10.1175/1525-7541(2004)005<0656:ALAOTA>2.0.CO;2.

Stohl A. and P.A. James (2005), A Lagrangian analysis of the atmospheric branch of the global water cycle. Part II: Moisture transports between Earth's ocean basins and river catchments. J. Hydrometeorol., 6, 961–984, doi:10.1175/JHM470.1.

Stohl A., G. Wotawa, P. Seibert and H. Kromp-Kolb (1995), Interpolation errors in wind fields as a function of spatial and temporal resolution and their impact on different types of kinematic trajectories. Journal of Applied Meteorology, 34(10), 2149– 2165, doi: 10.1175/1520-0450(1995)034h2149:IEIWFAi2.0.CO;2.

Stohl A., M. Hittenberger and G. Wotawa (1998), Validation of the Lagrangian particle dispersion model FLEXPART against large-scale tracer experiment data. Atmospheric Environment, 32(24), 4245–4264, doi:10.1016/S1352-2310(98)00184-8.

Stohl A., C. Forster, A. Frank, P. Seibert and G. Wotawa (2005), Technical note: The Lagrangian particle dispersion model FLEXPART version 6.2. Atmos. Chem. Phys., 5, 2461-2474, doi:10.5194/acp-5-2461-2005

Strey S.T., W.L. Chapman and J.E. Walsh (2010), The 2007 sea ice minimum: impacts on the Northern Hemisphere atmosphere in late autumn and early winter. J. Geophys. Res., 115, D23103, doi: 10.1029/2009JD013294

Stroeve J.C., T. Markus, L. Boisvert, J. Miller and A. Barrett (2014), Changes in Arctic melt season and implications for sea ice loss. Geophys. Res. Lett., 41, 1216–1225, doi:10.1002/2013GL058951.

Tang Q., X. Zhang and J.A. Francis (2014), Extreme summer weather in northern mid-latitudes linked to a vanishing cryosphere. Nat. Clim. Change, 4, 45–50, doi:10.1038/nclimate2065.

Tavolato, C. and L. Isaksen (2011), Data usage and quality control for ERA-40, ERA-Interim, and the operational ECMWF data assimilation system, ERA report series 7.

Trenberth K.E. and C.J. Guillemot (1998), Evaluation of the atmospheric moisture and hydrological cycle in the NCEP/NCAR reanalyses. Climate Dynamics, 14(3), 213–231, doi:10.1007/s003820050219.

Trenberth K.E., A. Dai, R.M. Rasmussen, and D.B. Parsons (2003), The Changing Character of Precipitation. Bull. Amer. Meteor. Soc., 84, 1205–1217, doi: 0.1175/BAMS-84-9-1205.

Trenberth K.E., J.T. Fasullo ans J. Mackaro (2011), Atmospheric moisture transports from ocean to land and global energy flows in reanalyses. J. Clim. 24 (18), 4907–4924, doi: 10.1175/2011jcli4171.1.

Trigo, I.F. (2006), Climatology and interannual variability of storm tracks in the Euro–Atlantic sector: A comparison between ERA-40 and NCEP/NCAR reanalyses. Clim. Dyn., 26, 127–143, doi:10.1007/s00382-005-0065-9.

Vihma T. (2014), Effects of Arctic Sea Ice Decline on Weather and Climate: A Review. Surv. Geophys., 35, 1175, doi:10.1007/s10712-014-9284-0

Vihma T., J. Screen, M. Tjernström, B. Newton, X. Zhang, V. Popova, C. Deser, M. Holland and T. Prowse (2016), The atmospheric role in the Arctic water cycle: A review on processes, past and future changes, and their impacts. J. Geophys. Res. Biogeosci., 121, 586–620, doi:10.1002/2015JG003132.

Walsh, J.E., X. Zhou, D. Portis, and M.C. Serreze (1994), Atmospheric contribution to hydrologic variations in the Arctic. Atmos.-Ocean, 32, 733–755.

Walsh J.E., J.E. Overland, P.Y. Groisman and B. Rudolph (2011), Arctic climate: Recent variations, in AMAP (2011) Snow, Water, Ice and Permafrost in the Arctic (SWIPA): Climate Change and the Cryosphere, 538 pp., Arctic Monit. and Assess. Programme (AMAP), Oslo, Norway.

Wang, M. and J.E. Overland (2009), A sea ice free summer Arctic within 30 years? Geophys. Res. Lett., 36, L07502, doi:10.1029/2009GL037820.

Wernli H. (1997), A lagrangian-based analysis of extratropical cyclones, II: A detailed case study. Quarterly Journal of the Royal Meteorological Society, 123(542), 1677-1706, doi:10.1002/qj.49712354211.

Whitefield J., P. Winsor, J. McClelland and D. Menemenlis (2015), A new river discharge and river temperature climatology data set for the pan-Arctic region, Ocean Modell., 88, 1–15, doi: http://dx.doi.org/10.1016/j.ocemod.2014.12.012.

Winton M. (2006), Amplified Arctic climate change: what does surface albedo feedback have to do with it? Geophys. Res. Lett., 33, L03701, doi: 10.1029/2005GL025244.

Wrona F.J., T.D. Prowse, J.D. Reist, J.E. Hobbie, L.M. J. Lévesque, R.W. Macdonald, and W.F. Vincent (2006), Effects of ultraviolet radiation and contaminant-related stressors on Arctic freshwater ecosystems, Ambio, 35(7), 388–401, doi: 10.1579/0044-7447(2006)35[388:EOURAC]2.0.CO;2

Wu P., R. Wood and P. Stott (2005), Human influence on increasing Arctic river discharges. Geophys. Res. Lett., 32, L02703, doi:10.1029/2004GL021570.

Yang X.-Y., J.C. Fyfe and G.M. Flato (2010), The role of poleward energy transport in Arctic temperature evolution. Geophys. Res. Lett., 37, L14803, doi: 10.1029/2010GL043934.

Yu L. (2007), Global variations in oceanic evaporation (1958–2005): The role of the changing wind speed. J. Clim., 20, 5376–5390, doi: 10.1175/2007JCLI1714.1

Yu L. and R.A. Weller (2007), Objectively Analyzed air-sea heat Fluxes for the global oce-free oceans (1981–2005). Bull. Ameri. Meteor. Soc., 88, 527–539

Yu L., X. Jin, and R.A. Weller (2008), Multidecade global flux datasets from the objectively analyzed air-sea fluxes (OAFlux) Project: Latent and sensible heat fluxes, ocean evaporation, and related surface meteorological variables OAFlux Project Tech. Rep. OA-2008-01, 64 pp., Woods Hole Oceanographic Institution, Woods Hole, Mass.

Zhang X., R. Brown, L. Vincent, W. Skinner, Y. Feng, and E. Mekis (2011), Canadian climate trends, 1950–2007. Canadian Biodiversity: Ecosystem Status and Trends 2010. Canadian Councils of Resource Ministers Tech. Thematic Rep. Series 5, 21 pp. [Available at http://www.biodivcanada.ca/default.asp?lang=En&n=137E1147-0.]

Zhang X., J. He, J. Zhang, I. Polaykov, R. Gerdes, J. Inoue, and P. Wu (2012), Enhanced poleward moisture transport and amplified northern high-latitude wetting trend, Nat. Clim. Change, 3, 47–51, doi:10.1038/nclimate1631.